Improving the Precision of Vehicle Fuel Economy Testing on a Chassis Dynamometer

Chappell, Edward

Award date:
2015

Awarding institution:
University of Bath

Improving the Precision of Vehicle Fuel Economy Testing on a Chassis Dynamometer

Edward Colin Chappell

A thesis submitted for the degree of Doctor of Philosophy

University of Bath

Department of Mechanical Engineering

March 2015

Abstract

In the European Union the legislation governing fleet CO_2 emissions is already in place with a fleet average limit of 130g/km currently being imposed on all vehicle manufacturers. With the target for this legislation falling to 95g/km by 2020 and hefty fines for non-compliance automotive engineers are working a pace to develop new technologies that lower the CO_2 emissions and hence fuel consumption of new to market vehicles. As average new vehicle CO_2 emissions continue to decline the task of measuring these emissions with high precision becomes increasingly challenging. With the introduction of real world emissions legislation planned for 2017 there is a development driven need to precisely assess the vehicle CO_2 emissions on chassis dynamometers over a wide operating range. Furthermore since all type approval and certification testing is completed on chassis dynamometers, any new technology must be proven against these test techniques. Typical technology improvements nowadays require repeatability limits which were unprecedented 5-10 years ago and the challenge now is how to deliver this level of precision.

Detailed studies are conducted into the four key areas that cause significant noise to the CO_2 emissions results from chassis dynamometer tests. These are the vehicle electrical system, driver behaviour, procedural factors and the chassis dynamometer itself. In each of these areas, the existing contribution of imprecision is quantified, methods are proposed then demonstrated for improving the precision and the improved case is quantified. It was found that the electrical system can be controlled by charging the vehicle battery, not using auxiliary devices and installing current measurement devices on the vehicle. Simply charging the vehicle battery prior to each test was found to cause a change to the CO_2 emissions of 2.2% at 95% confidence. Whilst auxiliary devices were found to cause changes to the CO_2 emissions of up to 43% for even a relatively basic vehicle. The driver behaviour can be controlled by firstly removing the tolerances from the driver's aid which it was found improved the precision of the CO_2 emissions by 43.5% and secondly by recording the throttle pedal movements to enable the validation of test results. Procedural factors, such as tyre pressures can be easily controlled by resisting the temptation to over check and by installing pressure sensing equipment. Using a modern chassis dynamometer with low parasitic losses will make the job of controlling the dynamometer easier, but all dynamometers can be controlled by following the industry standard quality assurance procedures and implementing statistical process control tools to check the key results. The implementation of statistical process control alone improved the precision of unloaded dynamometer coastdown checks by reducing the coefficient of variation from 6.6 to 4.0%. Using the dynamometer to accelerate the vehicle before

coastdown checks was found to approximately halve the variability in coastdown times. It was also demonstrated that verification of the dynamometer inertia simulation and response time are both critically important, as the industry standard coastdown test is insufficient, in isolation, to validate the loading on a vehicle.

Six sigma and statistical process control techniques have shown that for complex multiple input single output systems, such as chassis dynamometer fuel economy tests, it is insufficient to improve only one input to the system to achieve a change to the output. As a result, suggested improvements in each noise factor often have to be validated against an input metric rather than the output CO_2 emissions. Despite this, the overall level of precision of the CO_2 emissions and fuel consumption seen at the start of the research, measured by the coefficient of variation of approximately 2.6%, has been improved by over six times through the simultaneous implementation of the findings from this research with the demonstration of coefficient of variation as low as 0.4%.

Through this research three major contributions have been made to the state of the art. Firstly, from the work on driver behaviour an extension is proposed to the Society of Automotive Engineers J2951 drive quality metric standard to include the a newly developed Cumulative Absolute Speed Error metric and to suggest that metrics are reviewed across the duration of a test to identify differences in driving behaviours during a test that do not cause a change to the end of test result. Secondly, the need to instrument the vehicle and test cell to record variability in the key noise factors has been demonstrated. Thirdly, a universal method has been developed and published from this research, to use response modelling techniques for the validation of test repeatability and the correction of CO_2 emissions.

The impact of these contributions is that the precision of chassis dynamometer emissions tests can be improved by a factor of 6.5 and this is of critical importance as the new real world driving and world light-duty harmonised emissions legislation comes into force over the next two to five years. This legislation will require an unprecedented level of precision for the effective testing of full vehicle system interactions over a larger operating range but within a controlled laboratory environment. If this level of precision is not met then opportunities to reduce vehicle fuel consumption through technology that only has a small improvement on fuel consumption, which is likely given the large advances that have be achieved over the last few decades, will be missed.

Acknowledgments

I would like to express my gratitude and appreciation to Prof Chris Brace and Dr Sam Akehurst for their guidance, supervision and approachability throughout this research. Your feedback and continued encouragement has helped me no end.

I would also like to thank Allan Cox, Alan Jefferis, Don Blake, Tom Holley and Sam Hurley for their efforts in instrumenting, modifying and testing vehicles on the University of Bath chassis dynamometer with such high precision.

I would like to extend thanks and appreciation to all the management, engineering, technical, operational and maintenance staff from the commercial laboratory from which much of this work is based. Particular thanks must go those individuals with whom I worked closely, whilst you cannot be named for reasons of confidentiality, you know who you are and thank you.

The experimental work within the commercial laboratory was conducted with financial support from both a commercial organisation and the EPSRC, and their funding is acknowledged.

I would also like to thank all my colleagues within the PVRC for their support. Particular mention must be made to Prof. Gary Hawley, Dr. Andy Lewis, Dr. Richard Burke, Dr. Chris Bannister, Dr. Simon Pickering, Huayin, Karl, Deepak, Chris, Bob, James and Jim.

Last but not least I would like to thank my close friends and family for their unconditional support and encouragement throughout. I would also like to thank my parents for giving me the best possible opportunities to get this far, with particular thanks to my father who read through this thesis offering valuable advice and encouragement.

Table of Contents

Abstract 2

Acknowledgments 4

Table of Contents 5

List of Figures 11

List of Tables 24

Notation 26

Further Publications 28

Chapter 1. Introduction 29

1.1. Background and motivation 29

1.2. Fuel Economy and Emissions Testing 30

1.3. The combustion process and formation of vehicle emissions 30

1.4. UK and European Emissions Testing Procedure 31

1.5. The need for high precision, the importance of accuracy and the case for this research 35

1.6. Research Project with a Commercial Type Approval and Emissions Testing Laboratory 36

1.7. Aim and objectives 37

1.8. Scope of the Thesis 37

Chapter 2. Imprecision in Vehicle Fuel Economy Testing 39

2.1. The emissions chassis dynamometer 39

2.2. Vehicle Electrical System 40

2.2.1. The Electrical System 40

2.2.2. Electrical Ancillaries 40

2.2.3. Battery State of Charge 41

2.2.4. Electrical System Summary 45

2.3. Driver Behaviour 47
2.3.1. The Type Approval Driver 47
2.3.2. Speed Error 48
2.3.3. Other Driver Behaviours 49
2.3.4. Robot drivers 50
2.3.5. SAE J2951 Drive Quality Evaluation 50
2.3.6. Accelerator Pedal Busyness 53
2.3.7. Gear Shifting 53
2.3.8. Summary 54
2.4. The Dynamometer 54
2.4.1. The Emissions Chassis Dynamometer 54
2.4.2. Type Approval Road Load Determination 61
2.4.3. Inaccuracy and imprecision from chassis dynamometers 65
2.4.4. Dynamometer summary 69
2.5. Procedural Factors 70
2.5.1. Defining procedural factors 70
2.5.2. Vehicle alignment 71
2.5.3. Vehicle tyres 72
2.5.4. Vehicle restraints 76
2.5.5. Test Vehicle Mass 77
2.5.6. Engine oil level 77
2.5.7. The test room ambient conditions 78
2.5.8. Roadspeed fan 80
2.5.9. Vehicle run-in time 81
2.5.10. Procedural factor summary 82
2.6. The emissions measurement system 83

2.6.1. Overview of the TA emissions measurement system.....83
2.6.2. Sources of imprecision in the emissions measurement system.....84
2.6.3. Summary of the emissions measurement system.....87
2.7. All CO_2 noise factors.....87
2.8. Chapter Summary and Conclusions.....88
Chapter 3. Statistical Approach to Improving and Validating Test Precision.....90
3.1. Statistical confidence, accuracy and precision.....90
3.1.1. Obtaining confidence in results.....90
3.1.2. Precision, accuracy and resolution.....93
3.2. Modelling techniques.....94
3.2.1. Testing time.....94
3.2.2. Model classifications.....94
3.2.3. Design of Experiments.....95
3.2.4. Regression Modelling.....96
3.3. Process Improvement.....97
3.3.1. Statistical Process Control.....97
3.3.2. Control Charts.....97
3.3.3. Six Sigma.....99
3.3.4. DMAIC.....100
3.4. Chapter Summary and Conclusions.....100
Chapter 4. Highest precision fuel consumption measurement.....102
4.1. Introduction.....102
4.2. Experimental Method.....103
4.2.1. Battery State of Charge.....108
4.2.2. Engine Start Temperature.....109
4.2.3. Engine Oil level.....109

4.2.4. Pedal Busyness and Speed Error 109
4.2.5. Road Speed Fan 109
4.2.6. Vehicle Alignment and tie-down straps 110
4.2.7. Tyre Type and Tyre Pressure 110
4.2.8. Simulated Vehicle Mass 110
4.2.9. Ignition Timing 111
4.2.10. Initial Cell Air Temperature 111
4.2.11. Coastdown time 111
4.3. Results 111
4.3.1. Implementation of Statistical Tolerances 111
4.4. Response Modelling 115
4.4.1. Test Factors 115
4.4.2. Model Description 115
4.5. Test repeatability validation methodology 121
4.6. Chapter Summary and Conclusions 122
Chapter 5. Today's precision in a commercial setting 124
5.1. Introduction 124
5.2. The Commercial Emissions Testing Laboratory 125
5.3. Data mining for factors of imprecision in CO_2 emissions 130
5.4. Response Modelling 133
5.4.1. Vehicle A 133
5.4.2. Vehicle B 135
5.5. Introducing Engine Control Unit Logging on Vehicle A 136
5.6. Chapter Summary and Conclusions 141
Chapter 6. Vehicle Electrical System 143
6.1. Introduction 143

6.2. Sources of auxiliary electrical load variability 143
6.3. The effect of auxiliary electrical loads on CO_2 emissions 149
6.4. The effect of SLI Battery SoC on CO_2 emissions 156
6.4.1. Smart Alternator Technology 171
6.5. Chapter Summary and Conclusions 173
Chapter 7. The Driver 177
7.1. Introduction 177
7.2. Driver Rating Tools and Metrics in Industry 177
7.2.1. Predecessors to SAE J2951 177
7.2.2. SAE J2951 178
7.3. Driver's Aid Improvements 180
7.3.1. Experimental Approach 180
7.3.2. Experimental Results 182
7.3.3. Individual Driver Analysis 188
7.4. Comparing Driver Behaviour Metrics 196
7.5. Real-time Driver Feedback 201
7.6. CO_2 correction and tolerances for Drive Metrics 202
7.7. Chapter Summary and Conclusions 202
Chapter 8. Procedural 204
8.1. Introduction 204
8.2. Tyre inflation pressure 204
8.3. Engine oil level 207
8.4. Ambient Temperature 207
8.5. Chapter Summary and Conclusions 208
Chapter 9. The Chassis Dynamometer 210
9.1. Introduction 210

9.2. Dynamometer Load cell calibration 210
9.3. Dynamometer Base Inertia Calibration 213
9.4. Dynamometer Losses Calibration 214
9.5. Interaction of Calibrations 221
9.6. Coastdown Testing for Road Load Setting and Verification 221
9.7. The importance of dynamometer road load on CO_2 emissions 231
9.8. Six-Sigma Process Control and the Dynamometer Dashboard 237
9.9. Chapter Summary and Conclusions 251
Chapter 10. Conclusions 253
10.1. Summary 253
10.2. Conclusions 253
10.3. Outlook and further work 260
References 261

List of Figures

Figure 1-1: New European Drive Cycle [9].....32

Figure 1-2: WLTC [16].....34

Figure 2-1: Basic chassis dynamometer schematic showing key areas affecting engine load and measurement of CO_2 emissions 39

Figure 2-2: Simplified vehicle electrical system block diagram. Arrows indicate path and direction of energy transfer or indicate the path and direction of control signals.....40

Figure 2-3: Absolute effect on fuel consumption measured ordered and compared with the typical effect of change of oil's High Temperature High Shear value (HTHS) from 2.9cP to 3.5cP [8].....42

Figure 2-4: Results from the study of pre-test battery drain on CO_2 emissions, showing the wide range of results recorded from the same experiment performed on different vehicles [20] 43

Figure 2-5: Effect of energy supplied to the battery on gravimetric fuel consumption over the NEDC [8].....45

Figure 2-6: Example driver's aid speed display with tolerance lines shown 47

Figure 2-7: Test results showing the effect of optimised driving within the type I emissions test legal tolerances across 6 test vehicles. Vehicles 1-3 are SI and vehicles 4-6 are CI. The largest effects have been highlighted by the original author [20].....48

Figure 2-8: The University of Bath 48” single roller chassis dynamometer with DC electrical inertia simulation. This is a 2WD dynamometer and is housed in a climatic chamber. The vehicle is shown in the raised position above dynamometer on centralising mechanism.....55

Figure 2-9: Chassis dynamometer functional block diagram. Thick solid lines represent mechanical connections where rotational power is transferred between blocks. Dotted lines represent signal connections. An optional item is shown in the dotted outlined box. 56
Figure 2-10: Free body diagram for a vehicle driving up a gradient 57
Figure 2-11: Twin 20" roller chassis dynamometer with multiple clutch selectable flywheels and electrical inertia trimming 59
Figure 2-12: 48” single roller 4WD Horiba VULCAN chassis dynamometer [35] ... 60
Figure 2-13: CO_2 emissions from six test vehicles, tested at two chassis dynamometer road load settings and compared to baseline CO_2 emissions [10] . 63
Figure 2-14: Percentage change in road load versus percentage change in vehicle weight demonstrating non-linearity at low speeds. Dashed lines have been added by the author to demonstrate linearity for each vehicle if the error bars are used. [40] 65
Figure 2-15: Dynamometer quality assurance roadmap based on DPEQAP [49] . 67
Figure 2-16: Diagram of vehicle misalignment on a chassis dynamometer [8] 72
Figure 2-17: Correlation of wheel work to fuel economy [51] 74
Figure 2-18: Correlation of tyre surface temperature to tyre loss force [51] 75
Figure 2-19: combined effect of tyre related factors on the rolling resistance measured by coastdown time and on gravimetric fuel consumption [8] 76
Figure 2-20: CO_2 emissions from a variety of test vehicles tested at 15, 22, 25 and 28°C. The results are normalised against the CO_2 emissions at 22°C. [14] 79
Figure 2-21: Results from a study of the change in CO_2 emissions when soak temperature is increased from 22 to 28°C. Vehicles 1-3 are SI and vehicles 4-6 are CI. The largest effects have been highlighted by the original author [20] 80
Figure 2-22: Schematic diagram of a CVS system [27] 84

Figure 2-23: Possible error sources during exhaust emission testing on a chassis dynamometer [27] 86
Figure 2-24: Cause and effect diagram for the uncertainty of emissions measurement [27] 86
Figure 2-25: Fishbone diagram of the sources of fuel economy imprecision and inaccuracy 88
Figure 3-1: Total bag CO_2 emissions from 100 consecutive tests on a EURO 4 diesel light commercial vehicle 91
Figure 3-2: An illustration of the difference between precision and accuracy [67]. 93
Figure 3-3: Design of Experiments two level factoral design compared to OFAT for three factors [69] 95
Figure 3-4: Example X-bar and R chart. The x-axis is common to both plots and is the subgroup number. The y-axis for the X-bar chart shown at the top is the mean for each subgroup, the y-axis for the R chart shown at the bottom is the range from smallest to largest within each subgroup. The charts show example data that is not from experiments related to the research in this thesis. [78] 98
Figure 3-5: Example X and MR Chart. The x-axis is common to both plots and is the observation number. The y-axis for the X chart shown at the top is the raw value for each result, the y-axis for the MR chart shown at the bottom is the moving range from the previous to the current observation. The MR results therefore start at the second observation. The charts show example data that is not from experiments related to the research in this thesis. [78] 98
Figure 4-1: Diagram of the test sequence [83] 106
Figure 4-2: Diagram of the oil test sequence [83] 107
Figure 4-3: Schematic diagram of the test cell [83] 107
Figure 4-4: Fuel consumption results from the entire test programme [83] 112

Figure 4-5: Plots of the variability in the noise factors from overnight cold tests [83] 113
Figure 4-6: Plots of the variability in the noise factors from forced cold tests [83] 114
Figure 4-7: Plots of the variability in the noise factors from hot tests [83] 114
Figure 4-8: Main effects plot for the MLR model with the initial oil temperature removed [83] 117
Figure 4-9: Main effects plot for the optimised MLR model [83] 118
Figure 4-10: Initial potential difference at battery terminals for all test conditions [83] 119
Figure 4-11: Main effects plot for the optimised MLR model with initial oil temperature removed and including battery voltage [83] 120
Figure 4-12: Test validation method flow chart [83]..... 122
Figure 5-1: Vehicle A total CO_2 emissions results for all tests across all test cells. 128
Figure 5-2: Vehicle B total CO_2 results for all tests across all test cells. 129
Figure 5-3: Vehicle A, one number metrics (from left to right: Test cell i.d., Driver i.d., pre-test soak time, test cell temperature, test cell barometric pressure, test cell relative humidity, test cell ambient humidity, distance driven, post-test coastdown time, number of driver violations, driver violation time, road load force at 70 km/h, pre-test battery voltage, dynamometer minutes run in the last 2 hrs and dynamometer minutes since last run, respectively)..... 131
Figure 5-4: Vehicle B one number test metrics (from left to right: Test cell i.d., Driver i.d., pre-test soak time, test cell temperature, test cell barometric pressure, test cell relative humidity, test cell ambient humidity, distance driven, post-test coastdown time, number of driver violations, driver violation time, road load force

at 70 km/h, pre-test battery voltage, dynamometer minutes run in the last 2 hrs and dynamometer minutes since last run, respectively).....131
Figure 5-5: Vehicle A main effects plot for the MLR model, where the bars represent the pre-test soak time, test cell temperature, test cell barometric pressure, test cell relative humidity, post-test coastdown time, dynamometer minutes run in the last 2 hrs and dynamometer minutes since last run and the pre-test SLI battery voltage respectively.....134
Figure 5-6: Vehicle B main effects plot for the MLR model, where the bars represent the pre-test soak time, test cell temperature, test cell barometric pressure, test cell relative humidity, post-test coastdown time, dynamometer minutes run in the last 2 hrs and dynamometer minutes since last run and the pre-test SLI battery voltage respectively.....136
Figure 5-7: Main effects plot for the response model built from results on vehicle A, with both ECU data and test cell data. The bars represent the initial call air pressure, the normalised cumulative throttle position, normalised cumulative wheel speed, total coastdown time, normalised cumulative brake pedal input, normalised cumulative engine coolant temperature and the dynamometer thermal status given by the minutes since the dynamometer was last run.....138
Figure 5-8: Brake Mean Effective Pressure for a 2.2 litre displacement turbocharged diesel engine fitted to a light commercial vehicle and operating over the NEDC. Operating envelope is shown by the red line and the red circle shows the chosen steady state point for engine modelling. 139
Figure 5-9: Engine simulation results for steady state operation of 2.0 litre displacement gasoline engine running at 2bar BMEP and 2000 rev/min. 140
Figure 6-1: HIOKI current clamp configuration for vehicle auxiliary load experiments. VCU stands for vehicle connection unit and is part of the data

acquisition system in use within the commercial laboratory where the experiments were conducted. 145
Figure 6-2: Results of electrical load measurements during 2nd gear cruise at 28kph with seven different configurations of electrical auxiliary devices switched on 150
Figure 6-3: Results of tailpipe CO_2 measurements during 2nd gear cruise at 28kph with seven different configurations of electrical auxiliary devices switched on 151
Figure 6-4: Relationship between the average fuel power consumed by the engine and the average electrical power consumed by the auxiliary devices. Red data points were calculated from data recorded with auxiliary loads switched on and blue data points were calculated from data recorded with the auxiliary loads switched off. 152
Figure 6-5: Recorded total bag CO_2 emissions from repeated tests of a B-car on hot start TA style emissions tests in test cell 4 with all auxiliary loads switched on and off 153
Figure 6-6:Recorded cumulative modal tailpipe (TP) CO_2 emissions from repeated tests of a B-car on hot start TA style emissions tests in test cell 4 with all auxiliary loads switched on and off..... 154
Figure 6-7: Recorded change in total bag CO_2 emissions for all electrical loads and calculated change in total bag CO_2 emissions from individual electrical loads.... 156
Figure 6-8: Bar chart of total bag CO_2 emissions from a C-car with a turbocharged gasoline engine. For tests with battery charging during the preceding overnight soak and tests without any soak battery charging. Error bars show standard error of the mean at 95% confidence..... 158

Figure 6-9: Time series plot of a total bag CO_2 emissions from a C-car with a turbocharged gasoline engine. For tests with battery charging during the preceding overnight soak and tests without any soak battery charging 159
Figure 6-10: Histogram of total bag CO_2 emissions from a C-car with a turbocharged gasoline engine for tests with battery charging during the preceding overnight soak and tests without any soak battery charging 160
Figure 6-11: Vehicle C alternator current measured instantaneously during 24 NEDC tests. 7 tests where the SLI battery was charged overnight prior to the test (shown in blue) and 17 tests where there was no battery charging prior to the test (shown in red) 162
Figure 6-12: Vehicle C change in alternator energy during the emissions tests versus the change in the bag CO_2 emissions from the same tests. In both cases the changes are calculated from the mean alternator output energy and mean total bag CO_2 emissions from each of the emissions tests. A total of 24 tests are shown, 7 in red where the SLI battery was not charged and 17 in blue where the SLI battery was charged. 163
Figure 6-13: Vehicle C, overnight charge results using a CTEK smart charger to charge the vehicle SLI battery. The instantaneous current is shown in solid red and solid blue. The cumulative current in shown in dotted black and dotted pink. The chronological test number (taken from Figure 6-9) is shown above each plot. 165
Figure 6-14: Vehicle C, overnight charge results using a CTEK smart charger to charge the vehicle SLI battery. The instantaneous battery charger current is shown in blue and the instantaneous fusebox current in red. The chronological test number (taken from Figure 6-9) is shown above each plot. 167

Figure 6-15: The change in the battery charger energy during pre-test overnight soak versus the change in consumed fuel energy on the concurrent emissions test for vehicle C. The battery charger energy is calculated from charger on time until the first spike in the recorded current indicating the charger had turned off. 170
Figure 6-16: Example of recorded alternator current (blue), recorded battery voltage (red) and calculated alternator power (magenta) during an NEDC test on a vehicle equipped with smart alternator technology. 172
Figure 7-1: EER and SM drive metric results for phase 1 and 2 of NEDC chassis dynamometer emissions tests from the commercial laboratory. Y-axis shows fuel economy (FE) measured in miles per imperial (UK) gallon 179
Figure 7-2: An example of a typical drivers aid display with speed tolerances 180
Figure 7-3: An example of a typical drivers aid display without speed tolerances 181
Figure 7-4: Total Bag CO_2 Emissions for all drivers by driver's aid tolerance setting 185
Figure 7-5: Histogram of the total Bag CO_2 Emissions for all drivers grouped by driver's aid tolerance setting. 'Tol Off' stands for driver's aid tolerances switched off and 'Tol On' stands for driver's aid tolerances switched on 185
Figure 7-6: Boxplot of total bag CO_2 emissions for all drivers with driver's aid tolerances on. 186
Figure 7-7: Boxplot of total bag CO_2 emissions for all drivers with driver's aid tolerances off. 186
Figure 7-8: Histogram of Cumulative Absolute Speed Error (CASE) for all drivers and the two experimental cases, drivers aid tolerances on and off. 188
Figure 7-9: Boxplot of CASE for all drivers with driver's aid tolerances on. 189
Figure 7-10: Boxplot of CASE for all drivers with driver's aid tolerances off. 189

Figure 7-11: Instantaneous SAE primary metrics for driver 17 with driver's aid tolerances on and off.....190
Figure 7-12: Instantaneous CASE and SAE supplementary metrics for driver 17 with driver's aid tolerances on and off.....191
Figure 7-13: Instantaneous SAE primary metrics for driver 20 with driver's aid tolerances on and off.....192
Figure 7-14: Instantaneous CASE and SAE supplementary metrics for driver 20 with driver's aid tolerances on and off.....192
Figure 7-15: Instantaneous SAE primary metrics for driver 12 with driver's aid tolerances on and off.....193
Figure 7-16: Instantaneous CASE and SAE supplementary metrics for driver 12 with driver's aid tolerances on and off.....194
Figure 7-17: Instantaneous SAE primary metrics for driver 9 with driver's aid tolerances on and off.....195
Figure 7-18: Instantaneous CASE and SAE supplementary metrics for driver 9 with driver's aid tolerances on and off.....196
Figure 7-19: Comparison of vehicle speed error and pedal busyness as driver metrics for the first 200 seconds of a NEDC emissions test for high and low robot driver pedal oscillations. Plots show vehicle speed, the difference between high and low vehicle speed, the instantaneous pedal busyness, the difference between instantaneous high and low pedal busyness and the pedal busyness as developed over the test. 200
Figure 7-20: Relationship between difference in vehicle speed error and the difference in pedal busyness for high and low aggresivity drives over an NEDC recorded at 1Hz. Idle periods have been excluded. 201

Figure 8-1: Tyre inflation pressure measured from three quality check vehicles during soak conditions within the commercial laboratory. Vehicle A is a gasoline B-car, vehicle D is a C-car and vehicle B is a light commercial. FR is the front right tyre and FL is the front left tyre. All vehicles are front wheel drive. Representative FC sensitivity is shown using data from Brace et. al. [8]. 205
Figure 8-2: Histogram of pre-test ambient air temperature for a number of tests in a commercial laboratory and relationship between pre-test air temperature and total CO_2 emissions for the same tests. 208
Figure 9-1: Horiba results showing the achievable linearity (top plot) and the hysteresis (lower plot) for a VULCAN chassis dynamometer two sided load cell calibration [35]..... 212
Figure 9-2: Cell 14 and cell 4 loss calibration results for cold and warm states. Blue lines are for the cold dynamometer and red lines are for the warm dynamometer. In cell 4 two calibrations were run with the dynamometer in a warm state. Dashed lines show RMS fit error 215
Figure 9-3: Cell 4 loss calibration results for a cold, warm and cooling down dynamometer 218
Figure 9-4: Typical friction calibration results display on the University of Bath chassis dynamometer via the Sierra CP Engineering CADET host system 219
Figure 9-5: Coastdown test fishbone diagram..... 223
Figure 9-6: Comparison of coastdown time variability prior and post auto coastdown upgrade on the cell 12 dynamometer. Groups 1 - 4 are in order; vehicle A pre upgrade, vehicle A post upgrade, vehicle B pre upgrade and vehicle B post upgrade, respectively. 224

Figure 9-7: Boxplots of the error for each coastdown test run compared to the average result for a large number of manual and automatic transmission vehicles tested in the commercial laboratory. 225
Figure 9-8: Calculated inertia component of force applied by the dynamometer motor to the vehicle during a NEDC test and a coastdown test for a C-car tested on the University of Bath chassis dynamometer. Data collected at 10Hz. 228
Figure 9-9: Calculated total motor force, including inertia and dynamometer road load components, applied by the dynamometer motor to the vehicle during a NEDC test and a coastdown test for a C-car tested on the University of Bath chassis dynamometer. Data collected at 10Hz. 228
Figure 9-10: Calculated inertia component of force applied by the dynamometer motor to the vehicle during a NEDC test and a coastdown test for vehicle A tested on the cell 12 chassis dynamometer. Data collected at 1Hz. 230
Figure 9-11: Calculated total motor force, including inertia and dynamometer road load components, applied by the dynamometer motor to the vehicle during a NEDC test and a coastdown test for a vehicle A tested on the cell 12 chassis dynamometer. Data collected at 1Hz. 230
Figure 9-12: Proportion of total positive cycle power by driving mode and cycle phase for four vehicles tested over the NEDC. Vehicle A_1 is a high fuel economy version of vehicle A. 232
Figure 9-13: Proportion of the total cycle power by inertia and dynamometer road load force component and cycle phase for the four vehicles tested over the NEDC. Vehicle A_1 is a high fuel economy version of vehicle A. 233
Figure 9-14: Relationship between the positive work done by vehicle A against the dynamometer load and the instantaneous consumed fuel power for the same vehicle tested at in the commercial laboratory. 234

Figure 9-15: Proportion of the total CO_2 mass emissions by mode and phase for 29 tests on vehicle A at the commercial laboratory. 235
Figure 9-16: Proportion of total cycle CO_2 mass emissions for each mode of the NEDC averaged over 29 tests of vehicle A tested at the commercial laboratory. The error bars show the 95% confidence intervals based on the standard error of the mean. 236
Figure 9-17: Snapshot of the Dynamometer Dashboard front screen, with the cursor hovering over the inertia calibration result for cell 1, showing an example of the warning messages displayed to the user. 239
Figure 9-18: Dynamometer Dashboard load cell and calibration timeline plots... 241
Figure 9-19: Close up print preview style view of the SPC page 1 from the Dynamometer Dashboard. 244
Figure 9-20: Close up print preview style view of the SPC page 2 from the Dynamometer Dashboard. 245
Figure 9-21: Snapshot of the Dynamometer Dashboard quality assurance roadmap page. 247
Figure 9-22: Snapshot of the Dynamometer Dashboard test checker page with an example test from Cell 12 loaded to show the typical results that are displayed. 248
Figure 9-23: Distribution of unloaded (dynamometer only) coastdown times before and after the implementation of the Dynamometer Dashboard within the commercial laboratory. 250
Figure 10-1: Summary of the measured improvements made to the precision and the measured maximum effect of key noise factors made by the author in this thesis. The red bar shows the level of precision of CO2 emissions before the work started and the green bar shows the level of precision of CO2 emissions achieved through this work, both on the primary y-axis. The blue bars show the precision of

input factors measured through metrics with the baseline shown in dark blue and the improvement in light blue, both on the primary y-axis. The grey bars show on the secondary y-axis the maximum effect of individual noise factors possible during one emissions test. 259

List of Tables

Table 1-1: European Diesel Emissions Limits (# sourced from [1], * sourced from [13])....33

Table 1-2: European Gasoline Emissions Limits (# sourced from [1], * sourced from [13])....33

Table 1-3: Comparison of operating conditions on NEDC and WLTC [16]....35

Table 2-1: Procedural factor effect summary....82

Table 3-1: Amalgamated SPC control chart criteria for identifying special cause variation....99

Table 4-1: Main findings from the previous study conducted by Brace et. al. [8, 83]....103

Table 4-2: Response model factors [83]....116

Table 5-1: The commercial laboratory test cell capability in 2010....126

Table 5-2: Vehicle Specifications from the study....127

Table 5-3: Imprecision in total bag CO_2 emissions for both vehicles in the study130

Table 5-4: Vehicle A correlation matrix for MLR model with the two largest coefficient in bold. Variables V1 – V8 are defined as the pre-test soak time, test cell temperature, test cell barometric pressure, test cell relative humidity, post-test coastdown time, dynamometer minutes run in the last 2 hrs and dynamometer minutes since last run and the pre-test SLI battery voltage respectively....134

Table 5-5: Vehicle B correlation matrix for MLR model with the largest coefficient in bold. Variables V1 – V8 are defined as the pre-test soak time, test cell temperature, test cell barometric pressure, test cell relative humidity, post-test coastdown time, dynamometer minutes run in the last 2 hrs and dynamometer minutes since last run and the pre-test SLI battery voltage respectively....136

Table 6-1: Electrical loads read from HIOKI power analyser. Readings highlighted in blue are approximate due to noisy readings.....146
Table 7-1: Driver behaviour metric results for all drivers by driver's aid tolerance setting 182
Table 7-2: Driver Behaviour Metric Classifications.....198
Table 7-3: DoE test conditions and corresponding end of test driver metric results 199

Notation

AHU	Air Handling Unit
ASCR	Absolute Speed Change Rating
BMD	Bag Mini Diluter
BMEP	Brake Mean Effective Pressure
BSFC	Brake Specific Fuel Consumption
CARB	Californian Air Research Bureau
CASE	Cumulative Absolute Speed Error
CFV	Critical Flow Venturi
CI	Compression Ignition
CoV	Coefficient of Variation
CVS	Constant Volume Sampling
DET	Drive Evaluation Tool
DMAIC	Define Measure Analyse Improve Control
DoE	Design of Experiments
DPEQAP	Dynamometer Performance Evaluation and Quality Assurance Procedures
DR	Distance Rating
EBDR	Energy Based Driver Rating
ECU	Engine Control Unit
ER	Energy Rating
EER	Energy Economy Rating
EPA	Environmental Protection Agency (United States of America)
EPSRC	Engineering and Physical Sciences Research Council
ETW	Equivalent Test Weight
EU	European Union
FE	Fuel Economy
FC	Fuel Consumption
GSI	Gear Shift Indicator
GUI	Graphical User Interface
HVAC	Heating Ventilation and Air Conditioning
ICE	Internal Combustion Engine
IQR	Inter-Quartile Range
JRC	Joint Research Council
LHV	Lower Heating Value
MLR	Multiple Linear Regression
NEDC	New European Drive Cycle
OEM	Original Equipment Manufacturer
OFAT	One Factor At a Time
PAS	Power Assisted Steering
PC	Personal Computer
PEMS	Portable Emissions Measurement System(s)
PID	Proportional Integral Derivative
PMEP	Pumping Mean Effective Pressure
PRESS	Predicted Residual Sum of Squares
PVRC	Powertrain and Vehicle Research Centre
REF	Research Excellence Framework
RH	Relative humidity
RMSSE	Route Mean Square Speed Error
RLS	Road Load Simulation

SAE	Society of Automotive Engineers
SAO	Smooth Approach Orifice
SI	Spark Ignition
SLI	Starter Lighting and Ignition (battery)
SM	Smoothness Rating
SoC	State of Charge
SPC	Statistical Process Control
TA	Type Approval
TP	Throttle Position
VCA	Vehicle Certification Authority
WLTC	World harmonised Light-duty Test Cycle
WLTP	World harmonised Light-duty Test Procedure

Further Publications

The research that is presented in this thesis has led to the further publications that are listed below.

Journal Articles

The work presented in Chapter 4 led to publication in the pier reviewed and internationally recognised Institution of Mechanical Engineers Journal of Automobile Engineering.

Chappell, E, Brace, C and Ritchie, C, ***The control of chassis dynamometer fuel consumption testing noise factors and the use of response modelling for validation of test repeatability***, Proc Inst Mech Eng Part D, J Auto Eng, 227(6), 2013, pp 853-865.

REF Impact Case Study

The research from this thesis underpinned and led to an impact case study (REF3b) that formed part of the 2014 Research Excellence Framework submission for the University of Bath.

Journal Articles in Preparation

The research presented in Chapter 7 has been drafted into a journal paper article which is planned for submission to a peer reviewed journal during 2015. The draft paper is entitled**: The impact of driver behaviour on CO_2 emissions measurement precision on chassis dynamometers.**

Chapter 1. Introduction

1.1. Background and motivation

Regulation of harmful pollutants from vehicle tailpipes has been in place for many years, for example in the UK the first emissions limits, known as EURO 1, were published around 20 years ago [1]. Typical harmful pollutants covered by these legislations are carbon monoxide (CO), unburned hydrocarbons (HC), oxides of nitrogen (NOX) and particulate matter (PM). These harmful gases emissions are typically referred to as criteria pollutants. Over this time period the CO_2 emissions and thus fuel consumption have remained unregulated. However despite their being no regulatory motivation, vehicle fuel consumption has improved, for example a 14% reduction has been recorded between 1995 and 2006 [2]. Unfortunately this improvement has been offset by a vast increase in the size of the European fleet and the net effect has been an increase in European transport related CO_2 emissions of 26% between 1990 and 2004 [2]. In the midst of the growing concern over increases in global greenhouse gas emissions, CO_2 being a primary component of greenhouse gas and dwindling hydrocarbon fuel reserves, the European Commission introduced legislation in 2009 governing the new passenger car fleet average CO_2 emissions. The legislation outlined a roadmap for the tightening of the limits on fleet average CO_2 emissions culminating in a target of 95g/km CO_2 in 2020 [3]. The target is being gradually phased in; an initial limit of 130g/km was set to cover 65% of each manufactures' fleet average new cars sales for 2012. This was increased to cover 100% of each manufactures' fleet for 2015. From 2012 for every g/km that a manufacturer's fleet average CO_2 exceeds these limits is fined of up to €95 per registered vehicle, per g/km of CO_2 [4]. For large manufacturers making millions of vehicles each year, non-compliance with these regulations could clearly be a substantial threat to profitability. Similar legislation was adopted in other countries including Japan and the USA. The results from legislative type approval (TA) chassis dynamometer emissions tests forms the basis for manufacturers to demonstrate compliance against this new regulation along with the criteria pollutants. This has forced an increased interest in understanding how these results are obtained and how their precision can be improved.

Automotive researchers are being pushed to search more areas for fuel economy improvements to address the European Commission CO_2 targets. As a result of the large advances in the last few decades, these improvements are likely to be as a result of combined small effects. Examples of such effects are changes in fuel or oil properties and changes in auxiliary drive arrangements resulting in typical improvements in the range of 0.2 to 10% [5-7]. With potentially such small improvements, traditional repeatability limits of around 1% coefficient of variation (CoV) at a 95% confidence level are likely to be

insufficient. It is therefore of critical importance that rigorous approaches are developed for future chassis dynamometer testing to allow the highest precision testing, with repeatability targets of <0.5% CoV at a 95% confidence level, to be adopted as the norm. This level of precision is a significant challenge in a commercial testing environment but it a CoV of 0.5% has been demonstrated as achievable, with significant effort, in an academic testing context through the work of Brace et. al. [8].

1.2. Fuel Economy and Emissions Testing

The focus of this research is the use of modern chassis dynamometers for legislative type approval (TA) vehicle fuel economy and emissions testing. Fuel economy and emissions testing is a necessary and key part of daily business for OEMs developing new vehicles due to the need to assess legal compliance, known as type approval, of new vehicle emissions against the current emissions limits and targets imposed by the governing authorities [9, 10].

All types of legal emissions testing require the use of exhaust gas analysers to measure the concentrations of harmful pollutants in the vehicle exhaust gases. Arguably the most common system in use in Europe is the constant volume sampling (CVS) system. The basic layout of a CVS system allows diluted exhaust emissions to be collected into bags which are analysed at the end of a period of driving to give the overall mass of pollutants emitted by the vehicle during that period. The operation of the CVS system is described in section 2.6. At the present time, the most common alternative system for emissions measurement on chassis dynamometers is the Bag Mini Diluter (BMD) system, which is the most commonly used system in the USA.

Legislative emission test procedures follow differing protocols around the globe, for example, Europe, the United States of America and Japan all have different legislation. This presents challenges to OEMs to produce vehicles that meet these different legislations along with individual market needs whilst minimising development costs.

1.3. The combustion process and formation of vehicle emissions

Both gasoline and diesel fuels are primarily composed of hydrocarbon molecules and when these are burnt in an internal combustion engine the primary products are carbon dioxide and water [11]. Additional pollutants are generated such as oxides of nitrogen (NOx), un-burnt hydrocarbons from the fuel, particulates and carbon monoxide (CO) due to incomplete combustion. Emissions analysis systems make a measurement of the vehicle fuel consumption by an analysis of the concentrations of the carbon containing emissions, of which the carbon dioxide is normally the greatest [12]. The concentrations

are combined with a measure of the exhaust flow rate to determine the mass of the carbon containing emissions. Based on the assumption that the carbon containing emissions must have originated from the fuel, with the exception of background carbon compounds in the atmosphere, the mass of fuel burnt can be calculated. It is therefore often assumed that correlations with fuel consumption are equivalent to correlations with CO_2 emissions and this assumption will be used throughout this thesis [12].

1.4. UK and European Emissions Testing Procedure

The legislative emissions test procedure for use throughout Europe is defined within UN ECE reg no. 83-06 [9]. The regulation contains requirements to test the vehicle at several conditions, involving static testing and driven testing using a chassis dynamometer. Arguably the most involved of these tests is the 'type I' TA test which is the ambient cold start emissions test. The test is intended to replicate normal vehicle driving conditions over a standardised driving pattern on a chassis dynamometer, thereby allowing the controlled measurement of vehicle emissions and fuel economy. The primary requirements for a type I test are:

- Test cell ambient temperature between 20 and 30°C
- Minimum vehicle soak time 6 hours
- Vehicle is 'run-in' and must have completed at least 3000km prior to testing
- The vehicle shall be driven using the NEDC test cycle
- A tolerance of ±2kph on the demanded vehicle speed combined with a tolerance of ±1.0s on the time

The NEDC is made up of two parts, the urban cycle (part one) and the extra-urban cycle (part two), see Figure 1-1. Part one is made up of 4 repeats of the elementary urban cycle, each lasting 195s and part two lasts for 400s making the total cycle time 1180s [9].

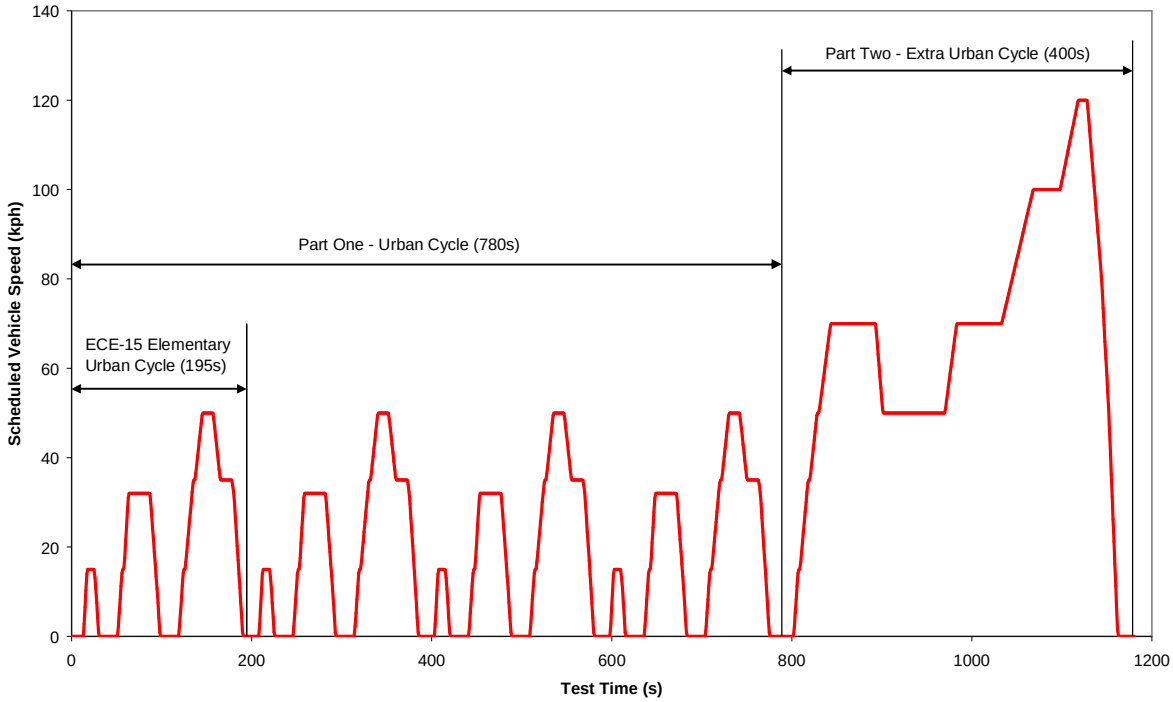

Figure 1-1: New European Drive Cycle [9]

In the UK there are additional requirements imposed by the Vehicle Certification Authority (VCA) for example the requirement that each legislative emissions test is supervised by a VCA representative.

For an OEM conducting legislative TA testing in Europe, the primary purpose of the type I test is to two fold; firstly to determine the vehicle has met the emissions limits defined by the European Union (EU) such that the vehicle can legally be sold in the EU and secondly to determine the official vehicle fuel consumption and CO_2 emissions. These figures form the basis for regional taxation and are used in official sales literature for the vehicle. The emissions limits are set by the European Commission and are set in agreement with vehicle manufacturers throughout Europe.

The first set of emissions limits within Europe was called EURO 1 and came in to force in 1992. Since that time the standards have evolved and updated primarily as a consequence of heightened awareness in the environmental impact of harmful vehicle emissions and the consumer need for lower fuel consumption due to the increasing cost and taxation on road fuels. At the time of writing the current European emissions standard is EURO 6. The EURO emissions limits are shown in Table 1-1 and Table 1-2.

Table 1-1: European Diesel Emissions Limits (# sourced from [1], * sourced from [13])

Emissions Standard	Enforcement Date	CO	THC	NMHC	NOx	HC + NOx	PM	PN
		(g/km)						(#/km)
EURO 1#	**1993**	2.72 (3.16)	-	-	-	0.97 (1.13)	0.14 (0.18)	-
EURO 2#	**1996**	1.0	-	-	-	0.7	0.08	-
EURO 3#	**2000**	0.64	-	-	0.50	0.56	0.05	-
EURO 4#	**2005**	0.50	-	-	0.25	0.30	0.025	-
EURO 5+*	**2009**	0.500	-	-	0.180	0.230	0.005	$6x10^{11}$
EURO 6*	**2014**	0.500	-	-	0.125	0.215	0.005	$6x10^{11}$

Table 1-2: European Gasoline Emissions Limits (# sourced from [1], * sourced from [13])

Emissions Standard	Enforcement Date	CO	THC	NMHC	NOx	HC + NOx	PM	PN
		(g/km)						(#/km)
EURO 1#	**1993**	2.72 (3.16)	-	-	-	0.97 (1.13)	-	-
EURO 2#	**1996**	2.2	-	-	-	0.5	-	-
EURO 3#	**2000**	2.3	0.20	-	0.15	-	-	-
EURO 4#	**2005**	1.0	0.10	-	0.08	-	-	-
EURO 5+*	**2009**	1.000	0.100	0.068	0.060	-	0.005	-
EURO 6*	**2014**	1.0	0.1	0.068	0.060	-	0.005	$6x10^{11}$

Vehicle manufacturers are required to demonstrate compliance with the emissions standards as well as measuring the CO_2 emissions using new, run-in, vehicles prior to the vehicle being certified for sale. However the CO_2 emissions recorded during the TA are not necessarily the CO_2 emissions that are declared and taken forward for the official declaration of a particular vehicle as there is an allowed tolerance of up to 4% between the results recorded in the TA tests and the declaration by the manufacturer [14]. This tolerance exists because of the need for the manufacturer to demonstrate compliance with their declared CO_2 emissions for vehicles tested after manufacture, known as in-service compliance testing.

Over recent years there has been substantial criticism by pressure groups, the press and technical bodies of the existing TA test procedures and the NEDC on the basis of a growing gap between legislative emissions and real world emissions. This is a concern for both consumers, who are buying vehicles expecting to be able to achieve the fuel consumption stated by the manufacturer and for the population as a whole; since inner city emissions, in particular NO_X emissions are not falling in line with the rate of decline in emissions standards [15]. The legislators are reacting to this criticism and are making two drastic changes to emissions legislation over the next two to five years. The first of these will be the introduction of real driving emissions, known as RDE, legislation as part of

EURO 6c in 2017 and the second the introduction of a drastically overhauled laboratory testing procedure is planned to take over sometime between 2017 and 2020.

The RDE requirement within EURO 6c will involve the use of portable emissions measurement systems known as PEMS which will be installed into vehicles and used to measure criteria pollutants during real world on the road driving. The exact details of the testing conditions are not yet fully agreed although Jon Caine of the Ford Motor Company, speaking at the 2015 Future Powertrains Conference gave some insight into the current status; stating that the boundary conditions could include a temperature range between 0 and 30°C, with the possibility of negative temperatures not ruled out, up to 700m altitude, driving to include a split into thirds of urban, rural and motorway lasting for 90 to 120 minutes in duration. This represents a substantial increase from the NEDC in the operating envelope within which the vehicle must be compliant with the emissions standards for criteria pollutants.

The new laboratory testing procedure, due to come into force somewhere between 2017 and 2020, is known as the World Light-duty Harmonised Test Procedure or WLTP [14], [15]. All the details are yet to be finalised but the most significant changes that are going to be brought about by the WLTP will be a completely new test cycle, known as the World Light-duty Test Cycle or WLTC, possibly a change to ambient temperature for laboratory tests, vehicle specific gear shift points and vehicle specific test mass including optional extras [16]. The WLTC is by far the most drastic of these changes and was created by analysing data from thousands of vehicles on the road. The cycle is shown in Figure 1-2.

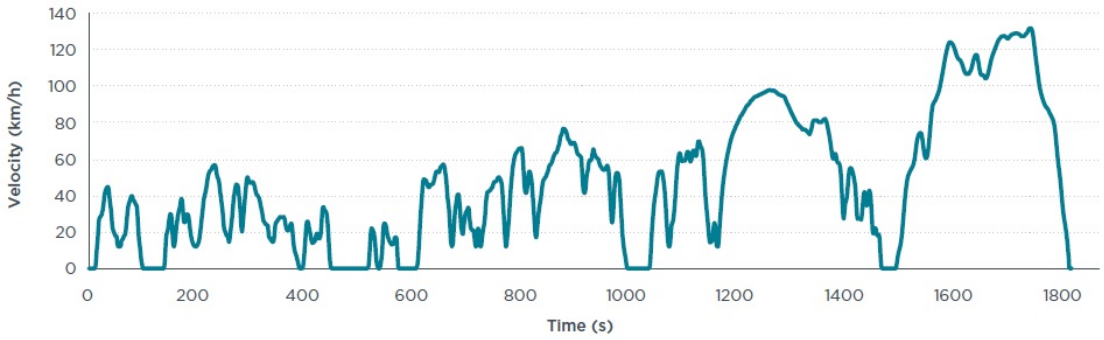

Figure 1-2: WLTC [16]

Compared with the outgoing NEDC, the WLTC represents a large increase in the vehicle operating envelope that will be assessed by chassis dynamometer TA tests. As Table 1-3 shows the cycle is longer, more transient as it involves over double the time spent accelerating and decelerating compared with the NEDC and the idle time is approximately halved. In addition the maximum accelerations and minimum decelerations have both increased substantially. The WLTC was determined by examining data from a large fleet of vehicles being driven on the road and therefore the author has high confidence that it

represents real world driving quite accurately. This is a large leap forward compared with the NEDC which is certainly not representative of real world conditions.

Table 1-3: Comparison of operating conditions on NEDC and WLTC [16]

	Units	NEDC	WLTC
Start condition		cold	cold
Duration	s	1180	1800
Distance	km	11.03	23.27
Mean velocity	km/h	33.6	46.5
Max. velocity	km/h	120.0	131.3
Stop phases		14	9
Durations:			
• Stop	s	280	226
• Constant driving	s	475	66
• Acceleration	s	247	789
• Deceleration	s	178	719
Shares:			
• Stop		23.7%	12.6%
• Constant driving		40.3%	3.7%
• Acceleration		20.9%	43.8%
• Deceleration		15.1%	39.9%
Mean positive acceleration	m/s^2	0.59	0.41
Max. positive acceleration	m/s^2	1.04	1.67
Mean positive 'vel * acc' (acceleration phases)	m^2/s^3	4.97	4.54
Mean positive 'vel * acc' (whole cycle)	m^2/s^3	1.04	1.99
Max. positive 'vel * acc'	m^2/s^3	9.22	21.01
Mean deceleration	m/s^2	-0.82	-0.45
Min. deceleration	m/s^2	-1.39	-1.50

1.5. The need for high precision, the importance of accuracy and the case for this research

There have been substantial reductions in passenger car fuel consumption over the last few decades for example European transport related CO_2 emissions have fallen by 26% between 1990 and 2004 [2]. This downward trend is likely to continue for years to come, although possibly at a different rate. It is likely that this will predominately be driven by legislation and fuel taxation, the foremost affecting the nature of the vehicles built by manufacturers, the latter affecting the customer demand for fuel efficient vehicles.

The majority of opportunities for large reductions in vehicle fuel consumption, greater than 10%, have already been implemented over the last few decades and therefore automotive engineers are required to search for more advanced areas for fuel economy improvements and such improvements are correspondingly likely to be as a result of combined small effects. Examples of such effects are changes in engine lubricating oil properties and changes in auxiliary drive arrangements resulting in improvements as

small as 0.2% [5-7, 17]. Repeatability limits of ±0.5% at a 95% confidence level will be required as the norm, with tighter limits if possible to allow effective arbitration of such changes. It is therefore becoming increasingly important to achieve the highest precision in emissions test results from every test to allow effective arbitration of any technological change no matter how small. Furthermore with the upcoming changes to emissions legislation within EURO 6c RDE and the WLTP there will be a need to evaluate vehicle CO_2 emissions over a much wider operating envelope. Since the emissions will be measured from the vehicle during real world driving, traditional methods for evaluating engine only emissions on an engine dynamometers are likely to be superseded by the need to test a complete vehicle on a chassis dynamometer so that all system interactions are included just as they are when driving in the real world. Therefore to be able to have the very high precision that is relatively well understood and achievable on an engine dynamometer but on a chassis dynamometer is going to become increasingly important.

In addition to achieving high precision it is also important to maintain a high level of accuracy. With only high precision an experimenter would have good statistical confidence in their results but would not know the magnitude of the effect measured was correct. This is of key importance when technology changes being considered are tested under type approval conditions where the testing might be conducted by another experimenter who might be using more accurate equipment or procedures.

1.6. Research Project with a Commercial Type Approval and Emissions Testing Laboratory

The research presented in this thesis utilises data, processes and knowledge gained from a research project conducted between the University of Bath Powertrain and Vehicle Research Centre and a commercial emissions testing laboratory. For reasons of confidentiality and to avoid any bias the identity of this laboratory is confidential. The aim of the project was to identify how the precision of the fuel economy and hence CO_2 emissions results could be improved from the daily emissions testing carried out within such a laboratory. A specific target was set to achieve at least a 0.5% coefficient of variation in the CO_2 emissions. The laboratory in question is certified to complete TA emissions tests for homologation of new to market vehicles as well as performing many development and research emissions tests. The Laboratory has many staff members working between three shifts to achieve near constant 24 hours a day, 7 days a week operation. The entire laboratory is climatically controlled for both temperature and humidity, it has around a dozen chassis dynamometer test rooms, a large number of vehicle soak bays and completes thousands of emissions tests per month. In other words

it is typical of most commercial emissions test laboratories around the world in both the OEM and tier 1 domains.

1.7. Aim and objectives

The aim of this thesis is to identify the sources of imprecision affecting vehicle fuel consumption from chassis dynamometer tests, to understand the fundamental physical mechanisms that cause these factors to be important, to propose and finally if possible demonstrate methods for controlling these sources.

From the overall aim several objectives were identified and these are listed below:

1. Review the literature relating to sources of imprecision and inaccuracy for chassis dynamometer based vehicle tests. Use existing data to attempt to rank the sources and establish the factors that have the largest impact on variability of CO_2 emissions.

2. Examine statistical methods for determining confidence in small differences between results and explore the application of regression modelling to chassis dynamometer testing

3. Understand the current best practice for high precision chassis dynamometer testing by analysing data recorded from a series of chassis dynamometer emissions tests where the knowledge and recommended tolerances gained from the literature are implemented.

4. Understand the standard practice in a commercial setting by gathering historical data from a commercial laboratory. Perform a data mining exercise to identify any sources of imprecision that are exposed by this data.

5. Guided by the findings from the literature perform detailed studies into the most significant sources of imprecision, identifying the root causes of their effects, proposing methods to improve the precision and if possible demonstrating these methods by controlling the factors.

1.8. Scope of the Thesis

The work presented in this thesis is organised into ten chapters. An overview of these chapters is given in the following paragraphs.

Chapter 2 presents a survey of the literature, summarising and critiquing the available information regarding sources of imprecision in TA style chassis dynamometer testing.

The noise factors are also ranked based on the magnitude of the effects recorded by the authors.

Chapter 3 examines statistical methods for determining confidence in results and explores the theoretical application regression modelling for identifying and quantifying noise factors. Useful statistical tools are explained such as statistical process control, six sigma and the DMAIC toolbox.

Chapter 4 applies the tolerances and recommendations, found in the literature, to a chassis dynamometer experimental programme to determine the current standard of best case high test precision testing in a tightly controlled environment and to determine if there is scope for further improvements.

Chapter 5 analyses data obtained in a commercial environment where multiple test vehicles, drivers and dynamometers are used. A data mining exercise identifies the important factors of imprecision in the commercial environment.

Chapter 6 explores the sources of imprecision from the vehicle electrical system, quantifies what contribution they make to imprecision in CO_2 emissions then proposes methods to measure and control these sources.

Chapter 7 explores the effect of a simple change to the driver's aid system on driver behaviour. Various driver metrics are examined and compared to determine which are most useful for improving the precision of driver behaviour.

Chapter 8 explores three important procedural factors to determine if these are likely to be significant in a commercial test environment. The tyre pressure, engine oil level and ambient temperature are studied.

Chapter 9 explores the sources of imprecision from the chassis dynamometer machine and its operation. The industry standard coastdown validation technique is analysed and a fully automated statistical process control tool is developed for utilisation in a commercial environment.

Chapter 10 summaries the findings from this research and closes the thesis. The overall aims and objectives are revisited to draw the final conclusions from this work.

.

Chapter 2. Imprecision in Vehicle Fuel Economy Testing

2.1. The emissions chassis dynamometer

A TA emissions chassis dynamometer test cell has thousands of constituent parts and as will become apparent in this chapter a large number of these can become sources of imprecision in the vehicle out CO_2 emissions results. The aim of this chapter is to review the literature, identifying which of these components are sources of variability in vehicle CO_2 emission results and to determine the magnitude of the effects such that the factors can be ranked. To aid this task the chassis dynamometer test cell has been split into five key subsystems; the vehicle electrical system, the chassis dynamometer, driver behaviour, procedural factors and the emissions measurement system. These classifications are relatively arbitrary and simply provide a convenient way break up the discussion of the literature. Each of these subsystems is identified pictorially in Figure 2-1.

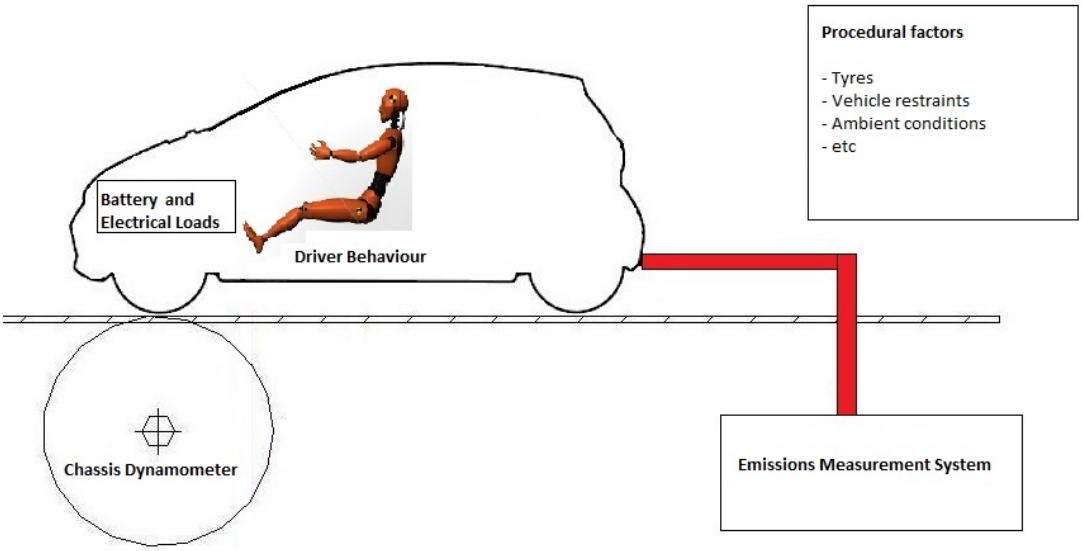

Figure 2-1: Basic chassis dynamometer schematic showing key areas affecting engine load and measurement of CO_2 emissions

A survey of the literature has been conducted to populate each of these five areas with sources of variability that have been identified and shown to cause imprecision in the vehicle fuel consumption and emissions results. This will also serve to highlight where there are gaps in the current literature.

2.2. Vehicle Electrical System

2.2.1. *The Electrical System*

The principle components in most passenger vehicle electrical systems are the starting, lighting and ignition (SLI) battery, the alternator and the vehicle ancillary electrical loads [18, 19]. The function of the alternator is to convert rotational mechanical energy from the internal combustion engine into electrical energy that can be used to recharge the battery and or meet the demands of the vehicle ancillary loads [19]. A simple block diagram of this system is shown below.

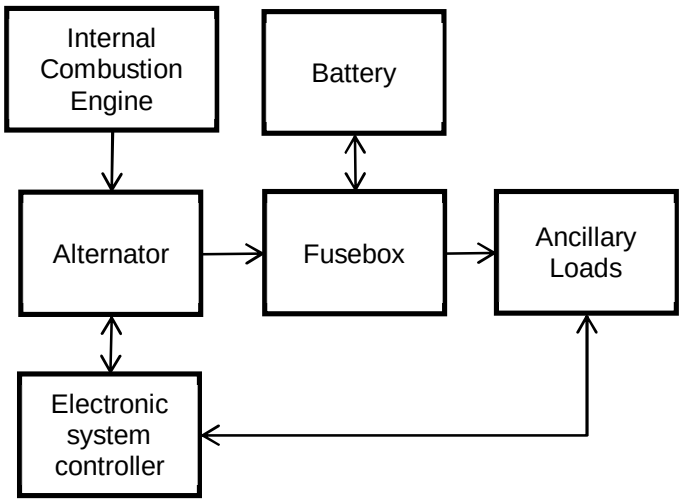

Figure 2-2: Simplified vehicle electrical system block diagram. Arrows indicate path and direction of energy transfer or indicate the path and direction of control signals.

Several authors have shown that the electrical load placed on the alternator during an emissions test affects the vehicle fuel consumption and hence CO_2 emissions [8, 14, 15, 20]. This electrical load can either be from a requirement to recharge the vehicle battery or a requirement to meet the demands of in-vehicle electrical ancillaries or a requirement to meet some combination of both demands [15]. There are no direct controls for either of these factors during TA emissions tests.

2.2.2. *Electrical Ancillaries*

Vehicle electrical systems are becoming ever more complex and now play an important role in vehicle design, functionality and desirability. In the past, the vehicle electrical system existed purely for basic functions such as engine starting, ignition and vehicle lighting [21]. Now the widespread adoption of electrically powered ancillaries such as power steering, cooling pumps and HVAC systems means the standard vehicle electrical system has to meet a much higher load. Even relatively simple modern vehicle electrical

loads are now in excess of 1.5kW [22], with future vehicle architectures requiring nearer or above 3kW [23]. Market trends indicate that vehicle electrical architectures will become even more complex in the coming years as manufacturers add functionality such as radar guided cruise control, automatic accident avoidance, internet connectivity and inter-vehicle communication. All of which are likely to drive even higher alternator loads in future vehicles. For TA legislative emissions testing the regulations state that all ancillary electrical loads are turned off for the duration of the testing [9, 14]. This would suggest that ancillary electrical loads could be ruled out as a source of imprecision. However for development or research testing or testing on prototype vehicles it is entirely conceivable that ancillary loads can be mistakenly switched on causing unexpected changes in the vehicle CO_2 emissions. The effects of switching on ancillary loads can be very large and this is a key factor in the differences between real-world and legislative TA fuel consumption [14, 24]. Studies attempting to quantify the differences between TA and real-world CO_2 emissions have recorded changes to the CO_2 emissions in the range of +5 to +50% depending on the number of accessories and magnitude of the electrical load [14].

2.2.3. *Battery State of Charge*

The effects of battery SoC on fuel consumption or CO_2 emissions are well documented in the literature [8, 14, 15, 20]. Several authors in the literature have examined the effect of starting an emissions test with a range of battery SoC. They have all recorded effects on vehicle FC or CO_2 emissions. For TA emissions, testing the battery SoC change during the test is not directly legislated. Some authors suggest that the regulations target a 100% battery SoC for legislative tests [15]. However the regulations for TA only specifies that the vehicle is run through a conditioning cycle prior to be soaked for between 6 and 30 hours without any battery charging [9]. It is therefore possible to enter the actual legislative test with a range of battery SoC depending on the vehicle behaviour during the conditioning cycle. In the literature Brace et. al. [8] discharged the battery of a diesel engine passenger vehicle by operating the headlamps continuously for 90 minutes prior to completing a NEDC emissions test. They recorded an 8.7% increase in FC, a change that was statistically significant at a 99% confidence level [8], see Figure 2-3. A limitation of their study is that the testing was conducted at -7°C and lead acid battery charge acceptance is reduced at low temperatures. This would suggest that the FC effect would be reduced if the testing were repeated at TA temperatures, namely between 20 and 30°C.

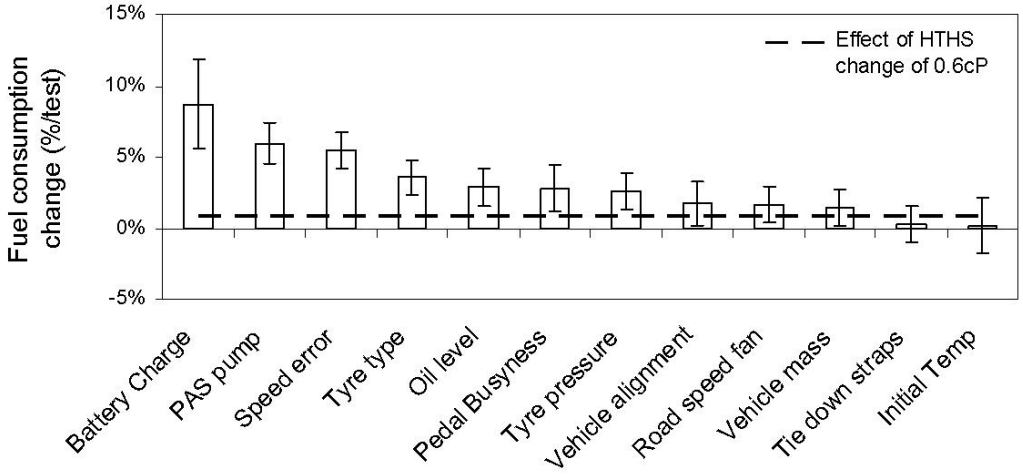

Figure 2-3: Absolute effect on fuel consumption measured ordered and compared with the typical effect of change of oil's High Temperature High Shear value (HTHS) from 2.9cP to 3.5cP [8]

A similar study by Schmidt on behalf of the TuV Nord [20] involved discharging the batteries of several test vehicles to a low level prior to completing TA style emissions tests. The actual level of discharge is not stated. However they recorded increased CO_2 emissions from all the test vehicles of between approximately 8 and 30% depending on the vehicle [20]. Conversation with the Schmidt revealed that the claimed level of discharge was very high, the vehicle batteries having been discharged to a point where they were just able to start the vehicle. It is surprising that there is such a wide range of results recorded across the vehicles and this shall be discussed later in this section. Kadijk et. al. [14] reporting the results of a selection of other authors states that the battery SoC is one of the key sources of test variability, with effects on CO_2 emissions generally up to 30%. Kadijk et. al. go on to state that one can expect a 1% reduction in CO_2 emissions for starting a TA emissions test with a battery that has been fully charged immediately prior to the test versus starting with a battery that has not been fully charged but has been charged in the recent past. A report from a confidential commercial source in which a vehicle with a turbocharged gasoline direct injection engine was tested recorded a linear correlation between during test battery SoC change and CO_2 emissions, the coefficient of determination being 0.67. The same study also tested a vehicle equipped with a turbocharged diesel engine and found a much stronger linear correlation, coefficient of determination 0.87, between battery SoC change and CO_2 emissions.

It is interesting that all the authors have recorded quite different magnitudes for the effect of pre-test battery SoC on CO_2 emissions. Some of these differences are of little surprise and can be attributed to experimenters investigating differing sized perturbations in battery SoC, whilst in other cases the differences are less obviously explained. For example the

study conducted by Schmidt [20] recorded quite different effects on CO_2 emissions within their own experiment, see Figure 2-4.

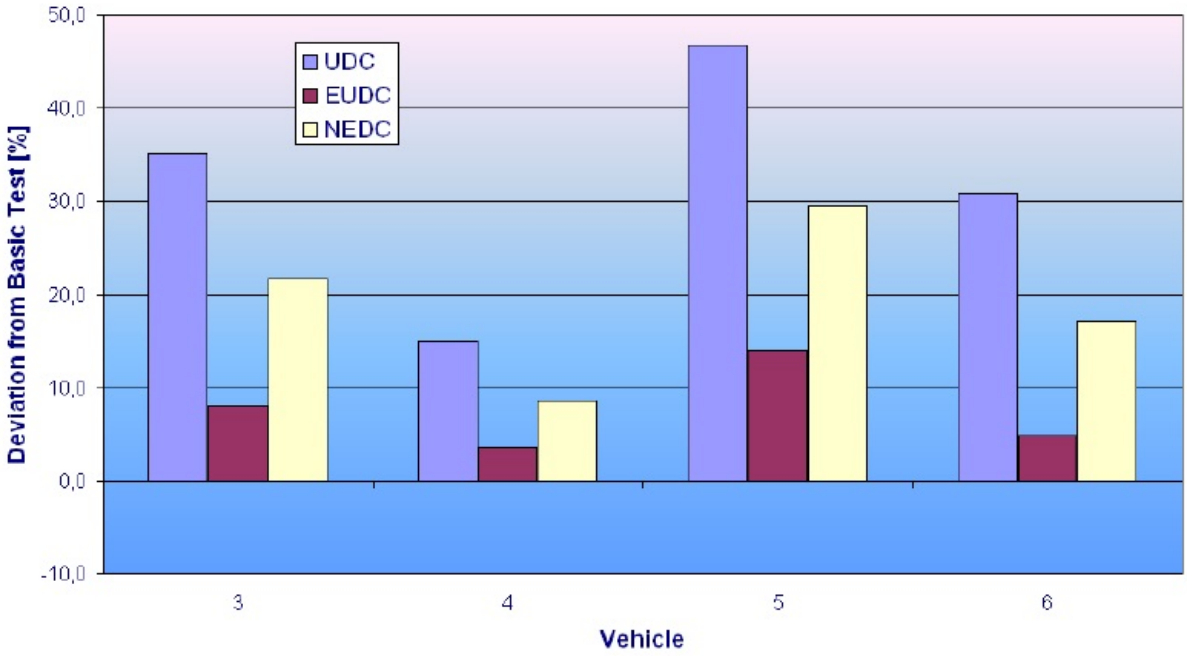

Figure 2-4: Results from the study of pre-test battery drain on CO_2 emissions, showing the wide range of results recorded from the same experiment performed on different vehicles [20]

Schmidt does not state what efforts were made to minimise test to test variability and prevent interactions with other factors, which is one explanation for the different results recorded from the vehicles. As the number of tests is unknown it is not possible to determine the statistical confidence in their results, nor if the differences between the vehicles are statistically significant. Furthermore very little detail is given about the procedure; the identities of the test vehicles are unknown, other than vehicles 1 through 3 are equipped with positive ignition engines and 4 through 6 are equipped with compression ignition engines [20]. By reference to the basic electrical system block diagram, see Figure 2-2, it is possible to identify the system components that are affecting the CO_2 emissions in these studies. For the testing carried out by Schmidt (#70} the battery was discharged prior to the test, so during the emissions test the electrical system controller must regulate the alternator output to recharge the battery. There are several ways to achieve this. Traditionally the alternator would be operated and loaded continuously to meet the electrical system demands regardless of the engine operating condition. However, nowadays an increasing number of manufacturers are adopting smart alternator technology. Smart alternators are an enhancement that has been enabled by the adoption of electrical control over the alternator output and also the development of in-vehicle current clamps to monitor battery SoC. A smart alternator is only switched on during periods of zero or low engine load such as during in-gear deceleration events were

the engine is being motored by the vehicle inertia. During acceleration modes the alternator is switched off completely and for cruise modes the alternator load is limited depending on the vehicle ancillary loads [25]. By using the vehicle inertia to indirectly drive the alternator through the engine no fuel is burnt and there is a corresponding saving in fuel consumption over test cycles. Kadijk et. al. [14] quote the work of a TuV Nord report which measured a decrease in CO_2 emissions of 2.4% from the adoption of selective charging during an emissions test. Whilst Montalto et. al. [25] report a saving of between 2 and 3% over the NEDC from the adoption of 'smart' alternator technology. A theoretical further utilisation of smart alternator technology is optimise the SoC balance over the course of an emissions test. For example Montalto et. al. [25] describe the scenario of starting an emissions test with a near to fully charged battery, as would be expected for TA conditions, and as a result ending with a lower SoC, perhaps around 85% as is required for satisfactory smart alternator operation [25]. It is possible some vehicles in Schmidt's study had these features and some didn't, so this could be part of the reason for the recorded difference between the test vehicles.

Other possible explanations for the differences in the CO_2 emissions recorded from different test vehicles can be attributed to the other components shown in the system block diagram, see Figure 2-2. The efficiency of the internal combustion engine will dictate how much fuel is burnt by the engine to generate the required shaft power to drive the alternator. Engine efficiency is dependent on many factors related to base engine design, engine management and combustion efficiency. The alternator efficiency will dictate the electrical current delivered to the battery for a given shaft power input from the ICE. Finally the charge acceptance and the capacity of the battery will dictate to what extent the battery SoC increases for a given charging current from the alternator. All these factors can be different when comparing test vehicles. For example the battery capacity is generally much smaller for low capacity positive ignition engines compared with large capacity compression ignition engines.

Despite these potential sources of variability that make inter vehicles comparisons difficult, Brace et. al. [8] developed a battery discharge sensitivity by conducting testing at an intermediate level of discharge, this time only 45 minutes with the headlamps, compared with 90 minutes as was reported previously. From these results a linear fit was developed between the fuel consumption and the electrical energy transferred to the battery, as measured by current clamps fitted to the vehicle, see Figure 2-5.

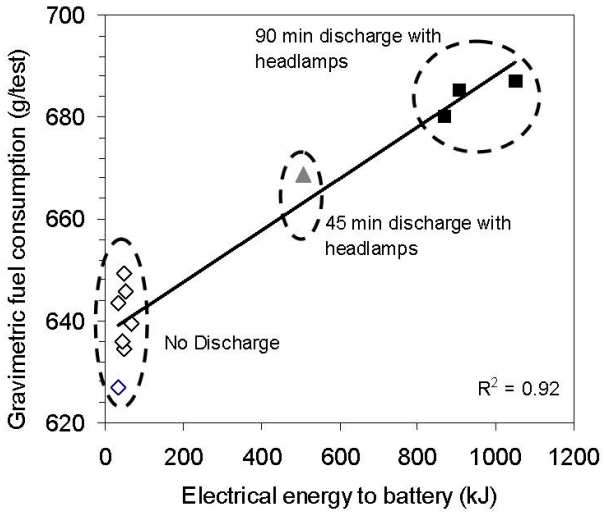

Figure 2-5: Effect of energy supplied to the battery on gravimetric fuel consumption over the NEDC [8]

For Brace et. al.'s [8] study the battery was discharged immediately prior to the NEDC test using the vehicle headlamps for a period of between 45 and 90 minutes. In the UK the standard headlamp bulb is rated at 55W, the side light bulb 5W and the tail light bulb at 5W. Assuming the vehicle was discharged using two headlamps, side lights and tail lights the total battery load would have been 130W. When this is summed over the 90 minute period the total battery discharge would have been approximately 16Ah. Knowing that the test vehicle was a C-car passenger vehicle equipped with a common rail diesel engine and assuming the vehicle was equipped with the manufacturer's standard fit battery the nominal battery capacity would have been approximately 70Ah. Therefore the battery discharge was 23%; approximately one quarter of the battery capacity. The strength of the linear correlation gives confidence that the results obtained by Brace et.al. are robust and not unduly affected by other factors. Taking the 8.7% fuel consumption effect and the 16Ah battery drain, gives a sensitivity of approximately 0.5% change in fuel consumption per 1Ah battery discharge. Of course this sensitivity must be treated as specific to that test vehicle given the variety of other factors that have already been highlighted and contribute to the relationship.

Brace et. al. [8] also carried out a statistical tolerancing exercise on their results and found that a tolerance on battery discharge of ±0.2V is required to obtain a FC repeatability target of 0.5%. This finding was based on measured open circuit battery voltage immediately prior to the start of the emissions test.

2.2.4. *Electrical System Summary*

The demand placed on the vehicle alternator is primarily controlled by two factors; the need to power vehicle auxiliary devices and the need to recharge the vehicle SLI battery. Electrical loads from vehicle auxiliaries and from a requirement to charge the vehicle's SLI

battery can both have large effects on the TA emissions test vehicle out CO_2 emissions. The importance of these factors has received considerable attention within the available literature.

The study of auxiliary loads has been reported in the context of the difference between real-world and TA CO_2 emissions in the work by Kadijk et. al. [14] who report that the effect of vehicle electrical auxiliaries on CO_2 emissions is in the range of +5 to +50%. No other studies exist in the literature for the effect of electrical auxiliaries on CO_2 emissions and therefore no detailed information exists on the causality of what is such a large reported range of effects. No studies have attempted to rank electrical auxiliaries or quantify their individual effects and so this would be useful area for further investigation.

Many authors have reported on the effect of SLI battery SoC on CO_2 emissions or FC by discharging the battery prior to an emissions test and recording the change on CO_2 emissions or FC. The reported effects range from 8.7% change in FC at 95% confidence reported by Brace et. al., to a 8-13% change in CO_2 emissions reported by Schmidt [20] and up to 30% reported by Kadijk et. al. [14]. There is quite a large discrepancy in the reported magnitude of the effects not only between authors but also within author's own studies. The reasons for this are likely to be a mixture of both a basic difference in the amount of discharge pre-test and also differences in the electrical/prime mover efficiency in converting fuel energy into electrical energy to recharge the battery.

It has been shown in the literature by more than one independent author that changes in vehicle out CO_2 emissions are linearly correlated with changes in the electrical load, be that from auxiliaries or from a requirement to recharge the battery.

Kadijk et. al. [14] reported that a 1% reduction in CO_2 emissions can be achieved by charging the SLI battery immediately prior to each emissions test. They are the only authors to report this finding and it is only covered briefly in their report. Verification of Kadijk et. al.'s result in the context on TA emissions testing on a chassis dynamometer would be a useful piece of work allied with detailed analysis of the effect of battery charging on both the SLI battery and on the CO_2 emissions. The discovery of a method for determining a well correlated relationship between consumed fuel energy by a vehicle and alternator energy would advance understanding in this important area.

The proposal of methods to identify, correct for and ultimately avoid electrical load variability error from battery SoC and vehicle auxiliaries is an essential finding for the improvement of precision in vehicle CO_2 emissions.

2.3. Driver Behaviour

2.3.1. *The Type Approval Driver*

During a TA emissions test a driver is shown a real time display of the vehicle speed against a target speed trace on a device known as a driver's aid [26].The driver's aid display normally consists of a computer monitor positioned either in front of the windscreen or by the driver's side front window. The driver's aid screen will likely show several small displays, often positioned around the edge of the screen, indicating the health of the various dynamometer test systems. However the centre point of the display is always a moving, real-time, graphical representation of the real time dynamometer speed against the target. An example of the type of graphical display being described is shown for the first 40 seconds of a TA style NEDC test in Figure 2-6.

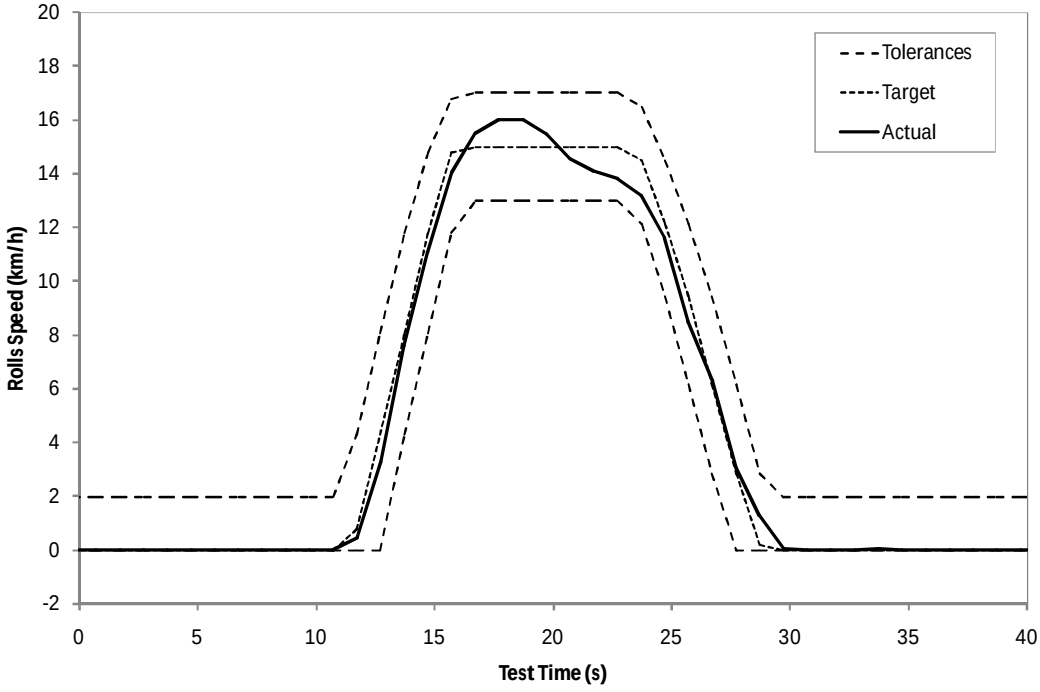

Figure 2-6: Example driver's aid speed display with tolerance lines shown

During the test the driver must control the vehicle speed to ensure it stays within the prescribed tolerance and ensure that they change gear when prompted to do so by the display on the driver's aid. The driver must therefore control the accelerator, brakes, change gear and start/stop the engine at the beginning/end of the test. For a vehicle with an automatic transmission the gearbox must, by current regulation, be operated in fully automatic mode [9]. For a TA emissions test the target speed trace is subject to a speed tolerance of ±2 kph and ±1 s [9].

2.3.2. *Speed Error*

The TA speed tolerance represents quite a wide window in which a variety of driving styles can be accommodated. The significance of variations in driver speed errors, within or reasonably close to these tolerances, on vehicle emissions, fuel consumption and hence CO_2 emissions are mentioned many times in the literature [8, 14, 15, 20, 27-30]. Kadijk et. al. [14] state that the *"influence of the driver using the (speed) tolerances in the drive cycle"* is one the key flexibilities in the current TA legislative emissions test procedure and state that driving variation within the tolerances can cause changes to CO_2 emissions of up to 4%. Kadijk et. al. also completed some theoretical modelling using a simulation tool developed by Ricardo. They simulated the effect of a change in driving style within the legal speed tolerances, which they described as *"(using) minimum speed and acceleration"*, for which a 1.2% reduction in CO_2 was found over the NEDC [14]. A report by Schmidt on behalf of the TuV Nord [20] examined the effect of *"taking advantage of the permissible tolerances of the driving curve"* across six different test vehicles and recorded quite different effects on the CO_2 emissions for the vehicles. Figure 2-7 is taken from his report and summarises his results.

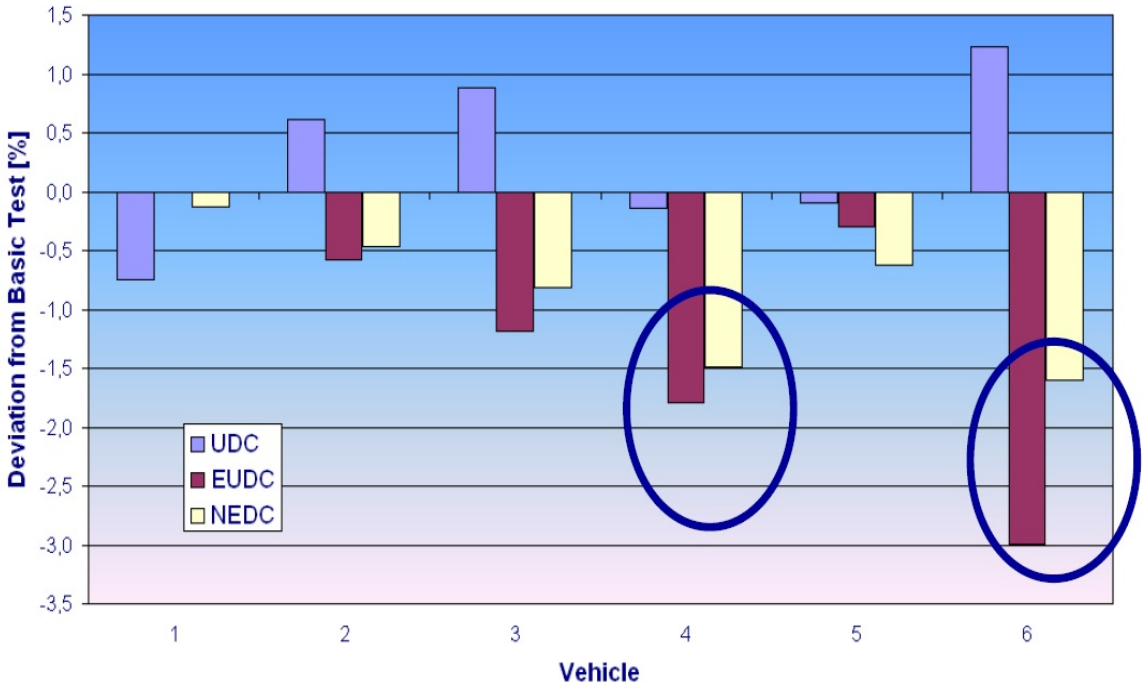

Figure 2-7: Test results showing the effect of optimised driving within the type I emissions test legal tolerances across 6 test vehicles. Vehicles 1-3 are SI and vehicles 4-6 are CI. The largest effects have been highlighted by the original author [20]

The largest effects were recorded for vehicles 3, 4 and 6, which are a mix of SI and CI. Interestingly for all but vehicle 1, the largest effect is seen in the faster second phase of the NEDC, known as the EUDC cycle. The same pattern is seen in the simulation results of Kadijk et. al. [14]. This strong dependence between the speed the vehicle is driven and the fuel consumption change can be understood by examination of the underlying

principles. To drive a vehicle of a certain mass at a certain speed requires an input of energy to the vehicle, which for a motor vehicle comes from burning fuel in the engine to release energy and convert it into mechanical rotational power at the wheels via the transmission. When a vehicle is travelling at a certain velocity it must have a certain kinetic energy expressed by Equation 2-1.

$$KE = \frac{1}{2}mv^2$$

Equation 2-1

Where KE is the kinetic energy, m is the mass and v is the speed. If the speed is doubled the kinetic energy is quadrupled and hence given perfect conditions for conversion of fuel into rotational power, four times as much fuel would be required. By reference to Figure 1-1 the EUDC is a much higher speed portion of the cycle and given that the vehicle kinetic energy increases with the square of the speed it is of little surprise that changes in speed with the same sized tolerance at a much higher nominal speed will have a much more significant effect on the CO_2 emissions.

Some authors have examined speed errors that fall outside of the legal tolerance. This is relevant because during research and development testing, with a vehicle running an immature calibration it might be quite difficult to keep within the tolerances and results from these tests will still be useful in the vehicle development process if they are repeatable. To this end Brace et. al. [8] found that a consistent speed error of +3kph during the cruise modes of the NEDC resulted in a 5.5% change in the vehicle fuel consumption, which was statistically significant at a 99% confidence level [8]. However this finding was derived from testing one vehicle so whilst it gives a useful indication of the effect, it cannot be used to provide a robust sensitivity that can be applied to other tests.

2.3.3. *Other Driver Behaviours*

Speed errors are not the only way that drivers can change their behaviour and cause effects to vehicle CO_2 emissions. Bielaczyc et. al. [27] list some driver behaviours that are also important to the CO_2 emissions namely; *"throttle (pedal) operation, (driving) experience and starting the engine"*. The authors also add clutch control, pullaway and speed of gear change to this list. Some of these factors, such as clutch control and pullaway are important factors but are very difficult to quantify universally and there are no metrics to directly define these factors in the literature. For the moment these are factors that have to be judged individually and commented on subjectively.

2.3.4. *Robot drivers*

One perceived way of improving driver precision is to use robot drivers since these are computer controlled and programmed to perform the same operation for every single emissions tests. In the early years, robot drivers were generally repeatable but did not drive vehicles at all like a human driver would. With advances over the years in the field of robotics, the driving styles of robots have become a lot more representative of human driving. However despite these advances, robot drivers are still not the default choice for emissions testing. There are several reasons for this. Firstly emissions regulations in many countries including Europe still require human drivers for certification testing [9]. Secondly despite the advances in robot technology, when compared with a human driver, some cheaper robot drivers still require significant in-vehicle installation and optimisation time to achieve satisfactory performance. Lastly during the vehicle development process human feedback on driveability is often an essential part of the refinement of vehicle calibrations. Surprisingly some authors go one step further and suggest that there is no reason to prefer a robot driver since the highest precision is not achieved with robot drivers and instead with skilled human operators [31, 32]. Although the author would argue that these conclusions are drawn due to using unsophisticated or non-optimised robot drivers as the authors experience from witnessing modern robot drivers is that they are highly precise.

2.3.5. *SAE J2951 Drive Quality Evaluation*

Industry experts have recently joined forces to develop a driver behaviour assessment standard known as the Drive Quality Evaluation for Chassis Dynamometer Testing which is published by the Society of Automotive Engineers under the standard number SAE J2951 [28].The drive quality standard recognises that there is significant scope for driver behaviour variability within the TA speed tolerance and therefore aims to provide better resolution on driver behaviour by providing: *"drive quality metrics intended to enable improved monitoring and characterization of driver-related variability"* [28]. The standard explains how to use and calculate a series of metrics that are all based on taking a simple 10Hz measurement of chassis dynamometer roller speed. The metrics and their uses shall be outlined in the following paragraphs.

The SAE J2951 standard consists of a number of metrics which are classified as either primary or supplementary. The Energy Rating (ER) is a primary metric from the SAE J2951 drive quality standard. It provides a measure of the percentage difference between the target cycle drive energy and the driven cycle drive energy. To determine the ER it is necessary to calculate the driven and target cycle energies, CE_D and CE_T respectively, from the positive road load forces. The calculation method is explained in full detail in the

SAE J2951 standard [28]. For brevity only the equation for the CE_D shall be quoted here, see Equation 2-2.

$$\boldsymbol{CE_D = \sum_{i=1}^{N}\left[\left(1.015 \cdot ETW \cdot a_{Di} + F_0 + F_1 V_{Di} + F_2 V_{Di}^2\right) \cdot d_{Di}\right]^+}$$

Equation 2-2 [28]

Where CE_D is the actual driven cycle energy, ETW is the equivalent vehicle test weight and a_{Di} is the driven acceleration at each timestamp i. F_o, F_1 and F_2 are the road load coefficients, with units of N, N/(ms^{-1}) and N/(ms^{-2}) respectively. V_{Di} is the driven vehicle speed at each timestamp i and d_{Di} is the total driven distance at each timestamp i. By examination of Equation 2-2 the cycle energy is therefore calculated by multiplying the vehicle mass by its acceleration to determine the acceleration force. Adding the acceleration force to the road load force at the given speed and then multiplying the overall result by the distance to give the work done and hence energy. More detail on the road load coefficients is given in section 2.4.1. The ER is then given by the percentage difference between the CE_T and the CE_D, as per Equation 2-3.

$$\boldsymbol{ER = \frac{CE_D - CE_T}{CE_T} \cdot 100}$$

Equation 2-3 [28]

Where ER is Energy Rating, CE_D is the actual driven cycle energy and CE_T is the target cycle energy. The Distance Rating (DR) is a primary metric from the SAE J2951 drive quality standard [28]. It measures the percentage difference between the total driven distance and the target distance. It is calculated as shown by Equation 2-4.

$$\boldsymbol{DR = \frac{D_D - D_T}{D_T} \cdot 100}$$

Equation 2-4 [28]

Where DR is the Distance Rating, D_D is the driven distance and D_T is the target distance.

The Energy Economy Rating (EER) is another primary metric from the SAE J2951 drive quality standard [28]. It combines the ER and DR ratings to provide a rating that correlates with CO_2 emissions and fuel consumption in a mass per unit distance format, this is particularly useful as it should correlate with emissions results which are conventionally reported in the same mass per unit distance format, for example g/km. Its calculation is shown Equation 2-5.

$$EER = \left[1 - \frac{DR/100+1}{ER/100+1}\right] \cdot 100$$

Equation 2-5 [28]

Where EER is the Energy Economy Rating, DR is the Distance Rating and ER is the Energy Rating.

The Root Mean Squared Speed Error is a supplementary metric from the SAE J2951 drive quality standard [28]. It is calculated by squaring the result of the subtraction of the driven speed from the target speed at each timestamp. These results are then summed over the duration of the test and then the root mean square is determined to provide a one number per test metric. The calculation is shown by Equation 2-6.

$$RMSSE = \sqrt{\frac{\sum_{i=1}^{N}(V_{Di}-V_{Ti})^2}{N}}$$

Equation 2-6 [33]

Where RMSSE is the Root Mean Squared Speed Error, V_{Di} is the actual driven speed at timestamp i, V_{Ti} is the target speed at timestamp i and N is the number of timestamps. The Absolute Speed Change Rating is a supplementary metric from the SAE J2951 drive quality standard [28]. It is calculated by first summing the absolute acceleration at each timestamp from the test for both the target and the driven speed traces. These calculations yield the absolute speed change for the target and driven speed traces, ASC_T and ASC_D respectively. The calculations for these are given by Equation 2-7 and Equation 2-8.

$$ASC_T = \Delta t \sum_{i=1}^{N} |a_{Ti}|$$

Equation 2-7 [28]

$$ASC_D = \Delta t \sum_{i=1}^{N} |a_{Di}|$$

Equation 2-8 [28]

Where ASC_T is the target driven Absolute Speed Change, ASC_D is the actual driven Absolute Speed Change, a_{Ti} is the target acceleration at timestamp i and a_{Di} is the driven acceleration at timestamp i. The Absolute Speed Change Rating (ASCR) is then the percentage difference of the ASC_T and ASC_D, as shown by Equation 2-9.

$$ASCR = \frac{ASC_D - ASC_T}{ASC_T} \cdot 100$$

Equation 2-9 [28]

Where ACSCR is the Absolute Speed Change Rating.

2.3.6. *Accelerator Pedal Busyness*

Prior to the publication of the SAE J2951 standard, Brace et. al.[8] found that a useful metric for quantifying driver behaviour is a measure of how oscillatory the driver's accelerator pedal movements are when integrated for the length of the test cycle. They named this metric the 'pedal busyness' and defined it as the sum of the absolute rate of change of the pedal position at each timestamp. By using a robot driver and re-calibrating its PID controller such that the pedal busyness was doubled over the NEDC they recorded a 2.8% change in the fuel consumption, a change which was statistically significant at a 99% confidence level. Bielaczyc et. al. [27] also mention driver accelerator pedal movements as being important from their work but do not suggest how this should be measured or what the exact effect is on CO_2 emissions.

2.3.7. *Gear Shifting*

It has also been found that the timing of the gear shift points in the cycle can cause significant changes in the fuel consumption and emissions [14, 30, 31]. The gear shift points for a vehicle without a gear shift indicator (GSI) are fixed, with respect to vehicle speed, by the emissions testing regulatory body [9]. However many new vehicles have dashboard mounted gear shift indicators which tell the driver when to change up and down gear. In this case, for legislative TA emissions tests, the driver must change gear when the vehicle indicates [9]. This allows manufacturers to tune their vehicle shift indicators to provide the best possible gear change strategy for the NEDC. When tuning a GSI calibrators will have to make assumptions about what loads the driver places on the engine during a TA test. Clearly it is possible to calculate the engine load using the target NEDC speed trace. However the previous discussion has demonstrated how there is a wide range of driving styles that can be adopted within the TA speed tolerance. Naturally this results in a certain amount of interaction between the vehicle, the GSI and the driver. For example a driver might need to minimise their speed and acceleration within the TA tolerance to maximise the benefit of the GSI. If they don't the GSI's effect will be limited. Authors have found that the resulting variability in the timing of the gear shifts causes significant variability in the fuel consumption and emissions results [14, 30, 31]. Vagg et. al. [30] simulated a novel calibration of GSI using experimental data obtained on a chassis

dynamometer and found a 4.3% decrease in FC and a 4.5% decrease in CO_2 emissions during cold start NEDC tests.

2.3.8. *Summary*

Variations in driver behaviour are an important factor influencing the precision of CO_2 emissions from TA style emissions tests. The speed error has been identified to cause changes to CO_2 emissions or FC in the region of 0.1 to 5.5% over the NEDC, whilst the modification of the gear shifting patterns has caused measured effects of 4.5% to the CO_2 emissions. Interestingly the authors in the literature acknowledge that there are many driver behaviours that are not easily quantified numerically but can have a significant effect on CO_2 emissions; the SAE J2951 drive quality standard has gone some way to filling this gap but no literature exists showing the usefulness of the standard's metrics or which ones are most suited to different test applications. This is an area were useful additional insight could be given to build on the information already available in the literature.

2.4. The Dynamometer

2.4.1. *The Emissions Chassis Dynamometer*

The purpose of the chassis dynamometer is to load the test vehicle powertrain via the vehicle tyres and simulate vehicle resistance as a function of speed that the vehicle experiences when driving on a conventional road albeit while the vehicle structure is held stationary [10, 26, 34, 35]. A good way of visualising this is to consider the following quote from D'Angelo et. al.; "*While the vehicle is driven on the rolls, the loading that the dynamometer applies must result in the vehicle achieving the same speeds, accelerations and decelerations that it would have on the road if driven with the same throttle movement profile*" [34].

In its most basic form a chassis dynamometer consists of one or more rollers that are positioned in contact with the vehicle driven wheels. These rollers are coupled to a device, such as a flywheel set or an eddy current dynamometer, which is capable of absorbing the power generated at the vehicle wheels when the vehicle is driven. This basic layout is commensurate with typical garage chassis dynamometers that are often used for assessment of engine performance, where it may only be necessary to measure basic dynamometer characteristics such as speed, load and acceleration. Modern advanced laboratory chassis dynamometers typically combine a single 48" diameter roller dynamometer with fast response AC motors and a high speed computer control system allowing full simulation of road driving including real time simulation of the vehicle

aerodynamic drag and inertia [36]. Figure 2-8 shows the University of Bath's chassis dynamometer, which is typical of a modern laboratory chassis dynamometer.

Figure 2-8: The University of Bath 48" single roller chassis dynamometer with DC electrical inertia simulation. This is a 2WD dynamometer and is housed in a climatic chamber. The vehicle is shown in the raised position above dynamometer on centralising mechanism.

The load applied to the vehicle wheels by the dynamometer is highly correlated with vehicle fuel consumption, CO_2 emissions and diesel NOx [8, 9, 37, 38]. The chassis dynamometer road load also accounts for an extremely high percentage of the load applied to the engine. Kadijk et. al. [10] quantified this importance via simulation and found that for a broadly representative modern passenger vehicle the engine load is comprised of road load forces, inertial forces and engine losses which comprise 63%, 25% and 12% of the total engine power output respectively.

The principle components of a chassis dynamometer and their interconnections can be demonstrated by considering a block diagram of the system as shown in Figure 2-9.

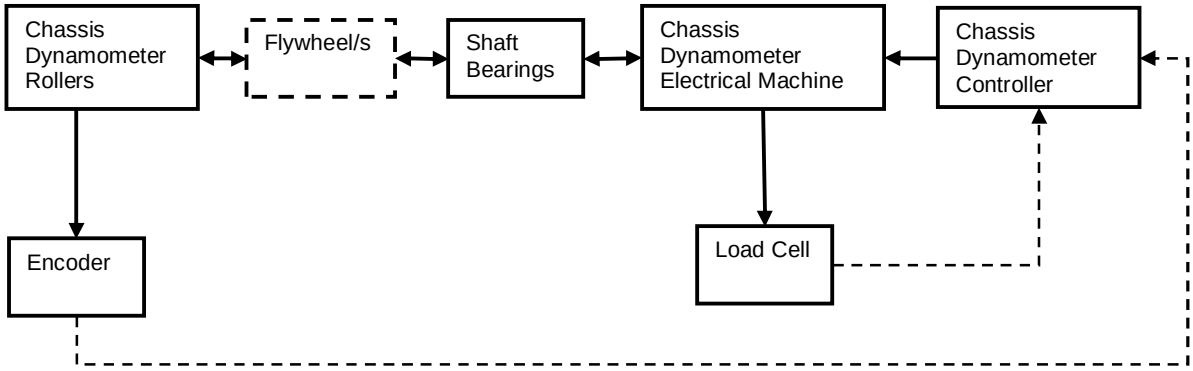

Figure 2-9: Chassis dynamometer functional block diagram. Thick solid lines represent mechanical connections where rotational power is transferred between blocks. Dotted lines represent signal connections. An optional item is shown in the dotted outlined box.

During testing the vehicle is mounted onto the dynamometer such that its driven wheels are in contact with the rollers and in the case of a 2WD vehicle the non-driven wheels are firmly affixed to the floor. A 4WD vehicle must be tested on a 4WD dynamometer which in essence is two standard 2WD dynamometers mounted on the same bed frame with a wheelbase adjustment mechanism. The rollers are the interface between the vehicle and the dynamometer and there are several designs in the field. The most common nowadays is the 48” single roller. In this case the vehicle’s driven wheels are each in contact with only one roller that is 48” in diameter. The large diameter is beneficial because the curvature of the surface in contact with the vehicle tyres is minimised, making it more like a real world flat road surface. An older but still widely used design of roller is the twin 20” roller configuration. In this instance the vehicle’s driven wheels rest down between two 20” rollers. This design means each driven tyre is subject to two contact points with the dynamometer rollers; it was originally perceived this would help in simulation accuracy since the two extra contact patches would account for those missing on account of the stationary non-driven wheels [39], however the tyre deformation is not equivalent to that on the road due to the small diameter of the rollers. Even on large diameter rollers there are greater frictional losses on a curved surface than on a flat road [34].

During real world on road driving the vehicle powertrain must produce enough tractive force at its driven wheels to overcome the losses placed on the vehicle, namely; aerodynamic drag, tyre rolling resistance, gravitational pull and drivetrain losses. It must also provide force to overcome the vehicle inertia and provide the acceleration demanded by the driver. During testing on a chassis dynamometer the rollers are loaded by what is collectively known as the inertia simulation system to replicate these real world loads. To

understand how this is achieved it is necessary to consider a free body diagram and the equations of motion for a vehicle driving along a road, as shown in Figure 2-10.

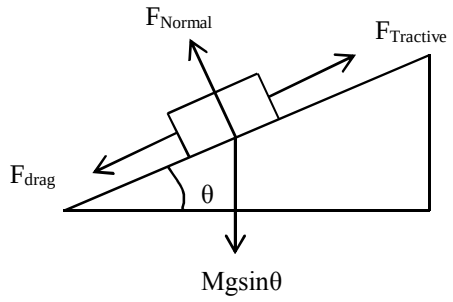

Figure 2-10: Free body diagram for a vehicle driving up a gradient

The components of force which act on the vehicle and cause it to move are made up to two elements; those known as the road load forces and those known as the inertial forces. The road load forces are made up of the resistive forces; aerodynamic drag, rolling resistance, losses and the force resulting from the slope of the road. The relative magnitude of these forces depends on whether the vehicle is stationary and the angle of the slope. When stationary the aerodynamic drag is zero and when on the flat there is no force resulting from the slope, leaving only the rolling resistance force component. These forces that comprise the overall road load force are expressed in Equation 2-10.

$$\boldsymbol{F_{road\ load} = C_{rr}N + \frac{1}{2}\rho V^2 C_d A + Mgsin\theta}$$

Equation 2-10 [37, 40]

Where F_{drag} is the tractive force, C_{rr} is the coefficient of rolling resistance, N is the normal tyre force, ρ is the density of air, C_d is the coefficient of aerodynamic drag, A is the vehicle frontal surface area, M is the mass of the vehicle, a is the vehicle acceleration, g is the acceleration due to gravity, and θ is the angle of the slope being driven. Since TA testing is always to simulate flat roads [9] the gradient component can be ignored and since direct determination of the individual coefficients is not necessarily straight forward they can be combined into a polynomial and the equation simplified as demonstrated by Equation 2-11.

$$\boldsymbol{F_{road\ load} = F0 + F1V + F2V^2}$$

Equation 2-11 [10, 34, 35, 40, 41]

Where F0, F1 and F2 are the road load coefficients. A second order polynomial is usually sufficient to represent the drag since the highest order term in Equation 2-10 is second

order, bearing friction is approximately linear with speed [42] and the F0 term is dominated by the tyre force [37].

When the vehicle is moving the inertia of the vehicle comes into play and is derived from Newton's second law as shown in Equation 2-12**.**

$$\mathbf{F_{inertial}} = \mathbf{Ma} = \mathbf{M}\frac{\mathbf{dV}}{\mathbf{dt}}$$

Equation 2-12 [34, 35, 41]

Where M is the mass of the vehicle, a is the vehicle acceleration and V is the vehicle speed. The total force acting on the vehicle is the sum of these two components as shown in Equation 2-13

$$\boldsymbol{F} = \mathbf{F_{road\ load}} + \mathbf{F_{inertial}} = \mathbf{F0} + \mathbf{F1V} + \boldsymbol{F2V^2} + \mathbf{I}\frac{\mathbf{dV}}{\mathbf{dt}}$$

Equation 2-13 [34, 35]

Where I is the equivalent vehicle inertia. To simulate these force components the dynamometer must employ a simulation system, typically comprising of an electric motor coupled to a fixed inertia system.

For the inertia component the dynamometer has a fixed inertia resistance, known as the dynamometer base inertia coupled to an inertia simulation system. The base inertia is comprised of the inertia of the dynamometer rollers, shafts, couplings and the rotating components of the electrical machine. The inertia simulation system then either up or down scales the base inertia to suit the test vehicle by adding or adsorbing the force from these components in the form of an electrical motor torque. The other drag components such as aerodynamic drag and any difference between tyre rolling resistance in the real world and on the rollers must be simulated by the dynamometer inertia and or road load simulation system. There are two main designs of the inertia simulation system. The oldest type of system is the mechanical inertia simulation system. These systems use a series of flywheels that are selectively coupled to the rollers via a series of clutches. The flywheels take up a large amount of room and therefore tend to be mounted on a separate shaft necessitating the use of many support bearings and often a toothed belt to connect the auxiliary shaft. The control system allows the operator to choose the desired flywheel that is closest to the effective mass of the test vehicle. A big disadvantage of this system is that it is limited, for accurate testing, to testing vehicles that have an effective mass that matches the available flywheels. Since it's only physically possible to fit a certain number of flywheels within the typical chassis dynamometer pit the TA authorities at the time were

forced to introduce the set of fixed stepwise inertia classes that are in fact still used today [15]. Fixed mechanical inertia dynamometers tend to go hand in hand with twin roller setups on the basis that the second tyre contact patch provides the extra rolling resistance that is normally given by the non-driven wheels [34]. An enhancement of the mechanical flywheel inertia simulation system is to couple in a relatively small electrical machine, either AC or DC. The electrical machine can be used to reduce the number of flywheels required by providing partial electrical inertia simulation to the base machine inertias. An example of the enhanced mechanical flywheel inertia simulation dynamometer is shown in Figure 2-11.

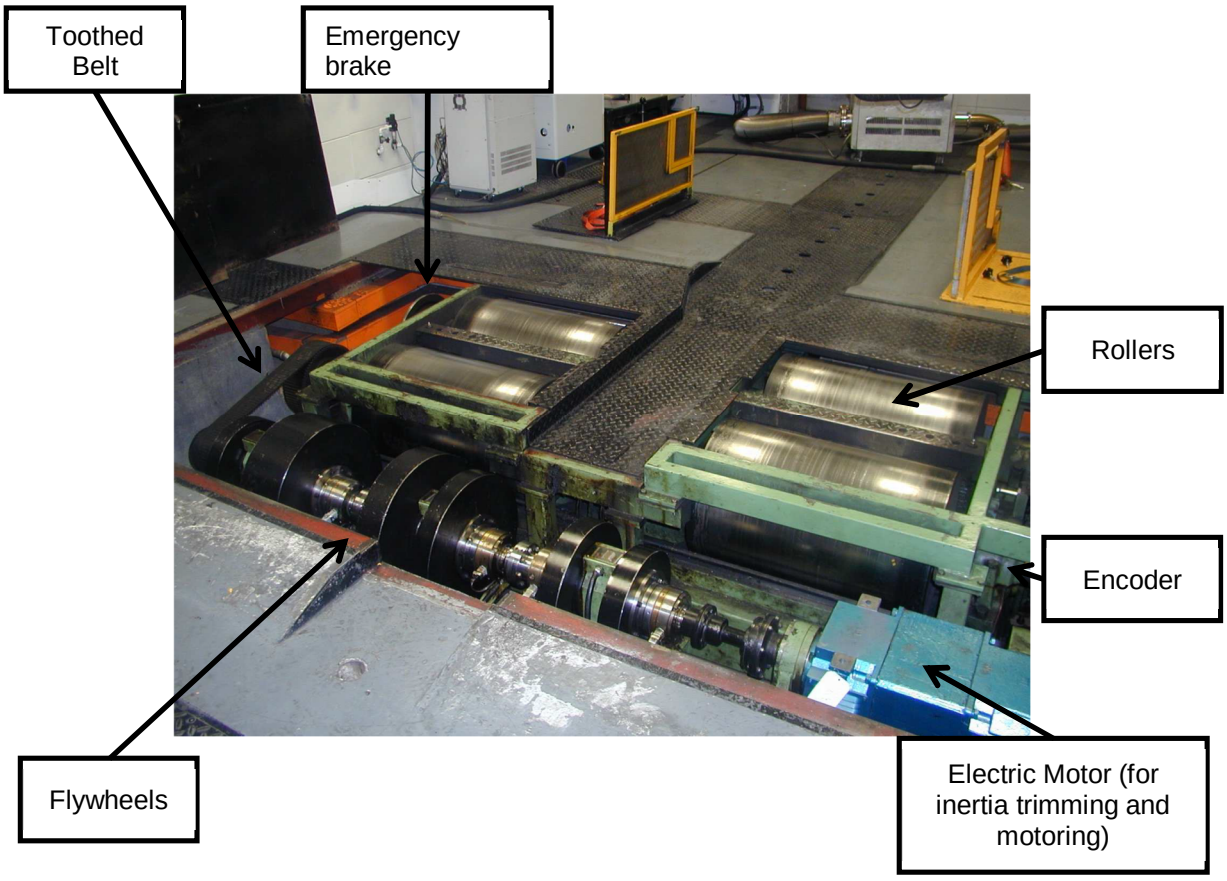

Figure 2-11: Twin 20" roller chassis dynamometer with multiple clutch selectable flywheels and electrical inertia trimming

The second type of inertia simulation system and the most common place today is the fully electric system. Fully electric inertia simulation systems will usually consist of one AC motor with a power rating between 150 and 300kW [43] mounted in the middle of two 48" diameter rollers. This configuration is known as 'motor in the middle' and has substantial advantages since there is no requirement for external shafts or bearings. An alternative layout of the same system is two use two smaller AC motors, one driving the left hand roller and one the right hand. For TA testing the regulations stipulate that such designs must install a rigid mechanical coupling between the two rollers [9]. A final alternative

within the fully electric inertia simulation systems is to use DC motors in place of AC, these tended to be used in the early days of electrical inertia simulation and have effectively been superseded by the AC motor due to its improved response time.

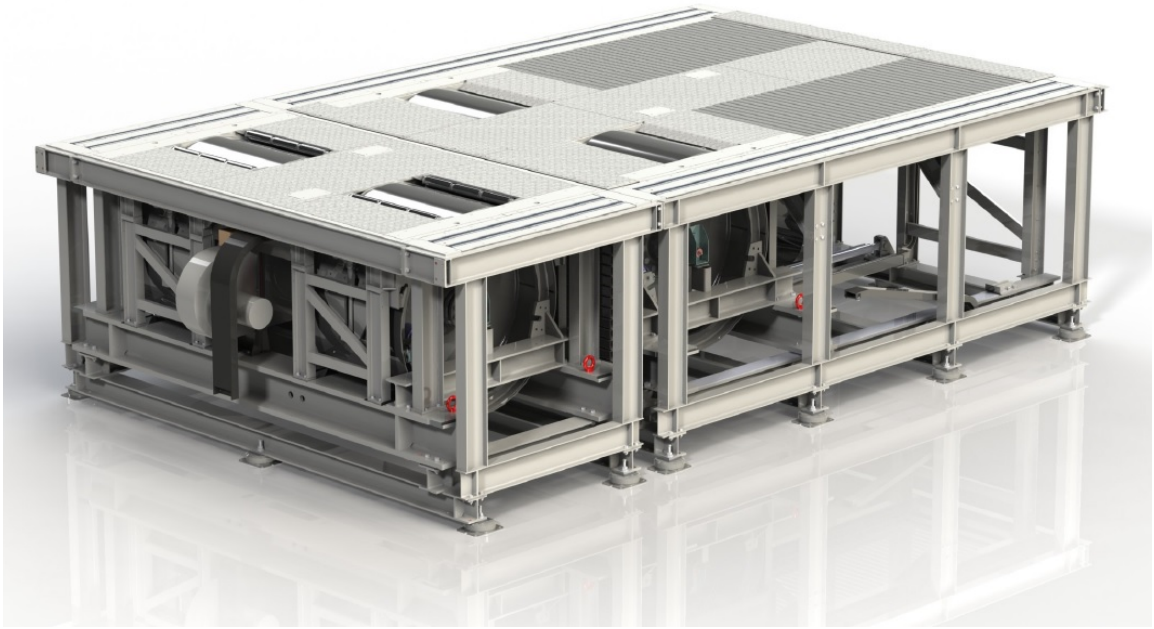

Figure 2-12: 48” single roller 4WD Horiba VULCAN chassis dynamometer [35]

In operation the dynamometer control system is given a definition of the dynamometer road load it must apply to the vehicle during testing in the form of the equivalent vehicle mass plus the three coefficients, F0, F1 and F2 as defined by Equation 2-11. The dynamometer controller takes a measure of the roller speed from one or often two encoders positioned on the roller shafts. The force applied by the electrical machine is measured by a load cell positioned between the chassis dynamometer bed frame and a lever arm attached to the electrical machine housing. Often the dynamometer electrical machine will be configured so that the inertia and road load simulation is not active when the rollers are stationary. Consider a vehicle starting from rest on a chassis dynamometer; the vehicle must therefore initially accelerate only the base inertia of the rollers, the vehicle wheels, driveline and the mechanical couplings in the dynamometer. Once the roller speed is above a certain threshold, typically less than 5kph, the motors become active and the dynamometer controller can adjust the motor current to achieve the desired road load and inertia simulation force for the given speed and acceleration rate. Since the load cell only gives a measure of the motor force, the controller must have an estimation of the loss force between the motor output and the roller surface to calculate the load applied to the vehicle. These losses arise primarily from bearing friction, flywheel and roller windage and motor coast torque losses [34, 42]. Bearing losses are reported to be

approximately linear with increasing speed and vary with viscosity of the lubricating medium and bearing preload, both of which are dependent on bearing temperature variations [42]. The estimation of the total losses is typically obtained by a separate test where the rollers are accelerated and decelerated at a fixed rate and the error in the motor force is measured. From this test the dynamometer losses can be defined by a quadratic equation, as shown by Equation 2-14, which is similar in format to Equation 2-11.

$$F_{Dyno\_Loss} = A0 + A1V + A2V^2$$

Equation 2-14

Where F_{Dyno_Loss} is the dynamometer loss force, A0, A1 and A2 are the loss force coefficients and V is the dynamometer roller surface speed.

2.4.2. *Type Approval Road Load Determination*

Before a TA vehicle is tested on a chassis dynamometer it will be taken to a test track and be subject to the legislative TA procedure for determining the track road load curve. The TA procedure is defined in ECE regulation 83-06 [9] and allows two options for the determination of the track road load along with a third option to use pre-defined dynamometer road loads known as 'cookbook loads'. The first method involves accelerating the test vehicle using the vehicle's powertrain and a human driver to 10kph above the maximum test speed, selecting neutral and measuring the time taken to coast down to the lowest test speed. This process is known as coastdown testing and is defined across two SAE standards; J1263 [44] and J2263 [45]. The times must be recorded when driving in both directions and the average taken. The recorded times are used to calculate the track road load forces which must be matched when the vehicle is then tested on the chassis dynamometer by adjusting the dynamometer load to suit. The alternative method is to use wheel torque transducers, accurate to ±2%, to measure the driving torque on the track at a set of constant speeds. On the chassis dynamometer the coastdown test is again used, either with or without wheel torque transducers to ensure the wheel torque or chassis dynamometer load is matched to the track wheel torque or load. This process is defined in the SAE standard J2264 [46]. Cookbook loads are another option and are dynamometer road loads that are pre-defined in the TA regulations and their use negates the need to match road loads [9].

The TA regulations [9] define tolerances for the accuracy of the chassis dynamometer system, which are equally applicable to whichever method is used for the dynamometer road load determination. Firstly it must be possible to read the chassis dynamometer load to within ±5% and the dynamometer load must be accurate to within ±5% when checked at 10 km/h speed intervals between 120 and 20 km/h. At 20 km/h the load must be

accurate within ±10% and below this the dynamometer absorption must be positive. The inertia of the dynamometer, including electrical simulation, must be within ±20kg of the target inertia class. The vehicle speed must be accurate to ±1km/h at speeds above 10km/h.

Several authors in the literature have noted that there is considerable flexibility in these procedures and tolerances meaning that there is often a sizable difference between the track road load used for TA road load matching and the real world road load [10, 14, 15]. This source of error is not directly applicable to sources of imprecision in chassis dynamometer testing, particularly when comparing test to test results. However the results do set the scene for the importance of chassis dynamometer road load as a factor of the load placed on the vehicle and hence the vehicle CO_2 emissions. As will be discussed in later sections of this thesis, there are considerable sources of imprecision with respect to dynamometer road load for chassis dynamometer testing in isolation. Therefore data that are presented by the literature in relation to the error between real world and chassis dynamometer testing may be helpful if it has been expressed with a transfer function between road load force and CO_2 emissions, regardless of whether this refers to error originating from track or chassis dynamometer testing.

Kadijk et. al. [10], quantified the differences between real world and TA track road loads by comparing the TA data submitted by vehicle manufacturers against Kadijk et. al.'s own in-house track coastdown tests. It was found that the real world track road loads were up to 30% heavier at speeds below 60 km/h and up to 70% heavier at higher speeds. This is a very large error, however by subjective examination of the data most vehicles are in the region of 50% heavier loads at low speeds and 20% heavier at higher speeds. Interestingly the larger differences were for the newer Euro 5 and 6 vehicles, which is why Kadijk et. al. indicate that the maximum error is an important metric when looking to new vehicle TA testing. Kadijk et. al. also quantified the decrease in Euro 6 road loads compared with Euro 5 and it was found that on average the decrease in road load was 18%. This decrease was modelled in a simulation environment and found to yield an 11% decrease in CO_2 emissions which is equivalent to a 0.61% change in CO_2 emissions per 1% change in road load. This result is a good match for the modelling result reported by the Kadijk et. al. in a separate report [14] where by a 0.63% change in CO_2 was predicted for a 1% change in road load. Despite reporting two very similar results the complete lack of details about the simulation in the Kadijk et. al.'s report means it is difficult to have high confidence in the findings.

Kadijk et. al. preformed further TA style tests on six Euro 5 and 6 vehicles with two chassis dynamometer road load settings; the manufacture's TA road load and Kadijk et.

al.'s coastdown derived real world chassis dynamometer road load. The CO_2 emissions results from these tests were compared to the baseline CO_2 emissions from the manufacture's TA tests, the results are shown in Figure 2-13.

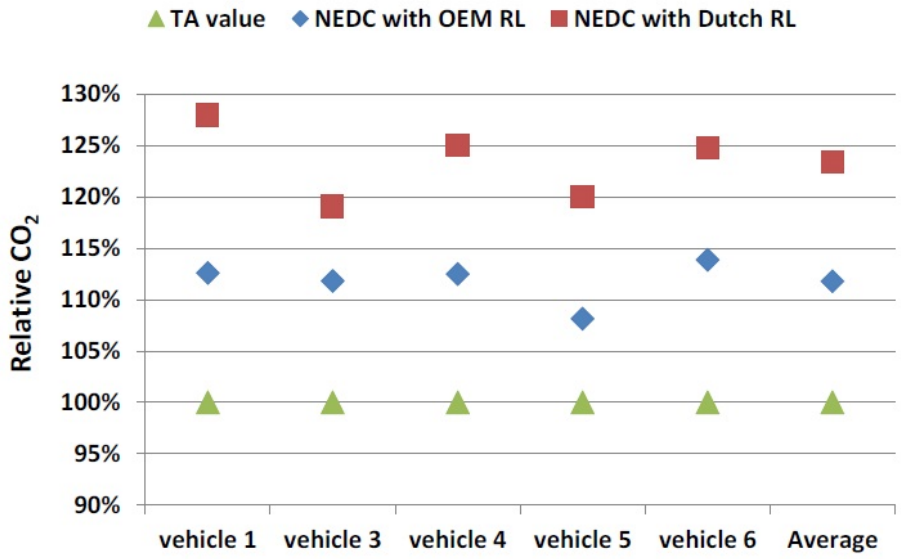

Figure 2-13: CO_2 emissions from six test vehicles, tested at two chassis dynamometer road load settings and compared to baseline CO_2 emissions [10]

By reference to Figure 2-13 it can be seen that for these vehicles the CO_2 emission results from tests run on the TA chassis dynamometer road load were 11% lower than those completed using Kadijk et. al.'s real world chassis dynamometer road load. Additionally there is a gap between the manufacturer declared CO_2 emissions and the TA chassis dynamometer road load of 12%, making a total gap between declared CO_2 and real world of 23%. This means a vehicle declared at 130 g/km CO_2 is actually emitting somewhere in the region of 160 g/km when tested in real world conditions. For this thesis the particularly interesting results are the difference in CO_2 emissions between the two sets of tests completed by the Kadijk et. al. since these data are from two experimental results obtained on a chassis dynamometer whereas the later uses a declared figure which is not taken from a chassis dynamometer test. It is incredibly difficult to make a valid comparison and objective conclusions from the reported differences between the manufacturers declared CO_2 emissions and the Kadijk et. al.'s recorded CO_2 emissions since the tests were performed in different test labs, by different people using different equipment. The differences could therefore easily be nothing to do with road loads and comprised of administrative subtractions made by the manufacturers as part of their CO_2 declaration, a legal flexibility in the existing procedure, or through differences in the CVS system optimisation. Unfortunately Kadijk et. al. do not directly quantify the magnitude of the difference in chassis dynamometer road load that caused the 11% average change in CO_2 emissions between the real world and TA tests. This makes it impossible to derive any

form of generic transfer function between road load and CO_2 emissions and is a big limitation of Kadijk et. al.'s study.

Many authors across a variety of reports propose broadly the same list of factors for the sources of these various discrepancies in road loads which are responsible for shifts in CO_2 emissions. For TA test vehicles manufacturers commonly use low rolling resistance tyres, optimising the tyre pressures for minimum rolling resistance and some use special tyre preparation techniques to further reduce rolling resistance, the details of which are not explicitly given in the literature [10, 14, 15]. The importance of tyres as a source of chassis dynamometer imprecision is discussed in detail in section 2.5.1.

Other reasons for the discrepancies are cited as the use of special low rolling resistance test track surfaces, test track inclination and optimisation of vehicle mass [10, 14, 15]. Test track inclination is controlled by the TA regulations, which allow a maximum gradient of 1.5% [9]. Kadijk et. al. [14] quantified the effect of fully utilising this tolerance via a Ricardo simulation tool and found a 0.3% decrease in CO_2 emissions. This effect is unlikely to be seen as a source of imprecision during chassis dynamometer testing since the gradient is either included in the original track road load determination for a vehicle model line and or is set as a variable within the chassis dynamometer control system. The later error state is easily identifiable since almost all systems will report the dynamometer settings used for each test. Kadijk et. al. point out that despite the regulations insisting that runs are performed in both directions, they do not preclude the design of a test track that slopes downwards in both directions [9, 10]. It is said that manufacturers typically optimise the vehicle mass so that the lightest possible TA vehicle is tested at the track. The TA regulations state that the test vehicle must have no optional extra equipment fitted, a courtesy which is readily utilised by the manufacturers [9]. Carlson et. al. [40] investigated the effect of changing the vehicle mass by 10% at the test track. Attempts were made to isolate drag changes by spacing the suspension to ensure the aerodynamic drag remained the same. When the three vehicles, which comprised a mix of gasoline, gasoline hybrid and fully electric vehicles, were tested over TA style tests a change to the vehicle energy consumption of between 2.4 and 4.1% was recorded [40]. These results are interesting but it should be noted that they are not comparable to European TA results, since the testing was conducted over the US drive cycles, namely the UDDS, HWFET and US06 cycles [40]. Carlson et. al. rightly point out that whilst these results are a useful indicator of the magnitude of possible errors, they are also specific to these vehicles. Interestingly a non-linearity was observed in the results that indicated that increasing mass impacted the road load less than decreasing by the same mass, see Figure 2-14 [40].

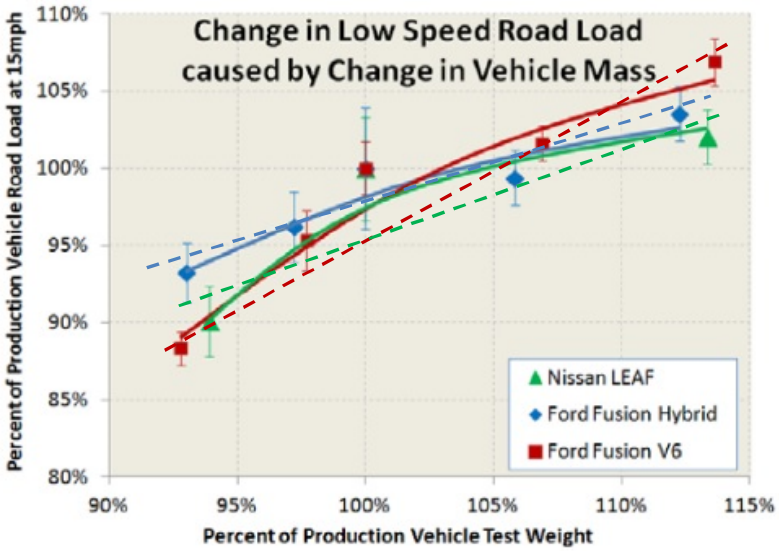

Figure 2-14: Percentage change in road load versus percentage change in vehicle weight demonstrating non-linearity at low speeds. Dashed lines have been added by the author to demonstrate linearity for each vehicle if the error bars are used. [40]

Classical texts on the subject of rolling resistance dependence on speed, see section 2.5.1 for details, state that the relationship is linear so it is of some surprise, even to Carslon et. al. [40], that these results indicate non-linearity. However by examination of Figure 2-14 it is possible on all three vehicle's 'curves' to fit a linear straight line fit through the data if one utilises the 95% confidence intervals. This suggests that the non-linearity is actually demonstrated in Carlson et. al. 's test error rather than being a fundamentally new finding.

Kadijk et. al. [14] tested a light commercial vehicle over the TA NEDC using two chassis dynamometer road loads, the first derived via matching to in-house track coastdown testing of the vehicle and the second being a cookbook road load taken straight from the regulations. The CO_2 emissions were on average 2.7% lower on the cookbook dynamometer road load, highlighting that the cookbook road loads are often an advantageous choice for manufacturers. This is generally only true for heavy vehicles which are more likely to have poor aerodynamics such as light commercial vehicles. In providing the cookbook road loads the regulators must represent a middle band road load for any given inertia class which means that lighter passenger vehicle's loads are often over estimated and heavier less aerodynamic vehicle's loads are typically underestimated.

2.4.3. *Inaccuracy and imprecision from chassis dynamometers*

Chassis dynamometers have been used since as early as the 1920's with the advent of Carl Schenck's 4WD dynamometer [35] but methods for understanding and controlling their accuracy did not start to appear until the very end of the 1970's [47]. Initial efforts to

improve the accuracy and repeatability of the chassis dynamometer where hampered by the lack of sophisticated equipment; however as these issues started to be overcome from the 1980's the EPA started to form work groups to focus on the sources of imprecision and error. This work initially culminated in 1991 with the publication of the EPA request for proposal for "Specifications for Electric Chassis dynamometers, Attachment A" [48]. This is a 40 page document outlining the requirements for emissions chassis dynamometers along with acceptance tests for ensuring it is fit to test. The document, commonly known as 'attachment A', provided an excellent standard at the time it was published. However as equipment, particularly computer control systems, have improved the standard has become more and more out of date. As early as five years after the publication of attachment A, some authors were eager to point out its shortcomings in not fully covering some of the important factors, such as response time and simulation accuracy [34]. A new working group was formed comprised of members from CARB, EPA, and seven major OEMs; resulting in the publication of the 'Dynamometer Performance Evaluation and Quality Assurance Procedures' or DPEQAP in 2000 [49]. The DPEQAP builds on the information presented in attachment A and effectively supersedes it. It presents eighteen procedures of which twelve are intended for the evaluation of a new dynamometer and six are quality assurance procedures for determining if the dynamometer is fit for test.

The report highlights many factors that are important to achieving accuracy and repeatability including but not limited to; load cell calibration, roller diameter and run-out, time verification, speed measurement, response time, base inertia evaluation, acceleration performance, parasitic losses compensation, roller surface texture and load cell calibration [49]. The report also defines a roadmap for ensuring that any chassis dynamometer is 'ready to test' from a quality perspective [49]. The roadmap has been summarised in Figure 2-15.

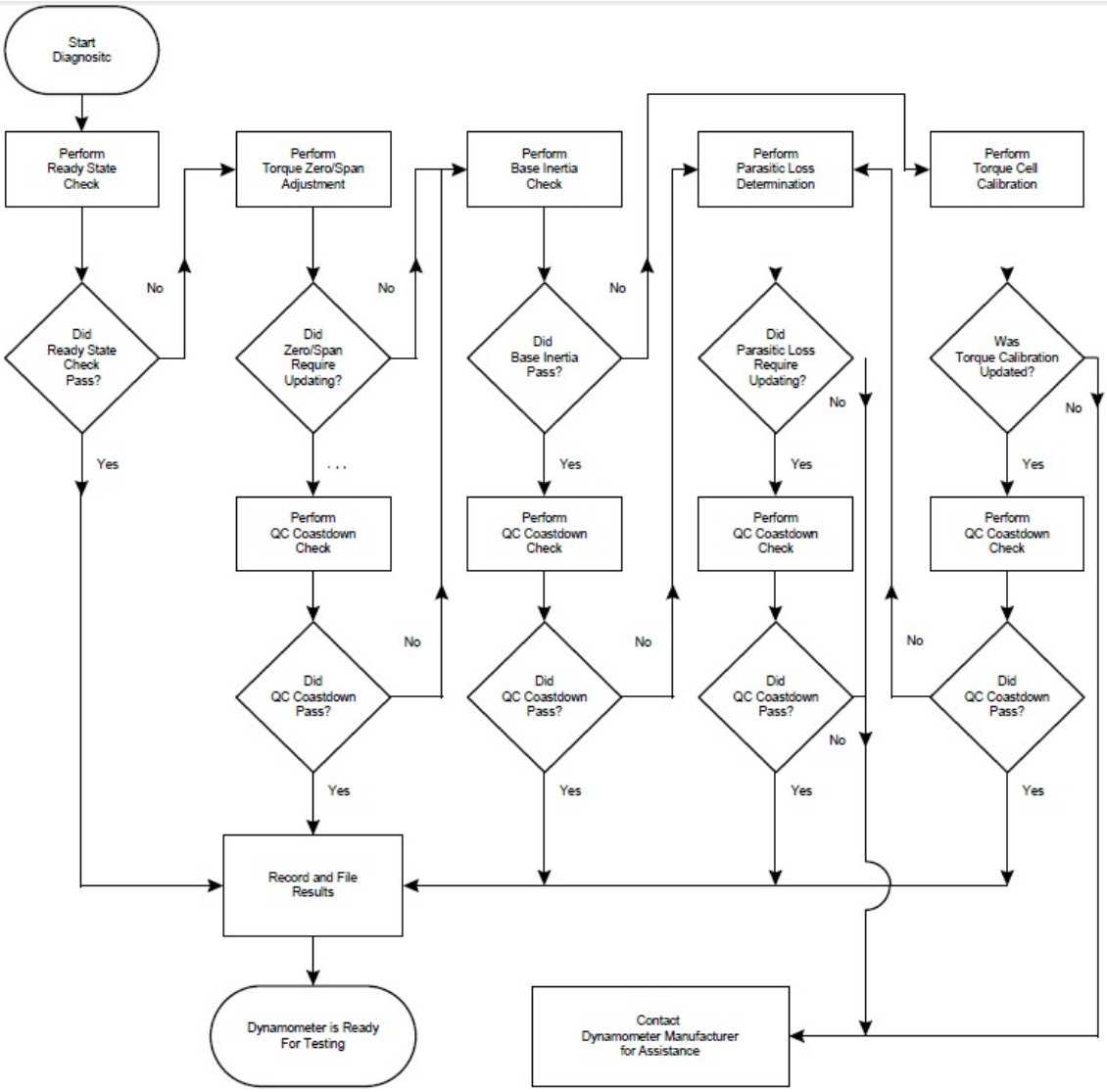

Figure 2-15: Dynamometer quality assurance roadmap based on DPEQAP [49]

The principle of the DPEQAP roadmap [49] is that each stage must be checked each time the dynamometer is used to ensure the highest quality results with minimum imprecision. Some stages require a straight forward yes/no check. Other stages require more detailed evaluation of results against DPEQAP defined specification limits. The following paragraphs will explore the nature and effects of errors within the individual stages of the DPEQAP roadmap.

The first stages in the DPEQAP roadmap are concerned with checking the calibration system, namely the load cell and encoders [27, 49]. The motor load cell is typically calibrated by applying dead weights to exercise the load cell to known forces. The gain and offset of the load cell amplifier can then be adjusted by the chassis dynamometer controller to ensure the readings from the load cell match the known forces applied by the series of dead weights [49]. The DPEQAP [49] recommends that the load cell calibration acceptance criteria are ±0.1% for accuracy, ±0.1% for linearity, ±0.1% for hysteresis and

±0.05% for repeatability. This is a much tighter tolerance than specified by the TA regulations which state that it shall be possible to read the indicated road load with an accuracy of ±5% and that the load of the dynamometer shall be matched to the real life road load within ±5% at 120, 100, 80, 60, 40kph and within ±10% at 20kph [9]. Below 20kph the dynamometer absorption shall be positive [9].

The chassis dynamometer system must have an accurate calibration of its base machine inertia for the control system to be able to correctly control motor current to achieve the desired roller force during road load simulation [49, 50]. As previously mentioned the common method for the determination of the base inertia is to accelerate and decelerate the rig at fixed rates whilst measuring the motor force. From newton's second law it is then straight forward to determine the mass of the rotating components. The DPEQAP gives a tolerance for the machine base inertia of ±0.2% of the manufacturers stated value [49]. This is a good standard for new machines, however on older systems where there has been substantial wear to the roller surface or large deposits of tyre rubber it may be more appropriate to use a value taken from an average over recent machine runtime. This has not been investigated in the literature but would warrant further consideration in the author's opinion since wear or deposits could alter the mass and it is currently unquantified if the change in mass is significant.

The chassis dynamometer must have an accurate model of the internal dynamometer losses to ensure the motor force that is applied will result in the correct force at the roller surface. One source of these losses is bearing friction which is highly dependent on the bearing temperature [42]. It is therefore important to thoroughly warm the dynamometer and bearings before a test to minimise imprecision arising from changing losses during the emissions test. Two authors have directly identified dynamometer thermal state as an important source of road load and therefore CO_2 imprecision [27, 49]. The relative magnitude of the loss force to the applied road load force will be important in determining the magnitude of this source of imprecision which has not been directly quantified in the literature. The DPEQAP report [49] specifies a procedure to verify that the compensation of the dynamometer parasitic losses is accurate. The procedure involves operating the dynamometer in speed mode up to a pre-defined test speed, then switching to RLS mode with F1=F2=F3=0 and recording the final speed after 60 seconds. If the parasitic losses are correctly compensated then the speed should not change, so a tolerance is specified in the force domain of ±0.1hp [49].

The final checks in the DPEQAP roadmap [49] are concerned with validating whole machine performance on the assumption that individual component validation does not guarantee that the whole system functionality is desirable. This is achieved via a

procedure known as an unloaded or dynamometer only coastdown test. For this test there is no vehicle on the dynamometer and the road load coefficients are adjusted to account for this. The DPEQAP recommends that the target inertia is the machine base inertia and that the road load coefficients are set to F0=20lbs, F1=F2=0. The resulting coastdown forces for each 10mph speed gate must be within ±2.2lbs.

Possibly the most obvious source of error and imprecision test to test from the chassis dynamometer is the use of incorrect settings for emissions tests. For example a user might accidently enter or select the incorrect inertia or dynamometer road load coefficients in the dynamometer control system. The effect of this error state has been investigated by authors in the literature. Brace et. al.[8] varied the load applied by the dynamometer through increasing the simulated inertia weight by 9.3% from the baseline condition. This was found to cause a 1.5% change in the vehicle fuel consumption, a change that was statistically significant at a 95% confidence level demonstrating the high robustness of the result. A change in the simulated inertia weight only affects the load applied by the dynamometer during transient events and does not affect the load applied during steady state cruise conditions. This means its effect on the overall emissions is highly dependent on the transient nature of the drive cycle. In the case of the NEDC there is a good proportion of both cruise and transient events [12] giving greater confidence in the result obtained by Brace et. al. and indicating that inertia errors are an important factor. Jourmard et. al. [31] report testing carried out by the TNO who tested five vehicles, each over five TA style emissions tests with three settings for road load and inertia. A detailed summary of the results is not given, however Jourmard et. al. describe that clear influence was found on all gaseous emissions, but only with significance on the CO_2 emissions, FC and diesel NOx emissions [31].

2.4.4. *Dynamometer summary*

The impact of variations in the road load applied to a vehicle on its CO_2 emissions have been commented on several times in the available literature. Most authors have focused their work on the quantification of the difference between the real world track road load, the TA track road load and the TA chassis dynamometer road load, both in terms of applied force and vehicle out CO_2 emissions. The differences between real world and TA are the focus of considerable attention within both the media and published literature, particularly with the development of new regulatory legislation that is currently taking place within the industry. As such the focus of these works is normally regarding the utilisation of test flexibilities that yield results which are incomparable to the real world which is a slightly different focus to that of this thesis. There is very little literature from the academic field which takes an in depth analysis of the chassis dynamometer with a view to

improving the precision of results. However the literature that is available still provides useful background on the sensitivity of vehicle emissions to changes in road load, since the sensitivity is likely to be very similar in the real world, on a track or when it is being tested on a chassis dynamometer. Within the available literature the Kadijk et. al. [10] have been the most vocal, stating modelling results that yield a sensitivity of 0.63% CO_2 per 1% change in applied road load force along with simulation results for the effect of gradient which yielded a sensitivity of 0.2% CO_2 per 1% change in gradient. Also reporting that the use of cookbook dynamometer road loads compared with track matched road loads gives on average a 2.7% lower CO_2 result from a vehicle. Carlson et. al. [40] examined the effect of vehicle mass and reported results that yield a sensitivity of between 0.24 and 0.41% consumed fuel energy per 1% change in vehicle mass. However their results were recorded over highly transient US test cycles and therefore the sensitivities are less valid for European TA or NEDC testing.

Other authors have examined the effect of incorrect use of the chassis dynamometer. Brace et. al. [8] increased the inertia simulation weight and recorded results that yield a sensitivity of 0.16% change in FC per 1% change in inertia simulation weight, a change that was statistically significant at a 95% confidence level. Jourmard [31] tested vehicles at three settings for road load and inertia and reported a clear influence on all emissions with significant changes to CO_2, FC and diesel NOx. Given that satisfactory dynamometer operation and setup has a clear influence on the vehicle CO_2 emissions a group of engineers from various OEM's worked together to understand the factors that are important to ensuring good machine performance. These factors have been identified in their report, the Dynamometer Performance Evaluation and Quality Assurance Procedures or DPEQAP, however the procedures are lengthy and arguably need to be streamlined to be useful applied to an industrial testing environment. For example basic principles like warming the dynamometer prior to usage are well known but the length of the required warm up and hence the relative importance of thermal state has not been quantified. Such a quantification of the important factors would allow useful trade-off of the importance of individual DPEQAP procedures. Ultimately no author to date has attempted to answer the question; is a modern chassis dynamometer capable of giving high enough precision and accuracy to meet the needs of today's testing requirements?

2.5. Procedural Factors

2.5.1. *Defining procedural factors*

The term 'procedural factors' has been coined to cover a variety of sources of variability that are all predominately linked to human actions performed by test technicians during the setup and completion of chassis dynamometer emissions tests. Examples include the

alignment of the vehicle when installing it onto the chassis dynamometer, the setting of the vehicle tyre pressures and the tightening of the vehicle restraints. The following sections will describe each of the known procedural factors and the available literature to understand their effects.

2.5.2. *Vehicle alignment*

When a vehicle is installed onto a chassis dynamometer, there are two main approaches. The first is for a front loading dynamometer, in which case a front wheel drive vehicle would be pushed backwards over the dynamometer rollers, with the roller brakes applied, until the non-driven wheels are clear and the driven front wheels are resting in the well of the rollers. The second is for a rear loading dynamometer, in which case a front wheel drive vehicle is pushed front first onto the dynamometer rollers until the wheels are resting in the well of the chassis dynamometer. Since it is not possible to align the vehicle completely perpendicular to the rollers during this initial installation the dynamometer must be used to centralise the vehicle once the wheels are resting in the rollers. For a twin roller dynamometer the centralising procedure is simply to slowly motor the rollers at less than 5km/h. If the vehicle is misaligned it will self-steer until it is perpendicular to the rollers. On a 48” single roller dynamometer it is necessary to have a centralising mechanism that provides the function of positioning the vehicle tyre on the crown of the roller. This normally consists of two small pinch rollers that move up the roller circumferentially until they hold the vehicle on the roller crown. The centralising procedure is then the same as for a twin roller dynamometer.

From the author’s experience there are two most likely modes of failure in centralising a vehicle. Firstly the vehicle can be rolled onto the dynamometer at such a severe angle that the rollers are not wide enough to align the vehicle via the self-steer principle. In this instance the vehicle will swerve off the dynamometer rollers and collide with the guards unless it has previously been loosely restrained to the test cell floor. The second and much more likely mode of failure is for the operator to forget to align the vehicle at all after installing it on the dynamometer. Brace et. al. [8] examined the effect of a misalignment that might occur from this mode of failure by purposely misaligning the vehicle by 75mm when measured as indicated by their diagram, see Figure 2-16.

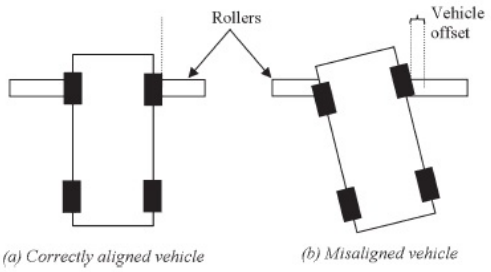

Figure 2-16: Diagram of vehicle misalignment on a chassis dynamometer [8]

When NEDC tests were run with the vehicle misaligned, a 1.7% increase in vehicle FC was found from the 75mm misalignment, a change that was statistically significant at a 95% confidence level. This is quite a small change compared to some the factors considered earlier in this chapter; indeed the factor appears quite far along the pareto chart taken from the Brace et. al.'s [8] paper, ranking eighth in the size of the effect, see Figure 2-3. No work exists in the literature identifying methods to detect or correct for this factor and only the study by Brace et. al. appears to have documented this factor.

2.5.3. *Vehicle tyres*

It has been shown in numerous studies throughout the literature that variability in the vehicle load resulting from changes to rolling resistance from tyre preparation can result in significant variability in the fuel consumption from chassis dynamometer tests [3, 8, 10, 14, 15, 27, 40, 41, 51-55]. The rolling resistance of a free rolling tyre is mainly caused by internal friction within the tyre carcass whilst windage losses, drag and slippage are generally much smaller effects at moderate speeds, typically accounting for only a few percent each [53-57]. The losses within the tyre carcass occur because in the contact area between the tyre and road there is deformation of the tyre and the energy dissipated to deform the tyre is not completely recovered when it springs back as the tyre rolls forwards [55]. The magnitude of these losses and hence the rolling resistance can be affected in a number of ways during TA road load determination and during TA emissions testing. The most commonly discussed factors affecting the rolling resistance are the tyre inflation pressure, wear, alignment, rolling radius, inertia, road surface friction, temperature, width and compound. Genta [55] documents the theoretical expected trend for some of these factors, stating that the rolling resistance of a radial tyre decreases with increased wear. Genta also states that the internal damping of rubber decreases with increased temperature and hence the hysteresis losses within a tyre will reduce, lowering the rolling resistance. In addition the lower rolling resistance will stabilise the temperature of the tyre since there is less energy dissipation within the tyre carcass and therefore less heat generated through the tyre deformation. Genta also states that an increase in the

inflation pressure or a reduction in the normal load will reduce the rolling resistance. Genta quotes a formula which expresses the rolling resistance coefficient as a function of the inflation pressure and speed, see Equation 2-15 [55].

$$f = \frac{K}{1000}\left(5.1 + \frac{5.5x10^5 + 90F_Z}{p} + \frac{1100 + 0.0388F_Z}{p}V^2\right)$$

Equation 2-15 [55]

Where f is the rolling resistance coefficient, K is a coefficient that takes a value of 0.8 for radial tyres, p is the inflation pressure, V is the speed and F_Z is the normal force. Equation 2-15 shows that the rolling resistance coefficient is linearly related to the inflation pressure. This linear relationship between inflation pressure and rolling resistance, exists only for the normal operating range of the tyre since extreme deflation leads to non-linearity in the carcass deformation. The linear relationship between inflation pressure and rolling resistance is further confirmed by several other authors work from the literature [53, 54, 57-60]. Of course the inflation pressure is directly linked to the normal force since it is impossible to increase the pressure without reducing the normal force. TA emissions testing legislation states that the tyre pressure must be set before testing when the vehicle is cold, however no specific temperature is stipulated [14], [9]. Kadijk et. al. [14] identify that by setting the tyre pressure when the vehicle is very cold it is possible to ensure the highest pressure and therefore the lowest rolling resistance during the test, when the vehicle is hot. Most authors have quantified the effect of tyre pressure changes when combined with other factors, however Brace et. al. [8] studied inflation pressure in isolation. It was found that a 7psi decrease in the tyre pressure of the conventional tyre caused a 2.6% change in the measured fuel consumption at a 99% confidence level; this is shown in Figure 2-3 [8]. This gives a sensitivity of 0.4% increase in FC per 1 psi tyre deflation. In the literature most authors have studied combinations of the factors that affect rolling resistance in lumped case studies. For example Fontaras et. al. [3] state that by improving the rolling resistance by between 10 and 20% a fuel consumption benefit in the region of 1 and 2.5% can be expected. Kadijk et. al. [14] state that the maximum possible change to fuel consumption or CO_2 emissions is in the region of ±20% as a result of the optimised play off of all possible rolling resistance related noise factors.

Tyre type is another important factor in the rolling resistance. Sports vehicles are typically equipped with high grip tyres and therefore have a high rolling resistance when compared with convention passenger vehicle tyres. A newer type of tyre that has gained popularity in recent years is the low rolling resistance tyre. Manufactures' typically use these on specifically branded eco models [14]. Brace et. al. [8] studied the change in the tyre type from conventional to a sports tyre and found a 3.6% increase in the measured fuel

consumption over the NEDC, a change that was statistically significant at a 99% confidence level, see Figure 2-3. The effect of low rolling resistance tyres has not been quantified in isolation in the literature. It is of course unlikely that the tyre type on a vehicle would change during a test programme, since the NEDC is a relatively low power cycle [12] and hence tyre life is likely to be high. However it is possible that the tyre type and manufacturer can vary when vehicles of the same make and model are tested at different labs and at different times. It is therefore important to monitor the tyre specification, including tread depth and tyre pressure when comparing batches of test results.

Sato et. al. [51] took an interesting approach in their study by examining the variation in wheel work rather than any physical change in the tyre setup or configuration. It was found that variation in wheel work, measured using a wheel torque transducer, was well correlated with fuel consumption results from the Japan 10-15 test cycle, see Figure 2-17.

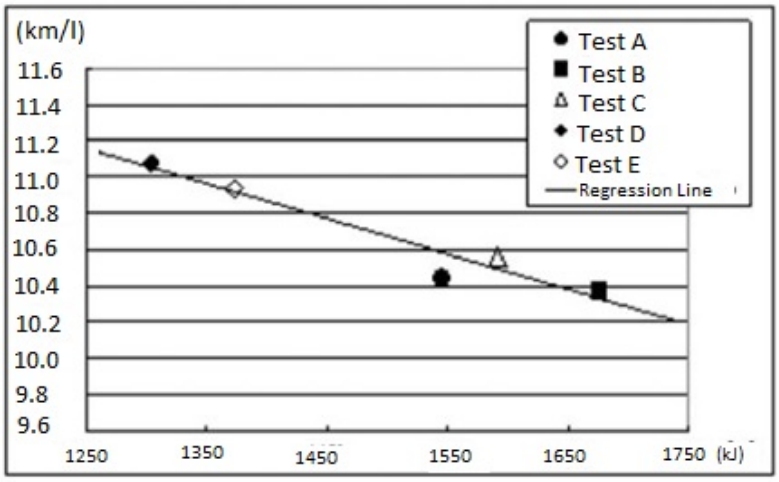

Figure 2-17: Correlation of wheel work to fuel economy [51]

The variation in wheel work was found to have been caused by variations in the tyre losses, which were in turn were found to correlate highly with the tyre surface temperature [51] which is exactly as predicted by the theory presented by Genta [55]. The correlation between tyre surface temperature and tyre loss is shown in Figure 2-18. The level of fit is good with a coefficient of determination, or R^2 value of 0.9, indicating that 90% of the variability in tyre losses can be attributed to variations in the tyre surface temperature and that there is a linear relationship between tyre surface temperature and tyre loss force.

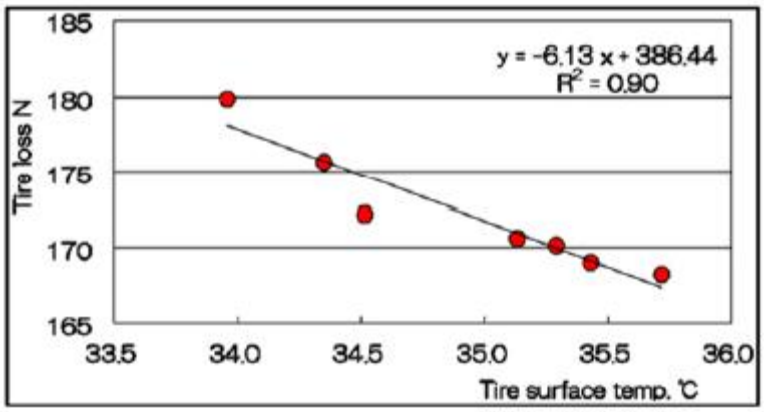

Figure 2-18: Correlation of tyre surface temperature to tyre loss force [51]

Unfortunately in the study carried out by Sato et. al. [51] the only link between variation in tyre losses and fuel economy is the correlation with wheel work shown in Figure 2-17. To make use of this correlation for TA emissions testing would necessitate the time consuming installation of expensive wheel torque transducers and the modification of the test vehicle, it is therefore unlikely to be feasible in a commercial environment. However the correlation of tyre temperature with tyre loss does show there is a case for ensuring consistent tyre temperature during TA emissions tests, although further work is required to determine the magnitude of the emissions response.

So far the effect of changes to the vehicle tyres on fuel consumption has been explored, however changes to the vehicle tyres can also be used to affect the coastdown time during TA dynamometer road load determination. Brace et. al. [8] summarised the cumulative effect of several tyre related factors on the coastdown times and also linked these to the fuel consumption, see Figure 2-19.

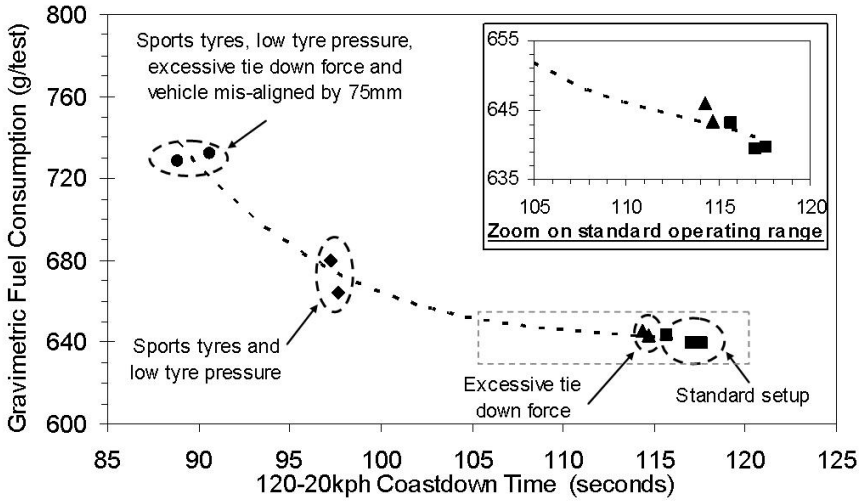

Figure 2-19: combined effect of tyre related factors on the rolling resistance measured by coastdown time and on gravimetric fuel consumption [8]

Their results show that an increase in the FC of approximately 12% was found when underinflated sports tyres were used over a NEDC, highlight just how significant the effect from the tyres can be. Brace et. al. state that these results also give more insight into their study of chassis dynamometer noise factors by allowing the data to be re-processed to take into account the coastdown time as a measure of all rolling resistance factors rather than individual measurements of the factors affecting coastdown time. When that was done it was found there is was 2% change in FC for a 10 second change in coastdown time which according to the data presented could occur from a 0.5 bar change in tyre pressure [8]. This highlights that it is important to examine the coastdown data from chassis dynamometer tests as it gives valuable insight into the variability in the rolling resistance and hence the potential CO_2 emissions. Of course a coastdown test will only give a measure of the end of test rolling resistance and hence it is also important to consider variables that can be controlled before the test is started, for example the tyre inflation pressure. Something that has not been considered within the literature is the expected variation in tyre pressure and therefore the best methods for controlling this and other factors relating to rolling resistance.

2.5.4. *Vehicle restraints*

An increase vertical load imparted on the vehicle through the tie down straps should result in an increase in the rolling resistance of the tyres, by reference to Equation 2-15, with a corresponding fuel consumption penalty. The study conducted by Brace at. al. [8] showed no statistical significance in the measured effect of the strap tension. However Peralta et. al. [61] found a reduction in the criteria pollutants and an improved precision in CO_2 emissions when comparing rigid restraint poles to flexible straps. For the study conducted by Brace et. al. it must be assumed that by changing the angle of the straps from

horizontal to being tied down to the floor does not impart a high increase in vertical tyre load and that the angle of the straps is likely to be a minor factor effecting the vehicle fuel consumption. However Brace et. al. [8] did not measure the strap tension directly or the vehicle suspension deflection when the straps were attached to the floor and therefore it is not possible to know how much vertical load was placed on the wheels. For example if the straps were still quite loose when angled to the floor it would be of little surprise that there was no effect on fuel consumption. Conceivably an operator could tighten the straps so tight that there is considerable increase in vertical load and hence a significant change to FC. Peralta et. al.'s study shows that by reducing the opportunity for the restraints to deform the load on the vehicle is more constant with an equivalent improvement in the vehicle CO_2 emission precision. However Peralta et. al. do not attempt to give any statistical confidence to their findings and it is clear from their results that the basic level of precision in their study is not ideal or necessarily totally in control meaning their results can only be taken as indicative at best.

2.5.5. *Test Vehicle Mass*

The vehicle mass is usually a variable that is optimised at the track road load determination stage of vehicle development where the vehicle inertia class is being determined. The effects of changes to the vehicle mass during road load determination have been discussed in detail in section 2.4.2. However it is also possible for the physical mass of the test vehicle that is installed onto the chassis dynamometer to vary. For example the volume and therefore mass of fuel in the vehicle's fuel tank, the weight of the driver and any passengers along with the weight of any optional extras installed into the test vehicle. The effect of increases in the physical mass of the test vehicle has the effect of increasing the vertical load on the vehicle tyres and therefore increasing the rolling resistance. Some laboratories have therefore adopted techniques to control the variation in the weight of the driver by asking lightweight drivers to take additional ballast into the vehicle when they drive an emissions test. The fuel tank mass is typically less important on a front wheel drive vehicle, since the fuel tank is usually located above the rear wheels, however in any case it is easily controlled by ensuring the tank level is maintained within a sensible tolerance with post-test refuelling.

2.5.6. *Engine oil level*

The effect of engine oil level on the CO_2 emissions during TA emissions tests is not widely discussed in the literature. Only Brace et. al. [8] have attempted to experimentally measure the effect of oil level on a C-car passenger vehicle by testing the vehicle with both a full fill and with 2.5 litres of engine oil removed. A decrease in the fuel consumption of 2.9% resulted from removing the 2.5 litres of engine oil, a change that was statistically

significant at a 99% confidence level. However this is quite a large decrease in the engine oil level and is likely to result in a level that is below the dipstick minimum. It's therefore unlikely to occur during normal vehicle operation on a chassis dynamometer, unless it is a deliberate test condition. Interestingly the TA regulations do not directly state a control measure for the engine oil level.

2.5.7. *The test room ambient conditions*

Chassis dynamometers used for TA emissions testing are always housed in climatic chambers or rooms since there is a legal requirement for TA emissions tests to maintain the test cell temperature within 20 to 30°C [9]. The TA legislation also stipulates that the engine coolant and oil must be within ±2K of the recorded laboratory ambient temperature at the start of the test [9]. For the most part, where a small chamber is used around only one test room the temperature is often very well regulated, since it is physically much easier to control a small volume of air. However in a commercial setting where there might be a large area with vehicle soak bays and test rooms all controlled by one air conditioning system it is more conceivable that there could be localised variations in temperature or humidity.

Several authors have found that variations in the temperature can cause variation in vehicle fuel consumption and emissions [8, 14, 15, 20, 31]. Whilst all authors indicate some form of temperature dependence, many authors do not state a correlation between ambient temperature and emissions and those that do found the effects were small. Brace et. al. [8] found that a 3°C increase in the engine start temperature caused only a 0.2% change in the vehicle fuel consumption, a change that was not statistically significant. Joumard et. al. [31] report that an increase in soak temperature from 10 and 20°C will cause a reduction in CO_2 emissions of 2% with no indication of statistical confidence. Kadijk et. al. [14] reported the findings of two studies by JRC. The first of these studies recorded the CO_2 emissions from multiple vehicles tested under replicate TA emissions test conditions at four different soak temperatures; 15, 22, 25 and 28°C. The results at 22°C were taken as a baseline for normalisation and a linear regression line was fitted through the results, see Figure 2-20. Unfortunately there is a very large scatter in the results, perhaps due to a lack of control of other noise factors and the resulting coefficient of determination of 0.214 for the linear fit is very low.

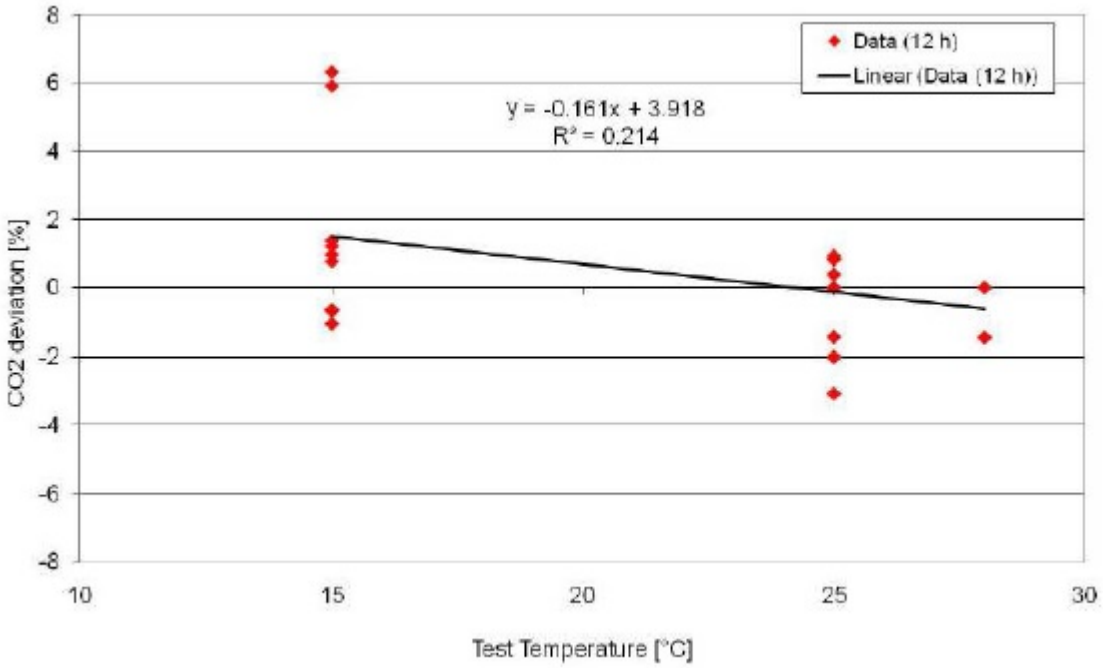

Figure 2-20: CO_2 emissions from a variety of test vehicles tested at 15, 22, 25 and 28°C. The results are normalised against the CO_2 emissions at 22°C. [14]

The second study by the JRC that is referenced by Kadijk et. al. investigated the effect of vehicle temperature prior to starting TA style emissions tests by varying the vehicle soak times from only one hour through to 24 hours in one hour increments. The results were used to derive a relationship between engine start temperature and reduction in CO_2 emissions from baseline of 0.17 % CO_2 per one degree kelvin. Kadijk et. al. imply that since the gradients from the two JRC studies are approximately equal there is high confidence in findings. However given the incredibly low coefficient of determination from the first study and the lack of any statistical confidence analysis, the author would suggest that low confidence must be placed on Kadijk's findings. Kadijk et. al. [14] also state within a table in their report that a difference in CO_2 emissions of 4% can be expected when results from 20 and 30°C laboratory ambient are compared. No reference is given for this finding, which is more than double the predicted 1.7% change from their reported JRC studies.

Schmidt [20] also investigated the effect of laboratory ambient soak temperature by testing vehicles at 22 and 28°C. The results reported by Schmidt have a large variance between the test vehicles and also between the test phases for some vehicles, see Figure 2-21.

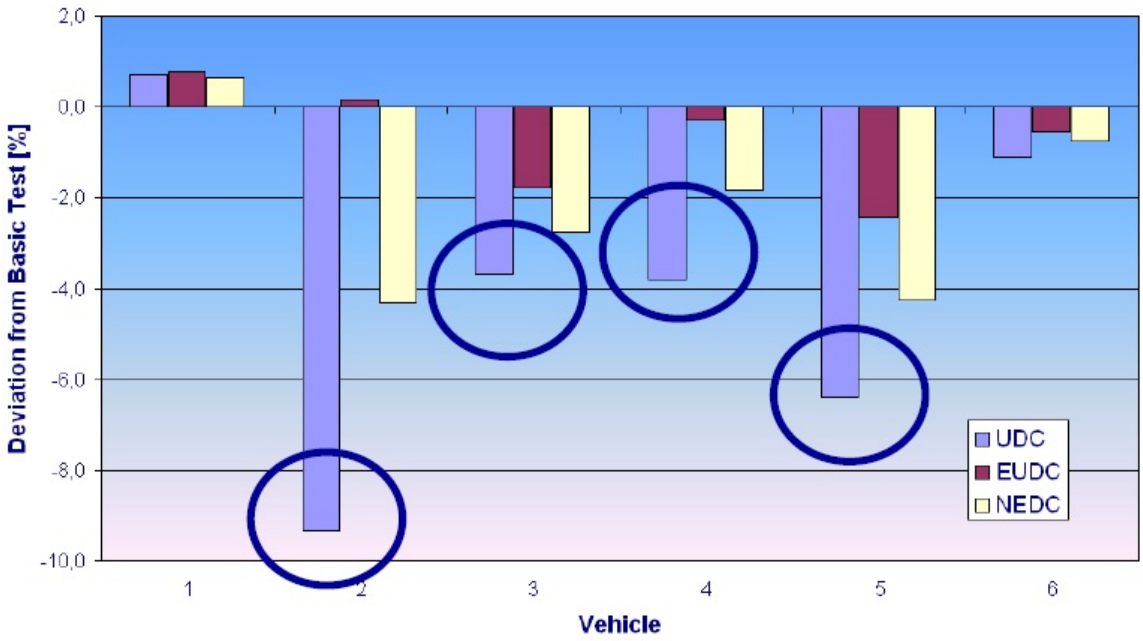

Figure 2-21: Results from a study of the change in CO_2 emissions when soak temperature is increased from 22 to 28°C. Vehicles 1-3 are SI and vehicles 4-6 are CI. The largest effects have been highlighted by the original author [20]

For vehicles 1 and 6 the change in soak temperature has had very little effect on the CO_2 emissions which have been changed by less than 1%. Conversely the other vehicles have shown large changes in the CO_2 emissions with overall NEDC emissions reduced by between approximately 3.5 and 9.5%. For test vehicles 1 and 2 the results are approximately in line with those reported by other authors; being in the region of 1%. Yet the results for the remaining vehicles show much larger effects than other authors report. For each of these vehicles the greatest change occurs in the first phase of the test which is not surprising since the vehicle will be warming up during this phase and will likely be warmed up by the time the second phase starts. Much like the other studies, Schmidt does not give an indication of statistical confidence in their results making it difficult to know how important the vehicle soak temperature is for the vehicle CO_2 emissions. A possible explanation that is supported by Schmidt's findings is that the importance of vehicle soak temperature is different for each vehicle. Perhaps this could be due to differences in the thermal mass of the engine or perhaps differences in the engine compartment shielding for heat retention. It is not possible to be sure with the information that is currently available in the literature.

2.5.8. *Roadspeed fan*

All chassis dynamometers for TA emissions testing use a road speed modulated fan, positioned 30cm from the front of the vehicle, to keep the engine cool and to replicate the air flow over the engine during normal driving [9]. There are three main factors that can

cause variability in the airflow from the road speed fan to the vehicle. Firstly, whilst the fan position is dictated in emissions legislation, it is often reliant on the user to correctly position the fan prior to each test and if this procedure is not tightly controlled, variability will be present. This is particularly the case for the angle of the fan which is simply required by legislation to point at the vehicle radiator and is therefore open to user interpretation. Another noise factor is the incorrect calibration of the fan wind speed to the vehicle speed. For TA emissions tests there is a legal tolerance on the calibration of the air speed at the fan exit, which could mean that the impact of this factor is likely to be relatively small. For reference the TA legal tolerance is that the air speed must be within ±5 km/h of the dynamometer roller speed between 10 and 50 km/h. At speeds above 50 km/h the air speed must be within ±10 km/h [9].

Brace et. al. [8] investigated the effect of a 40% overspeed in the fan over the duration of the NEDC which was found to have caused a 1.7% increase in fuel consumption, a change that was statistically significant at a 95% confidence level. A 40% fan overspeed is likely to result in an increase in air speed that is well outside the legal TA tolerance, so it is surprising that the measured effect is only very small. However Brace et. al. tested the vehicle over the NEDC which is a cold start cycle and is a relatively low speed and low power cycle, see Table 1-3. Therefore for the majority of the cycle it is likely that the engine was still warming up. Furthermore given the low ambient temperature of -7°C during Brace et. al.'s work combined with the slow speed and multiple idle periods during the first phase of the cycle, the author speculates that the fan overspeed may not have as large an effect as perhaps might be first thought. In addition Brace et. al. changed the fan demand from 100% of roller speed to 140% of roller speed and therefore it highly possible that the fan output saturated before it reached 40% overspeed since the output airflow was not measured or discussed in their study and no details of the fan characteristic are given. However their experimental findings would suggest that a study investigating the effect of air speed errors within the legal tolerance would struggle to find significant changes in CO_2 emissions. Of course it is also possible that the effects are highly vehicle specific and for example dependent on the extent of the engine compartment shielding.

2.5.9. *Vehicle run-in time*

For a TA emissions test the vehicle must be run in and have been driven at least 3,000km and this includes the vehicle tyres which must have a tread depth between 90 and 50% of the new depth [9]. However in the literature it has been identified that there is flexibility in these tolerances and that emissions results can vary by optimising the run-in time of the test vehicle [14]. An increased run-in time is advantageous since driveline, bearings and engine friction is reduced as components bed-in and component fit tolerances widen. Also

it has been demonstrated that tyres with a lower tread depth have a reduced rolling resistance compared with new tyres [55]. Kadijk et. al. [14] report the results of a study by Ricardo which found that by extending the run-in time from 3,000 to 15,000km the CO_2 emissions can be reduced by up to 5%. However Kadijk et. al. report that it is perceived by OEM's that modern vehicles would have a much reduced gradient of CO_2 reduction for run-in time. Kadijk et. al. claim that most TA test vehicles have only completed around 5,000km at the start of TA testing. The CO_2 improvement is also reduced if the vehicle is taken back to the track and new coastdown data recorded for a dynamometer road load match. Vehicles being tested on a cookbook dynamometer road load will therefore show a larger CO_2 reduction from an increased run-in time [14].

There is relatively little data in the literature for the effect of vehicle run-in time on CO_2 emissions however the effects of reduced rolling resistance for warn down tyres and a bedded-in driveline are widely accepted. It must therefore be concluded that the effect of run-in time will vary depending on the degree of optimisation of new vehicle losses. Kadijk et al. [14] estimate that for most modern vehicles the CO_2 reduction from increased run-in time is only in the region of 0.5% [14].

2.5.10. *Procedural factor summary*

The examination of the literature has identified several procedural factors. For some of these there is no numerical data to give an indication of the magnitude of the factor effect on CO_2 emissions; such factors include the vehicle restraint tension and the actual vehicle mass. The literature includes data from a least one experimental study for the remaining factors that allows an approximate quantification of the magnitude of each factor on the CO_2 emissions. These are summarised in Table 2-1.

Table 2-1: Procedural factor effect summary

Procedural factor	Size of effect on FC or CO_2 emissions	Author (s)
Vehicle alignment	1.7% FC	Brace et. al. [8]
Tyre inflation pressure	0.3 – 2.6% FC	Brace et. al. [8]
Tyre type	3.6% FC	Brace et. al. [8]
Vehicle restraints	Unknown	N/A
Actual test vehicle mass	Unknown	N/A
Engine oil level	2.9% FC	Brace et. al. [8]
Ambient temperature	0.2% FC	Brace et. al. [8]
	2 - 4% CO_2	Jourmard et.al. [31], Kadijk et. al. [14], Schmidt [20]
Roadspeed fan	1.7% FC	Brace et. al. [8]
Vehicle run-in time	0.5 – 5% CO_2	Kadijk et. al. [14]

By examination of Table 2-1 the largest effects are from the factors that relate the tyre condition, the engine oil level and the ambient temperature. Further work to identify and design control mechanisms for these factors would be a useful addition to the literature.

2.6. The emissions measurement system

2.6.1. *Overview of the TA emissions measurement system*

This section will give the reader an insight into the vastness of the emissions measurement system as a potential source of imprecision and inaccuracy in the measured CO_2 emissions from the vehicle during TA style emissions tests. All of the factors identified in earlier sections of this thesis can be considered to be affecting the vehicle out CO_2 emissions or FC. However consideration of the emissions measurement system means considering that the CO_2 emissions measured during a study might be varying due to the measurement system rather than due to the factor being investigated. The emissions measurement system is a large and complex system and there are many sources of imprecision and inaccuracy. Studies of the system looking at ways to improve the accuracy and precision are therefore a very important part of the chassis dynamometer testing field. However since the scope of work into improving the precision of the emissions measurement system is so vast that it could easily form the basis of an entire thesis in its own right it had to be excluded from in depth investigations within this thesis. But of course readers should not ignore the emissions measurement system when considering the precision and accuracy of their results.

The regulation emissions measurement system for TA emissions testing is the constant volume sampling or CVS system [9]. Figure 2-22 shows a basic schematic of the system.

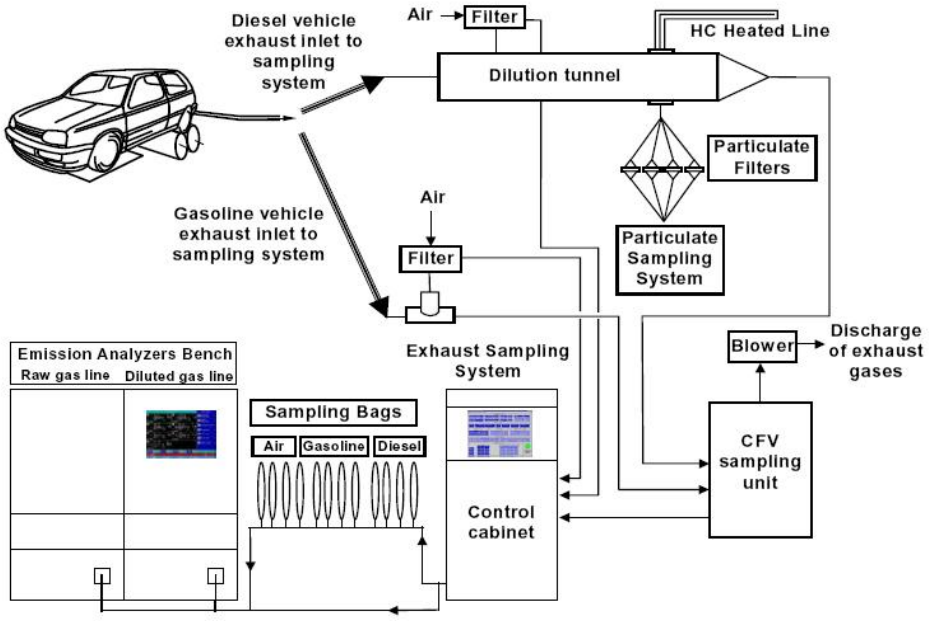

Figure 2-22: Schematic diagram of a CVS system [27]

The system works by taking the tailpipe exhaust flow from the vehicle and mixing it with ambient dilution air in a mixing tee. The diluted exhaust gas is then drawn through a critical flow venturi (CFV) which controls the flowrate at a fixed value, typically between 3 and 12m^3/min. The dilution ratio therefore varies, depending on the vehicle exhaust flowrate [62]. The diluted exhaust is then trapped in bags and the concentrations of the pollutants are measured by analysers at the end of the test. The concentrations can be converted to mass either by taking a measure of the ratio of the CO_2 concentration in the exhaust region of the mixing tee to that in the bag or by making a direct volume flowrate measurement. Currently the most popular methods for direct flowrate measurement include the smooth approach orifice (SAO) which is used to measure the dilution air flowrate and the ultrasonic flow meter which is used to measure the undiluted exhaust gas flowrate [27, 62-64]. To allow for the measurement of particulate emissions as part of the latest emissions standards, the mixing tee is replaced by a dilution tunnel with filter cartridges to catch the particulate emissions at the end of the tunnel [27].

2.6.2. *Sources of imprecision in the emissions measurement system*

There are many potential sources of error in the CVS system and in the exhaust gas analysers, Bielaczyc et. al. [27] neatly summarises these in a diagram of the typical chassis dynamometer test room, see Figure 2-23. Some of the factors identified by Bielaczyc et. al. [27] are sources of inaccuracy and not uncertainty, however in most cases the sources of inaccuracy can also vary on a test-wise basis meaning that they can also be sources of imprecision, hence it is valid to consider most of the factors in the context of this research.

Looking specifically at the emissions analysers Bielaczyc et. al. [27] identify the following sources of error; basic accuracy, measuring ranges, zero/span adjustment, linearization curve, calibration, measurement device temperature, gas divider accuracy and calibration gas accuracy. Other authors are in agreement with some of these error sources and have identified additional error sources including system contamination from previous tests, system out-gasing, dilution air contamination and water condensation [63]. All of these sources of error only become factors of imprecision if they vary between tests, for example a typical calibration gas bottle standard is the alpha standard, which has an accuracy of ±1%. If, between tests, the bottle standard is changed for one of a lower specification with a reduced accuracy. There will of course be a corresponding reduction in the accuracy and there will also be a reduced precision if test results are compared from analyser calibrations done on both bottles. If test results are compared from analysers calibrated using only one of the bottles then only the accuracy is affected.

Looking specifically at the CVS system Bielaczyc et. al. [27] identify the following sources of error; venturi calibration, temperatures, system leaks, dilution factor, mixing effects, pressure and condensation. Other authors are in agreement with these sources of error [63]. Again these factors are typically sources of inaccuracy, however most factors can cause imprecision when they are varied on a test-wise basis. For example when a vehicle is removed and reinstalled onto a chassis dynamometer and the exhaust connections are made, broken and remade, a system leak is quite possible and may result in imprecision when compared to results from previous tests.

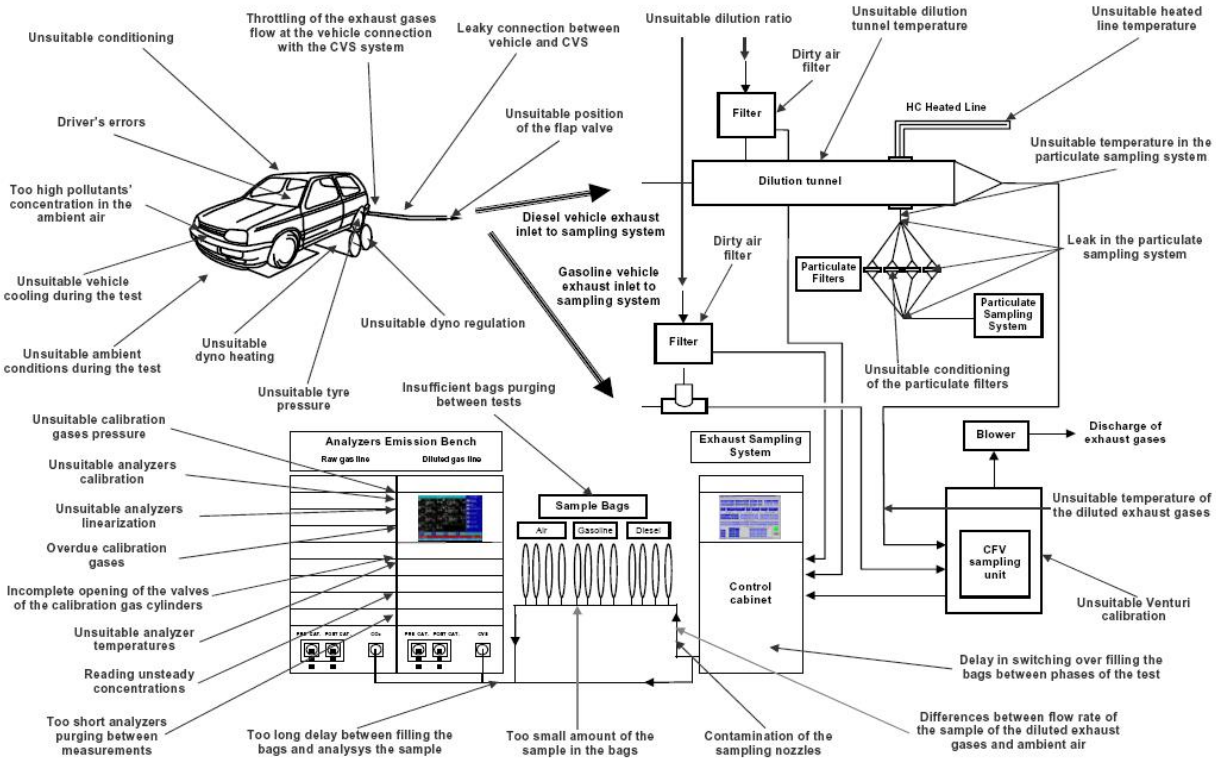

Figure 2-23: Possible error sources during exhaust emission testing on a chassis dynamometer [27]

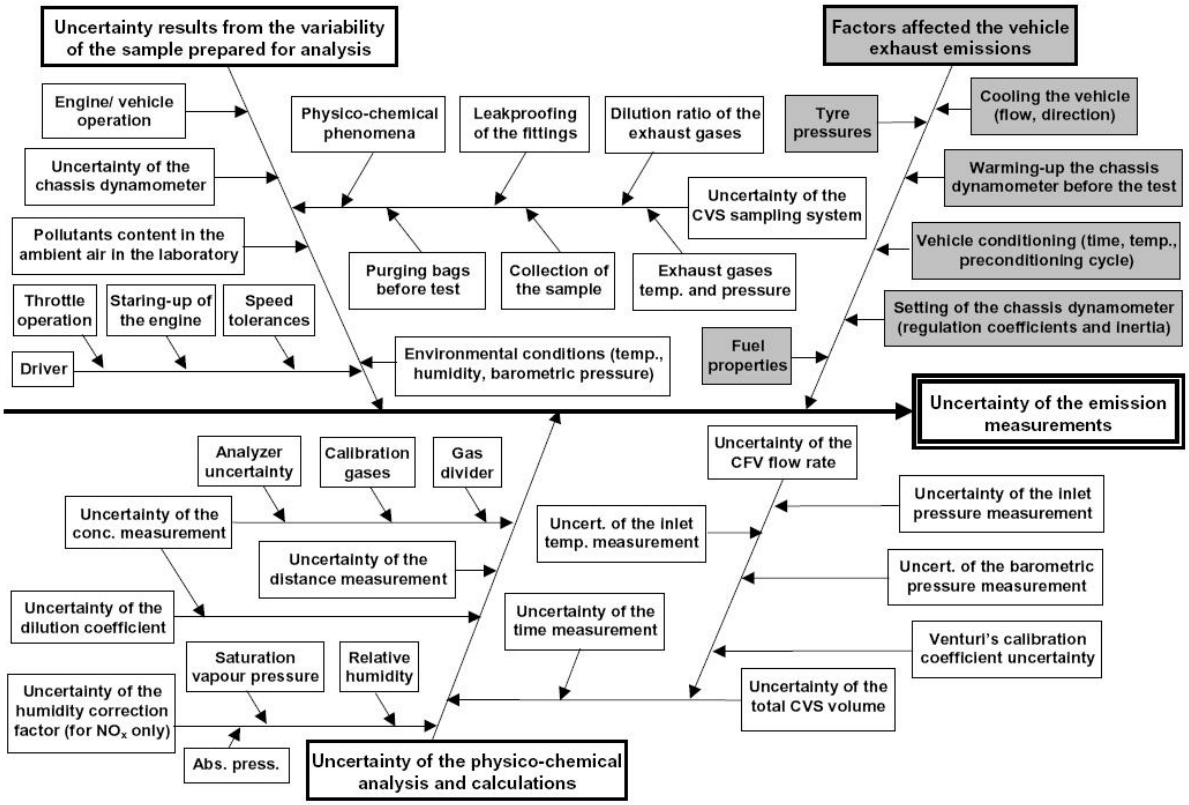

Figure 2-24: Cause and effect diagram for the uncertainty of emissions measurement [27]

When the sources of error and imprecision are compounded in an error analysis some authors have found some very high worst case uncertainties for regulated pollutants at the EURO 5 level. For example Bielaczyc et. al. [27] found that the worst case NO_x emissions error was 53% and 27% for gasoline and diesel vehicle emissions respectively. For the CO_2 emissions the corresponding worst case errors were found to be below 11% in both cases. These errors are high, however it is the author's opinion that the errors in the CVS and analysis system are unlikely to compound to give measurement errors that swing to an extreme high or low. Instead it is physically much more likely that errors will compound such that their individual effect is cancelled out somewhat and the overall effect is reduced. Since the publication of the research of Bielaczyc et. al. [27] there have been some enhancements to the CVS and analysis system such that the magnitude or the errors observed may be reduced. Some of these improvements are mentioned by Bielaczyc et. al. [27]; for example the improvement in exhaust flowrate determination via the use of a dilution air SAO.

2.6.3. *Summary of the emissions measurement system*

This section will have given the reader an introduction to the key sources of inaccuracy and imprecision from the TA emissions measurement system. The number of factors is quite vast and therefore errors can be large in magnitude, for example Bielaczyc et al. [27] state that the theoretical worst case CO_2 error is 11%. In reality the worst case error scenario is the most unlikely to occur during normal testing so errors and perhaps imprecision can be considered to be contained within a much smaller window. Determination of the magnitude of these errors would require significant additional work such that is outside the scope of this thesis.

2.7. All CO_2 noise factors

A fishbone diagram was created to summarise all the noise factors identified from the literature. The effects of each factor, extracted from the literature, are shown in brackets on the diagram as well as the largest possible effect for each area. This is shown in Figure 2-25 below.

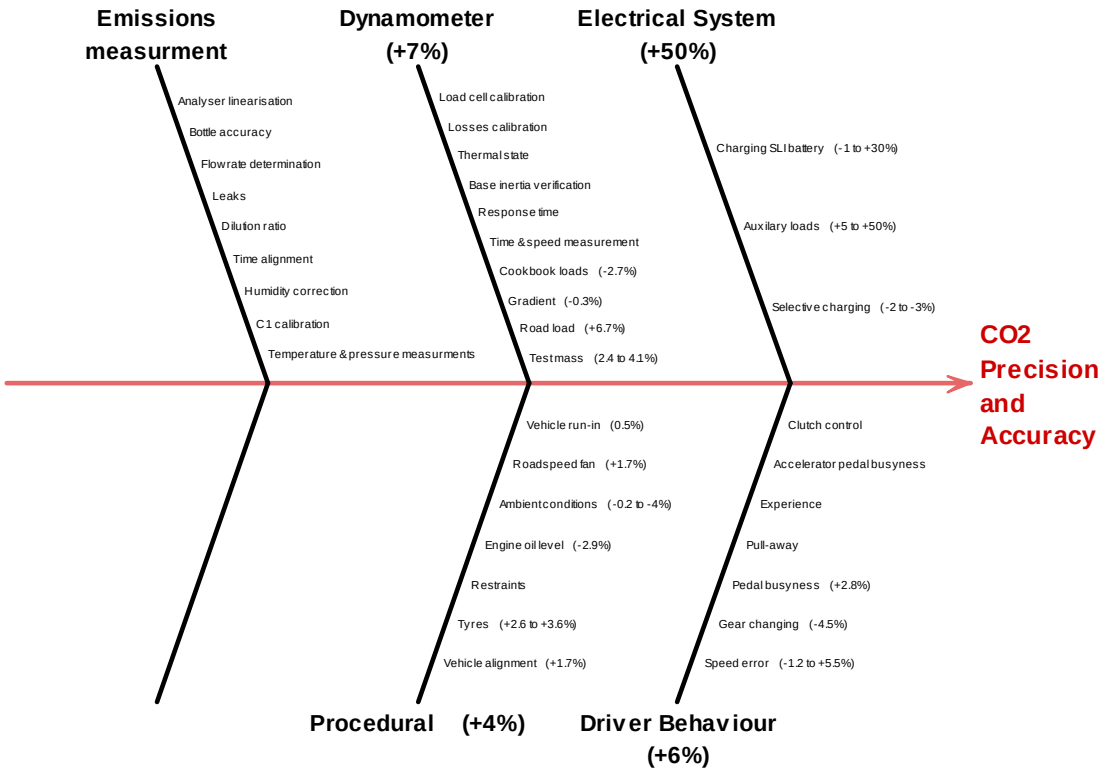

Figure 2-25: Fishbone diagram of the sources of fuel economy imprecision and inaccuracy

2.8. Chapter Summary and Conclusions

In this chapter the literature has been reviewed to determine the causes of imprecision in vehicle CO_2 emissions from chassis dynamometer tests. From this review the following conclusions are drawn:

- The vehicle electrical system is important in determining the precision of vehicle CO_2 emissions. The key factors are auxiliary loads and battery charging. Authors have shown effects for both factors can vary between as little as 1 and as much as 50% change in CO_2 emissions, showing that large perturbations are easily possible from this factor.

- Driver behaviour is important in determining the precision of vehicle CO_2 emissions. Authors have measured changes to CO_2 emissions between 0.1 and 5.5% from speed errors and 4.5% from variation in gear changes. Many authors acknowledge that there are several factors which are important in drive behaviour for which there are no quantitative metrics. The SAE J2951 drive quality standard is intended to partially address this but the standard is in its infancy and no published studies yet exist which use the standard.

- The chassis dynamometer and the load it applies to the vehicle are important in determining the precision of vehicle CO_2 emissions. One author reported a 0.63% sensitivity of CO_2 emissions per 1% change in applied road load and a 0.2% sensitivity in CO_2 emissions per 1% change in driving gradient. Another authors reported a 0.16% change in FC per 1% change in dynamometer simulation weight. The root causes of variability in a chassis dynamometer machine seems to be well understood and have to date culminated in the publishing of the DPEQAP.

- Procedural factors are important in determining the precision of vehicle CO_2 emissions. The factors that have been identified from the literature include vehicle alignment, tyre inflation pressure, tyre type, vehicle restraints, test mass, engine oil level, ambient temperature, roadspeed fan and vehicle run-in time. The magnitude of the effect recorded by authors for these factors varies in the region of 0.2 – 4% change in FC or CO_2 emissions, showing that the size of the effect from procedural factors is typically less than those from the electrical system, dynamometer or driver.

- The emissions measurement system is important in determining the precision of vehicle CO_2 emissions. A large amount of literature exists examining multiple factors resulting from the vehicle emissions measurement system and the scope of this area is outside the scope of this thesis. For this thesis it will be assumed that the vehicle CO_2 emissions can be measured in a precise and accurate way.

Chapter 3. Statistical Approach to Improving and Validating Test Precision

3.1. Statistical confidence, accuracy and precision

3.1.1. *Obtaining confidence in results*

For the most part engineers perform experiments in an attempt to validate a theory or measure the effect of a technological change to hardware. In an ideal world engineers would be able to record the entire population of results that would allow the theory or change to be validated. In reality the entire population of results is normally so vast that its measurement is totally impractical and would take far too long, for example an entire population of results could be all the FC results from all examples of a vehicle model in its lifetime. Engineers are therefore forced to conduct smaller experiments measuring only a batch of results and making inferences about the population. The resulting data set is known as a sample.

Traditionally when experiments are conducted the results are recorded more than once in an attempt to validate the experimental result. If upon repeating an experiment the results are the same, the experimenter has arbitrarily more certainty in the measured result and if the results are different the experimenter is forced to continue repeating the experiment or change the experimental setup on the assumption that there are other factors influencing the results. If the experimenter chooses to continue repeating the experiment a distribution of results will be obtained. An example of this is shown by plotting the CO_2 emissions from 100 consecutive TA style emissions tests completed on a chassis dynamometer, see Figure 3-1.

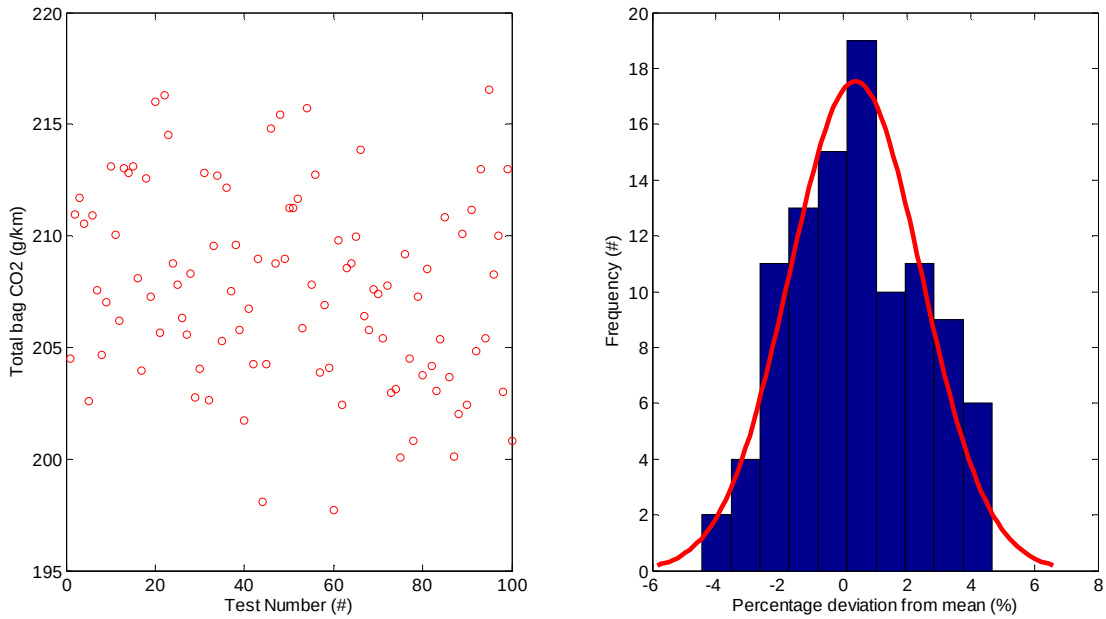

Figure 3-1: Total bag CO_2 emissions from 100 consecutive tests on a EURO 4 diesel light commercial vehicle

The sample mean is an important measure of the location of the data, however it gives no information about the spread, for which the standard deviation is commonly used measure of spread, see Equation 3-1.

$$s = \sqrt{\frac{\sum(y - \bar{y})^2}{n - 1}}$$

Equation 3-1 [65]

Where s is the standard deviation, y is the individual experimental results, y bar is the mean of the experimental results and n is the number of results. The standard deviation is given in the units of the experimental measurement, in this case g/km of CO_2. This means that it is not possible to use the standard deviation to make valid comparisons of experimental variability between experiments unless the results of the experiments are measured in the same units. It is therefore commonplace to express the standard deviation as a percentage of the mean since this allows for direct comparison of experimental variability. This is known as the coefficient of variation (CoV), see Equation 3-2

$$CoV = \frac{Standard\ deviation}{mean} \times 100$$

Equation 3-2 [65]

Given a sample of results an experimenter is usually left wondering if their results are correct or in other words how accurately does the sample mean represent the population mean. To this end the standard deviation can be used to calculate the statistical confidence interval. This is a statistical measure of the range in which the true result is expected to be; since the results of an experiment are considered to be a true random sample of the total population of results. The confidence intervals are calculated using Student's t distribution at a desired confidence level. The 95 and 99% confidence levels have become industry standard yardsticks for satisfactory confidence in an experimental result. Box et. al., [65] state that "*you should be somewhat convinced of the reality of a discrepancy (result) at the 5% level and fairly confident at the 1% level*". As an example the formula for the 95% confidence interval is shown in Equation 3-3.

$$95\%\ confidence\ interval = \frac{s}{\sqrt{n}} \times t_{n,95\%}$$

Equation 3-3 [66]

Where s is the standard deviation, n is the number of tests and t is the probability factor obtained from student's t distribution for the number of experimental tests at a 95% confidence level. The calculated 95% confidence interval can used to state the range in which 95% of the experimental results will lie; ± the calculated 95% confidence interval. Confidence intervals provide a simple way to assess the significance of differences between sets of experimental results. For example if an experimenter is wanting to compare two samples of results from before and after a technological change to a vehicle. The experimenter can calculate the confidence intervals for the two samples and if these are not coincident they can conclude that the average difference between the two samples is a real effect or a result of random variation.

In the world of chassis dynamometer emissions testing it is often the case that new and potentially expensive vehicle technologies need to be assessed on the chassis dynamometer to determine if they have a real effect on the TA emissions. If the improvements to be measured in emissions or FC are very small then the confidence intervals for the samples also need to be small. By reference to Equation 3-3 there are three ways to reduce the confidence intervals:

- Reduce the spread in the results, therefore decreasing the standard deviation
- Adopt an alternative confidence level, such that the t value is reduced
- Perform more repeat tests, thereby increasing the value of n and reducing the t value

Performing more repeat tests affects the equation in two ways firstly the denominator is increased and secondly the t value is reduced. Unfortunately this option is not very desirable since more repeat tests increases the cost of an experimental programme, which means the experimental programme will take longer, causes problems with test rig availability and can potentially introduce problems with drift over time.

Adopting an alternative confidence interval is also undesirable. As previously mentioned the 95 and 99% confidence intervals have become a statistical yardstick and therefore a reduction in confidence level below 95% is usually not allowed by the test customer, particularly in the field of automotive testing.

Reducing the spread in the results can be achieved by improving the repeatability of the experiments and reducing the random variation by identifying the important factors that are causing it. Once these factors are identified controls can be designed for them and if they cannot be controlled it may be possible to develop corrections for the factors. This too can be a costly option, however it remains by far the most desirable. It is this area that is the focus of the work presented in this thesis.

3.1.2. *Precision, accuracy and resolution*

This thesis is concerned with improving the precision of vehicle fuel economy testing on a chassis dynamometer and includes some aspects associated with improving the accuracy. It is therefore necessary to define these terms precision and accuracy and this is best achieved by considering a target as shown in Figure 3-2.

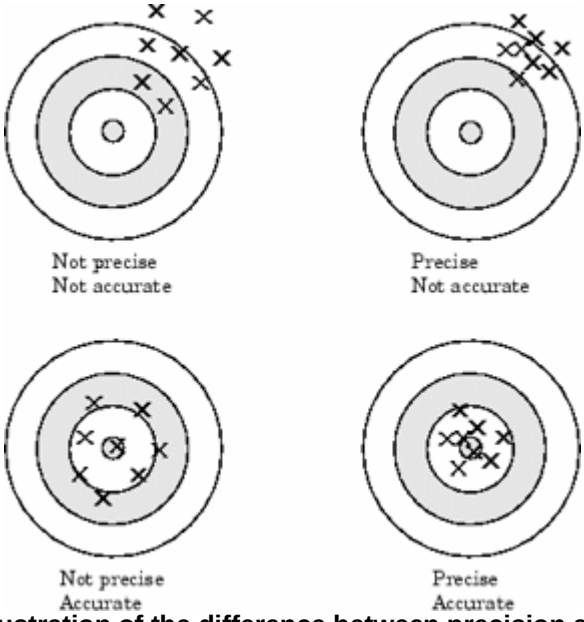

Figure 3-2: An illustration of the difference between precision and accuracy [67]

The picture in the top left of Figure 3-2 shows results that are neither precise, nor accurate; the results are scattered and off target. The picture in the top right shows results

that are precise but not accurate; the results are consistent and repeatable but off target, the target being the true answer or result. The picture in the bottom left shows results that are not precise but are accurate; the results are scattered but centred on the target. Finally the picture in the bottom right shows results that are both precise and accurate; the results are tightly clustered and on target.

The aim of this thesis is to improve the precision which, as introduced in section 3.1.1, can be measured by the standard deviation or the coefficient of variation. The accuracy of experimental results is also important and again as introduced in section 3.1.1, can be quantified by the standard error of the mean. These are therefore key metrics for the research presented in this thesis.

It is important for experimenters to ensure that the resolution of the measurement system in use is much high than the level of accuracy and precision that is required, otherwise it will not be possible to differentiate between small enough values for the target level of precision. However the resolution of the measurement equipment is not normally a cause for concern in the field of chassis dynamometer emissions testing since the equipment used is well designed and the problem of low resolution is generally well understood such that manufacturers are able to avoid these issues.

3.2. Modelling techniques

3.2.1. *Testing time*

Whenever an experiment is conducted it is important to plan the experiment such that the required data can be gained from the smallest number of experimental runs. With a large number of experimental variables, as is the case with chassis dynamometer testing, it is not practical to test every single experimental permeation. Design of experiments has become the tool of choice for satisfying this problem as shall be discussed in section 3.2.3.

3.2.2. *Model classifications*

Model based techniques have been used in the engine development and calibration communities for several decades. When combined with design of experiments techniques they can be used to quickly and efficiently develop a mathematical representation of an experimental space. Generally design of experiments is used to develop a set of experimental points that provide enough insight in the smallest number of tests possible. Modelling techniques are then used to develop a model of the resulting experimental data that represents the entire experimental space allowing the experimenter to optimise their experimental variables.

The models can be split into two classifications; physical models and data driven empirical models. A physical model is one that is built using a physical understanding of how a process works and is therefore best suited to relatively simple applications such as fundamental engine design problems. Engine calibration problems are normally too complex due to the physical, chemical and thermal processes involved in charge combustion. In these situations, where it is necessary to accurately and quickly represent the measured data, data driven empirical models have become the norm [68].

3.2.3. *Design of Experiments*

Design of Experiments (DoE) is a technique that allows the experimenter to explore a number of factors including their interactions at the same time whilst minimising the required number of tests. At the heart of design of experiments is the development of a test plan which covers the region of interest by varying factors simultaneously in a controlled fashion. One of the simplest test plans is the two level factoral design or 2^m factoral design. Such designs consist of all combinations of points at which the experimental variables take their maximum and minimum values. If one considers a two level factoral design with 3 factors when compared to a conventional one factor at a time (OFAT) approach. Figure 3-3 compares the experimental space of the DoE design to the OFAT approach. In this example the advantage of the DoE approach is that it allows the entire design space to be quantified, whereas the OFAT approach would only quantify the main effects of each factor. From the DoE approach the main factors can be estimated without the need to explicitly measure them, meaning that the main effects and their interactions can be quantified [69].

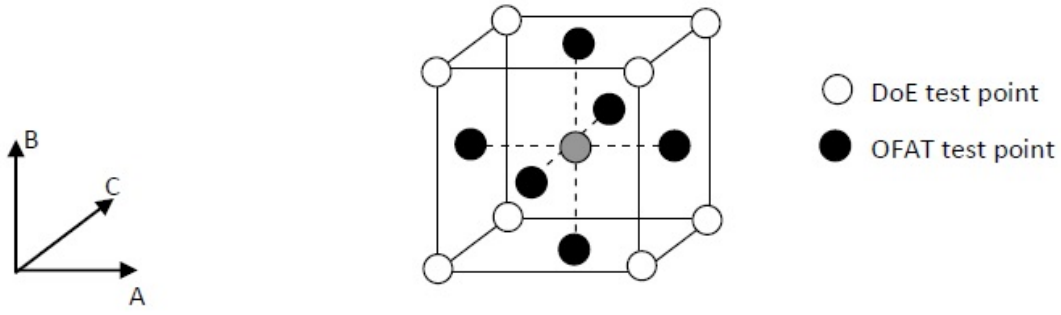

Figure 3-3: Design of Experiments two level factoral design compared to OFAT for three factors [69]

The DoE process falls hand in hand with regression modelling. To build a good data driven response model requires careful consideration of the nature of the results and the design of the experiment such that the necessary results are obtained to fit an accurate

model. There are many types of the DoE designs that can be used from the basic two level factoral designs, through full factoral, partial factoral, optimal and latin hyper cube designs. A full review of all these designs is beyond the scope of this thesis, however the basic principles that can be considered are that the choice of design will depend not only on the intended regression model but also on the experimental effort [65, 70].

3.2.4. *Regression Modelling*

In this thesis the traditional approach of starting from a clean sheet, using DoE to construct a test plan and then fitting the data to a pre-determined response model structure shall be reversed. This is because, for the most part experiments could not be planned well in advance nor was there much free capacity in the commercial laboratory environment for dedicated academic testing. Instead experimental data shall often be used from existing test programmes to construct a response model without any prior knowledge of the experimental design. In this case it is therefore most appropriate to use simple polynomial regression models, since any knowledge that guides the use of more complex techniques is unavailable. The downside with such an approach is that these regression models will likely encounter difficulties with highly non-linear responses. In such cases these factors will have to be examined on a case by case basis.

When fitting regression models a variety of methods shall be used to assist the selection of model parameters and achieve simple models with a good fit to the experimental data. Firstly a predicted residual sum of squares (PRESS) analysis shall be used. For this analysis each data point shall be removed in turn and the residual sum of squares error calculated for the remaining data points. If the model contains a parameter that causes over-fitting then the PRESS R^2 will be large since removing any one point will cause large errors [71].

Secondly a stepwise process shall be used for parameter selection. For this method the parameters are removed one at a time starting with a full model with all coefficients and removing the least significant term until all terms are significant on the basis of their confidence intervals. The method is equally applicable starting with an empty model and adding only those coefficients which are significant [71].

For models with large data sets it is not possible to use the PRESS or stepwise methods due to the large number of computations required. Instead an orthogonal least squares (OLS) method is used. The method does not require regression for parameter selection since the correlations between the output and each column of the regression matrix are assessed instead.

To determine the predictive power and goodness of fit of a regression model the following statistical tools shall be used. Firstly the coefficient of determination (R^2) which gives a measure of the variation explained by the model to the variation in the data. A downside of the R^2 method is that an increase in the number of model parameters will always cause the R^2 to increase due to increased explanation for variation by the model. The adjusted R^2 overcomes this problem by adjusting for the number of parameters in the model and will only be affected if more parameters cause a significant explanation for more of the variation in the data. An analysis of the residuals will give a measure of the size of the errors between the model predictions and the data. A PRESS analysis can also be used in much the same way that it can be used to help parameter selection. Finally if more experimental data is collected the model can be validated with an independent data set [70-72].

3.3. Process Improvement

3.3.1. *Statistical Process Control*

Statistical Process Control (SPC) is a quality control technique that utilises statistical methods to determine if a process is capable of producing the desired defect level and also if it is in control producing defect free products with a minimum of waste. Process capability is about determining if the fundamental ability of the system is good enough to achieve the desired specification. Process control is about determining if, when running the process is achieving the desired effect rate without special cause variability. A process in statistical control is only affected by common cause variability and is free of special cause variability. Common cause variability is the inherent natural variability present in any process. Special cause variability is variability caused by unusual or out of the ordinary events. A process can be in statistical control but still not be producing products that are within specification. Specification limits can be set by customer demand or expectation rather than being based off a mathematical formula. Process capability is a part of SPC that is concerned with the quantification of how close a process is to producing products that are within the specification limits [73-75].

3.3.2. *Control Charts*

Control charts are used to plot either individual results or subgroups of results with the intention of identifying if all special cause variability has been removed and therefore is the process is in control. The most basic set of control charts are the X-bar and R charts [76]. For this chart the mean of each subgroup is plotted on the X-bar chart and the range of each subgroup is plotted on the R chart. X-bar and R charts are typically used were data can be classified into subgroups of between 4 and 8 measurements and at least 20

subgroups are required as a rule of thumb [77]. An example X-bar and R chart is shown in Figure 3-4.

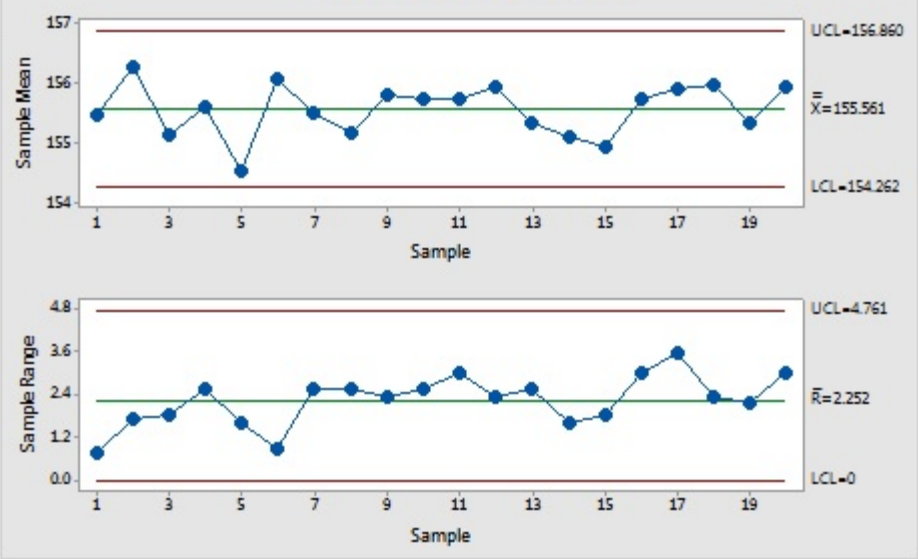

Figure 3-4: Example X-bar and R chart. The x-axis is common to both plots and is the subgroup number. The y-axis for the X-bar chart shown at the top is the mean for each subgroup, the y-axis for the R chart shown at the bottom is the range from smallest to largest within each subgroup. The charts show example data that is not from experiments related to the research in this thesis. [78]

If measurements cannot be classified into subgroups it is necessary to use the X and MR chart. For this chart the individual measurements are plotted on the X chart and the moving range between the individual points is plotted on the MR chart.

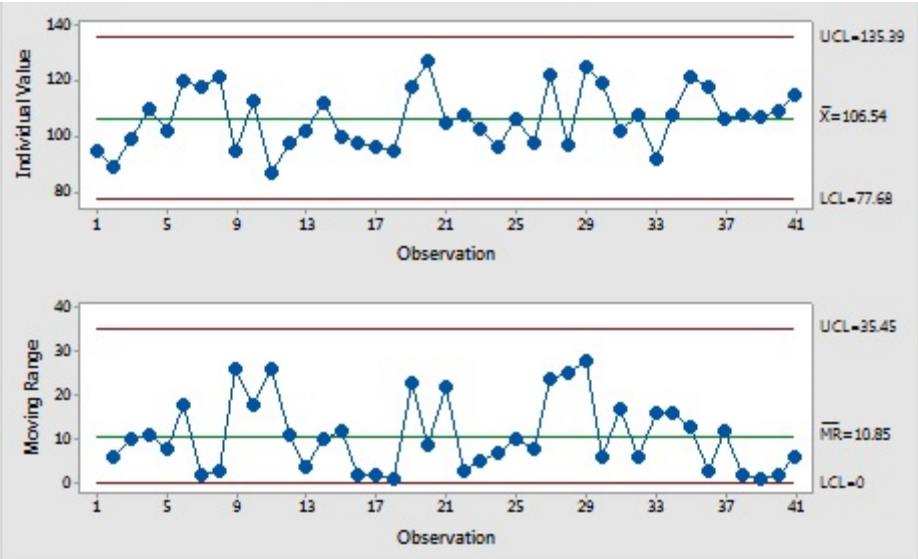

Figure 3-5: Example X and MR Chart. The x-axis is common to both plots and is the observation number. The y-axis for the X chart shown at the top is the raw value for each result, the y-axis for the MR chart shown at the bottom is the moving range from the previous to the current observation. The MR results therefore start at the second observation. The charts show example data that is not from experiments related to the research in this thesis. [78]

For both types of control chart there are upper and lower control limit lines (UCL and LCL respectively). There are standard formulae for these lines based on the chart type and are quoted in most texts on the subject [73, 77, 79], but for brevity shall not be included here.

Additionally for the control charts there is a generic set of criteria that can be applied to identify if the process is in control and identify if there are any special cause variations. These criteria are relatively universal across the literature, however there are some subtle differences between sources and therefore an amalgamation of these has been made and is presented in Table 3-1.

Table 3-1: Amalgamated SPC control chart criteria for identifying special cause variation

Key indicators of an out of control process	Reference
One point outside the control limits	[73, 77, 79, 80]
Eight or more consecutive values on the same side of the mean	[73, 77, 79, 80]
A run of six or seven alternating high and low values	[79]
A run of fourteen alternating high and low values	[73, 80]
A trend of six or seven consecutive increasing or decreasing observations	[73, 79]
2/3 of the points greater than two standard deviations from the centreline	[73, 77, 79, 80]
4/5 of the points greater than one standard deviation from the centreline	[73, 77, 80]
Fifteen consecutive points within one standard deviation of the centreline	[80]

Control charts are particularly useful in large commercial operations where processes need to be monitored to ensure that high quality is being maintained. The charts are therefore often used in manufacturing plants and could well prove useful in the commercial laboratory being investigated in this thesis.

3.3.3. *Six Sigma*

Six sigma is the name given to a set of techniques for data driven process improvement and the reduction of defects to achieve a specification limit for the mean of plus or minus six standard deviations. The techniques which were originally developed by Motorolla in the 1980's to achieve a higher quality product from manufacturing and improve profitability. In statistics the greek letter σ is used to denote the standard deviation which is a measure of the variability in a sample of data such as the results from a series of emissions tests, see section 3.1. For a process that is normally distributed, ±6σ encloses 99.9997% of the results around the mean. Therefore if a user sets a specification limit of ±6σ for their manufacturing process they are saying that 99.9997% of their products will be defect free. This was the tolerance that was chosen by the originators of the six sigma process, however the techniques and tools that developed from the evolution of the six

sigma process can equally be applied to any scenario where a process improvement is being made [76, 81].

3.3.4. *DMAIC*

Six sigma projects focused on improving an existing process typically use the DMAIC structure. DMAIC defines a five step process for process improvement with the five steps being called: Define, Measure, Analyse, Improve and Control. The Define stage is concerned with mapping out the potential business opportunity and determining the problem definition. The Measure stage is concerned with measuring the current state of the process, often this will necessitate installing new equipment to make the measurements possible. At the analyse stage the recorded data is used to determine the root cause of the problem. The improvement stage is concerned with implementing an improvement to the process to elevate the original problem. Finally the control stage is where sustained improvement is demonstrated [76, 81]. The DMAIC framework is a useful toolbox to guide any process improvement and is used extensively within the commercial field. It will therefore be applied to several sections of this thesis were individual noise factors are examined in depth.

Six sigma and SPC techniques have shown that for a complex process, such as emissions testing on a chassis dynamometer, with a large number of inputs which affect one output, it is insufficient to improve only one input when looking for an improvement on the output measure. Instead all inputs which affect the output must be improved simultaneously to expect a measurable improvement to the output [81, 82]. This is an important finding for the research in this thesis as it shows that all the significant factors must be considered and suggests that for individual factor studies it might be necessary to examine input metrics to see an improvement; knowing that ultimately an improvement in CO_2 precision would be seen if all factors are improved at once.

3.4. Chapter Summary and Conclusions

This chapter has looked at how confidence can be obtained from experimental results by improving the precision; how design of experiments based modelling tools are useful for determining important factors, how statistical process control techniques can be used to determine if a process is in control and how six sigma tools are helpful for achieving continuous improvement. Based on the findings from this chapter the following conclusions can be drawn:

- Confidence in experimental outcomes can only be improved by increasing the precision of the experiment.

- Six sigma and process control techniques have shown that in a complex multiple input single output system it is insufficient to improve the precision or control of one input factor. To achieve significant improvements in the output it is necessary to improve all important input factors.

- Statistical process control charts are extremely useful tools to identify special cause variability and therefore determine if a process is in control and capable of giving the required level of precision.

Chapter 4. Highest precision fuel consumption measurement

4.1. Introduction

A study conducted by colleagues of the author [8] which was analysed in detail in Chapter 2 used a design of experiments (DoE) approach to investigate the effect of relatively large changes in typical chassis dynamometer experimental setup parameters on fuel consumption. The study also included a control variable to simulate a typical technological change for improved fuel consumption in the form of removing the PAS pump. The findings of this study were that nine out of twelve of the experimental setup factors examined had a significant effect on the vehicle fuel consumption over an NEDC emissions test at a 95% confidence level. These findings are summarised in Table 4-1. All these effects were larger than that of removing the PAS pump, which caused a 0.6% decrease in fuel consumption. Six of these factors were also significant at a 99% confidence level. Statistical methods were used to derive tolerances for the experimental setup factors to achieve a 0.5% CoV in the measured fuel consumption [8]. The study focused on relatively large changes in the setup factors, e.g. a 90 minute battery discharge, however during normal testing programmes such large changes in setup factors are arguably less likely. This chapter aims to further the work carried out Brace et. al. [8] by implementing their recommended tolerances during a real test programme to assess the fuel consumption improvement of two candidate engine oils compared to the production (baseline) oil. These tolerances were determined to achieve a test repeatability of 0.5% CoV in the measured FC. In addition, based on the findings from section 3.2 a universally applicable method for validation of test repeatability is examined. The bulk of the work presented for this chapter was published in the IMechE Journal of Automobile Engineering [83].

Table 4-1: Main findings from the previous study conducted by Brace et. al. [8, 83]

Factor Description	Standard Condition	Perturbed Condition	Fuel Consumption change (%)	Significance 95%	99%	Recommended tolerance
Battery discharge (V)	Normal	90min discharge from headlamps	8.7	Y	Y	±0.2V
Engine start temperature	-7°C	-4°C	0.2	N	N	Insignificant
Engine oil level	Upper dipstick mark	Remove 2.5l	-2.9	Y	Y	±0.45l
Pedal busyness	Normal	Double pedal activity	2.8	Y	Y	±25%
Speed error	None	3kph fast on cruises	5.5	Y	Y	±0.3kph
Road speed fan	Normal	+40% over speed	1.7	Y	N	±20%
Vehicle alignment	0	75mm offset	1.7	Y	N	±25mm
Tie-down straps	Horizontal	Angled	0.3	N	N	Insignificant
Tyre type	Production	Sports	3.6	Y	Y	N/A
Tyre pressure	Normal	Low	2.6	Y	Y	±0.1bar
Vehicle mass	1479kg	1617kg	1.5	Y	N	±50kg
PAS Pump	Production	Removed	-0.6	Y	Y	N/A

4.2. Experimental Method

A test programme was conducted on a chassis dynamometer using a Toyota Aygo test vehicle with a 998cc naturally aspirated spark ignition gasoline engine with variable valve timing, coupled to a 5 speed manual transmission. The test programme was designed to assess any fuel consumption benefit of two candidate engine oils relative to a production and hence baseline engine oil. The engine oils were tested over a number of days with three NEDC tests being completed each day and a climatically conditioned overnight soak of approximately 15 hours between each test day. The primary requirement of the test programme was to determine the fuel consumption benefit during a cold start test, TA style emissions test, however there was also a requirement to assess the hot start performance. Therefore each day the three tests were performed two with a cold start condition and one with a hot start condition. Of the cold start tests, one was performed following an overnight soak and the other following forced cooling of the vehicle. The number of test days for each oil was approximately four, although this varied due to practical constraints. In-between each test candidate oil a flush and fill cycle was completed to prevent any contamination of the test oils from residuals in the engine sump or galleries. All tests and soak periods were conducted with the test cell conditioned at

25°C, to mirror the requirements of legislative TA emissions testing [9]. Prior to the start of the test programme the dynamometer road load was set for the test vehicle by iteration to achieve bag CO_2 emissions that matched the type approval value for the Toyota Aygo test vehicle. Once the type approval value of 108g/km [84] was achieved the dynamometer load was not adjusted for the duration of the test programme. During the road load setting process, the dynamometer was prepared for testing by operating it at a fixed speed for a period of time, as per manufacturer recommendations, to ensure the system, especially the bearings were warm and hence that the parasitic losses were stable. Then immediately following the warm up the dynamometer losses were evaluated and compensation coefficients derived. Then the dynamometer inertia simulation performance was verified, all these procedures were again completed in accordance with the dynamometer manufacturer's recommendations. Since the road load was not adjusted for the entire test programme the dynamometer was always prepared prior to each test using the same warming procedure and the same loss compensation coefficients. In addition an inertia simulation check was performed immediately prior to every test and all tests were immediately followed by a vehicle coastdown test. In the first instance this was to verify the dynamometer performance prior to each test and in the second to verify the dynamometer and vehicle loading immediately after a test.

To maintain the precision of the test conditions day to day the vehicle was always conditioned in the same manner prior to each test. The first cold start test of each day was referred to as the 'overnight cold' test, prior to which the vehicle was subject to an overnight soak in the conditioned cell with a target temperature of 25°C. The resulting typical engine sump temperature was 23°C and the authors believe that the reason for the slightly lower engine sump temperature was due to a low flow rate cold air draft over the engine sump from the dynamometer pit. The second cold start test is referred to as the 'forced cold'. This test was aimed to replicate the overnight cold test but instead used forced cooling. By iteration via experiments on the vehicle the following cool down procedure was developed and used throughout the test programme:

1. Immediately after overnight cold test, vehicle bonnet up
2. Roadspeed fan to 75% and cell temperature depressed to 15°C
3. Monitor oil sump temperature until it reaches 30°C
4. Raise cell temperature back up to 25°C and turn off roadspeed fan
5. Leave vehicle to soak for a minimum of 30 minutes

The cooldown procedure resulted in a typical oil sump temperature of 23°C immediately prior to the start of the test so the cooldown procedure was deemed to be as close a match to the overnight soak condition as was practically possible. For the hot start test condition each day, referred to as a ‘hot test’, the vehicle was warmed by driving it in 5th gear at 120-130 km/h until the oil sump temperature reached 90°C. Approximately 7miles of driving was required to achieve this. The vehicle was then brought back to a stationary idle and the emissions test was immediately started. Figure 4-1 shows the test sequence diagram.

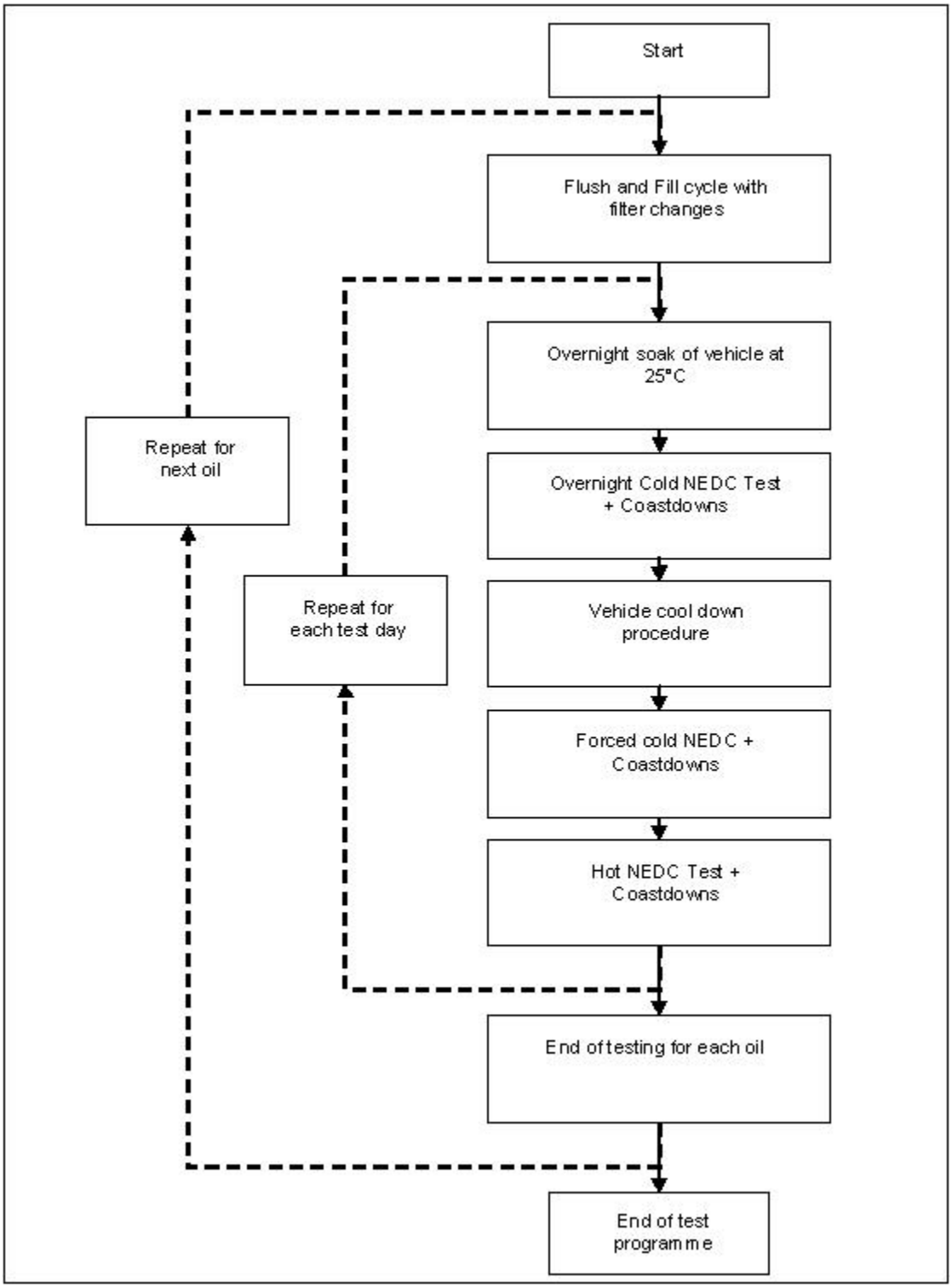

Figure 4-1: Diagram of the test sequence [83]

In an attempt to isolate any effect on fuel consumption caused by vehicle drift over time, each candidate oil was bracketed using the baseline oil. Figure 4-2 shows the test sequence for the oils tested. The baseline oil was chosen because it has a significantly higher viscosity than either of the candidate oils. It was therefore expected that a higher fuel consumption would be measured when the vehicle was tested with the baseline engine oil. The full properties of the oils including what additives they had was not known

by the author and therefore it was not possible to predict the likely change in fuel consumption between the candidates.

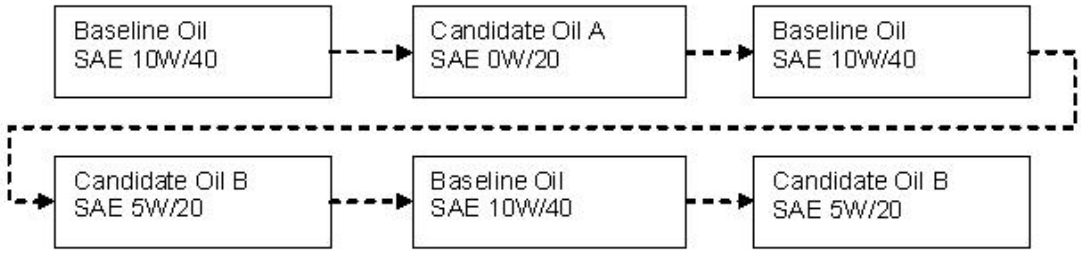

Figure 4-2: Diagram of the oil test sequence [83]

The fuel consumption was measured using the industry standard bag analysis method. For this method a carbon balance is performed on the exhaust gases collected over the entire NEDC emissions test [9]. Figure 4-3 shows a schematic of the experimental setup including the locations for the gas sample points.

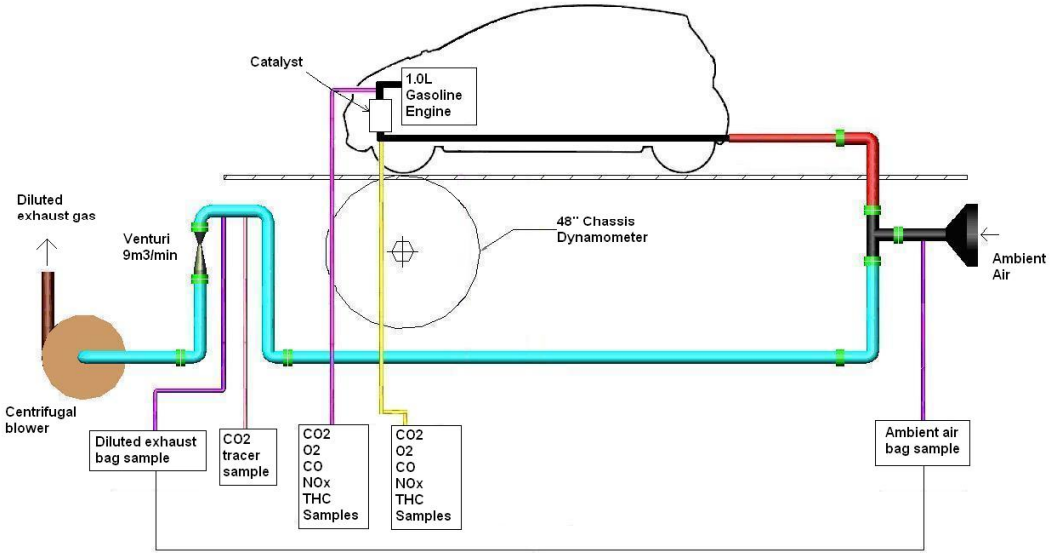

Figure 4-3: Schematic diagram of the test cell [83]

Throughout the test programme all the factors identified in the previous study [8] were controlled within the suggested tolerances where possible. The following sections describe how this was achieved in each case.

4.2.1. *Battery State of Charge*

Whenever the vehicle was not being tested the battery was put onto trickle charge from a conventional battery charger. Such battery chargers do not attempt to measure the SoC of the battery and instead continually apply a fixed voltage charge, allowing the current to reduce to near zero as the battery nears fully charged. Such chargers will therefore continue to charge a battery even once 100% SoC is reached, eventually resulting in damage to the battery. It is possible to gain an estimate of the battery SoC from measuring the open circuit voltage, providing care is taken to ensure the surface charge has dissipated which could give a false high reading. However estimating lead acid battery state of charge from open circuit voltage is not very accurate. It is also possible to take a sample of electrolyte into a hydrometer and determine the specific gravity of the electrolyte as a measure of SoC, since the electrolyte becomes heavier as the battery charge increases. However the accuracy of the reading is highly dependent on the electrolyte level and this method is practically hazards since it involves handling acidic electrolyte. The most accurate method is to do a discharge test, but this test results in a discharged battery and a battery that can't be used for the experiment [18]. Clearly measuring lead acid battery SoC is a difficult problem which highlights the need to make battery current measurements during testing, rather than attempt to quantify the SoC prior to the test. Therefore for these experiments the conventional battery charger was used and left attached to the battery between tests. If the time between tests was consistent, which was likely, given the experimental programme adopted with daily testing, the battery SoC should have been controlled consistently to near 100% at the beginning of each test.

Since a partially discharged battery at the beginning of a test will require charging from the vehicle alternator during a test there will be an uncontrolled increase in fuel consumption. Starting every test with a fully charged battery should ensure that there is a consistent charge by the alternator in the initial phases of the overnight and forced cold NEDC tests. This is because there is a consistent discharge from the battery at the start of these cold tests from the starter motor. For the hot test condition the engine is already running at the start of the test and the battery should be fully charged during the warm up driving period.

During every test a current clamp meter was installed onto the vehicle to measure the flow of current from and into the vehicle battery. Following each test a cumulative sum of the current flow was calculated to be used as an indicator of the net current flow consistency test to test.

The previous study by the authors used the battery voltage as an indication of the battery state of charge and a tolerance of ±0.2V was suggested, see Table 4-1 [8]. Conventional automotive battery chargers do not allow the user any control over the charging and

simply aim to fully charge the battery. Practically, this makes it very difficult to enforce the recommended ±0.2V tolerance. The best that can be achieved is to hope that by continually charging the battery, the voltage is within tolerance. A measure of the battery voltage was taken prior to the start of every test to enable an assessment of the battery voltage repeatability.

4.2.2. *Engine Start Temperature*

A thermocouple was installed into the engine oil sump so that a consistent oil sump temperature could be identified at the start of each test. The engine coolant temperature was also logged from the engine control unit (ECU), since this can often form the basis for ECU changes to spark or fuelling maps which may cause unforeseen changes to the fuel consumption.

4.2.3. *Engine Oil level*

During the flush and fill cycle for each candidate test oil only the quantity of oil recommended by the vehicle manufacturer was added; 3.3 litres. During a given test week the oil level was checked daily and never needed to be topped up. This meant that quantity of engine oil in the vehicle sump was controlled well within suggested tolerance of ±0.45l [8].

4.2.4. *Pedal Busyness and Speed Error*

A human driver was used throughout this test programme. Therefore driver measures such as pedal busyness and cumulative speed error could not be directly controlled. However a test validation criterion of ±0.5 km/h and ±1 % was implemented on the speed error, meaning the requirements of both the British standard and the legislative emissions testing regulations were met [9, 85]. The pedal busyness was calculated for every test using pedal position data logged from the ECU. The pedal busyness is defined as the cumulative rate of change in the pedal position over the drive cycle. It can be calculated by taking the derivative of pedal position and summing the absolute value of the derivative on a second by second basis over the entire drive cycle.

4.2.5. *Road Speed Fan*

Throughout this test programme the road speed fan was controlled by the chassis dynamometer control system with the speed of the fan being proportional to the simulated vehicle speed, as measured by the rollers. The road speed fan was therefore controlled well within the recommended tolerance of ±20% [8].

4.2.6. *Vehicle Alignment and tie-down straps*

The vehicle was aligned onto the chassis dynamometer (parallel to the rollers) at the beginning of the test programme. Once aligned the rear wheels of the vehicle where clamped to the floor and the front of the vehicle was held using tie-down straps during testing. Following the previous work by the Brace et. al. [8] these straps where positioned horizontally to prevent any vertical force being imparted onto the vehicle that might adversely affect the rolling resistance. To minimise differences in the vehicle alignment test to test, the vehicle was not removed from the dynamometer for the duration of the programme. However in-between each test the tie-down straps did have to be removed and re-attached and therefore before every test two checks of vehicle alignment were carried out. Firstly the position of the vehicle on the rollers was checked by measuring the distance from the tyre side walls to the edge of the rollers. Any movement outside of the suggested tolerance from the previous study (±25mm) [8] would have been corrected by re-aligning the vehicle although this was not necessary during the test programme. Secondly to check there were no variations in the vertical load on the front wheels, the height of each front wheel arch from the roller crown was measured prior to every test although again it was found that there were no measurable variations throughout the test programme.

4.2.7. *Tyre Type and Tyre Pressure*

Throughout this test programme the same tyres were used on the vehicle and the tyre pressures where checked at the start of each test day prior to the start of the overnight cold test. The checks were carried out using a calibrated gauge manufactured by ‘Intercomp’ with a stated accuracy of 0.1% of full scale deflection and a full scale measurement range of 99.99psi, yielding an expected error of 0.0999psi. The cold tyre pressure set point was 2.76bar and with the gauge used in this research, the pressure should have been controlled within the 0.1bar recommended tolerance from the work of Brace et. al. [8]. The tyre pressures where then not adjusted again for the rest of each test day as it was perceived that the consistent nature of the test scheme would result in consistent tyre pressures during each of the three test conditions (overnight cold, forced cold and hot). The procedure for checking the tyre pressures was to overinflate the tyre slightly and then to deflate the tyre until the specified pressure was measured on the gauge. This was done to remove any effect of hysteresis in the gauge.

4.2.8. *Simulated Vehicle Mass*

The simulated vehicle mass throughout the entire test programme was 875kg and this was not altered. An inertia verification check was performed prior to every test and the

CoV of the reported inertia result from this test was 0.1% over the entire test programme. For the 875kg test vehicle, a 0.1% inertia error corresponds to 0.875kg which is well within the suggested tolerance of ±50kg [8].

4.2.9. *Ignition Timing*

In addition to the testing factors already identified from the previous study, the ignition timing for cylinder 1 was also logged from the ECU. The timing is directly related to the efficiency of the combustion occurring in the engine and hence is inextricably linked to the fuel consumption [11]. The cumulative sum of the ignition timing was calculated from the recorded ECU data to provide an indication of variations test to test, despite the value having little direct physical meaning.

4.2.10. *Initial Cell Air Temperature*

The test cell air temperature was controlled to a target temperature of 25°C for the entire test program. The instantaneous air temperature at the start of the drive cycle was recorded for every test to check for repeatability. During the test programme the initial cell air temperature was very consistent, for all test conditions the temperature varied within approximately ±0.5°C. For the forced cold tests the initial cell air temperature was less variable; the CoV of initial cell air temperature falling from 1.5% for the overnight cold tests to 1.1% for the forced cold tests. This was probably due to the rigorous nature of the forced cool down procedure.

4.2.11. *Coastdown time*

Immediately following the end of every drive cycle test the vehicle was subjected to three coastdown tests to check the repeatability of the rolling resistance and road load simulation. For these tests the dynamometer was used to motor the vehicle up to 130 km/h and then the vehicle was allowed to coastdown and the time taken for the vehicle speed to drop from 120 to 20 km/h was recorded. This was repeated three times and the average time from the three runs was taken as the coastdown time for that test.

4.3. Results

4.3.1. *Implementation of Statistical Tolerances*

Figure 4-4 shows, at each test condition, the average fuel consumption results for the baseline oil and each candidate oil over the entire test programme. The coefficient of variation (CoV) for each data set is also shown which gives an indication of the repeatability. Of the total number of tests completed approximately 30% were identified as outliers. Of this 30%, two thirds were due to either technical malfunctions of the emissions

measurements system resulting in there being no FC data recorded or ECU data logger errors, again resulting in no data being recorded. One third of the outliers were caused by driver violations outside the legal tolerance as defined in section 4.2.4. Importantly no tests were made invalid unless one of these criteria was met and there was a reason to mark the test as invalid. In total there were 61 valid tests.

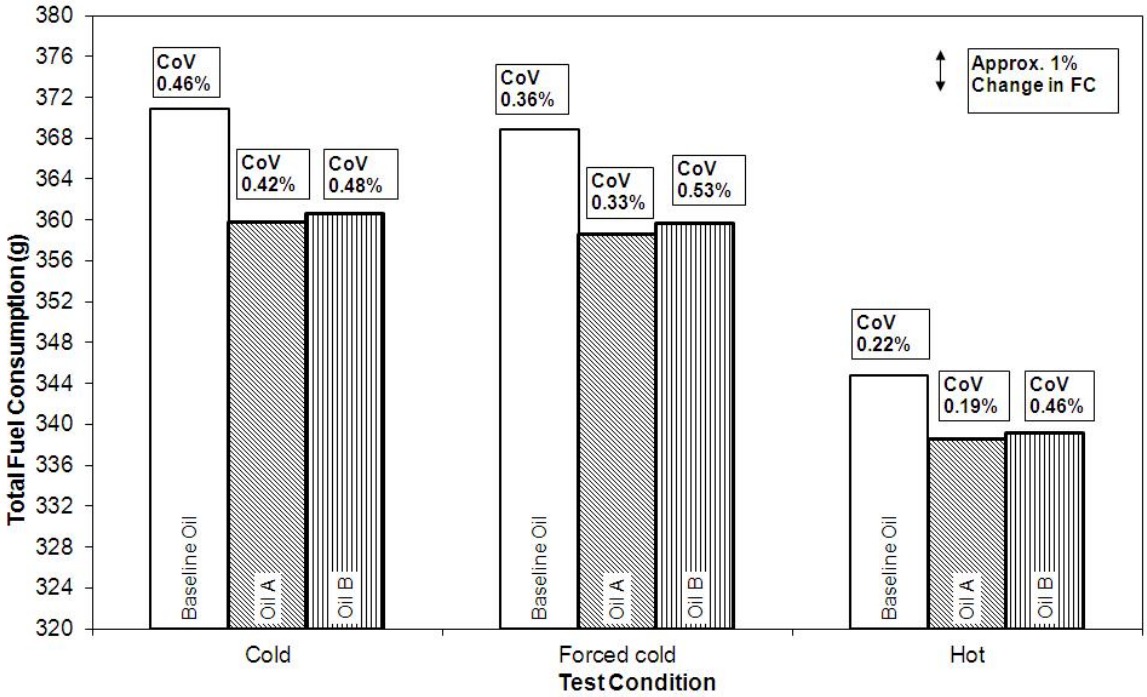

Figure 4-4: Fuel consumption results from the entire test programme [83]

The recommended tolerances from the work of Brace et. al. [8] were applied throughout the test programme. These statistical tolerances were developed with a repeatability target of 0.5% CoV, a target that has been achieved in all the data sets from this programme, thereby demonstrating that these tolerances can be successfully implemented.

For some of the data sets the required level of repeatability has only just been achieved, for example the 'forced cold' condition tests on oil B, whilst for others, for example the 'hot' condition tests on oil B the variability has been more than halved from the target. This inconsistency in the testing precision suggests that the testing could still be more tightly controlled and that there are still factors contributing to the variability beyond the factors previously identified.

As detailed in the experimental approach section, see section 4.2, several of the test setup factors that were sought to be controlled were also logged either continuously during each test, or once on a test-wise basis. Those factors which were logged continuously enabled the calculation of one-number metrics. For example the ignition timing was logged from the ECU throughout each test, enabling the cumulative ignition

timing to be calculated. Initially all such factors were examined as a time series to look for any large trends with fuel consumption and the resulting plots are shown in Figure 4-5, Figure 4-6 and Figure 4-7. Processed results were available for a total of eight test setup factors and these were:

V1 – Cumulative battery current

V2 – Initial oil sump temperature

V3 – Cumulative speed error

V4 – Pedal Busyness

V5 – Cumulative throttle position

V6 – Cumulative ignition timing

V7 – Initial test cell air temperature

V8 – Average total coastdown time

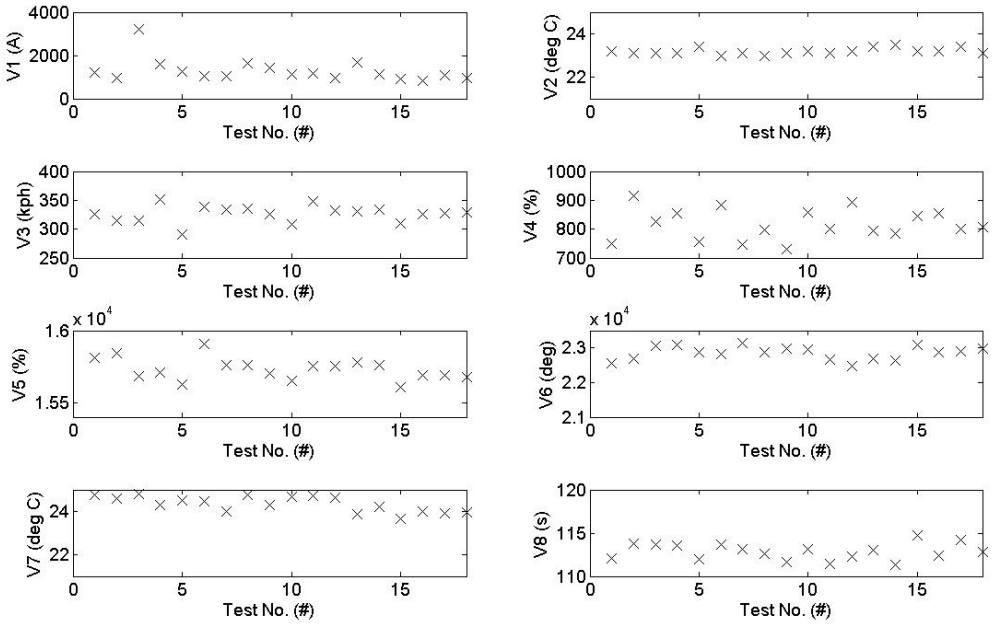

Figure 4-5: Plots of the variability in the noise factors from overnight cold tests [83]

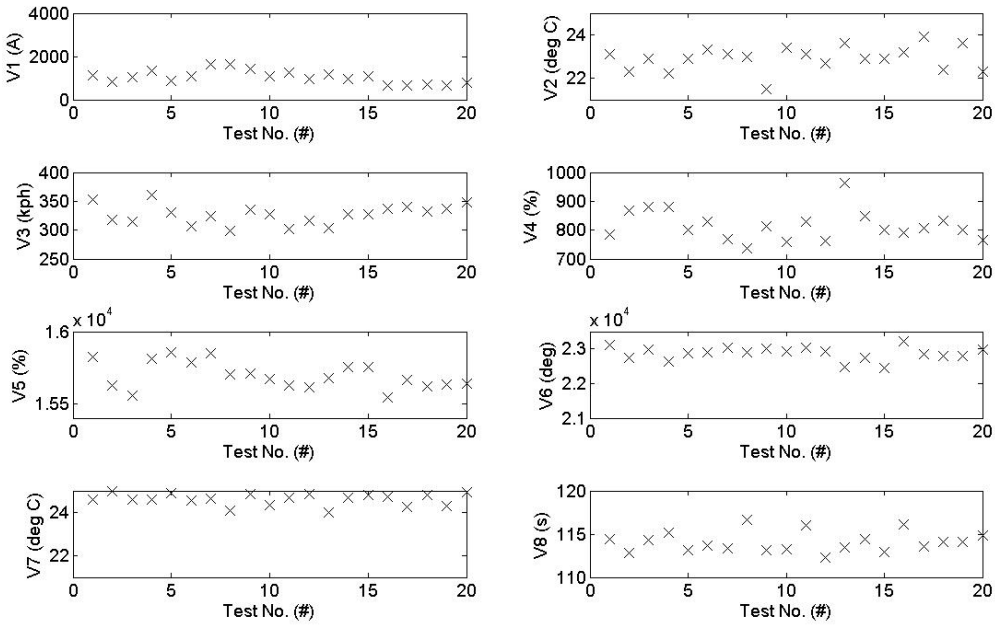

Figure 4-6: Plots of the variability in the noise factors from forced cold tests [83]

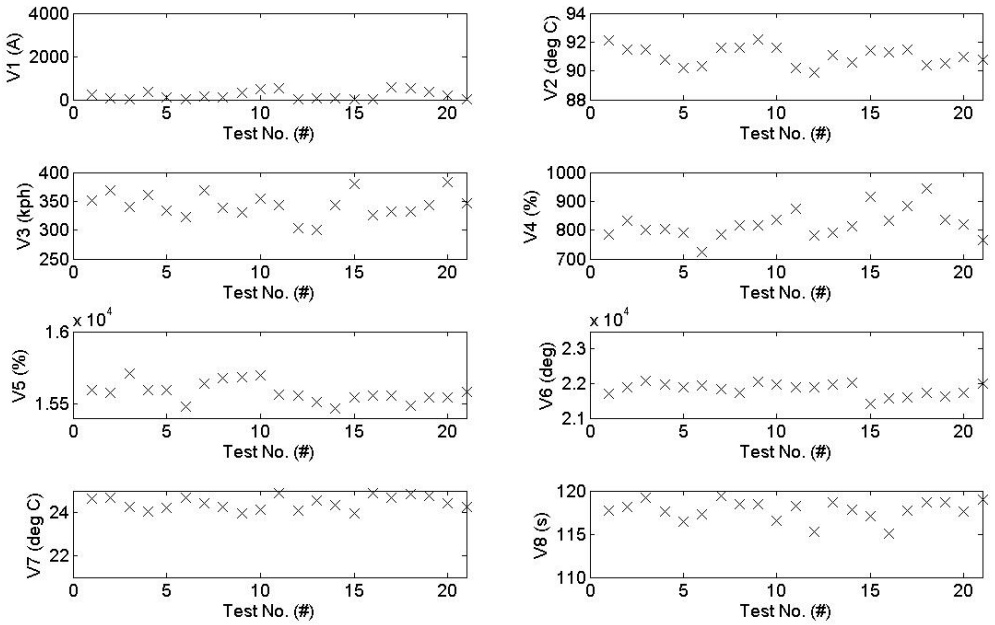

Figure 4-7: Plots of the variability in the noise factors from hot tests [83]

Figure 4-5, Figure 4-6 and Figure 4-7 show that most of the factors appear relatively consistent test to test, since there are only a couple of potential outlier tests. For example the third overnight cold test has a cumulative sum of battery current that is approximately doubled from the previous test, although this is not reflected in the fuel consumption result from that test. Aside from individual tests, the general trends of increased variability in some factors rather than others was not found to cause increased correlation with fuel

consumption when examined on a one factor at a time approach. However this straight forward methodology does not allow for variation that is a function of multiple factors; for that it is necessary to construct a regression response model including as many factors as possible.

4.4. Response Modelling

4.4.1. *Test Factors*

In the following sections several response models are constructed and these are based on the test factors which are listed in Table 4-1.

4.4.2. *Model Description*

A multiple linear response or MLR model was created and fitted for the data for all the eight factors identified in Table 4-2 and from the results of 61 valid tests. The form of the resulting model using the MLR technique can be written as shown in Equation 4-1 below.

$$y_u = \beta_0 + \beta_1 x_{1u} + \beta_2 x_{2u} + \cdots + + \beta_k x_{ku} + e_u$$

Equation 4-1 [86]

Where y represents the variable being fitted by the model with a number of variables equal to k and x dependant variables.

Table 4-2: Response model factors [83]

Identifier – Noise Factor (NFx) or Variable (Vx)	Factor	Units	Factor type (continuous data, one-number metric or qualitative)	Qualitative factor settings
NF1	Mileage	Miles	One-number	-
NF2	Cumulative Throttle Position	%	Continuous data	
NF3	Cumulative Battery Current	A	Continuous data	
NF4	Pedal Busyness	%/s	Continuous data	
NF5	Cumulative Ignition Timing	°	Continuous data	
NF6	Accumulated Speed Error	Km/h	Continuous data	
NF7	Average Total Coastdown Time	s	Continuous data	
NF8	Initial Oil Sump Temperature	°C	One-number	
V1	Test Oil	-	Qualitative	Baseline, A, B
V2	Test Type	-	Qualitative	Overnight Cold, Forced cold, Hot

There was a large range of values recorded between the noise factors, for example the cumulative ignition timing is four orders of magnitude different to the oil sump temperature for every test. To prevent this causing any problems when fitting a model, all the noise factor results and the fuel consumption responses were normalised by scaling their value between 0 and 1. Initially the modelling results showed extremely low confidence in the predicted effects of the noise factors and this was due to two of the model input factors being highly correlated; namely the initial oil temperature and the test condition, since these are both dependant on the temperature of the vehicle. To have confidence in any response model results it is important that the factors are independent. If two input factors are highly correlated it will be difficult for the model to determine which factor is responsible for the change in fuel consumption and therefore the confidence in the effects predicted by the model will be low [65]. The extent of the correlation between the input factors can be assessed by examination of the correlation coefficients. Brace et. al. [8] remark in their reference to McPherson: "*It is generally accepted that a correlation coefficient of greater than 0.8 and less than -0.8 indicates a strong relationship, greater than 0.5 or less than -0.5 a fair amount of correlation and below 0.2 or above -0.2 a weak correlation*". Examination of the correlation coefficients for the model with all factors highlighted that there was a strong correlation between the initial oil temperature and the test type as the corresponding correlation coefficient has a magnitude of 0.9. Physically it is logical that the initial oil temperature would be highly correlated with the test condition, as the criteria for the test conditions are based on the oil temperature, see section 4.2. It is therefore necessary to exclude the oil temperature from the modelling before proceeding.

Once the initial oil temperature was excluded as a variable from the model a good level of fit was achieved and this is shown in Figure 4-8.

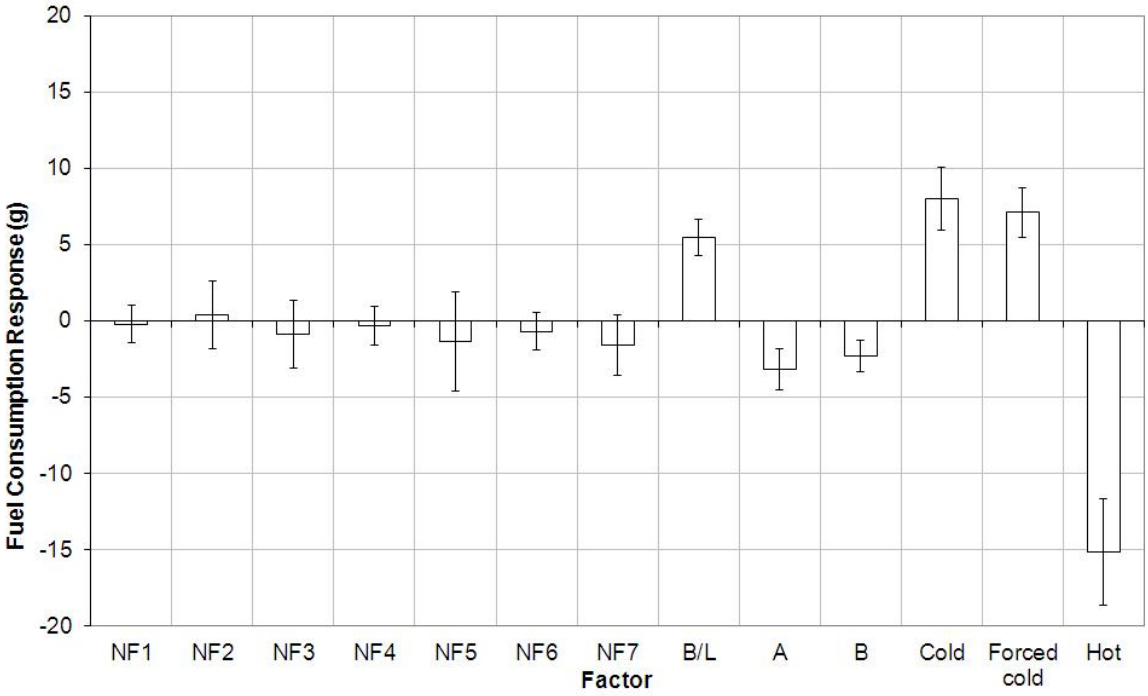

Figure 4-8: Main effects plot for the MLR model with the initial oil temperature removed [83]

The level of fit of the model is good with an R^2 value of 0.982 and an adjusted R^2 of 0.971. The level of fit gives an indication of how well the model fits the experimental data and can be assessed using the coefficient of determination, R^2. The coefficient of determination is a measure of the differences between the fitted model and the recorded data. The closer the R^2 value is to 1 the better the level of fit and in this case the model had an R^2 value of 0.982 and an adjusted R^2 value of 0.978. This means that 98% of the variability in the fuel consumption results can be explained by the eight noise factors, the test type and the oil type. The ability of the model to predict responses can be determined by performing a predictive residual sum of squares, or PRESS, analysis. PRESS analysis is conducted by removing points in turn from the data set and assessing the error between the full regression model fitted to all data points and the model fitted with each point removed. The PRESS R^2 value is based on these principles and can therefore be used to arbitrate the model's ability to predict data that has not been measured. It can also identify instances of model over fitting, where by a high R^2 value is obtained but the calculated PRESS R^2 is low [71]. Like the coefficient of determination the closer the calculated PRESS R^2 value is to 1, the better the model can predict the data. In this case the PRESS R^2 is 0.969 so the model's predicative ability is very good.

However, whilst the confidence in the model overall has been improved, the confidence in the predicted effects from the test factors is still very low. The greatest confidence in one

of these effects is seen for the average total coastdown time where the confidence interval spans a range approximately twice the magnitude of the model predicted effect. The confidence in the effects of the test type and the oil type are much greater than those of the test factors and the intervals for most of these effects do not cross the axis and are not overlapping indicating that they are statistically significant effects. Since there are extreme differences between the relative magnitudes of the confidence intervals and the predicted effects for the test factors compared to the test conditions, combined with the very good fit and predictive power of the model it is possible to conclude that none of the test factors have a significant effect on the fuel consumption. It is therefore possible using this technique alone to conclude that with the data recorded, all of the test factors that are known to cause significant changes to fuel consumption have been adequately controlled. That is, none of these factors are causing changes to fuel consumption that obscure the fuel consumption change as a result of the primary test variables, in this case the change in engine oil type and start temperature.

To improve the confidence in the model predictions further and to prove the predictive power of the model, the test factors were removed one factor at a time, starting with the effects with the smallest effect to confidence interval ratio. The resulting optimised model is shown in Figure 4-9.

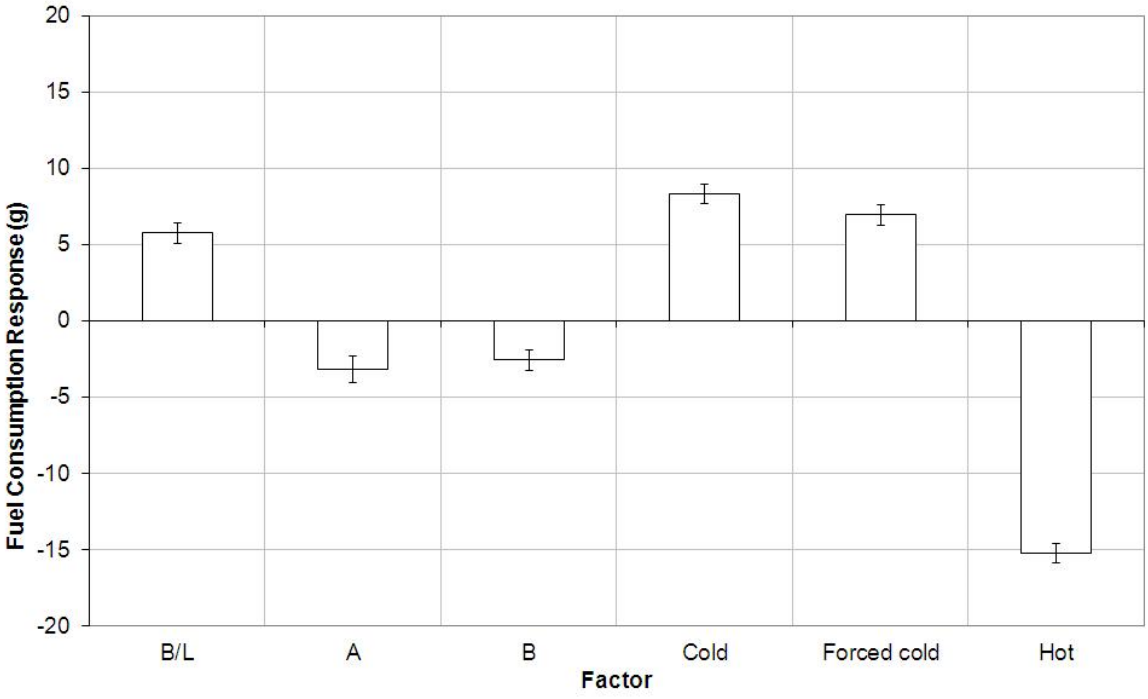

Figure 4-9: Main effects plot for the optimised MLR model [83]

For the optimised model the level of fit is very good with a R^2 value of 0.979 and an adjusted R^2 value of 0.977. The predicative power is also good as the PRESS R^2 is 0.975. By removing the test factors, the predictive power of the model has been substantially

improved as the ratio of the magnitude of the confidence intervals to the predicted effects has been increased throughout the model.

One factor that was discussed in the section 4.2.1 but has not included in regression response modelling is the battery voltage. This is because it was not recorded correctly for all 61 tests, instead it was only recorded for 52 tests. Figure 4-10 shows the results from the measurements of battery voltage.

Figure 4-10: Initial potential difference at battery terminals for all test conditions [83]

For the overnight cold and hot start tests the battery voltage has been approximately controlled within the ±0.2V tolerance, however for the forced cold tests the battery voltage spans a range of ±0.5V. This increased variability in battery voltage for the forced cold test is not replicated in the cumulative battery current results. Since the cumulative battery current results built into the previous response model, see Figure 4-8, showed that battery current was adequately controlled during the tests. The inference must be that the battery state of charge and voltage prior to the test were adequately controlled. To determine if the battery voltage variability was causing imprecision in the fuel consumption results a final response model was constructed for the smaller subset of tests where the battery voltage was recorded. Again the model was initially constructed with all the factors and the factors were removed one factor at a time until an optimised model was developed that included the effect of battery voltage and this is shown in Figure 4-11.

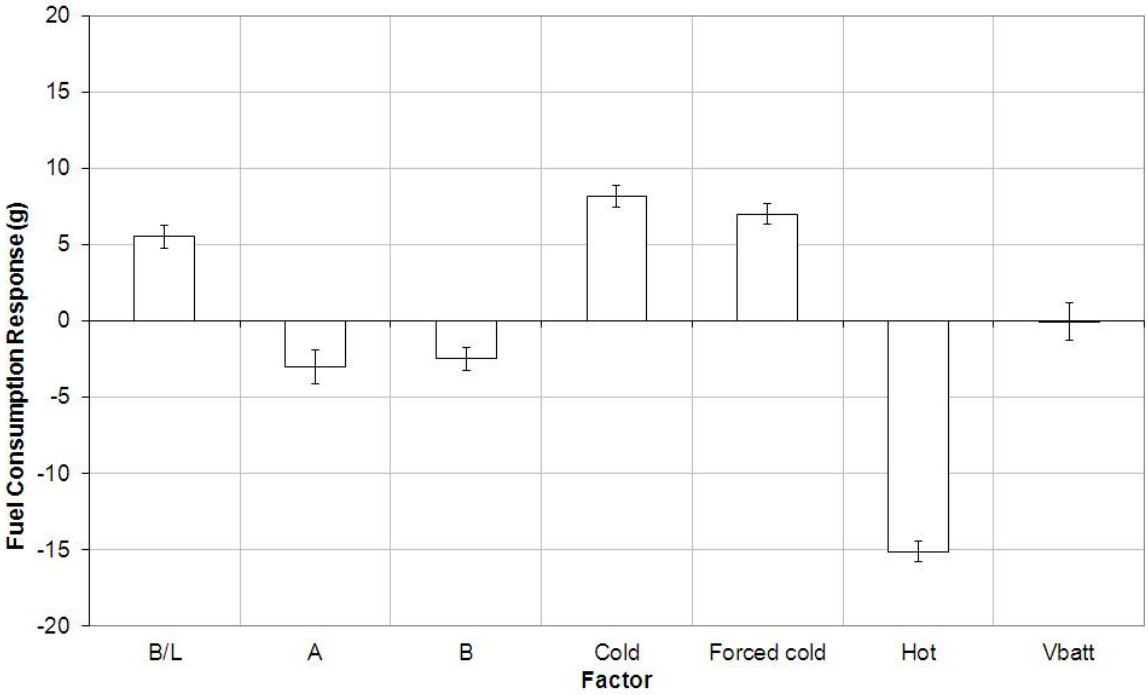

Figure 4-11: Main effects plot for the optimised MLR model with initial oil temperature removed and including battery voltage [83]

The response model of Figure 4-11 has a good level of fit with a R^2 of 0.980 and an adjusted R^2 of 0.978. The predicative power of the model is also good with a PRESS R^2 of 0.975. The confidence in the model is good as the confidence intervals for all the test conditions are small compared to the predicted effects. However for the battery voltage the confidence in the predicted effect is very low as the confidence interval spans approximately six times the range of the predicted effect. The predicted effect of the battery voltage variability is also very low. Therefore, despite the lack of control of the battery voltage within the required tolerance for the forced cold tests, the battery voltage has no statistically significant effect of the fuel consumption and it is therefore possible to conclude that overall the battery state of charge was adequately controlled and that since the battery current and voltage are not perfectly correlated it is important to recorded both variables.

The aim of the test programme that forms the basis of the work presented in this chapter was to determine the effect of two candidate engine oils compared to a baseline oil. Figure 4-4 shows that there is a large difference between the baseline oil and the two candidates at all test conditions and only a small difference between the candidates themselves. By examination of the response modelling results, see Figure 4-9, it is possible to conclude that there was an approximate 7-8g or 2% fuel consumption saving for using either candidate oil over the baseline and although the model indicates that candidate A yields the lowest fuel consumption, the difference between A and B is not statistically significant since the error bars are overlapping. The full properties of the oils were not known, but given that the viscosity index of oil A and B are similar, oil A being a

0W/20 and oil B being a 5W/20. When these are compared with the significantly thicker baseline oil which had a viscosity index of 10W/40 and only caused a 2% change in FC, it is not surprising that the experimental results did not show a statistically significant difference between the candidate oils.

4.5. Test repeatability validation methodology

In section 4.4 it has been shown that existing mathematical modelling techniques can be used to construct linear regression response models to verify that test setup factors have been adequately controlled so as to not cause a significant effect on the fuel consumption and therefore to mask the effect of a technology change under assessment through chassis dynamometer emissions testing. In the quest for the highest possible precision in fuel consumption measurement, it is suggested that these methods can be used for any test programme conducted on a chassis dynamometer to verify that controlled testing has been carried out. Although in the case of the testing conducted for this thesis, no factors were found to have a significant effect on the vehicle fuel consumption, if factors were found to correlate with the measured fuel consumption and the resulting response model has a good level of fit and predictive power, with high confidence in its predictions, the effects from the model could be used to determine the effect of the test variables as if the variability in the noise factors has not been present, i.e. the model would correct the fuel consumption results. This would allow better confidence in the recorded effects of the technological change under assessment, without the need to carry out repeat testing. A flow diagram is shown in Figure 4-12 to outline the procedure suggested by the author for the use of the response model technique.

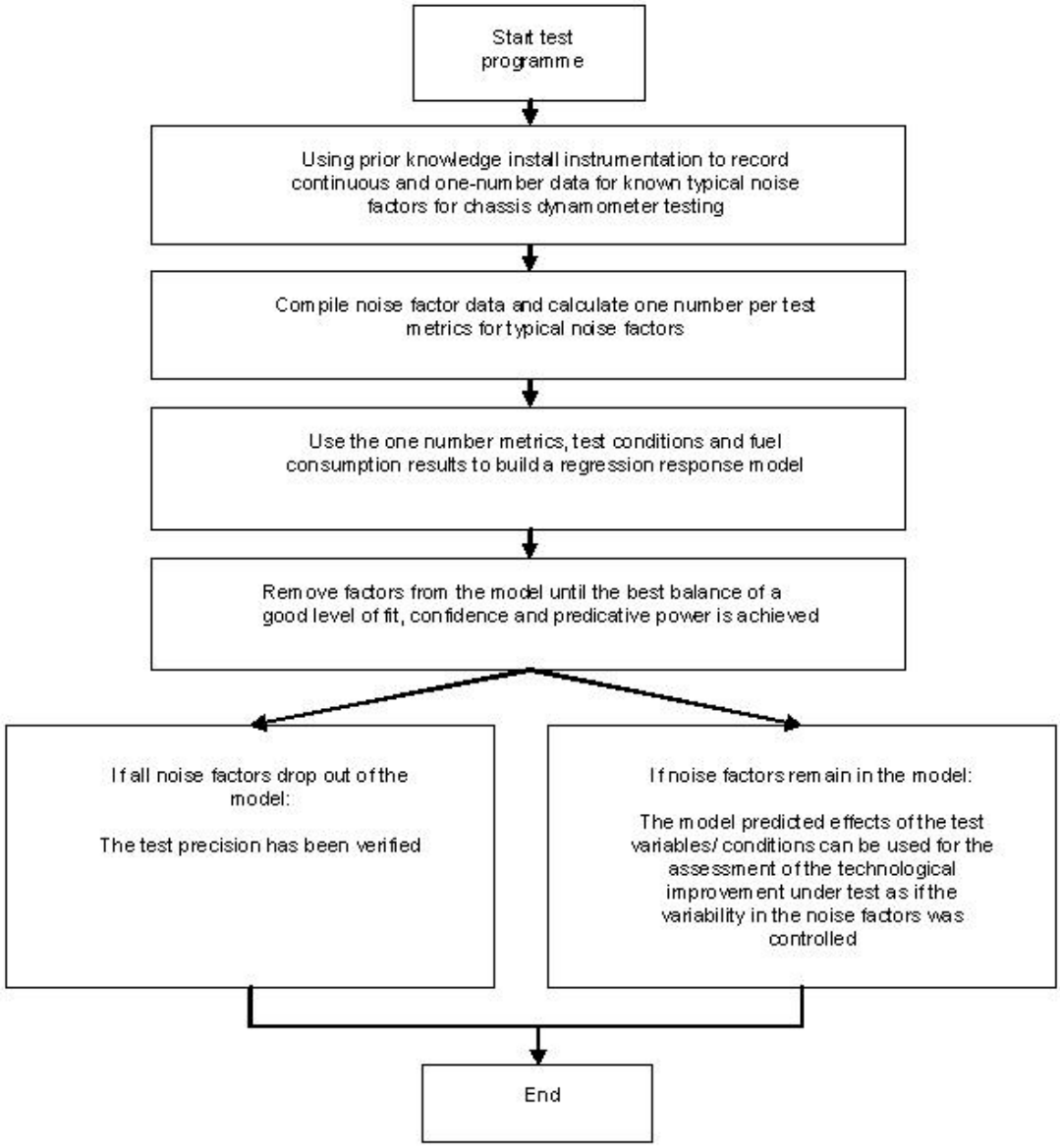

Figure 4-12: Test validation method flow chart [83]

4.6. Chapter Summary and Conclusions

In this chapter the recommended tolerances for noise factors from Brace et. al.'s work [8] were implemented along with additional controls based on knowledge gained from the literature and other studies. In addition the response modelling techniques introduced in Chapter 3 were used to propose a universal mechanism for the validation of test repeatability. The following conclusions can be drawn from this work:

- The suggested tolerances for test setup factors from the previous work carried out by Brace et. al. [8] have been successfully implemented during a chassis dynamometer based fuel consumption trial to assess the fuel consumption benefit of candidate oils compared to a baseline oil. Through the implementation of these tolerances the 0.5% CoV target for repeatability of the fuel consumption results was achieved.

- The use of the mathematical regression response modelling was successfully demonstrated to show that no recorded noise factor had a statistically significant effect on the vehicle fuel consumption that would mask or distort the fuel consumption change measured through the changes in oil and test type.

- A universally applicable method has been developed and described for the use of regression response modelling to verify that noise factors have been adequately controlled and to determine the effect of the test variables in isolation of these noise factors. This method can be used by any chassis dynamometer experimenter to correct CO_2 results if a noise factor has varied in an unexpected fashion providing a good fit can be obtained for the response model.

Chapter 5. Today's precision in a commercial setting

5.1. Introduction

In the previous chapter test noise factors were explored and controlled to produce high precision results within a test laboratory in an academic setting. A high level of precision was demonstrated with the highest variability being within the target of 0.5% CoV of CO_2 emissions and in some cases much less than the target. It has been shown that considerable effort is required to achieve these targets even within a relatively small academic test environment with only one test vehicle, chassis dynamometer and a relatively low test throughput. Whilst high precision in an academic setting is undoubtedly useful for research into next generation vehicles, there is of course much interest from industry into methods for improving the precision of chassis dynamometer results within commercial labs. In these environments that task is arguably much more challenging since many commercial outfits operate large laboratories with many chassis dynamometer test rigs, multiple CVS emissions measurements systems, multiple drivers and a high demand for tests resulting in high throughput. This chapter will use the lessons learnt so far to analyse data from such a commercial laboratory to understand the level of precision that is currently being achieved and what the primary sources of variability might be that would highlight ways in which the precision can be understood and improved in any large scale chassis dynamometer test facility.

As discussed in section 1.6 some of the research presented in this thesis is based on project with a commercial emissions testing facility. The project aim was to improve the precision of CO_2 emissions recorded during routine TA style chassis dynamometer emissions tests. The laboratory in question is typical of a commercial chassis dynamometer test facility with a reasonably high throughput; performing thousands of TA style emissions test per year. The staff of the laboratory report that high precision results have always been challenging to achieve due to the large number of variables that are thought to affect the CO_2 emissions during chassis dynamometer tests combined with a lack of time to focus on controls and improvements due to the high throughput.

The relatively large baseline variability in the total bag CO_2 emissions is clearly demonstrated by examining data from two vehicles tested in the lab which show that the normal variability in CO_2 emissions is approximately five times as large as the variability in CO_2 emissions recorded during the experiments of Chapter 4 where the results were obtained from a smaller scale test environment.

5.2. The Commercial Emissions Testing Laboratory

The chassis dynamometer emissions test cells within the laboratory in question consist of a mixture of test hardware and capabilities. For the purpose of clarity in this thesis each test cell has been given a number, unrelated to their actual identity. There are five diesel chassis dynamometer test rooms which are given the identities of cell 1 through cell 5. There are four gasoline chassis dynamometer test rooms which are given the identities of cell 6 through cell 9. There are three certification chassis dynamometer test rooms given the identities of cell 10 through cell 12. Finally there are two environmental chassis dynamometer test rooms which are given the names cell 13 and cell 14. Cell 14 is an altitude test cell and cell 13 is a cell that can be used for extreme temperature testing. Each test cell has its own chassis dynamometer and its own dedicated CVS gaseous emissions measurement system. A three shift manning operation works across all test cells and vehicles rather than having operators that are dedicated to a certain test cell or client.

The project from which this data was gained started in 2010 and the historical data analysed in this chapter covers the period up to 2010 for vehicles which were already active within the laboratory. The test cell capability is therefore summarised for the year 2010 in Table 5-1 noting that the capability of these test cells today in 2015 is much changed from the 2010 status.

Table 5-1: The commercial laboratory test cell capability in 2010

Test Cell i.d.	Chassis Dynamometer Type	Chassis Dynamometer Inertia Simulation	Fuel	Environmental conditions
Cell 1	Twin roller	Combined flywheel and electrical	Diesel	Regulatory (controlled) air temperature (20 - 30°C) Ambient (uncontrolled) air pressure Regulatory (controlled) air humidity
Cell 2	Single 48" roller	Electric		
Cell 3				
Cell 4	Twin roller	Combined flywheel and electrical		
Cell 5				
Cell 6			Gasoline	
Cell 7				
Cell 8				
Cell 9				
Cell 10	Single 48" roller	Electric	Diesel	
Cell 11			Gasoline or Diesel	
Cell 12				
Cell 13	Twin roller	Combined flywheel and electrical		Climatic test cell - 40 to +50°C
Cell 14			Gasoline	Altitude test cell

The commercial laboratory completes a vast number of both TA style emissions tests and R&D emissions tests each year. The vast majority of these tests are completed for external clients. Whereby the client owns their vehicle, controls their testing requests and whilst the laboratory provides the results from their tests the laboratory does not record any details about what was done during the test. For example if a client calibrating a new to market vehicle was using this laboratory, the laboratory would record the basic test setup parameters such as the vehicle make, model, the test type, test requestor along with of course the emissions results. During the client's series of tests the client might well be changing the ECU calibration of the vehicle on a test by test basis, this would have the effect of making the vehicle emissions unrepeatable on a test by test basis. This is a typical usage case for a vast number of commercial laboratories and clearly demonstrates why only limited analysis of precision or equipment status can be performed using client test results.

Due to the difficulties in using client tests for laboratory quality checks, the laboratory operates a round robin style internal correlation or quality checking exercise. The basic principle for this exercise is to test a small number, typically around four, production intent test vehicles around the laboratory with the aim of testing each vehicle once a day. The vehicles are tested on rotation such that they are approximately equally tested in all the test cells. The teams of operators rotate each week around the three daily shifts so that whilst the driver for each test is not randomly chosen there is variation in the drivers and in theory all drivers will test a vehicle multiple times during its life with the laboratory. On any

given week, for logistical reasons, drivers are normally assigned to one test cell. This policy means it is typical to see that the same driver has tested the correlation vehicle every day in that week. This has the theoretical advantage of reducing the variability in the way the vehicle is driven but additionally means that comparative data is not being recorded for all drivers. The quality check vehicles are dedicated to the purpose and a relatively strict procedure is documented for the testing of these vehicles, designed to mimic the TA test procedure with the most significant departure from the TA test procedure being that the vehicle SLI batteries are kept on charge between all tests.

In 2010 the laboratory was operating four quality check vehicles; two gasoline and two diesel vehicles. Unfortunately two of these vehicles, named for the purposes of this thesis vehicle C and vehicle D, were relatively new into the laboratory. When a new quality check vehicle comes into the laboratory it is subject to a lengthy process of preparation for testing. For example, along with instrumenting the vehicle, if the vehicle is brand new there must be a run-in period and similarly if the vehicle has been run-in on the road but not been tested on a chassis dynamometer before it is also subject to a shorter dynamometer based run-in. During this period the dynamometer load is iterated until an acceptable coastdown match to the TA track road load or some appropriate target data is achieved. At the time of this study these vehicles had therefore not completed a sufficient number of tests to be regarded as giving useful sample sizes of results and they had to be excluded from the study. The specification of the remaining quality check vehicles are summarised in Table 5-2. One vehicle is a B-car which is a small passenger car with a relatively small naturally aspirated gasoline engine. The other vehicle is a light commercial equipped with a much larger displacement internal combustion engine, which is a turbocharged diesel unit.

Table 5-2: Vehicle Specifications from the study

Vehicle I.D.	Type	Engine	Transmission	Fuel	Emissions standard
A	B-car	1.4 NA inline four cylinder	Manual	Gasoline	Euro 4
B	Light commercial	2.2 turbocharged inline four cylinder	Manual	Diesel	Euro 4 (i.e. no DPF)

The broad aim of the quality check vehicle testing is to identify problems with the results from test cells by testing the same vehicles repeatedly under the same conditions and comparing the historical results. The process is therefore based on the assumption that the same vehicles will produce the same emissions results when tested repeatedly. The large body of historical data from these tests provides a useful quantification of the test to

test variability in emissions and coastdown test results from the two vehicles. The procedure adopted at this laboratory is that all emission test results from the quality check vehicles are valid unless they fall significantly outside the normal range of results or a specific problem is encountered during the test to make the result questionable. These assessments are totally subjective. To give an initial picture of the test to test variability in the emissions results from the laboratory, the total CO_2 (g/km) emissions results for all tests from vehicle A are plotted, see Figure 5-1. At the time of writing there had been a total of 209 tests on this vehicle and of these only 6 tests had been identified as being invalid using the aforementioned procedure.

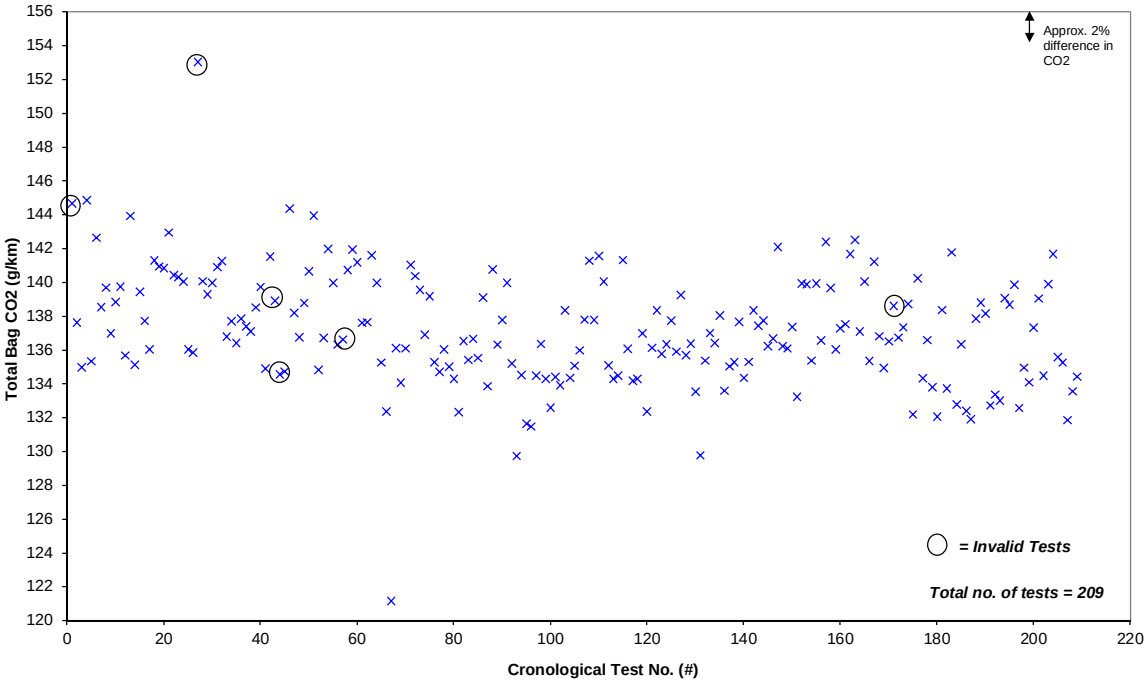

Figure 5-1: Vehicle A total CO_2 emissions results for all tests across all test cells.

Figure 5-1 shows that there is a large spread in the CO_2 test results from the vehicle A; most test results lie in a range that is approximately ±5% of the mean result, the CoV being 2.5%. A typical repeatability limit for vehicle emissions testing is ±0.5% at 95% confidence [8], a limit that is some ten times smaller than the variability seen here. With the exception of one extreme outlier with CO_2 emissions in the region of 153g/km, the results marked as invalid tests do not appear to be outlier tests in terms of CO_2 emissions. This draws question as to the suitability of the test invalidation process. As mentioned in the previous paragraph the procedure used by the laboratory for this is subjective and results are excluded for a mixture of reasons. When these reasons were examined it was found that some of these were acceptable reasons, such as a fault in the emissions measurement system meaning that an incorrect FC result is reported and others, such as not simply liking the result, are certainly not an acceptable reason for marking as invalid. Some of these ‘invalid’ results appear in the central band of results on Figure 5-1 which

clearly suggests that the wrong process is being used to identify outliers since the author would expect these to be valid without any detail to justify further. By means of comparison the results from vehicle B have also been plotted, see Figure 5-2.

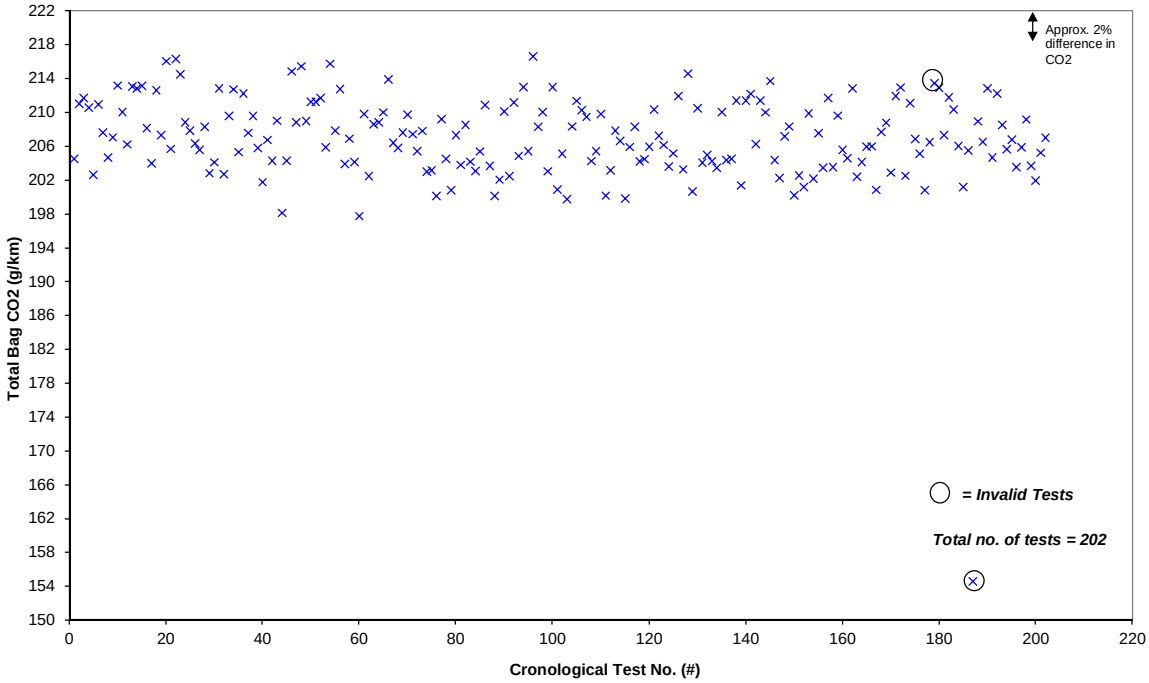

Figure 5-2: Vehicle B total CO_2 results for all tests across all test cells.

The overall spread in the CO_2 results from the vehicle B is approximately ±4% of the mean result, the CoV being 2.7%. Therefore the spread of results from the vehicle B is slightly smaller than that for the vehicle A. The reason for the increased CoV compared to the vehicle A, which was 2.5%, is due to the extreme outlier CO_2 result of 154.5 g/km, since if this is removed the CoV reduces to 1.96%.

Table 5-3 summarises the level of imprecision in the total bag CO_2 emissions from these vehicles when tested during the quality check programme in operation at this laboratory. By reference to Table 5-3 it is interesting to note that the number of tests for each vehicle is similar and whilst the standard deviation is much lower for vehicle A, the CoV is almost equal for the two vehicles. This means that whilst the absolute variability is lower for the vehicle A, the variability as a proportion of the mean is the same for both vehicles. The test to test variability for the two vehicles is five times as large as the variability in the recorded results from the test vehicle in Chapter 4. The results from the assumed stable production intent quality check vehicles have variability in the region of 2.5% CoV, this suggests that clients wanting to use the laboratory to assess the difference between two minor calibration changes across multiple drivers and test cells are very unlikely to be able to do so. But this is not the entire story, because as a study will demonstrate in Chapter 6 the test cells are capable if sufficient controls are put in place. One output of this thesis is therefore to determine which factors should be controlled to achieve this.

Table 5-3: Imprecision in total bag CO_2 emissions for both vehicles in the study

Vehicle I.D.	Number of tests	Mean total bag CO_2 emissions (g/km)	Standard deviation of total bag CO_2 emissions (g/km)	Coefficient of Variation of total bag CO_2 emissions (%)
A	209	137.2	3.4	2.5
B	202	206.9	5.5	2.6

The study is based only on the one-number-per-test results since the second by second results are not examined during the quality check testing exercise. Whilst the second by second data does exist it is captured in individual files for each test and thus there are considerable practical challenges to obtaining copies, processing and analysing each file for the 400 plus tests captured within the study.

When attempting to conduct a tightly controlled programme of testing it is normal to implement controls for test setup factors which could affect the results. When a control is implemented for one of these noise factors a numerical value can be recorded which is representative of the condition for each test. For example the battery state of charge could be controlled by implementing a charging regime and measured in Ah at the start of every test. These principles were introduced in section 4.2. In order to understand the significance of the factors which affect the variability in the CO_2 emissions it is necessary to make a measurement of all conceivable factors.

5.3. Data mining for factors of imprecision in CO_2 emissions

When this data mining exercise was conducted there were a limited number of test setup factors recorded for every test and therefore mining the data for correlations between test setup factors and results is limited. However 15 variables were routinely recorded. Initially the variables recorded were plotted against the total test bag CO_2 emissions to look for obvious correlations between the recorded variables and the CO_2 emissions, these plots are shown in Figure 5-3 and Figure 5-4.

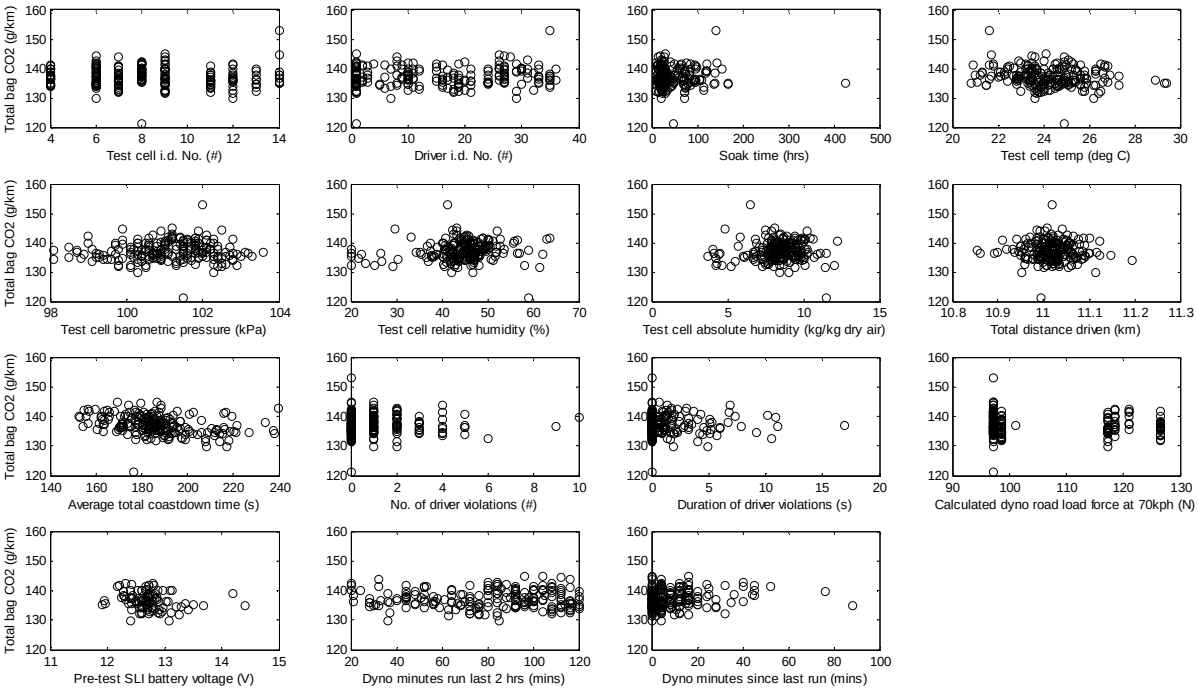

Figure 5-3: Vehicle A, one number metrics (from left to right: Test cell i.d., Driver i.d., pre-test soak time, test cell temperature, test cell barometric pressure, test cell relative humidity, test cell ambient humidity, distance driven, post-test coastdown time, number of driver violations, driver violation time, road load force at 70 km/h, pre-test battery voltage, dynamometer minutes run in the last 2 hrs and dynamometer minutes since last run, respectively)

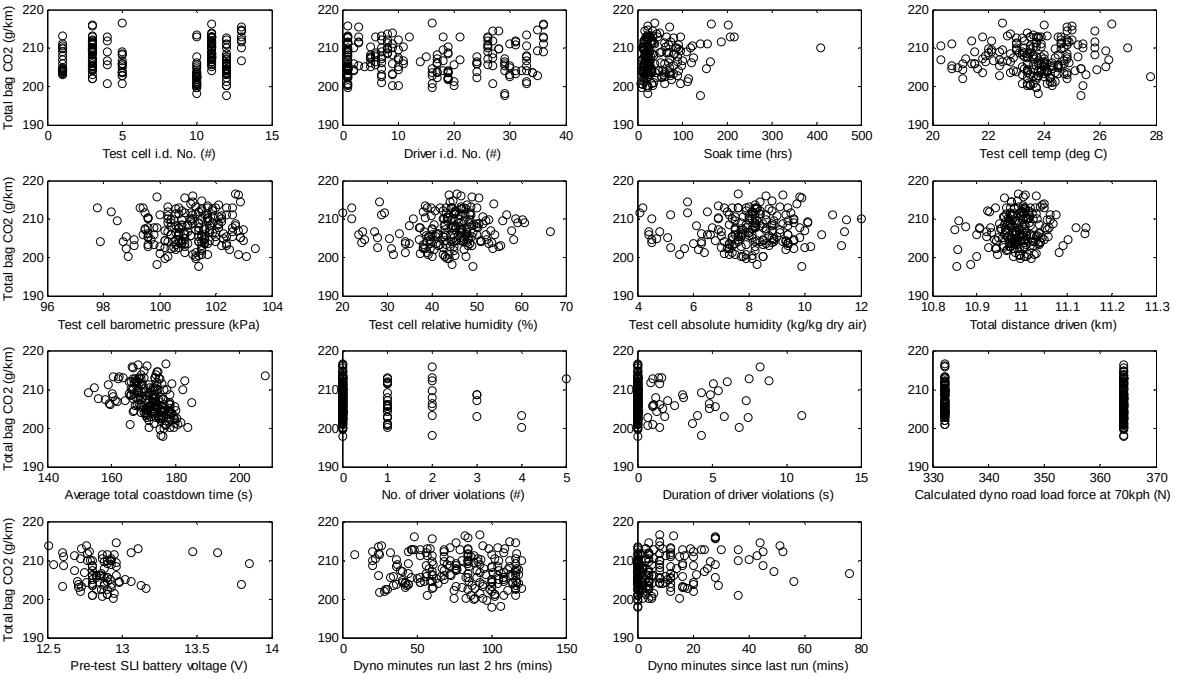

Figure 5-4: Vehicle B one number test metrics (from left to right: Test cell i.d., Driver i.d., pre-test soak time, test cell temperature, test cell barometric pressure, test cell relative humidity, test cell ambient humidity, distance driven, post-test coastdown time, number of driver violations, driver violation time, road load force at 70 km/h, pre-test battery voltage, dynamometer minutes run in the last 2 hrs and dynamometer minutes since last run, respectively)

For most of the 15 variables plotted as one-number-per-test metrics, in Figure 5-3 and Figure 5-4 there is no clear correlation between the plotted variable and the total bag CO_2 emissions. However there are some interesting results for some variables. The plots of the test cell i.d's show that the variability in CO_2 emissions is different for some of the test cells. However the trends are not the same for the two test vehicles, for example the cell 11 results from vehicle B have a higher mean than those from cell 10 or cell 12. Conversely for vehicle A the cell 10, cell 11 and cell 12 results all have approximately the same mean CO_2 result. For vehicle A, cell 4, cell 8 and cell 13 all have a similar range in the total bag CO_2 emissions, of approximately 10 g/km, a range that is smaller than the other test cells. This is difficult to explain physically, cell 4 and cell 8 are located very close to each other and received conditioned air form the same AHU so could have similarly stable environmental conditions. However the test cells immediately adjacent to cell 8 which are coincidently cells 9 and 7 are also served by the same AHU yet do not have the same variability making this explanation unlikely. It is evident from the plots that the cell 13 results are few in number, suggesting there is less confidence that the low variability is a real effect instead it seems more likely that the low variability is a result of only examining a small number of results. Cell 14 has the largest range of recorded CO_2 emissions, which is of little surprise given that the dynamometer is subjectively regarded to be the least repeatable in the laboratory with emissions measurement equipment that is by far the oldest and not fully maintained.

Overall all the drivers have a similar range from the lowest to the highest CO_2 results. Some drivers have a small spread in results compared with most, but it is not easy to tell from the plot if these drivers have completed more or less tests than other drivers. It looks like the spread in CO_2 emissions is slightly larger for the vehicle B results when compared with the vehicle A results.

Interestingly there is not an obvious correlation between the number of driver violations and the CO_2 emissions. Since a drive violation can be either an excursion above or below the target speed trace violations can result in either increases or decreases respectively in the expected CO_2 emissions. This probably explains why there is no correlation, since multiple violations could result in any combination of positive or negative changes in the CO_2 emissions. The drive violation time is the total time for each test that the drive spent driving outside the speed tolerance. The total time can similarly be comprised of any combination of positive or negative speed errors and the CO_2 effect of these could potentially cancel each other out when summed over the duration of a drive cycle. These findings clearly demonstrate that it is not sufficient to examine driver behaviour purely on

the basis of the drive cycle tolerance violations, an idea that is further expanded in Chapter 7.

For both vehicle A and vehicle B there are two regions of recorded data for the road load force and this is because the target dynamometer road load force is different for the single and twin roller dynamometers to counter for the increased rolling resistance of a twin roller dynamometer due to the two tyre contact areas per tyre. Within each cluster there is no obvious trend between the road load force and the CO_2 emissions.

The relative humidity or RH and absolute humidity show some degree of correlation for vehicle A as a slight slope is apparent in the data. However there is a large scatter in the humidity results so a linear fit would likely result in a very low coefficient of determination. Interestingly this there is no real indication of this trend in the vehicle B results. The author speculates that as the humidity of the air increases the extra quantity of water vapour in the air causes the specific heat capacity of the air to increase. Therefore when combustion takes place in the engine it is possible that more fuel is burnt to achieve the same combustion gas temperatures.

For both test vehicles there is a slope in the coastdown time data from Figure 5-3 and Figure 5-4. For vehicle A this suggests a weak correlation between coastdown time and CO_2 emissions, whereby the longer the coastdown time the lower the CO_2 emissions. This is physically logical since a longer coastdown time is indicative of a lower rolling resistance, reduced vehicle work during the test cycle and hence lower total CO_2 emissions. For vehicle B the angle of the slope is much steeper, however for both vehicles there is a lot of scatter in the results.

Plotting the recorded test variables one factor at a time against the total bag CO_2 emissions is a useful initial scoping exercise as some weak trends have been identified, the most notable of which being weak correlations for coastdown time for both vehicles and test cell humidity and for vehicle A. However a significant limitation is that it is not possible to examine the correlations without the interactions of the other variables. To achieve this it is necessary to use the response modelling techniques that were introduced in Chapter 3.

5.4. Response Modelling

5.4.1. *Vehicle A*

In the previous sections graphical representation of the test results was used to search for correlations between the test setup factors and the CO_2 results and there were no clear correlations evident through these techniques. A more rigorous approach is to build a

multiple variable regression response model, a technique that was introduced in Chapter 4. This method has the advantage of looking for correlations based on all the test setup factors and there inter relations. In this instance the Umetrics Modde programme was used to build a Multiple Linear Regression, MLR, model based on the eight noise factors examined in the previous sections. Figure 5-5 shows the main effects plot for the vehicle A and Table 5-4 shows the corresponding correlation matrix.

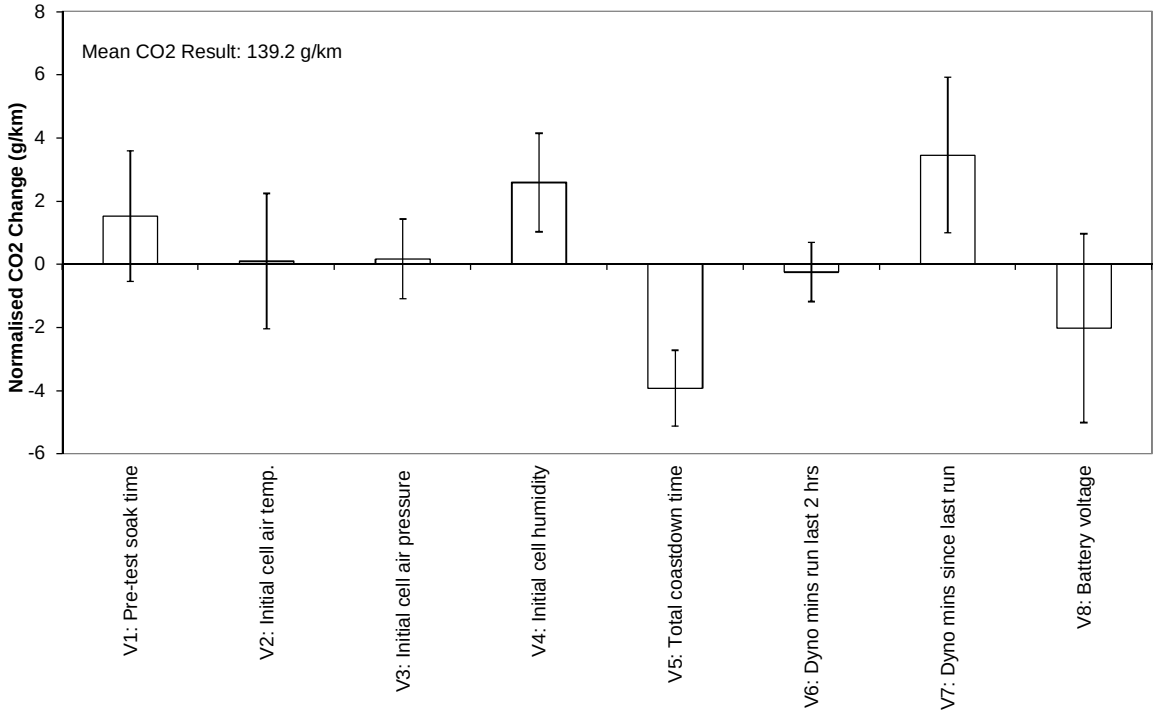

Figure 5-5: Vehicle A main effects plot for the MLR model, where the bars represent the pre-test soak time, test cell temperature, test cell barometric pressure, test cell relative humidity, post-test coastdown time, dynamometer minutes run in the last 2 hrs and dynamometer minutes since last run and the pre-test SLI battery voltage respectively

Table 5-4: Vehicle A correlation matrix for MLR model with the two largest coefficient in bold. Variables V1 – V8 are defined as the pre-test soak time, test cell temperature, test cell barometric pressure, test cell relative humidity, post-test coastdown time, dynamometer minutes run in the last 2 hrs and dynamometer minutes since last run and the pre-test SLI battery voltage respectively

Correlation Coefficient									
	V1	**V2**	**V3**	**V4**	**V5**	**V6**	**V7**	**V8**	**CO2**
V1		0.01	0.02	-0.13	0.08	0.02	0.00	**0.40**	0.00
V2			0.15	-0.17	0.10	-0.11	0.13	-0.26	-0.02
V3				-0.13	0.01	0.15	0.09	0.12	-0.01
V4					0.04	-0.01	-0.18	-0.17	0.23
V5						0.09	0.11	0.12	**-0.53**
V6							-0.28	0.02	-0.17
V7								0.04	0.15
V8									-0.19
CO2									

The level of fit of the model can be quantified by the coefficient of determination or R^2 value which gives a measure of the differences between the measured data and the fitted model. The closer the R^2 value to 1 the better the level of fit and in this case the R^2 value

is 0.432. This is a very low R^2 value and indicates that only 43.2% of the variability in the CO_2 results can be described by the eight noise factors.

For all noise factors in Figure 5-5, except the coastdown time, the 95% confidence intervals are greater than half the effect that the factor has on the CO_2 result. This suggests that there is a fair correlation between the coastdown time and the CO_2 result, agreeing with the slight downward trend evident in Figure 5-3. The corresponding correlation coefficient is -0.53, further indicating the presence of a fair amount of correlation, since generally a coefficient with a magnitude larger than 0.8 is required for strong correlation [8]. The model also suggests there is a fair amount of correlation between the soak time and the battery voltage. Physically this is logical, since a longer soak time should result in a longer battery charge time. However all these results should be taken with caution due to the lack of a good fit for the response model.

5.4.2. *Vehicle B*

Using the same processes and tools as the previous section a MLR model was constructed for vehicle B using the same eight noise factor and CO_2 results. Figure 5-6 shows the main effects plot for the model and the corresponding correlation matrix is shown in Table 5-5.

The coefficient of determination for the vehicle B model was 0.198. This is worse than the R^2 value for the model based on vehicle A's results and indicates that only 19.8% of the variability in the CO_2 results is described by the eight noise factors. Figure 5-6 shows that only the coastdown time has had an effect larger than half its corresponding confidence interval. However it is not possible to conclude there is anything more than a fair to weak correlation since the correlation coefficient is only -0.29.

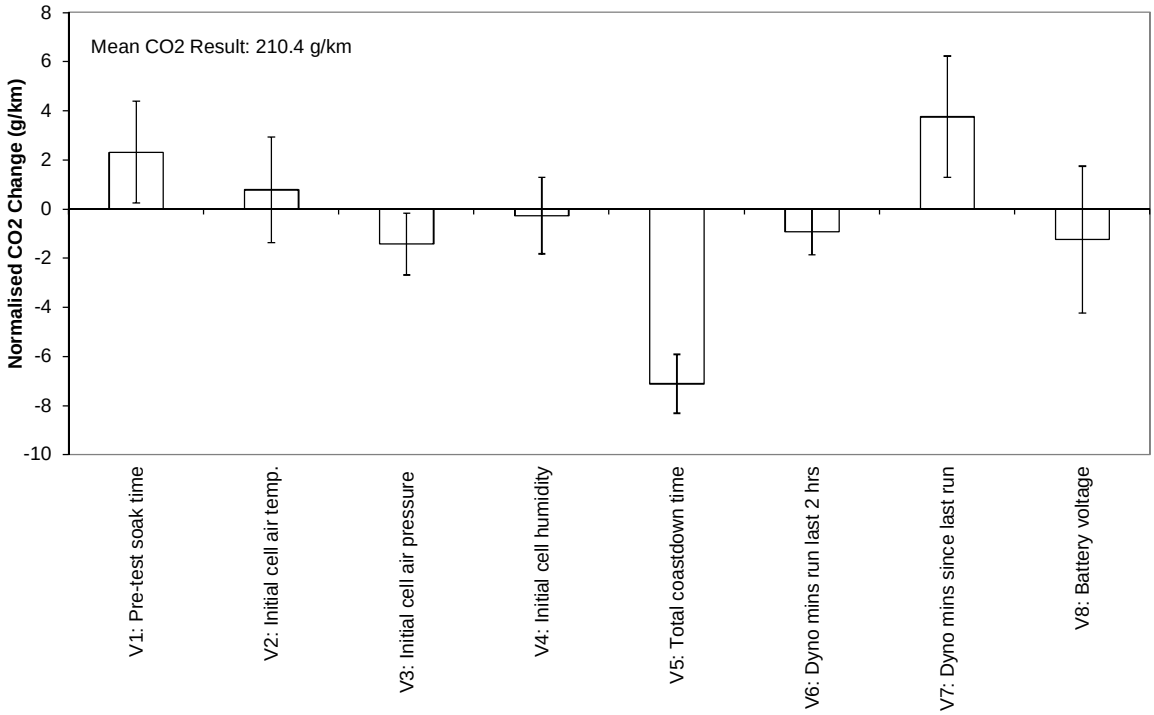

Figure 5-6: Vehicle B main effects plot for the MLR model, where the bars represent the pre-test soak time, test cell temperature, test cell barometric pressure, test cell relative humidity, post-test coastdown time, dynamometer minutes run in the last 2 hrs and dynamometer minutes since last run and the pre-test SLI battery voltage respectively

Table 5-5: Vehicle B correlation matrix for MLR model with the largest coefficient in bold. Variables V1 – V8 are defined as the pre-test soak time, test cell temperature, test cell barometric pressure, test cell relative humidity, post-test coastdown time, dynamometer minutes run in the last 2 hrs and dynamometer minutes since last run and the pre-test SLI battery voltage respectively

Correlation Coefficient									
	V1	**V2**	**V3**	**V4**	**V5**	**V6**	**V7**	**V8**	**CO2**
V1		-0.01	0.07	0.01	0.12	0.12	-0.07	-0.13	0.08
V2			0.14	-0.20	0.15	-0.19	0.03	-0.13	0.05
V3				-0.03	-0.14	-0.21	0.21	-0.23	0.06
V4					-0.07	-0.04	0.10	-0.10	0.03
V5						0.05	-0.03	-0.07	**-0.29**
V6							-0.25	-0.03	-0.19
V7								0.22	0.26
V8									0.01
CO2									

These modelling results highlight that the standard variables which are routinely recorded for a quality check emissions test within the laboratory are insufficient to describe the imprecision in the recorded CO_2 emissions. Additional variables must be logged to understand the root causes of the variability.

5.5. Introducing Engine Control Unit Logging on Vehicle A

The standard set of variables recorded as part of the quality check testing, which has been examined in the preceding section of this chapter gives little insight into the primary sources of variability in the recorded CO_2 emissions. A method was therefore sought to increase the number of measured variables.

In Chapter 4 ECU logging was used to record measures of driver accelerator inputs and also to measure vehicle control variables. For a pilot study this is a relatively simple form of logging to add to an existing chassis dynamometer test setup. Generally the most difficult element of installing ECU logging is the requirement to time align the emissions and ECU data during post processing. This is relatively easily worked around by the inclusion of a common signal in both data logs.

For this study a standalone ECU logger was installed into vehicle A and the resulting data from 35 tests was used to construct a new response model. Initially the model was fitted with all factors included, which unsurprisingly gave a low level of fit due to the presence of factors that were not at all correlated with CO_2 emissions and also due to the inclusions of multiple correlated inputs. Multiple correlated inputs are a problem because the model is unable to identify which of the correlated inputs is the cause and which is the effect. It is therefore necessary to try and only include one measure of each discrete variable. The minimise press routine was used within the Matlab model based calibration toolbox to achieve the model with the best compromise between the level of fit and the number of informative factors. The routine works by calculating the PRESS if each factor was individually removed and then removing the factor that results in a model with the smallest PRESS. This is repeated until a model with the best PRESS is achieved.

The level of fit of this new response model with both the test cell data from the previous sections, although not from the same tests, and the new additional ECU data is much improved. This is in spite of the significantly reduced number of tests, approximately 35 compared with 200. The coefficient of determination for the resulting response model is 0.802, the adjusted coefficient of determination is 0.751 and the PRESS R^2 is 0.696. This shows that by simply including the ECU data with the test cell data the resulting model is able to describe approximately 80% of the variability in the data compared with only approximately 40% from the test cell only modelling, thus highlighting the importance of both measuring the data in the first place to gain an understanding and also the importance of measuring ECU data.

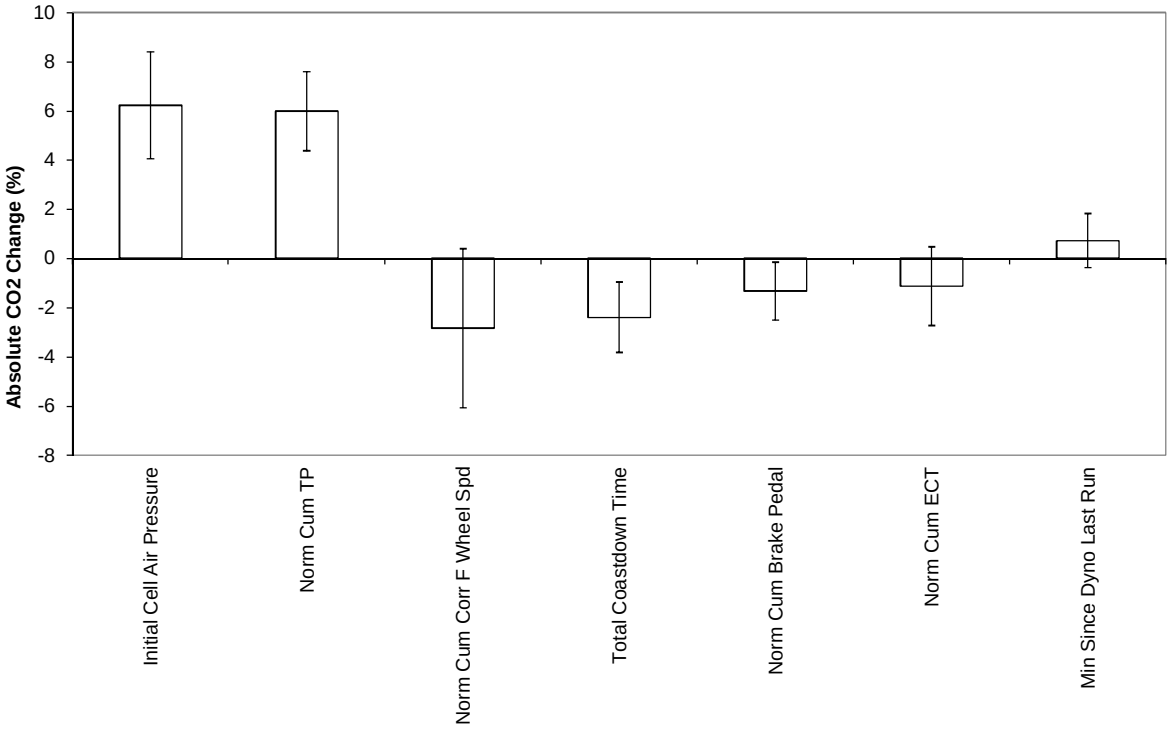

Figure 5-7: Main effects plot for the response model built from results on vehicle A, with both ECU data and test cell data. The bars represent the initial call air pressure, the normalised cumulative throttle position, normalised cumulative wheel speed, total coastdown time, normalised cumulative brake pedal input, normalised cumulative engine coolant temperature and the dynamometer thermal status given by the minutes since the dynamometer was last run.

The main effects plot of Figure 5-7 shows some variables that are in agreement with the test cell only model and some that are new. One of the most significant factors from the previous response modelling, the initial test cell humidity, has dropped out of this ECU and test cell model. Instead the initial cell air pressure is the only test cell environmental factor that is included. In fact it has the largest main effect of all the included factors with a predicted change of just over 6% in CO_2 emissions as a result of normal swings in cell air pressure within the test cell. In this experiment the initial cell air pressure varied from 98 to 102.3 kPa which are well within the normal range of expected air pressures for the UK. This fact is clearly demonstrated by examining the highest lowest and highest recorded air pressures in the UK at 92.6 and 105.6kPa respectively [87]. The effect of the ambient air pressure on the fuel consumption of internal combustion engines is not very widely published and the 6% change in CO_2 emissions predicted from the response model is surprisingly high. However some authors have examined the effect and have concluded that there is a fuel consumption penalty for operating a vehicle designed for sea level running at altitude but that the effect is reduced at very high engine loads [88]. To validate this an engine simulation model, constructed in the Ricardo Wave simulation package, was used. The model was of a turbocharged 2.0 litre displacement gasoline engine and had been optimised for steady state accuracy. Therefore instead of running the model over the entire NEDC a steady state operating condition was chosen that was

representative of a running condition from the NEDC. The chosen condition was 2 bar BMEP and an engine speed of 2000 rev/min which was selected by examining data from tests on an engine test bed using the same powertrain as fitted to vehicle B, these data are shown in Figure 5-8.

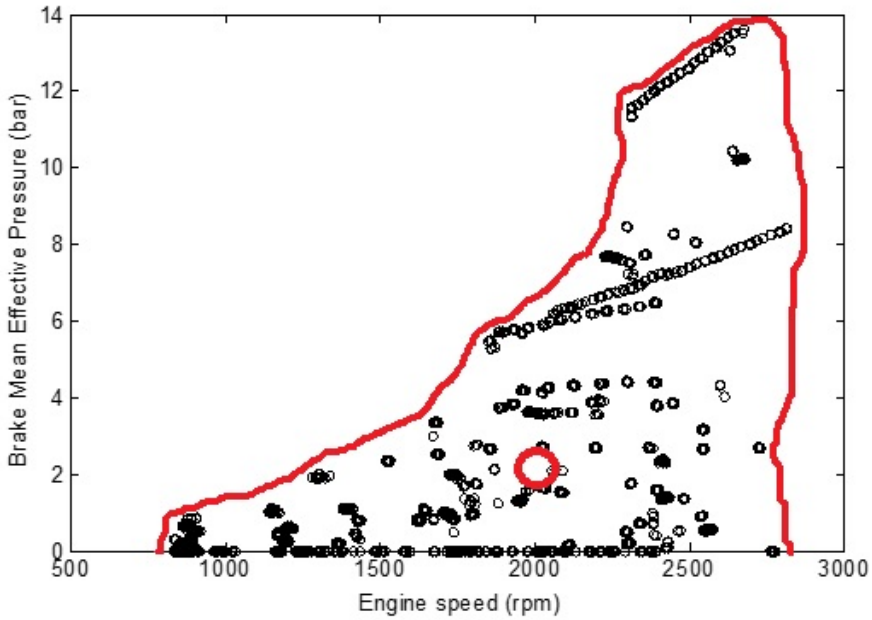

Figure 5-8: Brake Mean Effective Pressure for a 2.2 litre displacement turbocharged diesel engine fitted to a light commercial vehicle and operating over the NEDC. Operating envelope is shown by the red line and the red circle shows the chosen steady state point for engine modelling.

By examination of Figure 5-8 the chosen operating point, shown by the red circle, is well within the operating envelope of the engine over the NEDC. Although there are differences in the powertrain between vehicle A, vehicle B and the simulation model, the chosen simulation point is still likely to be well within the operating range for the NEDC, given its relatively central location within the data collected for vehicle B's engine, see Figure 5-8. The simulation was run over the approximate range of ambient cell air pressure that was recorded within the data captured for vehicle A and the output BSFC and PMEP were recorded. The results are shown in Figure 5-9.

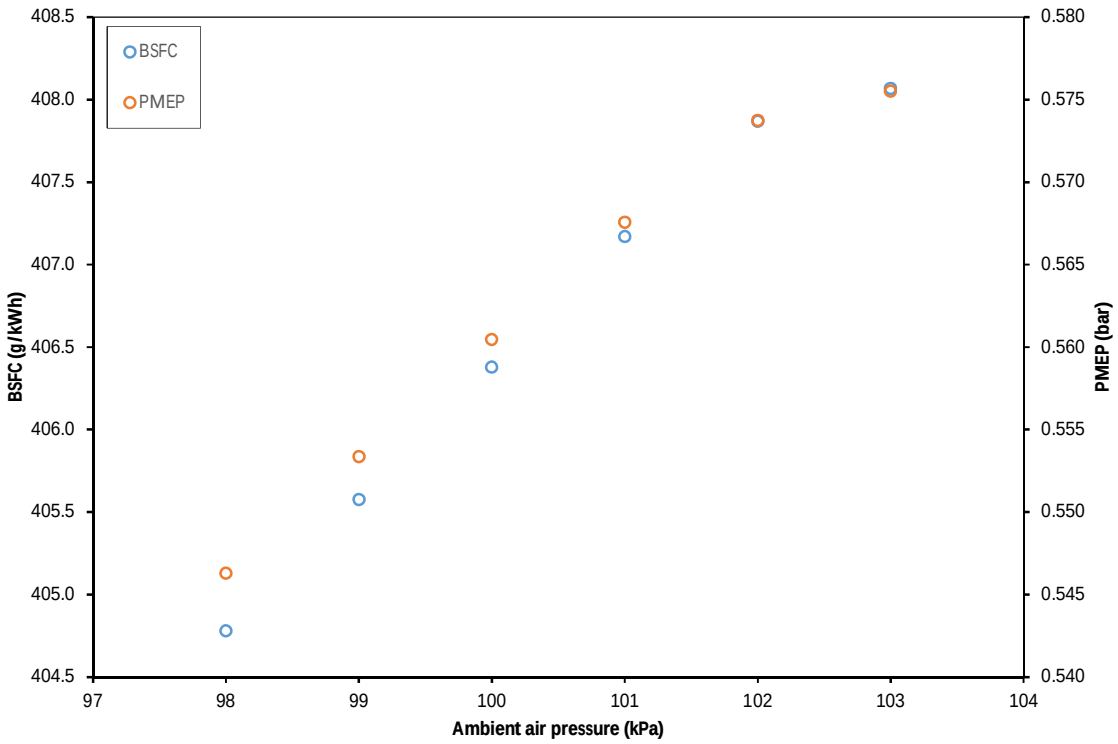

Figure 5-9: Engine simulation results for steady state operation of 2.0 litre displacement gasoline engine running at 2bar BMEP and 2000 rev/min.

The simulation results of Figure 5-9 show agreement with the trend observed in the response model of Figure 5-7. That is the fuel consumption and hence CO_2 emissions increase with increased ambient air pressure. The modelling results explain the reason for this, which is due to an increase in the absolute value of the pumping losses quantified by the PMEP. The engine must use more fuel to overcome these increased pumping losses which the author speculates are caused by an increased throttling of the engine in reaction to the increased air density from the increase in air pressure. The increase in pumping losses from the simulation was approximately 5%. However the magnitude of the effect to BSFC shown by the engine simulation is much smaller being approximately a 1% increase in BSFC over the range of ambient pressure. This is six times smaller than the main effect, of 6%, from the response model for vehicle A. One drawback of the Ricardo Wave simulation is that it uses a Viebe heat release model, so the heat release is fixed for a given condition. As such the effect of the increase in the in-cylinder density from the increased air pressure will be a small increase in heat release. The model will not show this effect and as such will under predict the magnitude of the effect on BSFC. This may go some way to explaining the discrepancy between the response model and Ricardo Wave results but is unlikely to explain all of the discrepancy. Another factor is that the confidence interval for the main effect of the response model was large, extending approximately ±2% from the absolute value for the main effect, so the effect could actually be lower than 6%. In addition the Ricardo Wave simulation results only examine one condition, where the response modelling uses data from a transient drive cycle. It is

therefore possible that the effect of air pressure is lower for the condition that was chosen for simulation. Finally it is also possible that differences in the controller behaviour for the two engines is contributing to some of the discrepancy between the simulation and response modelling results. Further work would be required to quantify these effects.

The second largest main effect is a metric called the cumulative throttle position. This is calculated by summing the throttle position data over the test cycle and therefore captures all throttle movements, both those accelerating and decelerating the vehicle. If a driver drives a cycle with a speed that is higher than the target speed they will inevitably hold higher accelerator pedal demands during cruises resulting in a higher end of cycle value for cumulative throttle position and higher CO_2 emissions due to the extra load placed on the engine to drive at a higher speed. Similarly if a driver is more oscillatory on the throttle pedal they will also record a higher value for cumulative throttle position and they will also generate more CO_2 since for each micro transient they will accelerate above their cruise speed then immediately loose that momentum by decelerating only to have to repeat the process again. This means that instead of operating at a fixed throttle position during cruises and therefore a fixed engine load where the engine would operating a constant point on its BSFC map it is instead oscillating from regions of higher and lower efficiency, the net result is most likely to be a reduced efficiency. The total coastdown time shows an effect of approximately 2% CO_2 with a confidence interval only just smaller than 2%, showing that whilst there is confidence that the factor is correlated with CO_2 emissions because the confidence interval is lower than the magnitude of the main effect, there is very little confidence in the effect being equal to 2%.

The other factors, vehicle wheel speed, coastdown time, cumulative brake pedal, cumulative engine coolant temperature and dynamometer status are all logical factors to be correlated with the variability in the CO_2 emissions. However given the large size of the error bars in relation to the predicted main effects it is not possible to have any statistical confidence in the validity of the correlation between these factors and the CO_2 emissions.

5.6. Chapter Summary and Conclusions

In this chapter historic data from a commercial laboratory was mined for sources of variability and to determine the base level of variability in bag CO_2 emissions. Post-test analysis, one factor at a time and response modelling techniques were used to determine the most significant factors. From these findings the following conclusions were drawn:

- The commercial laboratory's historic data sets show a relatively low level of precision when compared with results that are obtainable under highly controlled conditions of Chapter 4. The basic level of variability, measured by the coefficient

of variation, was found to be approximately 2.5%. This is five times larger than the level of variability seen in a tightly controlled study, such as that conducted by Brace et. al. [8] showing there is plenty of scope for improvement.

- Very few noise factors are routinely recorded within a commercial laboratory which had a significant influence on the CO_2 emissions. Only the coastdown time, the dynamometer status, measured in minutes since last run and the test cell humidity and the soak time looked to be having an influence on CO_2 emissions. However very low confidence was recorded in these effects as the standard errors were large. The inclusion of ECU data logging helped to improve the fit of the response models with the coefficient of determination of the being nearly doubled from 0.432 to 0.802.

- For a gasoline vehicle the initial cell air pressure has been shown to be a significant and newly identified factor. All other factors that have been identified as significant are all factors that have previously been found in the literature or experimental work to be important. With a R^2 of 0.802 from the best response model there is an indication that approximately 20% of the variability in the CO_2 results is currently unexplained by the recorded data. This shows that there are still important factors to be identified and controlled to improve the precision in CO_2 results.

- The relative difficulty in obtaining good fitting models to the data that describe the CO_2 emissions, highlights that the environment is nearly always too noisy to review the effect of one test setup factor on the overall output factor; the CO_2 emissions, reinforcing the conclusion from Chapter 3. Instead it is necessary to analyse metrics for each section of the noisy environment and know that whilst improving only one section might not produce tangible benefits to the precision of CO_2 emissions, if all sections are improved there will be an overall tangible benefit to the precision of the CO_2 emissions.

Chapter 6. Vehicle Electrical System

6.1. Introduction

The review of the literature highlighted the significance of reducing variability in vehicle electrical system loads and in pre-test battery SoC to achieve increased precision in measured CO_2 emissions. This is because variations in the total electrical load during a test will result in variations in the load placed on the engine via the alternator and hence variability in the tailpipe CO_2 emissions. There is very little data on the relative magnitude of the load from electrical auxiliary devices and the expected errors in CO_2 from these loads during an emissions test. Furthermore authors have only touched on proposed methods for reducing the electrical load variability to improve the precision of CO_2 emissions. The most notable being Brace et. al. [8] who calculated from their results that a tolerance of ±0.2V was necessary to achieve a FC repeatability target of ±0.5% at 95% confidence. However they do not provide a method for achieving this tolerance in practice and the author assumes that the tolerance would therefore be applied retrospectively in post processing of any test results. A more desirable outcome would be a method for controlling the SoC variability such that defect tests can be avoided.

6.2. Sources of auxiliary electrical load variability

The published works in the literature state that variability in the vehicle auxiliary loads which are switched on during vehicle emissions tests can cause changes to CO_2 emissions anywhere in the region of +5 to +50%. This is a vast range and is stated without any detailed evidence and without any results that allow for a proper understanding of the causality. Furthermore there are no guidelines for experimenters wishing to minimise this source of variability.

Variability in CO_2 emissions caused by auxiliary electrical loads can result from a variety of error states. Perhaps the most readily envisioned error state is that the driver manually and intentionally switches on an auxiliary load, such as the headlamps, in an uncontrolled manner part way through an emissions test. However there are also less obvious error states that the author proposes should be considered. For example the vehicle ECU may automatically switch on/off auxiliary loads. An example of which would be the switching on of the heated rear window when the ambient temperature is below a threshold to place extra load on the engine and speed the warm up process of the engine. Another example of a previously unconsidered auxiliary load error state is where auxiliary loads are either manually or automatically switched on immediately prior to an emissions test as part of the pre-test setup process. In large scale laboratories vehicles are soaked in dedicated bays away from the test cells and if the SLI battery is to be charged this will often take

place in the soak bays. When a vehicle is collected from soak, it will be disconnected from the battery charger and then wheeled to the test cell, which is the procedure in use in the commercial laboratory investigated within this thesis. The movement of the vehicle and the possible opening of the driver's door will certainly awaken the ECU and associated controllers. The ECU may also trigger a fuel pump prime in preparation for the engine starting when the driver's door is first opened from soak. The author proposes that this pre-test load could be highly variable depending on the number of movements and door openings prior to the test.

In order to understand more about the effect of vehicle auxiliaries during or prior to emissions tests, various tests were carried out using a passenger B-car with a 1.4 diesel engine which was tested in the commercial laboratory environment. The test vehicle used for this study was, by modern standards, a relatively simple one and hence not all electrical auxiliary loads could be tested. The test vehicle was instrumented with HIOKI 9278 current clamps connected to a HIOKI power analyser. The current clamps were of a split type and were positioned to measure the fusebox and battery currents from the vehicle. Figure 6-1 shows the schematic arrangement of the HIOKI current clamps on the vehicle. One clamp was positioned to measure the output from the alternator, whilst the other was positioned on the battery negative lead to measure the overall charge balance on the battery.

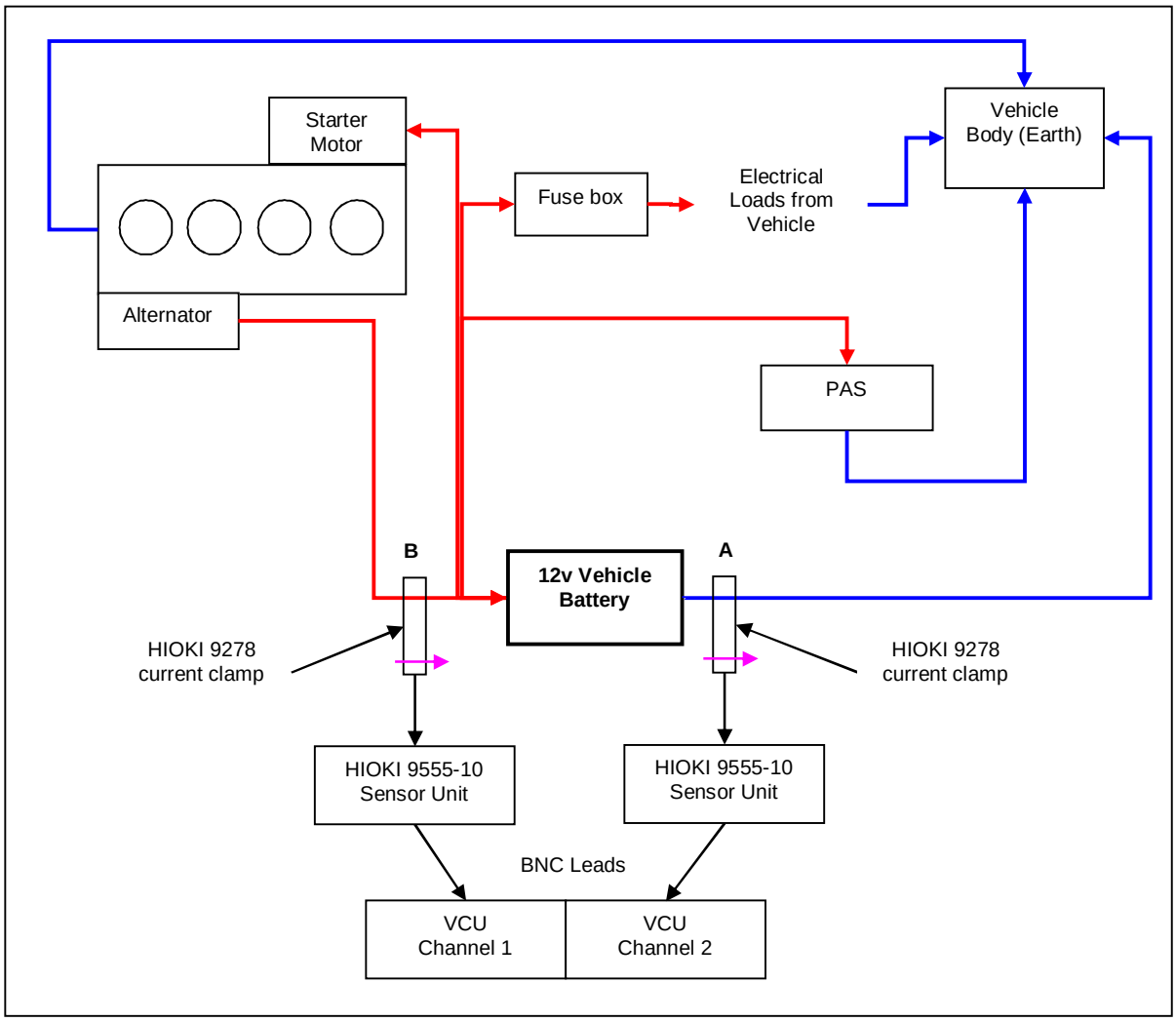

Figure 6-1: HIOKI current clamp configuration for vehicle auxiliary load experiments. VCU stands for vehicle connection unit and is part of the data acquisition system in use within the commercial laboratory where the experiments were conducted.

The HIOKI measurement system has a high accuracy and repeatability, conforming to the European hybrid vehicle regulations, known as ECE R101 [89]. The stated accuracy of the current clamps is ±0.5% reading and ±0.05% full scale. Initially readings were manually transcribed from the HIOKI power analyser display as the current clamps were installed into the vehicle, zeroed and then various auxiliary loads were turned on. The test was then repeated whilst the engine was idling with the vehicle in neutral. With the engine running the alternator current was very oscillatory and therefore impossible to read manually with any real certainty. Table 6-1 shows the results in the sequence they were recorded during the experiment. There were no delays in recording the results shown on each concurrent line of the table.

Table 6-1: Electrical loads read from HIOKI power analyser. Readings highlighted in blue are approximate due to noisy readings.

		Current (A)	
	HIOKI Channel:	***I1***	***I2***
	Current clamp position:	***Alternator***	***Battery***
No.	**Process**	**Clamp A**	**Clamp B**
1	Attach clamps	N/A	N/A
2	DEMAG	0.00	0.00
3	Driver door open	0.00	0.80
4	Driver door shut	0.00	0.80
5	Key on to ign. Initial peak	0.00	60.00
6	Key on to ign. SS	0.00	2.30
7	Blower 4	0.00	18.20
8	Blower 3	0.00	12.50
9	Blower 2	0.00	7.80
10	Blower 1	0.00	5.60
11	Heated rear window	0.00	15.60
12	Side lamps	0.00	5.00
13	Dipped beam	0.00	14.20
14	Main beam	0.00	15.65
15	LH indicator	0.00	6.00
16	Hazard	0.00	11.00
17	Radio @ 28 vol	0.00	0.30
18	Crank engine	0.00	60.00
19	6-8sec after engine fires	60.00	2.40
20	minutes after engine fires	25.00	2.40
21	10's of minutes after engine fires	3.00	2.40
22	Idling engine	unstable	2.40
23	Side lamps	unstable	5.30
24	Dipped beam	unstable	15.50
25	Main beam	unstable	17.20
26	Heated rear window	unstable	18.00
27	LH indicator	unstable	2.80
28	Drivers electric window fully down to fully up	15.00	10.50
29	Drivers electric window fully up to fully down	12.00	7.50
30	Drivers electric window motor stall	40.00	28.00
31	Air con on	40.00	33.00
32	Engine off	0.00	1.40
33	Door open	0.00	0.70
34	Key out	0.00	0.70

Many modern vehicles automatically prime the fuel pump either when the vehicle is unlocked or when the driver's door is opened in preparation for the driver starting the engine. This can be heard by the driver as a short duration, normally 1-2 second long 'whirring' noise either as one approaches the car or opens the door. In the case of diesel vehicles the author speculates that this could also include an initial glowplug heating phase. The results from Table 6-1 show that when the driver's door was opened on the test vehicle a load of 0.8A was placed on the battery. The author speculates that this is unlikely to have been attributed to a fuel pump priming since the current is too low for a fuel pump, unfortunately the test environment was too noisy to hear if the pump was

running or not. Another explanation could be that the ECU powers up when the driver's door is opened, this is perhaps more likely given the low current involved since the engine is not running the ECU will not be required to drive high current devices, only low power devices such as the instrument cluster. In either case it is likely that an interior courtesy light would illuminate on opening the door, if this was 5W bulb then it would draw a current of 0.4A at approximately 12v so this only accounts for half of the measured current. After opening the door the engine was started without significant delay and therefore it was not possible to determine if the 0.8A load changed with respect to time, but it can be seen that the load continued after the driver's door was shut perhaps adding validity to the theory that the load is from the ECU rather than a fuel pump. A load of 0.8A at the nominal system voltage of 12v, appropriate given that the engine was not running, equates to a power of 9.6W. If this load is indeed from the ECU switching on and is a process that continues each and every time the driver's door is opened it could become a significant factor if the vehicle is repeatedly disturbed during soak periods and the SLI battery is not on charge.

When the vehicle was keyed on there was an initial spike in the current then a second later the reading stabilised to 2.3A. The assumption is that this is the load from the glowpugs on this diesel vehicle. The next steps in the test from 7 through 17 consisted of switching various auxiliary loads on and off without the engine running. The highest loads are from the HVAC blower on maximum speed, 18.2A recorded, the headlights, 15.65A and the heated rear window, 15.6A. These devices have changed the vehicle current demand on the battery by a factor of between six and eight times from the steady state current with no auxiliary loads switched on. The radio in this vehicle was the lowest auxiliary load, with only 0.3A recorded. This is an interesting result since it is not unheard of for emissions test drivers to switch the radio on whilst driving during development tests and with a load of only 0.3A it is suggested that this would be unlikely to have a significant effect on CO_2 emissions. However it is not uncommon on luxury vehicles for the sound system to incorporate a power amplifier for the speakers, in which case the electrical load from the sound system would be much higher and switching it on during a test would be more likely to have a significant effect on CO_2 emissions.

Once the engine was started the next few readings show the alternator being loaded up to recharge the energy lost from the battery during the engine cranking. Readings 19 through 21 shows that the alternator current rapidly decays from a high value in the region of 60A to only around 3A in the space of just over 10 minutes. The battery load remained constant during this time at 2.4A and it is therefore assumed that this is the current required to run the ECU on this vehicle, with the engine running. There will likely be a difference for the ECU load with the engine on and off, due to the load from the injectors

when the engine is running. When a selection of the previous auxiliary loads were again switched on with the engine running to verify the results and it was found that the recorded current was different for the auxiliary loads with the engine running. The offset between the two sets of results was not constant; for the position lamps the difference was 0.3A, whilst for the main beam headlights the difference was 1.55A. It is hard to understand the reason for this difference without a deeper insight into the calibration of the vehicle electrical system which is outside the scope of this thesis. It is also possible that a portion of this variation is attributable to the accuracy of the measurement system. Perhaps a more robust approach for loads such as lighting is to read the bulb wattage and calculate the current, the same approach could be used for other items, providing the power requirement is known or stated on the component. The load from the electric windows was also measured in steps 28 through 30 and it was found, perhaps unsurprisingly that the load for raising the window, due to the gravitational force, is higher than lowering, 10.5 and 7.5A respectively. It was also found that holding the electric window switch in the up position after the window has closed caused a drain of 28A from the motor stalling. In most vehicles this stall is limited to a set period of time in the region of 1 second and therefore whilst the recorded current is high it is unlikely to have a significant effect on CO_2 emissions since the period is so small. One of the most significant electrical loads that could only be measured with the engine running is the air conditioning, which was found to draw in the region of 33A, making it the highest auxiliary load recorded on this vehicle. At the heart of any air conditioning system is the compressor, which is a mechanically driven device connected to the engine. Theoretically the only electrical load associated with the air conditioning system would be from the HVAC blower fan, however an earlier separate recording of the blower on maximum speed showed the load was only 18.2A. This leaves an unexplained electrical load of 14.8A on the battery with the air conditioning on. The author speculates that this load could have been to engage an electrically actuated clutch on the compressor pulley. Unfortunately it was not possible to verify if the vehicle had one fitted nor take a measurement to verify this. At the end of the test when the vehicle was switched off it was interesting to see that the battery load returned to almost the same value recorded at the start of the test, 0.7A compared with 0.8A giving confidence that the current measurement system had not drifted during the test.

The results from the static testing of the B-car test vehicle show that the electrical load from auxiliary devices varies considerably depending on the device and the likely duration of the load. The testing so far has shown the magnitude of electrical auxiliary devices in terms of current, but has yet to examine the effect of auxiliary loads in terms of CO_2. To that end a similar test was conducted except with the vehicle being driven and the CO_2 emissions recorded.

6.3. The effect of auxiliary electrical loads on CO_2 emissions

On the same B-car test vehicle as in previous section a test sequence was developed whereby the vehicle was warmed up by driving at a standard warm up cycle, then the vehicle was cruised at a constant speed of 28kph in 2nd gear whilst various electrical loads were switched on and off. The human driver attempted to maintain a constant speed during the testing. The industry standard CVS emissions measurement system installed in the test cell was used to analyse modal tailpipe emissions over consecutive 30 second sampling periods. The test was started with no auxiliary electrical loads switched on and the CO_2 emissions were sampled for 30 seconds. Then an auxiliary load was switched on and another 30 second sample was measured. In between each measurement with an auxiliary load switched on, a 30 second sample was taken with no loads switched on to verify that the baseline emissions had not changed. During the experiment, HIOKI 9278 current clamps connected to a HIOKI power analyser were used to measure the fusebox and battery currents from the vehicle, as per the setup used earlier in this chapter.

The results from the test are shown in Figure 6-2 which shows the recorded fusebox current and in Figure 6-3 which shows the corresponding modal CO_2 mass emissions. The fusebox current results show excellent agreement with the static results of Table 6-1. The largest electrical auxiliary loads are from the HVAC system, namely the air conditioning system, blower fan and heated rear window. The second largest group of loads is the headlights. The baseline current is very consistent, returning to almost exactly the same value of approximately 2.5A between each auxiliary load. For three of the auxiliary loads, namely the air conditioning, HVAC blower and heated rear window the current is not stable during the 30 second sampling window and is either increasing or decreasing. It is difficult to imagine a reason for the current changing with time since the electrical load is by definition constant with the possible exception of the air conditioning, where the system could be configured to operate at different set points based on the in-vehicle temperature demand. The variation in fusebox current is not correlated with vehicle speed, unlike the tailpipe CO_2 emissions which are highly correlated with vehicle speed. By reference to Figure 6-3 it can be seen that for the HVAC system, the main beam headlights and for some of the ‘off’ periods the gradual change in cruise speed is approximately proportional to the change in CO_2 emissions.

The vehicle speed was not well controlled during the 30 second sampling for the air conditioning and this was because the sudden and significant change in mechanical load on the engine from the air conditioning compressor caused a drop in vehicle speed to which the driver reacted by accelerating harshly, overshooting the target speed and then slowing back near the target 28kph. This speed excursion caused a marked effect on the

recorded CO_2 emissions which can be seen in Figure 6-3. The CO_2 emissions spike to very large value that is nearly double the steady state CO_2 recorded with no auxiliary loads switched on. The instability in the CO_2 emissions from the sampling period with the air conditioning switched on means that it is impossible to separate the CO_2 effect of the additional load placed on the engine via the mechanical compressor from the mechanical load from the alternator via the vehicle electrical system.

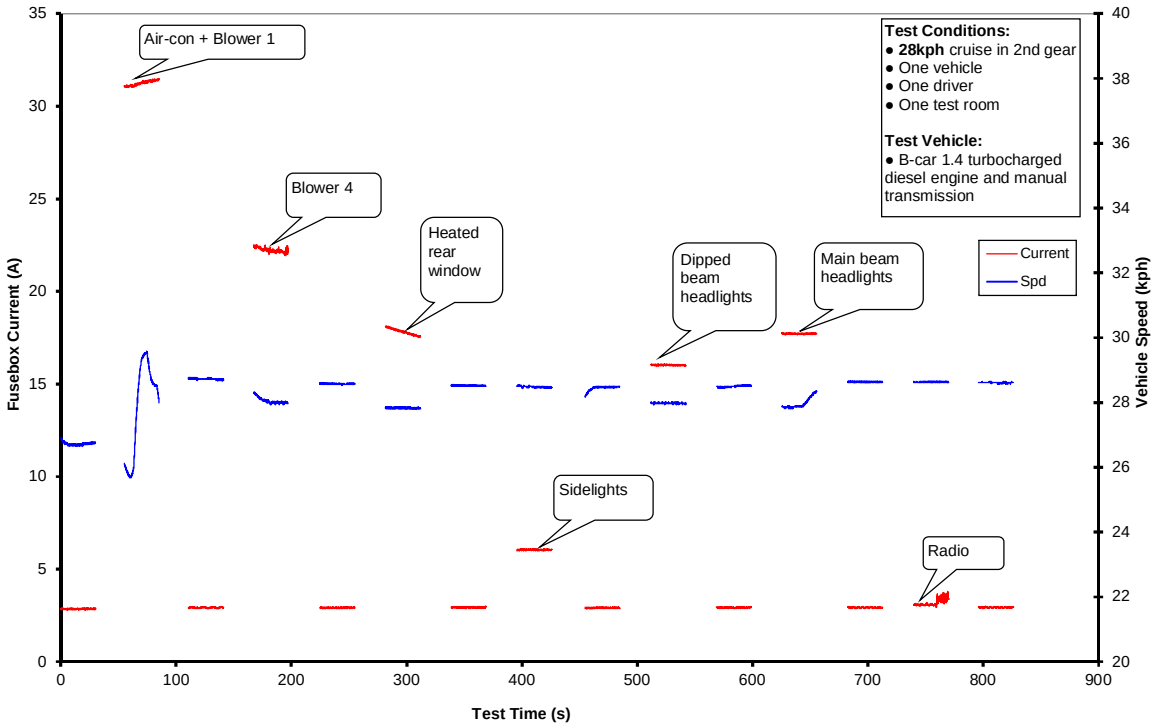

Figure 6-2: Results of electrical load measurements during 2nd gear cruise at 28kph with seven different configurations of electrical auxiliary devices switched on

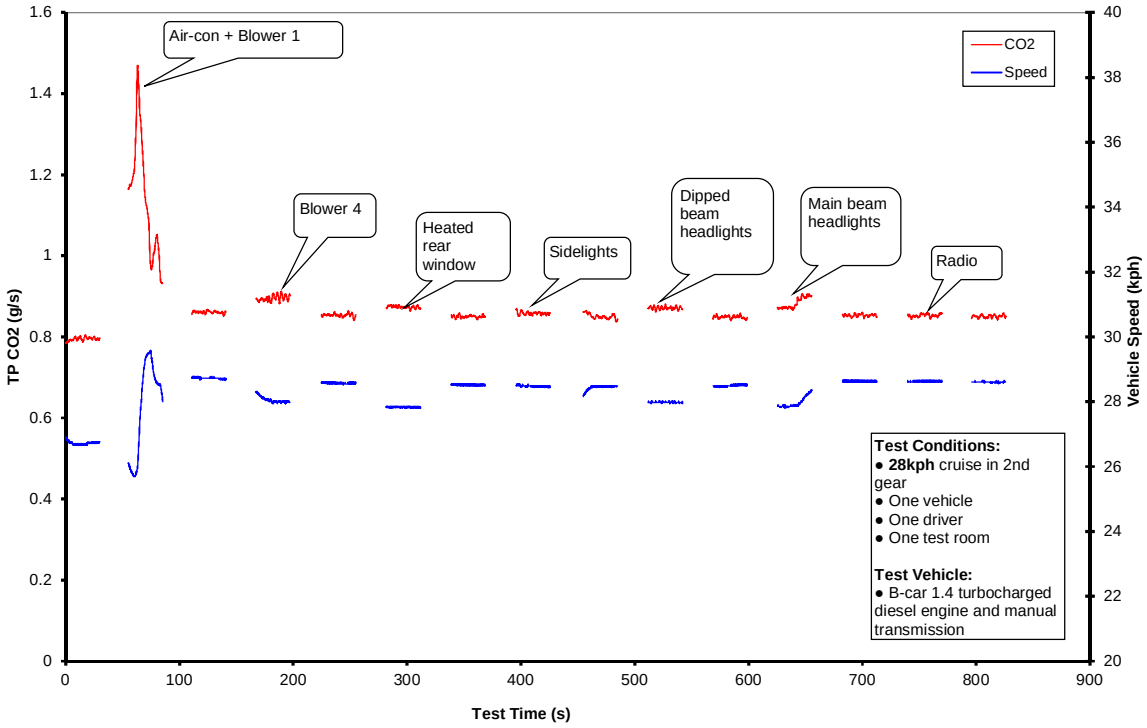

Figure 6-3: Results of tailpipe CO_2 measurements during 2nd gear cruise at 28kph with seven different configurations of electrical auxiliary devices switched on

For the auxiliary loads the change in CO_2 emissions seems to scale with the changes in current recorded previously. The largest consistent CO_2 emissions change is for the HVAC blower, main beam headlights and heated rear window, which were the also largest recorded electrical loads in both Figure 6-2 and Table 6-1.

By averaging the instantaneous alternator current and vehicle FC recorded during the 30s sampling windows the relationship between the average change in alternator current, from the baseline, and the average change in FC, again from the baseline can be determined. By assuming a constant system voltage of 14.4V, as is the case in a basic alternator equipped vehicle the average alternator power and fuel power can be calculated allowing the relationship between change in electrical power and consumed fuel power to be directly compared. The resulting relationship is shown in Figure 6-4.

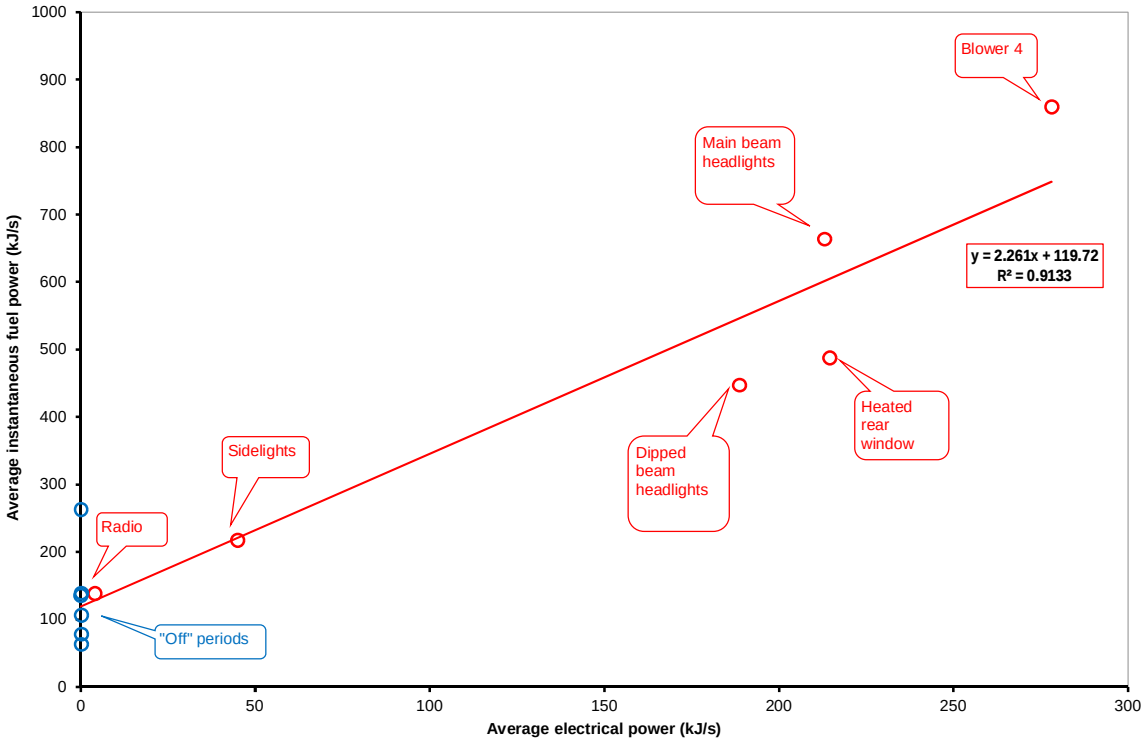

Figure 6-4: Relationship between the average fuel power consumed by the engine and the average electrical power consumed by the auxiliary devices. Red data points were calculated from data recorded with auxiliary loads switched on and blue data points were calculated from data recorded with the auxiliary loads switched off.

The exceptionally high coefficient of determination of 0.91 for the linear best fit in Figure 6-4 shows that the alternator power is directly proportional to the consumed fuel energy. For this vehicle, the gradient of the best fit line shows that an increase in the alternator energy from an auxiliary load requires an increase in the consumed fuel energy of just over twice the magnitude of the change in alternator energy. With no electrical loads switched on the engine is consuming approximately 120kJ/s of fuel energy to be driven at a steady 28kph in second gear. With the highest electrical auxiliary load switched on the rate of consumed fuel energy is increased by approximately seven times from the baseline, thereby highlighting the potential significance of variability in electrical auxiliary loads. The results from the sampling period with the air conditioning system switched on has been excluded from Figure 6-4 since it is a combination of mechanical and electrical loads making it an outlier with respect to the other data points.

Whilst the results collected thus far are useful for determining both what the relative CO_2 effect of auxiliary loads are, i.e. which auxiliaries should experimenters be most concerned about and what the likely power consumption of the loads is, the results do not allow a direct arbitration of the effect on bag CO_2 emissions over a TA style emissions test. To this end an experiment was conducted using the same vehicle and test cell as the previous experiments in this chapter. In this case the vehicle was tested over four consecutive TA style emissions tests. However in this case the tests were hot start. Hot

start tests were chosen primarily for expediency, so that all testing could be completed within one working shift. However there were other benefits, such as thermal stability of the vehicle, being able to use the same driver, the same test cell and emissions analyser for all tests. This minimises potential errors from all the other factors outside of the vehicle electrical system and means a good level of repeatability is much more likely since differences in factors such as the emissions measurement system, the load applied by the dynamometer and the way in which the vehicle is driven are all minimised. For the four tests the vehicle test condition was alternated between all auxiliary loads switched on and off in an A-B-A-B sequence. The results are shown in Figure 6-5 and Figure 6-6.

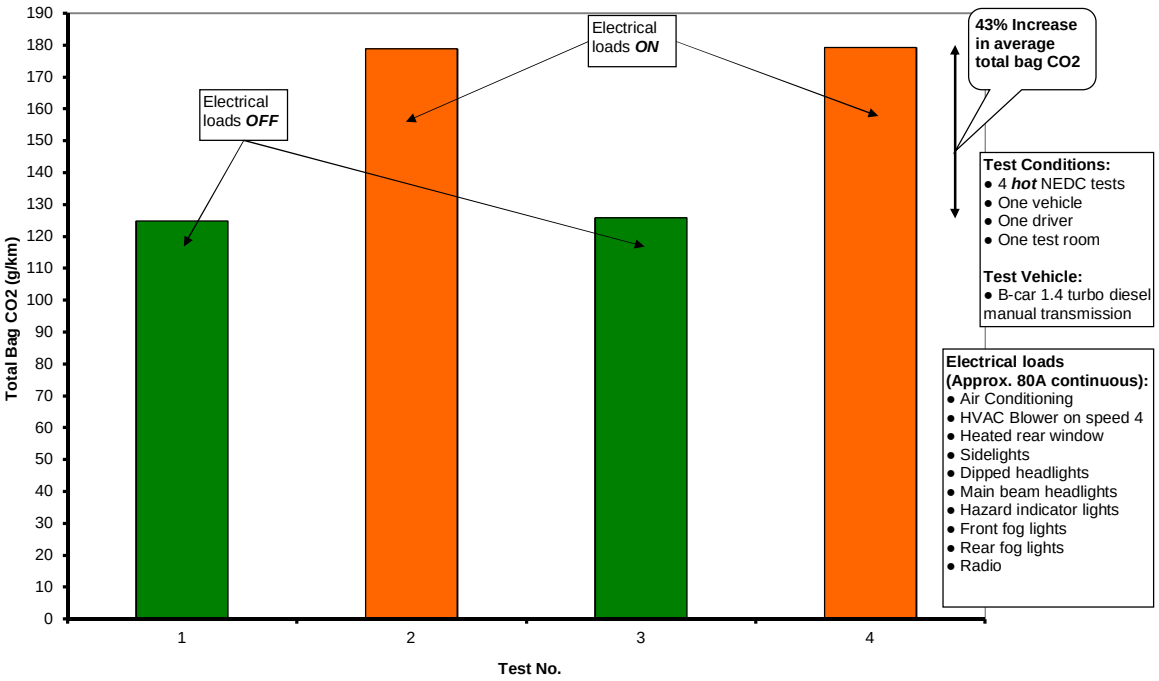

Figure 6-5: Recorded total bag CO_2 emissions from repeated tests of a B-car on hot start TA style emissions tests in test cell 4 with all auxiliary loads switched on and off

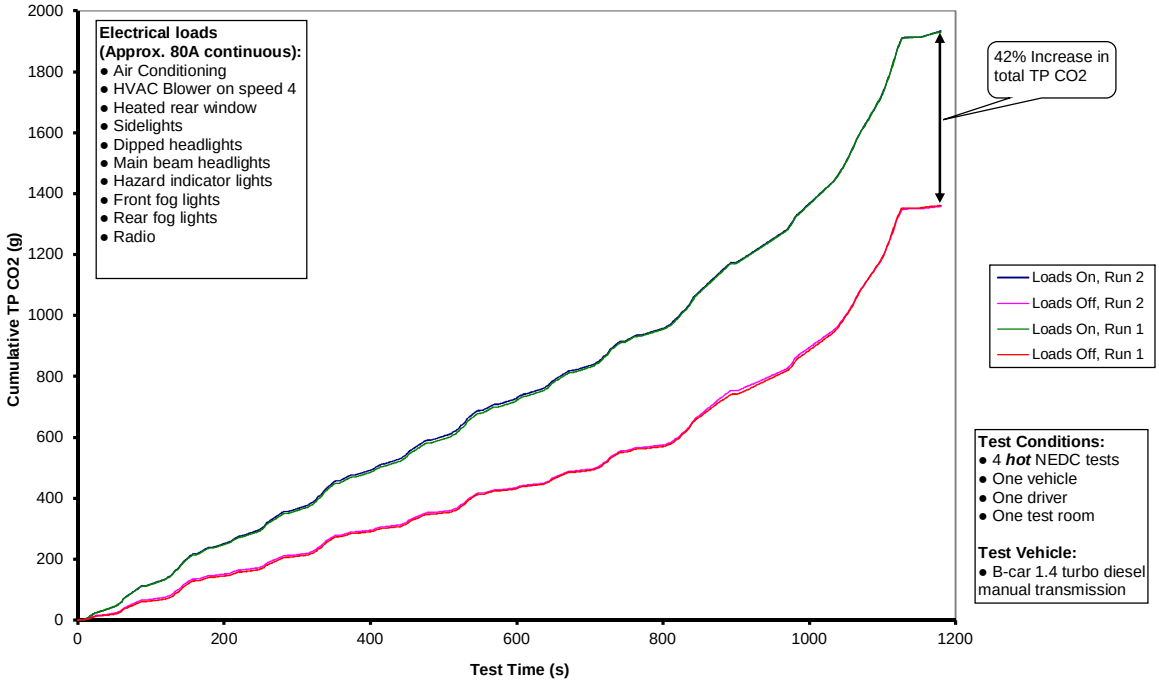

Figure 6-6:Recorded cumulative modal tailpipe (TP) CO_2 emissions from repeated tests of a B-car on hot start TA style emissions tests in test cell 4 with all auxiliary loads switched on and off

By examination of Figure 6-5 and Figure 6-6 it is apparent just how large the change in CO_2 emissions can be from electrical auxiliary loads when they affect the entire duration of an emissions test. In the previous sections of this chapter it has been shown that the highest individual loads cause changes to the vehicle battery current demand of up to eight times during static testing. During steady state cruising this equated to a change in the electrical power demand of up to approximately 275kJ/s. The resulting change in instantaneous consumed fuel power for each auxiliary load was approximately 2.2 times larger. From the drive cycle tests of Figure 6-5 it can be seen that with all electrical auxiliary loads switched on the change in CO_2 emissions is 43%. In addition Figure 6-6 shows that this difference was approximately constant for the entire duration of the test since the modal CO_2 lines are constantly diverging by the same amount. In the literature it was found that the expected range for the change in CO_2 emissions was 5 – 50% [14] from TA style tests and hence are in reasonably good agreement with the effect published in the literature. Of course the test vehicle used here was a reasonably simple one and therefore there are some auxiliary loads which are now more commonplace but could not be tested, e.g. heated windscreen, heated seats, stereo power amplifier, active cruise control and so on. These devices would increase the size of the difference between the two conditions, perhaps to a similar magnitude as reported in the literature, perhaps to an even higher magnitude. Conversely the air conditioning system was switched on for this test which as seen previously is a combination of mechanical and electrical loads. Therefore a proportion of the 43% change in CO_2 emissions will be a result of the increased mechanical load from the compressor rather than the alternator. Unfortunately

the tests could not be repeated with the air conditioning system switched off to isolate this effect.

The repeatability of the tests is also quite remarkable, when compared with the analysis of Chapter 5, from a test sequence performed in test cell 4 of the commercial laboratory. Figure 6-6 shows that the modal CO_2 recorded for the two tests at each condition which are so consistent that the traces are completely indistinguishable. It serves to highlight an important point that is relevant to the entirety of this thesis. It shows just what is capable with good vehicle and test cell pre-conditioning, a repeatable driver and emissions measurement system. The coefficient of variation with all electrical loads switched on was 0.15% and with all loads off was 0.58%. It shows that whilst it might not be possible to always see the effect of improvement in one aspect of TA style emissions testing due to a lack of control in other factors. It is possible to achieve the goal of a CoV of less than 0.5% from a small number of tests at within a commercial environment if the appropriate controls are implemented.

In the literature there was no information regarding where an experimenter might expect their results to lie within the stated +5 to +50% CO_2 effect from electrical auxiliary loads. The results from the literature have shown that the expected range of magnitude for the effect of switching on all electrical auxiliaries is in approximate agreement with the collected experimental data however the effect of individual electrical auxiliary loads has only been examined during steady state testing. Both the results reported in the literature from Brace et. al. [8] and the results from the steady state testing of this chapter, see Figure 6-4, have shown that there is a linear correlation between alternator electrical output and consumed fuel energy. On this basis the alternator current measurements taken during the steady state testing, see Figure 6-2, were used to scale the total bag CO_2 results from the hot start drive cycle tests and give an approximate indication of the expected change in bag results over a full NEDC test and the results are shown in Figure 6-7.

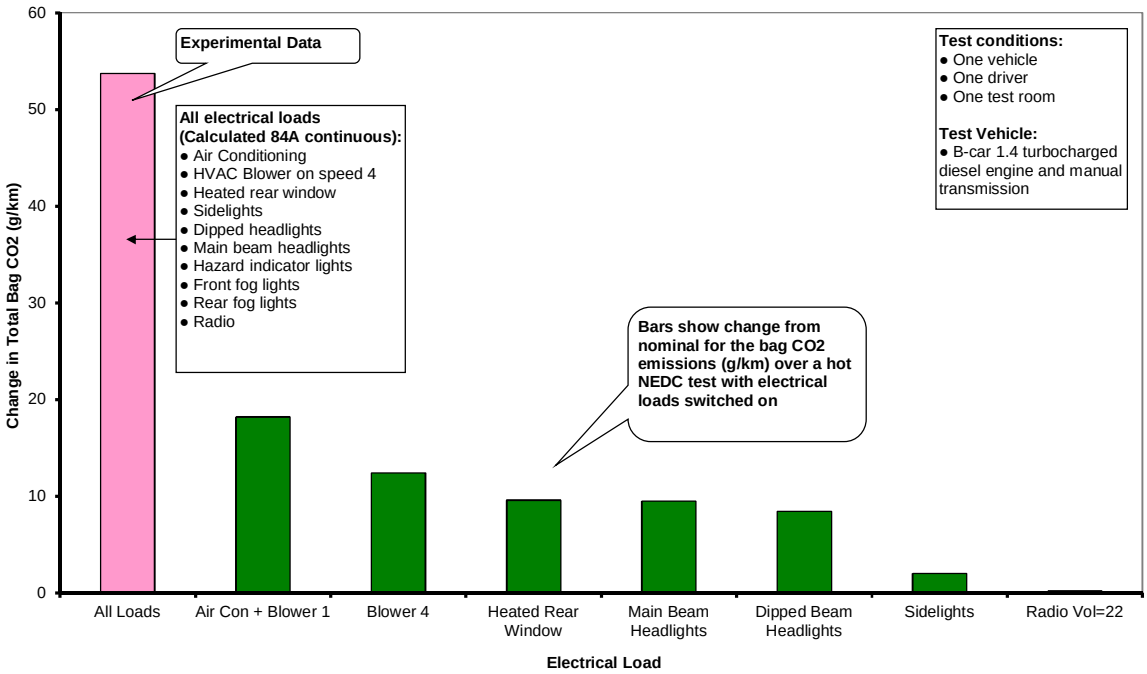

Figure 6-7: Recorded change in total bag CO_2 emissions for all electrical loads and calculated change in total bag CO_2 emissions from individual electrical loads

The results from Figure 6-7 show that the expected change in total bag CO_2 emissions from a hot start NEDC test range between approximately 18 and 0.2 g/km depending on the auxiliary load that is switched on during the test. For this vehicle, a B-car with a 1.4 litre diesel engine, the average hot start total bag CO_2 emissions were 125.3g/km so this range represents a change of between 14 and 0.16% for individual auxiliary loads.

6.4. The effect of SLI Battery SoC on CO_2 emissions

The literature review highlighted that control of the pre-test SLI battery SoC is important to maintain high precision CO_2 emissions results. Authors recorded quite different magnitudes for the effect of battery discharge on the CO_2 emissions with changes in FC or CO_2 emissions ranging from +5 to +30%. As discussed in the literature review, some of this variability in the results can be explained by the examination of different levels of battery discharge. For example Brace et. al. [8] recorded an 8.7% change in FC from a 45 minute discharge of the battery with the vehicle headlamps, whilst the Schmidt et. al. [20] recorded a 30% change in CO_2 from discharging a vehicle battery until it was only just able to start the vehicle. The authors even found different results within their own study which shows that relative magnitude of battery discharge on CO_2 emissions really can be thought of as vehicle specific. It is a function of several factors which include but are not limited to the engine efficiency, alternator efficiency, battery charge acceptance and the battery charging strategy.

The traditional methods for controlling pre-test battery SoC is either to charge the battery between each emissions test such that the experimenter aims to start each test with a 100% SoC. Or to run a conditioning cycle to stabilise the vehicle, then not to charge between each test but to make sure that the auxiliary loads are kept the same for each test via implementation of procedural controls, such as not operating electric windows and so on. The first method is often used in research testing environments since it provides the easiest way to maintain high precision. If the soak periods are maintained at the same duration between tests then the battery condition should be the same going into each test and the load on the vehicle electrical system from battery charging will be consistent. This is also the method that is used for the quality check test vehicles in the commercial laboratory for the same reasons. The second method is preferable for those calibrating vehicles with TA in mind and is therefore the method that is often used by clients. This is because it is closer to the method used for TA emissions tests and hence reduces the offset between development and final witnessed TA testing. One author in the literature attempted to quantify the difference between these two modes of testing and found that the effect was 1% in CO_2 emissions, with no stated statistical confidence [14].

The existence of these two methods creates a real difficulty for the quality department of a commercial laboratory when looking to identify equipment or process problems in test cells. For example a client of a laboratory might complain that they are getting imprecise CO_2 results from their TA style emissions tests. In this case the Quality Engineer is likely to examine the results from quality check vehicles and might find that these results show high precision in CO_2 emissions. There are many possible causes for this, but one that is relevant here is that the client vehicle might have highly variable battery SoC during soak, whilst the quality check vehicle battery SoC is, as will be shown later in the chapter, much more likely to be consistent due to the battery charging during soak periods. If both sets of results show a problem then the quality check vehicle might be kept in the problem test cell for an extended period. In the commercial laboratory examined in this thesis there are no battery chargers located in the test cell and therefore a previously stable quality check vehicle might suddenly become unstable due to battery SoC variation, masking any equipment issues in the test cell. This sequence of events has been witnessed by the author. Aside from test cell problems of imprecision, another important issue in the context of TA emissions tests is the absolute CO_2 emissions. The literature has already shown that there is a 1% difference in CO_2 emissions from the two battery charging processes. To gain confidence in this finding an experiment was conducted using the quality check vehicle C which was tested at Bath University alternating between the conditions of battery charging during soak periods and no battery charging. The test vehicle was a C-car with a 2.0 litre displacement turbocharged gasoline engine and an automatic transmission. The same human driver was used for all tests which were conducted at a

controlled test cell ambient of 25°C. The vehicle was not removed from the dynamometer for the duration of the test programme. In total seven tests were completed with the battery being charged during soak and 17 tests with the battery not being charged. Figure 6-8, Figure 6-9 and Figure 6-10 respectively show a bar chart of the results, a time series plot and a histogram.

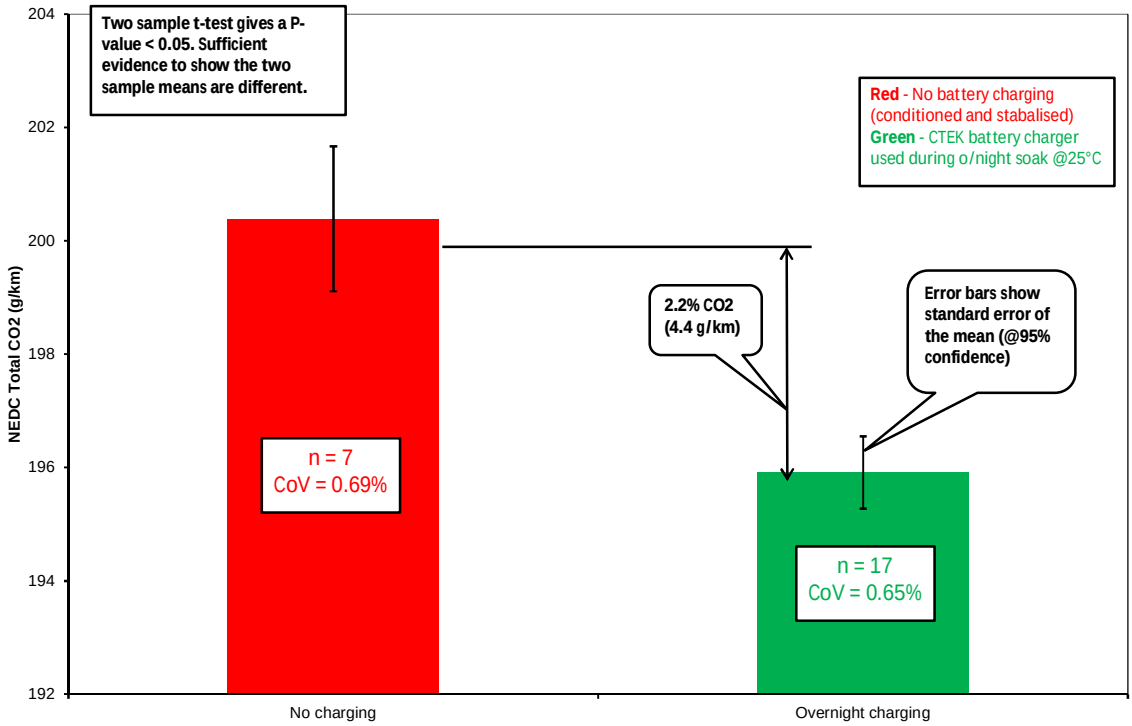

Figure 6-8: Bar chart of total bag CO_2 emissions from a C-car with a turbocharged gasoline engine. For tests with battery charging during the preceding overnight soak and tests without any soak battery charging. Error bars show standard error of the mean at 95% confidence

In this experiment a 2.2% difference was found in the total bag CO_2 emissions between the two conditions. A two sample t-test was conducted on the results which showed that the difference in the recorded CO_2 emissions was statistically significant at a 95% confidence level.

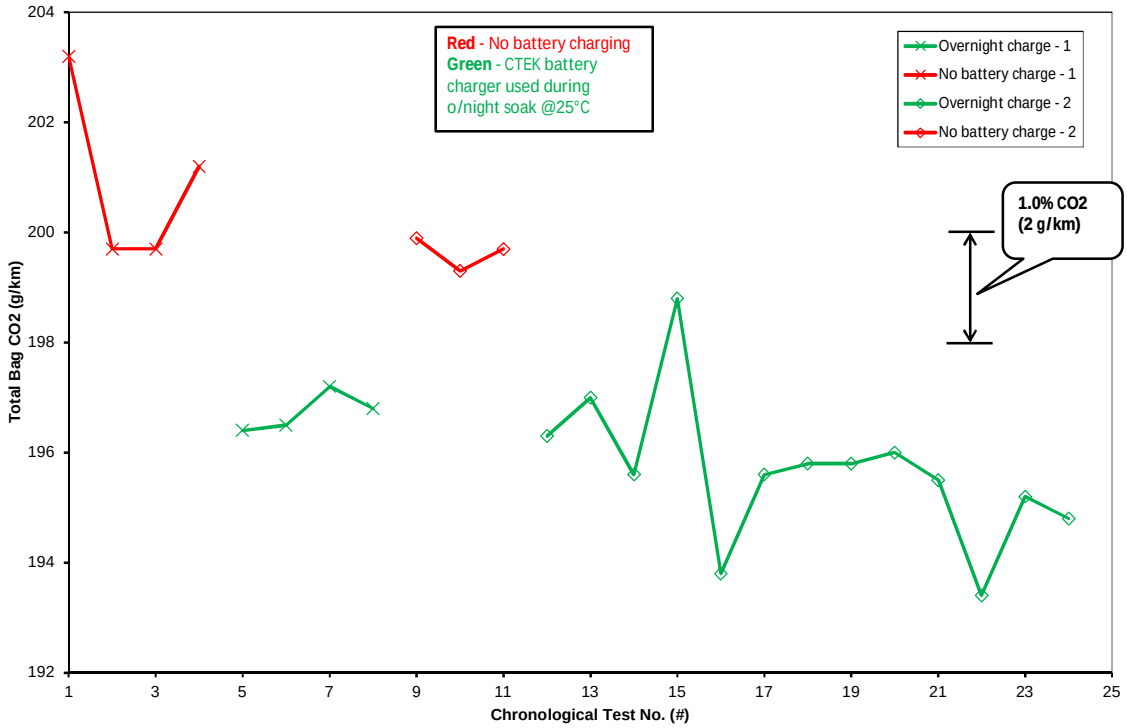

Figure 6-9: Time series plot of a total bag CO_2 emissions from a C-car with a turbocharged gasoline engine. For tests with battery charging during the preceding overnight soak and tests without any soak battery charging

The difference between the two test conditions recorded from this experiment is just over double the magnitude that was reported in the literature [14] thereby showing that even for a production intent vehicle there is a significant change in CO_2 emissions when the battery is not charged during the soak and even more importantly the change is immediate, so it is absolutely critical that the same process is adopted for every single soak period. The magnitude of the difference between the two methods is highly likely to be vehicle specific. For example if a vehicle has a problem and there is a permanent drain on the battery the effect will be much larger than a vehicle where there are no faults with the electrical system and hence little to no drain on the battery during soak periods. Also for conventional vehicles without smart alternator technology, whilst the alternator efficiency is likely to be similar between vehicles, the engine efficiency could be quite different, especially if comparing a diesel and a gasoline engine vehicle. From the time series plot of Figure 6-9 it can be seen that none of the individual data points from each method overlap adding to the result of the two sample t-test and giving more confidence in the recorded difference between the two methods. This point is further highlighted by the histogram of Figure 6-10.

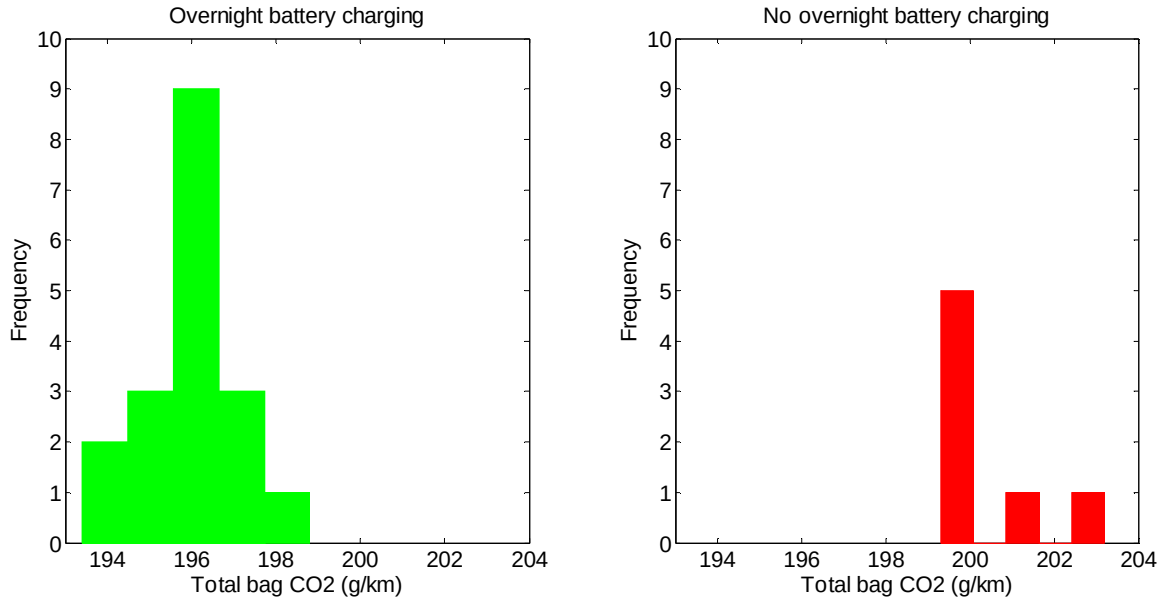

Figure 6-10: Histogram of total bag CO_2 emissions from a C-car with a turbocharged gasoline engine for tests with battery charging during the preceding overnight soak and tests without any soak battery charging

It is interesting to examine the variability in the results from the two groups. The repeatability is generally very good for the two methods with CoV's of 0.69 and 0.65% both being quite close to the target of 0.5% and much below the variability in typical results from the commercial laboratory quality check vehicles. However the variability is still higher than the author would like and there are clear spikes in the data, suggesting there could be outlier results on test days 1, 15, 16 and 22. An examination of the test diary reveals some of the difficulties that commonly affect this type of experiment. On test 12 the engineer decided to conduct a short dynamometer warm up without consent of the test owner. For test 17 the climatic plant was accidently switched off for the duration of the test meaning that the end of test temperature was 2-3°C higher than the target. Also on test 17 the key had been left in the vehicle overnight from the previous test. For test 21 the operator chose to run twice the normal number of coastdown tests requested by the test owner. On test 22 the battery charger was accidently left connected until over halfway through the emissions test with the unsurprising consequence that the CO_2 emissions are the lowest recorded for any of the tests in the experiment. For many of the tests there were problems with the current clamps installed onto the vehicle, which will affect the analysis in the following sections of this chapter. For tests 5, 6 and 7 the clamps did not record any data due to low batteries. On test 15 the clamps were found to be showing a higher than normal fusebox current during the post-test running with a corresponding increase in alternator current. This snapshot of the problems encountered goes someway to explaining why it is so difficult to conduct a 'good' experiment with a high level of repeatability. Given that most of the issues in this experiment come from human error, it also indicates that with automation it is possible to minimise a lot of common errors.

Interestingly, despite these problems, it is only for test 22 that the recorded human errors correlate with a change in total bag CO_2 emissions.

So far the analysis of the results from this experiment has shown that a significant difference was recorded between the two methods, however the chassis dynamometer emissions test is such a large multiple input and output system that this result alone is not conclusive proof of the root causality of the difference between the two groups. To do this it is necessary to examine the detailed results recorded during the experiment which includes a measure of the alternator and vehicle fusebox current. Figure 6-11 shows the recorded instantaneous alternator current during the TA style emissions tests on vehicle C, from which there is a clear difference between the results from the two test conditions. The results plotted in blue, which represent the tests where the battery was charged, have a lower magnitude throughout the duration of the test. The difference is most clearly seen in the first 200 seconds, where most of the current traces for the 'charging' tests are about half the magnitude of the 'no charging' tests. Furthermore the tests where the battery was charged are much more repeatable than those were the battery was not charged. This shows that there is an improvement not only in the absolute magnitude of the alternator current but also an improvement in the alternator current precision. By reference back to Figure 6-8, this improvement is somewhat reduced for the CO_2 emissions where the improvement in the CoV was barely registered being only 0.04%. In fact there is very little difference in the precision of the CO_2 results from the two groups. As will be seen in other chapters of this thesis, it is clear that a measurable improvement in a test noise factor does not necessarily force an improvement in the overall system output, the CO_2 emissions, since there are too many variables in the system that are changing simultaneously. In this case a high precision of alternator current is not translated into an improvement in CO_2 emissions precision.

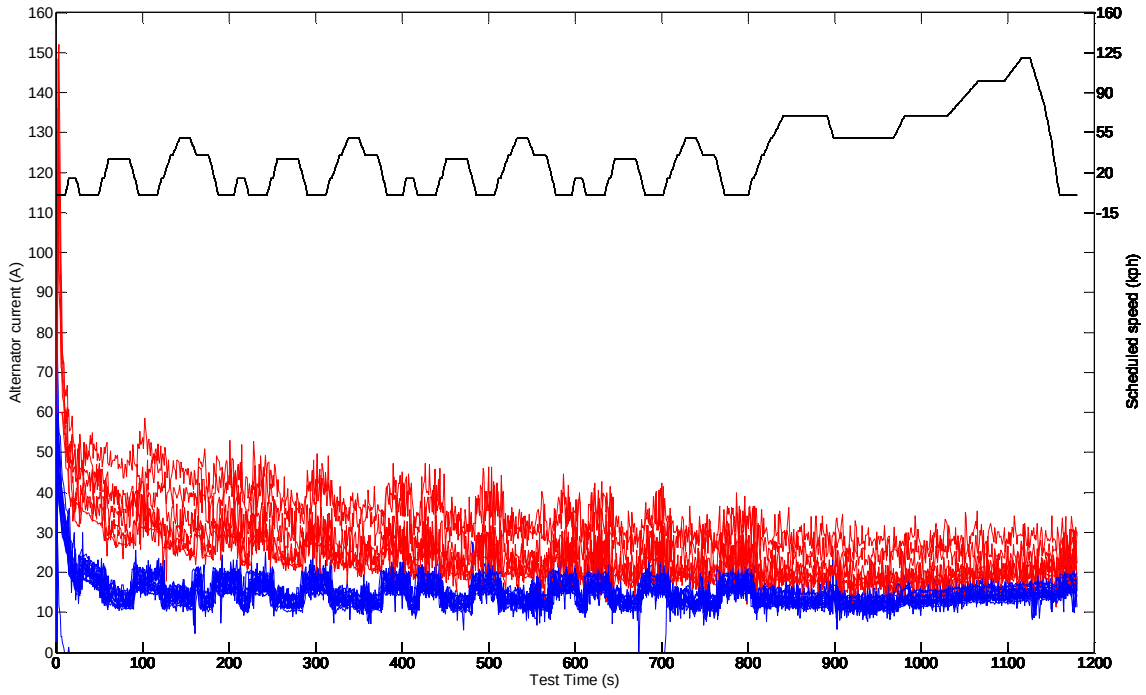

Figure 6-11: Vehicle C alternator current measured instantaneously during 24 NEDC tests. 7 tests where the SLI battery was charged overnight prior to the test (shown in blue) and 17 tests where there was no battery charging prior to the test (shown in red)

An interesting characteristic of the results in Figure 6-11 is that the current is not stable and instead increases or decreases by an approximately fixed value depending on the vehicle driving mode. This phenomenon is known as selective charging or smart alternator and is done to save fuel and hence reduce CO_2 emissions [25]. This concept was introduced in the literature review, see section 2.2.3.

Using the alternator current results recorded during the tests, see Figure 6-11, the change in total energy output from the alternator was calculated for each test on vehicle C and was plotted against the change in consumed fuel energy. This was done by assuming a constant system voltage of 14.4v for the duration of the test and calculating the total electrical energy transferred for each individual test. These were then used to calculate the mean and the corresponding change from the mean for each test. The same principles were used to calculate the change in consumed fuel energy. The CVS system reports the total mass of fuel used for each test, which it calculates using the industry standard carbon balance technique and user inputted values for the carbon:hydrogen ratio of the fuel. The fuel mass was converted to energy using an approximate figure of 44 MJ/kg for the lower heating value of gasoline [90]. The lower heating value was chosen because it includes the energy required to vaporise the water during the combustion process and an approximate figure was chosen because the exact properties for the fuel used during the testing were not known. Both test conditions, with overnight charging and without were included in this analysis and the results are shown in Figure 6-12.

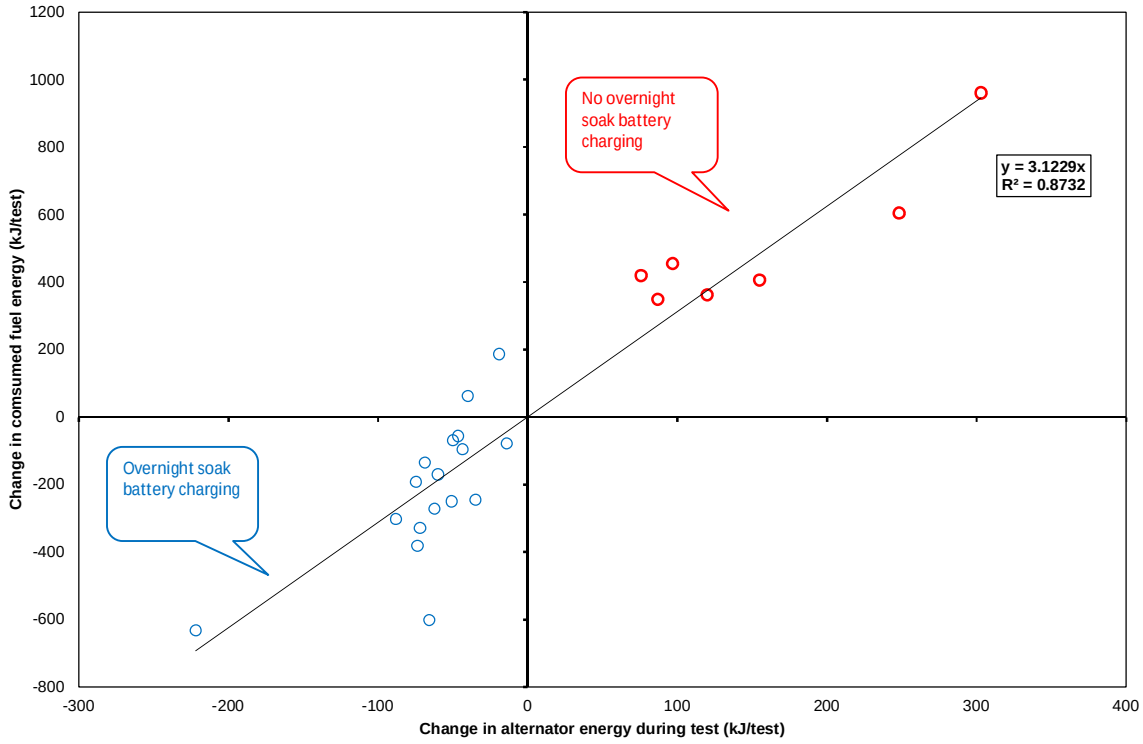

Figure 6-12: Vehicle C change in alternator energy during the emissions tests versus the change in the bag CO_2 emissions from the same tests. In both cases the changes are calculated from the mean alternator output energy and mean total bag CO_2 emissions from each of the emissions tests. A total of 24 tests are shown, 7 in red where the SLI battery was not charged and 17 in blue where the SLI battery was charged.

Figure 6-12 shows that there is a clear distinction between the two test conditions; with soak battery charging and without soak battery charging. When the battery is charged prior to a test, less energy is demanded from the alternator as the battery needs less recharging and hence less fuel is used. Conversely when the battery is not charged prior to the test the alternator demand is increased and more fuel is burned to meet this demand. The relationship between the change in alternator energy output during the tests and the change in consumed fuel energy during the tests is linear with a high coefficient of determination of 0.87 indicating the good level of fit. The gradient of the linear fit is approximately 3.12, so for each unit change in alternator output energy the consumed fuel energy is increased by just over three times. This is a steeper gradient than was found in Figure 6-4, where the gradient was only 2.26. The two experiments differ in the magnitude of the change in electrical energy output from the alternator; for the electrical auxiliary load testing the range was about half that seen here. However that should not affect the recorded gradient since the relationship is linear. The most significant difference between the two experiments is the test vehicles. In the case of the auxiliary load experiments the test vehicle was a B-car with a 1.4 litre displacement diesel with a manual transmission, where as in this experiment the test vehicle was a C-car with a 2.0 litre displacement gasoline engine and an automatic transmission. The author would therefore expect that the different ICE efficiencies would likely account for the difference in the gradient, since

diesel engines are more thermally efficient that gasoline engines and the losses in an automatic transmission are likely to be higher than a manual.

It is perhaps surprising, given that typical ICE efficiencies are normally in the 20% region during part load operation, that the efficiency that the gradients of both lines represent a system efficiency of between approximately 22 and 31%. However these values are based off a change in engine load and fuel used rather than taking into account the overall efficiency which would include the fuel used to counter pumping losses and engine friction. This is the engine load that is represented by the y-axis intercept on a Willan's line. A Willan's line being the straight line on a graph plotting engine load on the x-axis and fuel consumption on the y-axis [26].

During the test sequence a current clamp and logger were configured to measure the current output from the battery charger used to charge the SLI battery overnight between tests. The battery charger used for the experiment was a CTEK intelligent device and the author was interested to see the device's charging characteristic and to calculate the total charge being transferred to the battery before each test. Due to the long duration of the charging period (between 16 and 22 hours) the logging frequency had to be reduced to keep the data file a manageable size. Hence a logging frequency of 0.2Hz was selected. Initially the recorded data showed a large amount of noise and hence a low pass filter was added to the logging device by the test engineer. Unfortunately this filter was therefore not applied for some tests and applied for others. Once it was applied the raw unfiltered data was not recorded and so it was not possible to directly compare these results with any validity. This further highlights both the difficulty of recording good experimental data and also the importance of not changing the way parameters are recorded part way through a test sequence. Figure 6-13 and Figure 6-14 show the instantaneous battery charger and vehicle fusebox current recorded for a small subset of the tests were the battery was charged overnight prior to the test. The cumulative energy transferred by the battery charger is also shown along with the cumulative residual energy transferred to the battery, taking account of the vehicle energy demands. The residual energy was calculated by subtracting the vehicle fusebox current from the battery charger output current.

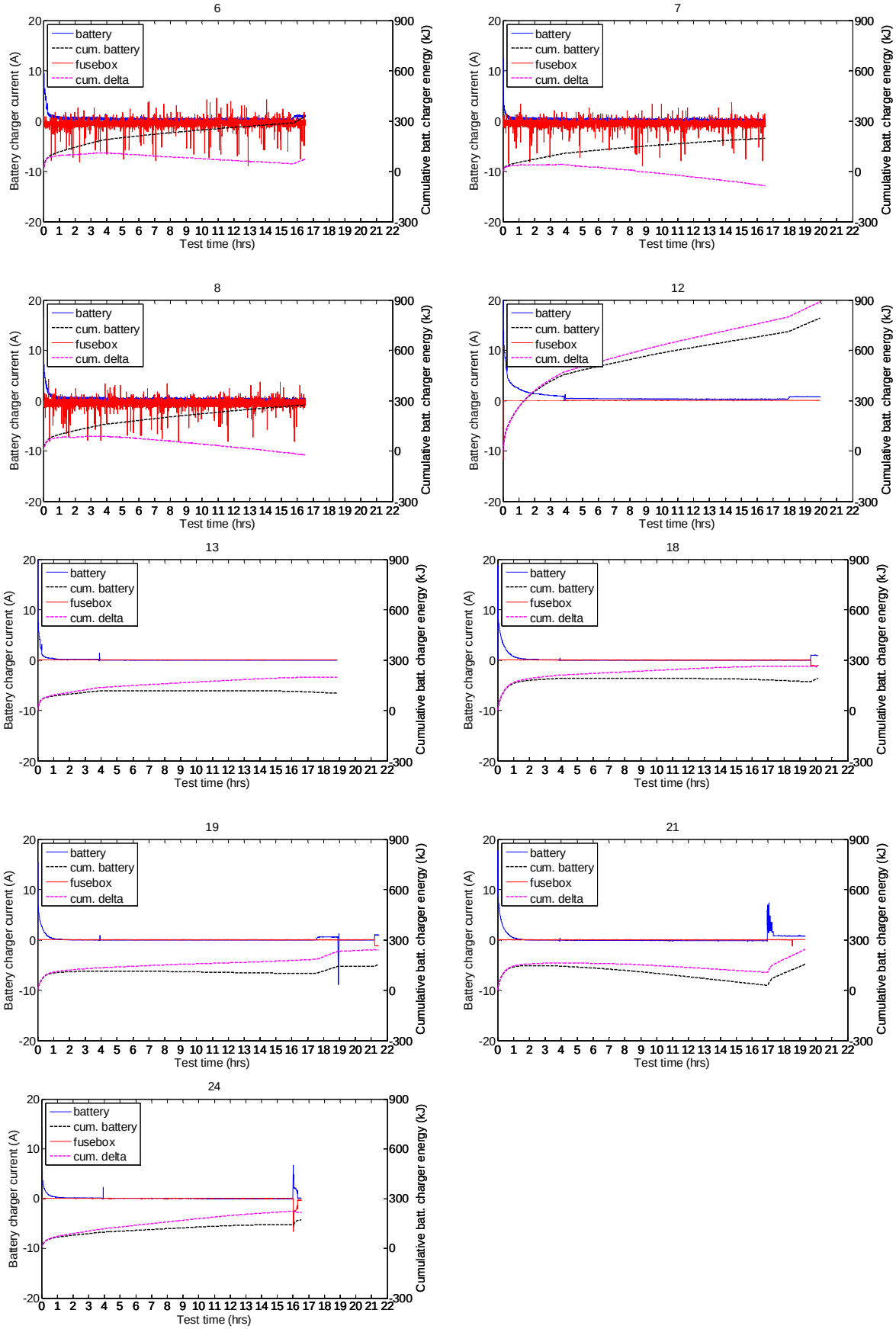

Figure 6-13: Vehicle C, overnight charge results using a CTEK smart charger to charge the vehicle SLI battery. The instantaneous current is shown in solid red and solid blue. The cumulative current in shown in dotted black and dotted pink. The chronological test number (taken from Figure 6-9) is shown above each plot.

Unfortunately the calculation of the residual current highlighted another problem with the recorded data. The current clamps used for this study were not the HIOKI devices used previously but much lower specification Picotech units. The Picotech units appear to be not very robust at accurately measuring current around zero. When the individual plots are zoomed in, see Figure 6-14, the vehicle fusebox current is sometimes recorded as zero for the majority of the test, sometimes as a slight positive current and sometimes a slight negative current. The author proposes that this is not a real affect, since there is no logical explanation for it and instead it is much more likely to a problem with the manual zeroing of the current clamps. When the difference between the two recorded current traces is calculated the result of this very small error over such a long period is very significant on the cumulative results. The final values for the residual current range from approximately -100 to 900kJ and for the first three tests the residual is lower than battery current, whilst for the other tests the pattern is reversed.

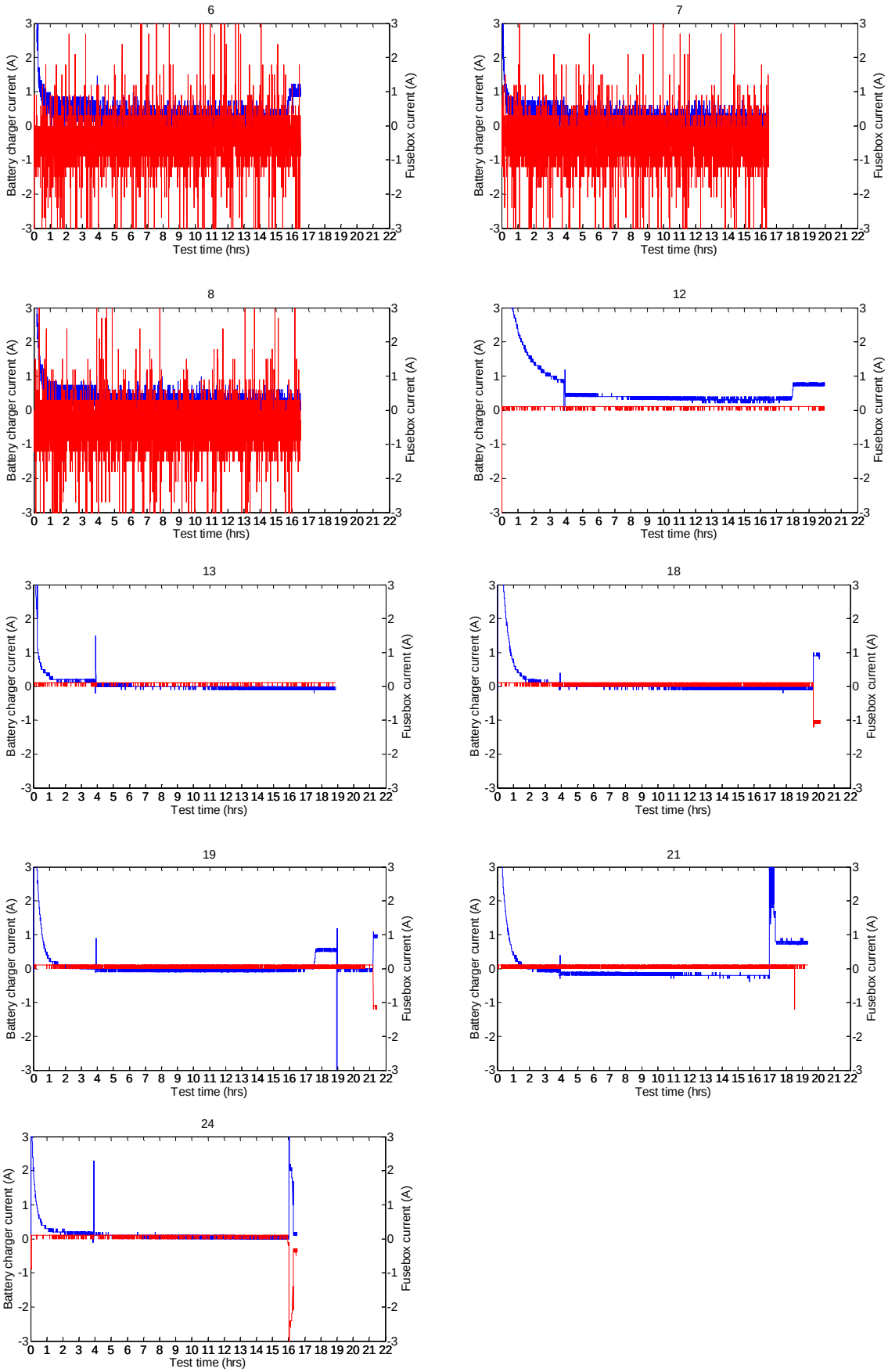

Figure 6-14: Vehicle C, overnight charge results using a CTEK smart charger to charge the vehicle SLI battery. The instantaneous battery charger current is shown in blue and the instantaneous fusebox current in red. The chronological test number (taken from Figure 6-9) is shown above each plot.

As mentioned earlier in this chapter, for the first three tests in the batch shown in Figure 6-13 and Figure 6-14 the test cell diary reveals that the test engineer had problems with the current clamps on day 6. The clamps are battery powered and low batteries were found. It appears from the results that this problem was not rectified until after day 8 and hence no real data was recorded for these days. This highlights the significant advantage in choosing mains powered clamps over battery powered clamps.

By examination of both Figure 6-13 and Figure 6-14 together it can be seen that for all tests the charging profile is reasonably similar; there is an initial exponential decay from a value of around 20A to a value between 1 and 0A which takes approximately 4 hours. At a very repeatable 4 hours into the battery charge, there is an instantaneous spike in the charging current and the charging current then takes a step change to a lower value. For most tests this lower value is around 0A; it is as if the charger is switching itself off. For all but one of the tests, towards the end of the charging period the battery charger rate takes a step change from near 0A to a higher value, which is initially a high spike in current that quickly settles to either a constant value or a profile that varies within the region of 1 to 2A. At the same time for each overnight charge the vehicle fusebox current is seen to follow a very similar profile but inverted and negative. The change in vehicle electrical load via the fusebox is due to the vehicle being ‘disturbed’ prior to the start of the emissions test. It has been seen earlier in this chapter that opening a vehicle door can cause the vehicle ECU to wake and the fuel pump to prime with a corresponding increase in battery load. This is exactly what is happening in these tests. What is of particular interest in relation to test precision is that in the case of these tests this increase in vehicle load has clearly been met by the battery charger and the result is that the battery is not drained prior to the test start. If however the battery charger had been disconnected at a different time in relation to the test start the vehicle load might have drained the battery instead. In this case there would have been an increase in the alternator load during the test, since the battery would be more discharged going into the test and there would be a corresponding increase in CO_2 emissions. This theoretically means that the variability in the difference between the total energy transferred to the battery during the overnight charge is correlated with the variability in the fuel energy consumed by the vehicle for the subsequent emissions test. Where the total energy transferred to the battery would be calculated using the balance of the battery charger output current and the vehicle fusebox input current. To prove this theory using the data from this experiment presents a few challenges. It has been seen previously that for tests for tests 6, 7 and 8 the fusebox current was not recorded properly, meaning that the energy balance cannot be calculated. By examining Figure 6-14 the same problem appears to have affected test 21. It can also be seen that for all tests the fusebox current is relatively constant until near the end of test, however the magnitude is zero for some tests and is a slight positive or slight

negative value for other tests. The accuracy of the current clamps varies between ±1.5% and ±4% depending on the measured current. For the magnitude of current being measured in this case, the stated accuracy would be either ±1.5 or ±2% depending on the measurement range used. 1.5% of the measurement range of the current clamp is 0.9A, so at the very least the clamps is highly unlikely to be able the measure 1A with a high degree of accuracy. Additionally the clamps must be zeroed, or de-magnetised, prior to each measurement to ensure an accurate zero point. If this is not done consistently, the author's previous experience with these clamps suggests the zero can easily be inaccurate within the 0 to 2A range. The approach taken was to therefore assume that for all tests the vehicle fusebox demand was met wholly by the battery charger and to analyse only the battery charger current recorded within the first four hours of the overnight charges up until the point where the current spikes and the charging rate drops. The current spikes were manually identified and the corresponding switch off times read from the raw data. The battery current was then multiplied by the typical alternator charging voltage of 14.4v since the actual voltage was not recorded. The corresponding instantaneous power was summed over the periods to find the cumulative energy transferred to the battery. For the vehicle TA style emissions tests which were conducted after each overnight charge, the mass of fuel burnt that is reported as standard from the CVS system was used to calculate the consumed fuel energy during each test. For this calculation a standard value for the LHV of gasoline of 44MJ/kg was used which was the same as used for the previous analysis in this chapter. The resulting plot of consumed fuel energy during the test versus battery charger input energy is shown in Figure 6-15.

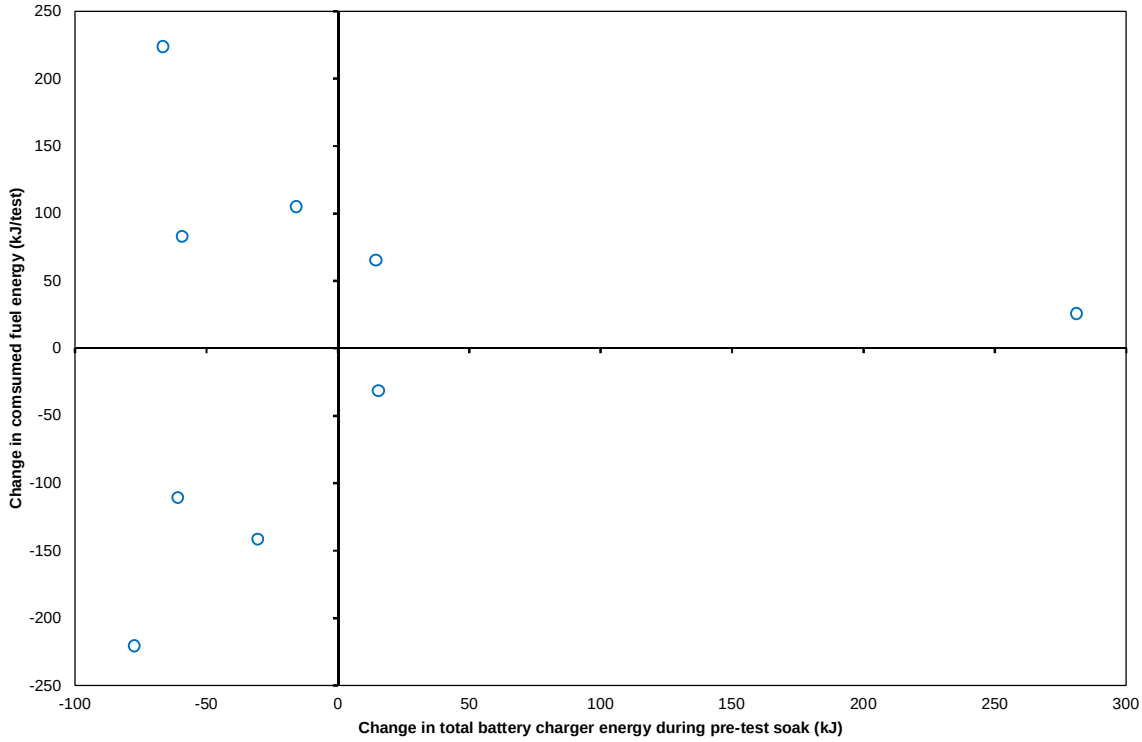

Figure 6-15: The change in the battery charger energy during pre-test overnight soak versus the change in consumed fuel energy on the concurrent emissions test for vehicle C. The battery charger energy is calculated from charger on time until the first spike in the recorded current indicating the charger had turned off.

Figure 6-15 shows that there is no clear correlation between the energy transferred to the battery during the overnight soak and the fuel energy consumed by the vehicle during the following day's TA style emissions test. Even if the outlier at approximately 280kJ change in battery charger energy, to the right of the figure, is excluded. This is surprising given that the theory clearly shows that these variables should correlate. However as the literature review highlighted, the variability in the consumed fuel energy is governed by many other factors, unrelated to the vehicle electrical system. Hence given the small magnitude of the variability in the battery charger energy, approximately 100kJ from smallest to largest with the outlier excluded it will be very hard to correlate to a change in consumed fuel energy. A reinforcement of this point the results of Figure 6-12 which showed a good correlation with change in fuel energy were taken from tests where the change in alternator output energy was approximately five times the size of the change in battery charger energy between overnight soak periods that is shown here.

For these tests, which were performed at Bath University, the battery charger was kept near the vehicle and the vehicle was not removed from the dynamometer for the duration of the test programme. The author is therefore reasonably confident that the charger was left connected up until very close to the start of each test. This is why the increased vehicle loads have been captured in the results. Conversely, as described earlier in this chapter, in the commercial laboratory the battery chargers are located with the vehicle in

the soak spaces and not in the test cell. It is therefore likely that almost all of the vehicle load from the pre-test 'disturbance' would cause battery drain and not be met by the battery charger. Although the test results from this thesis could not be used to determine the significance of the factor, it can be concluded that the timing of the battery charger disconnection in relation to the test start is a factor to consider during vehicle testing, as the duration of any 'disturbance' to the vehicle pre-test. The only potential exception to this is for vehicle equipped with a smart alternator system, for these vehicles if the change in battery SoC is relatively small and means the SoC remains within acceptable limits for the system, it is possible there will not be any effect on CO_2 emissions. This is explained in more detail later in the chapter, see 6.4.1.

6.4.1. *Smart Alternator Technology*

If a vehicle is fitted with smart alternator technology, as described in section 2.2.3 then it is conceivably possible that a change in pre-test battery SoC or a change in auxiliary loading during the test would not affect the end of test CO_2 emissions. This is because the alternator is predominately operated during throttle closed deceleration events to recover vehicle inertial energy and convert it to electrical energy to meet the vehicle demands without the need for burning more fuel and generating more CO_2. For this to be the case the change in electrical loading from either battery SoC or from auxiliary loads would need to fit within the envelope of available electrical energy from pedal off, coasting deceleration events. The available energy from these events is limited and hence the smart alternator system can only 'handle' relatively small changes to electrical demand whilst maintaining the same CO_2 emissions for the test.

To investigate the system further a vehicle equipped with a smart alternator system was tested over one TA style emissions test whilst instrumented with the same HIOKI current clamps as used in the previous experiments of this chapter. In addition the battery voltage was recorded to enable an accurate calculation of the alternator energy. The results are shown in Figure 6-16.

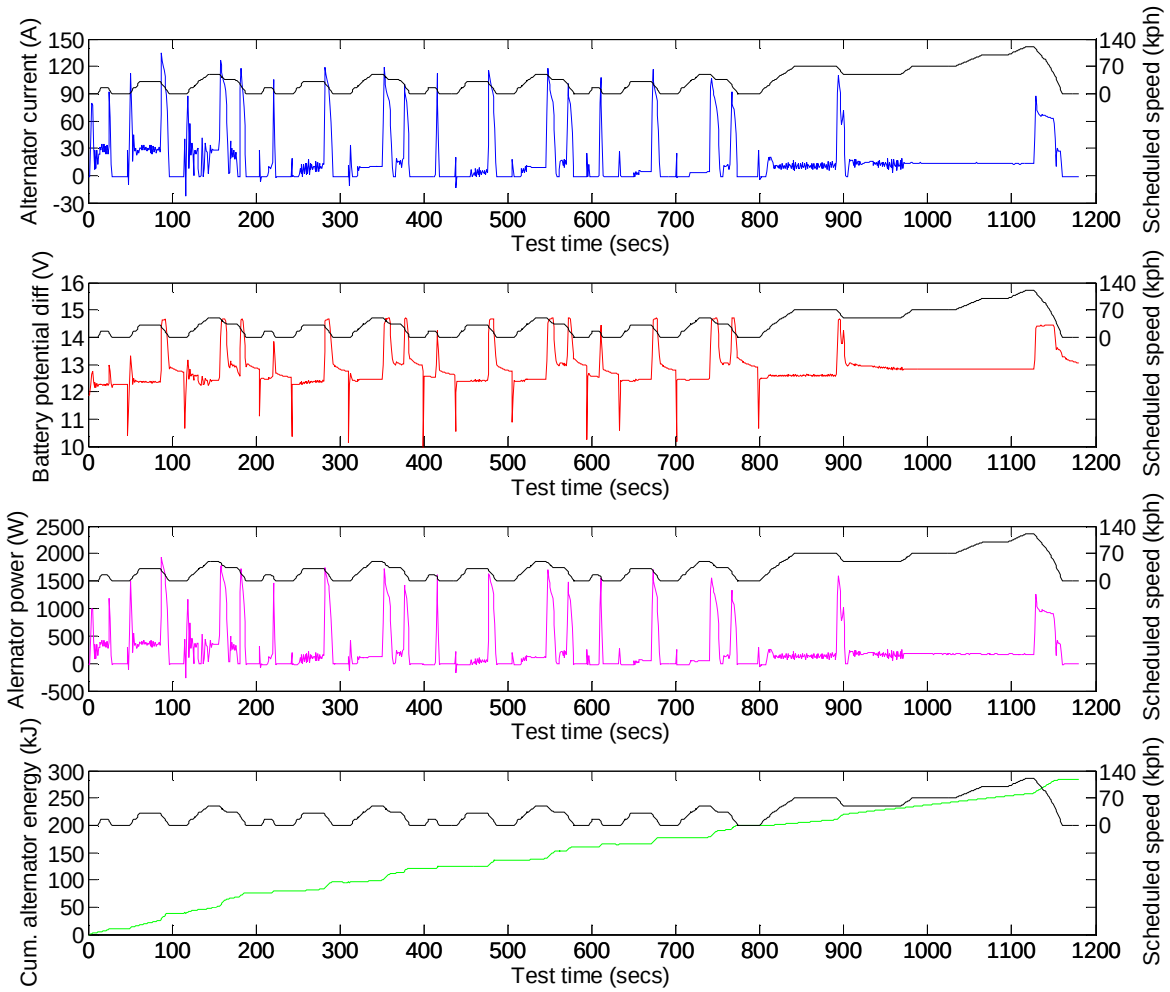

Figure 6-16: Example of recorded alternator current (blue), recorded battery voltage (red) and calculated alternator power (magenta) during an NEDC test on a vehicle equipped with smart alternator technology

By examination of Figure 6-16 it can be seen that the alternator output is actively controlled on this vehicle depending on the operating mode of the vehicle. During idle events the alternator output current is zero and the battery voltage is just below the nominal open circuit voltage of the battery. The voltage is reduced slightly because of the electrical load from the ECU and the alternator output is zero because the engine is switched off by the automatic stop-start system. During acceleration and cruise events the alternator is switched on but the output appears to be limited. The battery voltage rises but generally only reaches around 13v far below the conventional battery charging voltage of 14.4v. The battery is being trickle charged in these conditions and a compromise between re-charging the battery and increasing the CO_2 emissions is being met. On deceleration events the alternator output is maximised, since there is no CO_2 generation and the battery voltage reaches relatively constant peaks around the normal charging voltage of 14.4v. As a result the alternator power peaks between 1500 and 2000W during these events compared with the rest of the cycle where the alternator power is in the region of 0-500W.

During the test, the alternator output has been minimised and is only needed to meet two demands. Firstly the need to recharge the battery following the engine start event and secondly the need to recharge the battery following the discharge from the ECU during the periods where the alternator output is zero, in other words idle periods. These loads are the same on a conventional vehicle, except where the battery has not been charged between the tests, in this case there is an additional load due to need to recharge the battery fully to 100% SoC. If a conventional vehicle is charged between tests this demand should not exist since the battery will be at 100% SoC prior to each test. This is confirmed by examination of the average cumulative alternator energy for the tests on vehicle C in the previous experiment, see Figure 6-13 and Figure 6-14. Where the battery was charged between the tests the average cumulative alternator energy is approximately the same as that for the smart alternator equipped vehicle, being approximately 240kJ compared with approximately 275kJ on this vehicle. Where the battery was not charged between the test the average alternator energy was increased to nearly double the figure, being approximately 460kJ. This highlights how on a smart alternator equipped vehicle it may not actually be necessary to recharge the battery between every test since the same alternator output can be achieved on a vehicle that was not charged prior to the test.

6.5. Chapter Summary and Conclusions

In this chapter a series of experimental studies were conducted to understand the effect of noise factors from the vehicle electrical system on the CO_2 emissions.

In brief it was found that to ensure a high level of precision the vehicle battery needs to be charged between tests and that auxiliary loads must be switched off for the duration of tests since they can draw a large current and hence cause a significant change to the CO2 emissions. It is absolutely vital that the vehicle is instrumented with current clamp devices to measure the alternator and battery current. Without these key measures of the loading on the vehicle electrical system it is impossible to control the key noise factors.

From the studies that were conducted the following detailed conclusions can be drawn:

- A study of vehicle electrical auxiliaries on a relatively simply equipped 1.4L diesel engine B-car found that the highest current is drawn by the switching on the air conditioning system, 33A, followed by the HVAC blower at 18.2A, the headlamps at 15.7A and the heated rear window at 15.6A. The radio was found to draw a very small current at only 0.3A however the vehicle was not equipped with an amplifier, as many modern vehicles are, so this load could be higher in most cases. In the process of recording these results it was found that auxiliary load from the ECU and fuel pumps can be unintentionally triggered by opening the vehicle door.

Similarly the load from operating the electric windows was found to be between 10.5 and 7.5A for raising and lowering respectively. These loads are non-continuous and often act for only a very short period, so to have a significant effect on CO_2 emissions they would need to persist for a long period or all act on the same test or pre-test.

- By measuring the steady state modal CO_2 mass emissions during a 2nd gear cruise it was found that the auxiliary loads with the highest current, also caused the largest changes in CO_2 emissions. By calculation a linear fit with a high coefficient of determination and a gradient of approximately 2.3 was developed between the change in average electrical power and the change in average modal consumed fuel power. With no loads switched on the vehicle was found to be consuming 120kJ/s and with the highest pure electrical load, the HVAC blower, representing a change in alternator energy of 275kJ/s, the fuel energy consumption was increased to around 700kJ/s according to the linear fit. Due to noise in the experimental results this was actually recorded as approximately 900kJ/s.

- Over a series of four hot start TA style emissions tests it was found that with all the electrical auxiliaries switched on, even for the relatively basic test vehicle, the alternator current was increased by an estimated 80A continuous with the resulting change in total bag CO_2 emissions of 43%. When these effects were isolated individually it was predicted that the change in total hot bag CO_2 emissions would be between 14 and 0.16% depending on the load.

- The two methods for conditioning a SLI battery SoC pre-test were investigated, the first where the battery was not charged between the tests and the second where the battery was charged. A statistically significant difference, at 95% confidence, of 2.2% was found between the average total bag CO_2 emissions for the two methods. By examining the recorded alternator current from the tests it was confirmed that alternator load is reduced and the precision is improved when the battery is charged between tests. However within the noise of the recorded CO_2 emissions it was not possible to see this precision improvement in terms of CO_2. By calculation a linear fit, with a good level of fit and a gradient of 3.1 was developed between the change in alternator energy during the test and the change in consumed fuel energy. The change in alternator energy was found to be in the region of ±300kJ/test with a corresponding change in consumed fuel energy of approximately ±930kJ/test. The difference from the gradient for the B-car vehicle was attributed to the difference in the vehicle powertrain and electrical system efficiencies.

- The analysis of the battery charging behaviour of an intelligent CTEK charger found that the charger generally switched off after approximately 4 hours, having recharged the battery in a conventional exponential decay of current presumed to be at a fixed voltage. If the vehicle is disturbed prior to an emissions test, whilst the battery charger is still connected, it was found that the battery charger will power the vehicle auxiliary devices reducing the battery discharge prior to a test and potentially causing a change in CO_2 emissions during the test. Unfortunately these results did not correlate from this experiment due to a combination of problems with the logging. A further analysis of the energy transferred to the battery during the initial 4 hour charge found no correlation with the variability in consumed fuel energy calculated from the result of the emissions test the next day. This was attributed to relatively small magnitude in the variability of battery charger output, being only 100kJ from smallest to largest, meaning the effect was swamped by other test noise factors outside the scope of the electrical system.

- An initial review of smart alternator equipped vehicles suggests that they could vastly reduce the number of incidences of the alternator load related variability in CO_2 emissions, provided any perturbation in alternator load can be contained within the internal energy envelope of the test vehicle and electrical system efficiency.

- In summary it was found that without recording the alternator and fusebox current relatively little information can be gleamed into the electrical system as a source of imprecision in CO_2 emissions. Given the success of using relatively low cost current transducers it is suggested that current logging should be the norm for any emissions test. Furthermore there is a growing interest from the legislators in using the recorded data to correct the CO_2 emissions on the basis of the net battery current changes during a TA emissions test.

- Additionally auxiliary loads should be switched off for any testing and electric windows not adjusted mid test. During the pre-test period it is important to minimise disturbances to the vehicle unless the battery is still being charged.

- On a conventional vehicle, without a smart alternator, the battery should always be charged between tests when conducting research work, for development work or TA this is the decision of the test engineer and is dependent on the aim of the testing. However if the necessary steps are taken to measure battery current or interrogate the electrical system for battery SoC it should be possible to achieve high precision results with either method, providing the system is monitored and

errors are corrected straight away, by either procedural improvements or external battery charging.

Chapter 7. The Driver

7.1. Introduction

To achieve high precision emission test results from chassis dynamometer vehicle tests it is imperative to consider the impact of the driver behaviour variation between and during emissions tests. This has been clearly demonstrated through many sources covered in the literature review with authors measuring the effects of drive variations within the legal TA tolerance of anywhere between 0.1 and 4% change in CO_2 emissions.

The relatively recent publication of the SAE Drive Quality Standard SAE J2951 [33] has helped to provide an industry standard set of metrics for quantification of driver behaviour variations that correlate with vehicle out emissions. The metrics defined in this standard include the Energy Economy Rating (EER), Energy Rating (ER), Distance Rating (DR), Absolute Speed Change Rating (ASCR) and Root Mean Squared Speed Error (RMSSE). There are also alternative, non-SAE J2951, metrics that can be calculated. For example a novel metric which was defined by Chappell et. al. [83] is the Cumulative Absolute Speed Error, termed CASE. The calculation of the SAE J2951 metrics is explained in more detail in the literature review, see section 2.3.5 and other metrics are explained later in this chapter.

In this chapter a comparison of drive rating metrics and recommendations for how the metrics can be best utilised are made. This is done by examining the sensitivity of the metrics to changes in driver inputs during a controlled experiment to change the configuration of the driver's aid. The experiment was conducted across a large group of drivers using one vehicle and six chassis dynamometer emissions test cells within the commercial laboratory environment. A simple change was made to the driver's aid display such that the speed tolerances were removed and only the target trace was shown. Consideration is also given to the suitability of metrics for use in a real-time feedback tool.

7.2. Driver Rating Tools and Metrics in Industry

7.2.1. *Predecessors to SAE J2951*

In the years prior to the development of the SAE standard SAE J2951, driver behaviour classification and analysis could not be conducted against any global or national standard. As such any tools were developed by individual organisations and an example of such a tool was developed by the commercial laboratory discussed within this thesis. For reasons of confidentiality this tool will not be referred to by its real name and will instead be referred to within this thesis as the Driver Evaluation Tool, or DET. The DET results are

calculated real time during the emissions test by the test cell host computer but are only reported at the end of the test as one-number-per-phase results.

7.2.2. *SAE J2951*

The DET was developed by a team within the commercial laboratory that went onto form the basis of the working group for the SAE J2951 drive quality evaluation standard. As a result the DET has effectively been superseded by SAE J2951 and is no longer used within the commercial laboratory. The two systems are very similar, the DET reports four metrics; Energy Usage (EU), Distance Rating (DR), Energy Efficiency Rating (EER) and Smoothness (SM) which are almost directly comparable to the SAE J2951 metrics, ER, DR, EER and ASC respectively. The main differences are to do with the boundary conditions, for example speed signal filtering, the minimum speed below which values are taken to be zero, the adjustment of dynamometer coefficients to achieve track coefficients and the SM metric is speed based whilst the ASC is acceleration based. The DET is however worth mentioning because there exists data showing a good correlation between the DET metrics and the vehicle FE from chassis dynamometer emissions tests. As has been mentioned previously in this thesis, given the difficulty in making a change to just one input factor and obtaining statistically significant changes to the output emissions such data is not easily available. It is worth including because it validates that these metrics are useful tools for the assessment of driving behaviour against vehicle emissions and FE. The data was obtained from a series of controlled tests with the same vehicle and driver and found the EER and SM metrics correlated with the bag FE. These results are presented in Figure 7-1 below.

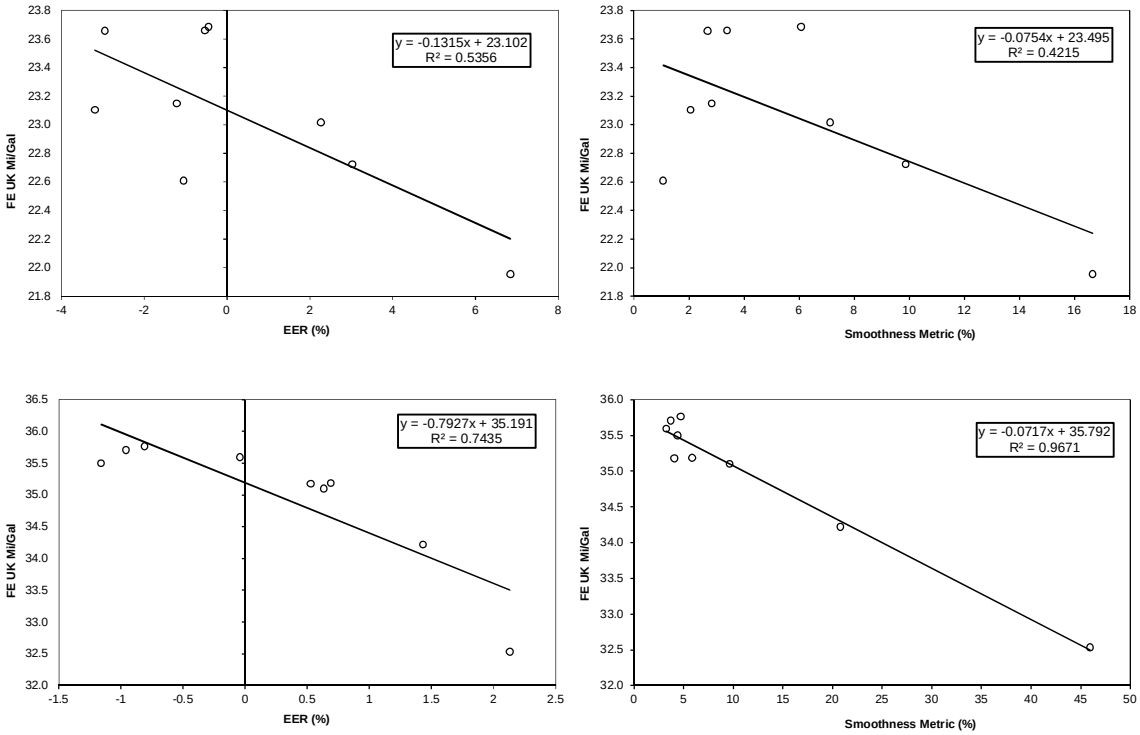

Figure 7-1: EER and SM drive metric results for phase 1 and 2 of NEDC chassis dynamometer emissions tests from the commercial laboratory. Y-axis shows fuel economy (FE) measured in miles per imperial (UK) gallon

The results of Figure 7-1 show that there is correlation between the DET metrics and the FE during TA style emissions tests. Interestingly there is less confidence in the correlation for phase 1 of the test as the coefficient of determination is only 0.54 and 0.42 respectively. The exact configuration for the tests where this data was obtained is unknown so there could be a multitude of reasons for the reduced confidence caused by a lack of control of the other factors known to be important for precise FE results. During phase 2 there is a good correlation between the DET EER and SM metrics with coefficients of determination of 0.74 and 0.91 respectively. At least where there has been a reduced certainty in the correlation this does not appear to be caused by a lack of perturbation of the driver style. In phase 1 the EER varies from approximately -5 to +7 with a low coefficient of determination, where as in phase 2 the EER varies from approximately -1.2 to + 2.2 with a much high coefficient of determination, which points to a lack of control of other noise factors being the most likely explanation of the reduced confidence in the correlation from phase 1.

7.3. Driver's Aid Improvements

7.3.1. *Experimental Approach*

As was introduced in the literature review, see section 2.3, during a chassis dynamometer emissions test where the vehicle is driven by a human driver a device known as a 'driver's aid' is used to inform the driver of how to drive the vehicle. Most drivers' aids offer a relatively basic display of the chassis dynamometer roller surface speed plotted in a real-time graphical format against a target speed trace. Most chassis dynamometer control systems are able to display the legal speed tolerances around the target speed trace and this is often the default configuration. However the display of these tolerances is usually optional and easily selectable within the chassis dynamometer/ test cell controller. In this study two driver's aid display configurations were used, one where the legal speed tolerances where displayed along with the target speed and the second where only the target speed was displayed. The aim was to determine if variation in driver behaviour was reduced for the scenario where the tolerances were not displayed. Figure 7-2 and Figure 7-3 show the two configurations which were the subject of the investigation.

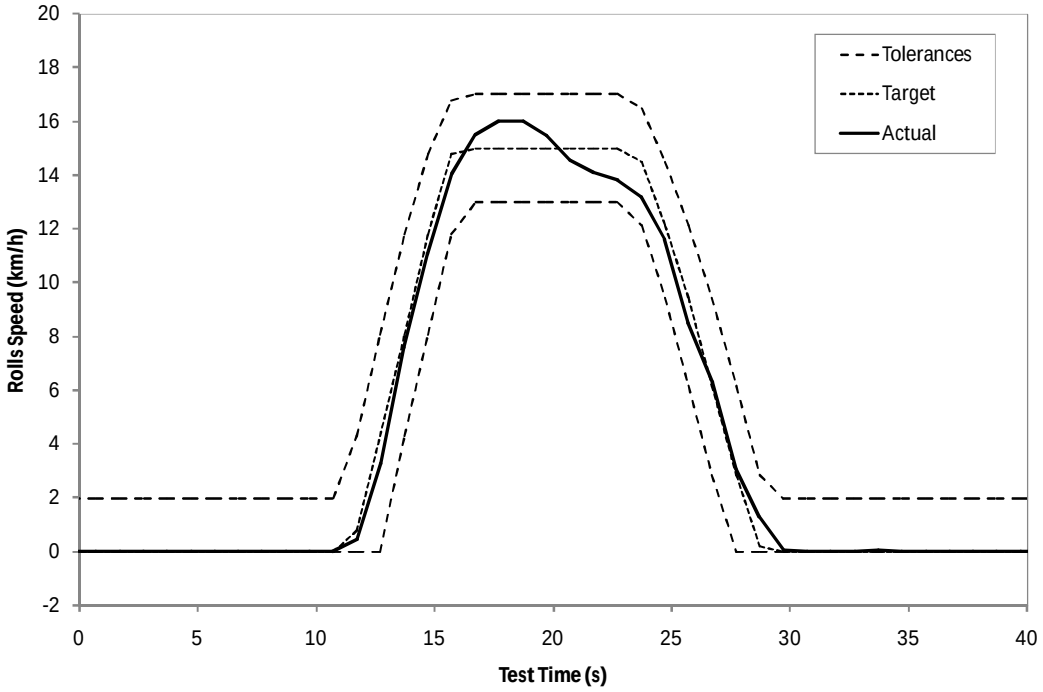

Figure 7-2: An example of a typical drivers aid display with speed tolerances

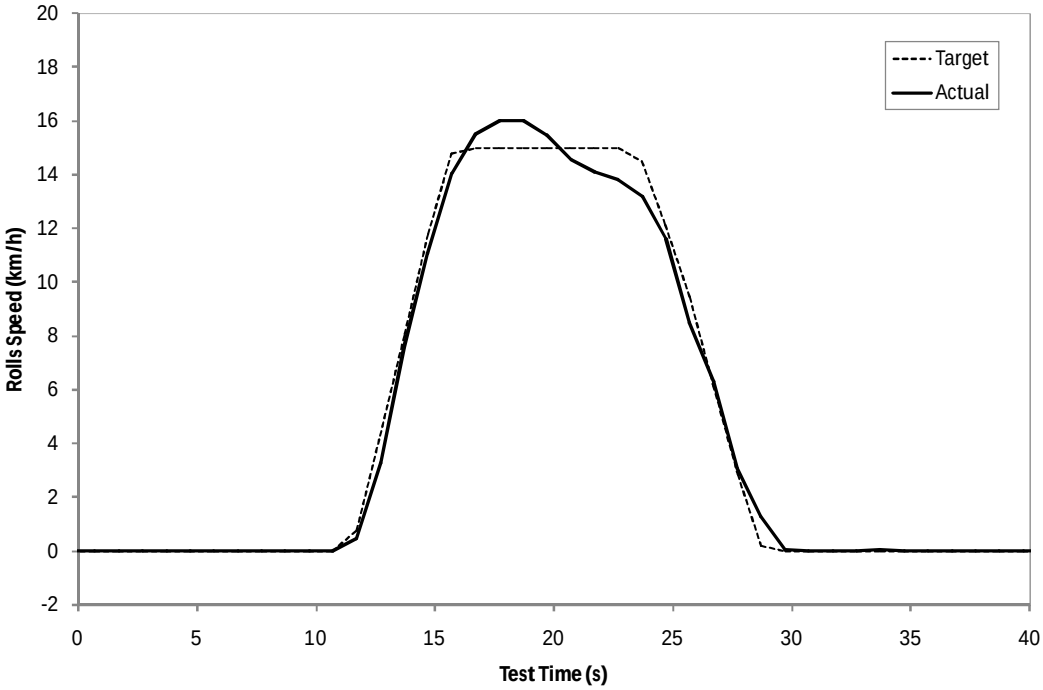

Figure 7-3: An example of a typical drivers aid display without speed tolerances

The study was conducted using a passenger vehicle which was tested over repeated TA style cold start NEDC tests in an automotive chassis dynamometer emissions test facility. The vehicle was tested for approximately 450 tests, across 6 chassis dynamometer test cells with 35 human drivers. In between each test the vehicle was soaked for at least 8 hours at the ambient lab temperature of approximately 25°C. During the soak periods the vehicle battery was charged. The test vehicle used for the duration of the study was the aforementioned vehicle A which is a B-car equipped a 1.4 litre displacement gasoline engine and a 5 speed manual transmission.

Initially the drivers for each test were asked to drive with the driver's aid configured to display both the target trace and the tolerances, as per Figure 7-2. After approximately 250 tests had been completed the drivers were asked to drive the vehicle with the driver's aid configured to only show the target drive trace, as per Figure 7-3. Approximately 200 tests were completed in this condition. For each test several driver performance metrics were calculated consisting of both SAE J2951 standard metrics and an alternative novel metric. The calculation of the SAE J2951 metrics is explained in section 2.3.5 but in addition a novel metric, introduced by the work of Chapter 4 and Chappell et. al. [83] was also calculated for the resulting data. This metric was the Cumulative Absolute Speed Error, or CASE, and is defined in section 4.2.4.

7.3.2. *Experimental Results*

Table 7-1 shows the mean and standard deviation driver behaviour metric results calculated across all drivers, for the two test conditions, driver's aid tolerances on and off.

Table 7-1: Driver behaviour metric results for all drivers by driver's aid tolerance setting

Drive Metric	Driver's aid tolerances on	Driver's aid tolerances off	Percentage change between tolerances on and off (%)
Mean Total Bag CO_2 (g/km)	135.4	134.9	**0.37**
Standard deviation total bag CO_2 (g/km)	4.46	2.52	**-43.5**
Mean Total EER (%)	-0.37	-0.24	**35.1**
Standard deviation EER (%)	0.60	0.51	**-15.0**
Mean DR (%)	0.08	0.06	**-25.0**
Standard deviation DR (%)	0.36	0.25	**30.6**
Mean ER (%)	-0.28	-0.18	**35.7**
Standard deviation ER (%)	0.73	0.65	**-11.0**
Mean CASE (km/h)	606.3	539.0	**-11.1**
Standard deviation CASE (km/h)	131.1	97.3	**-25.8**
Mean RMSSE (km/h)	0.78	0.68	**-12.8**
Standard deviation RMSSE (km/h)	0.17	0.11	**-35.3**
Mean ASCR (km/h)	3.72	3.83	**2.96**
Standard deviation ASCR (km/h)	1.40	1.17	**-16.4**

It has been seen many times in the literature that during controlled experiments driver variations can have a significant effect on the CO_2 emissions from chassis dynamometer vehicle tests. Yet by examination of Table 7-1 there is only a very small difference between the mean total CO_2 emission results for the two test cases in this experiment; the percentage change being only 0.37%. This result is not surprising given, firstly, the simple difficulty in obtaining statistically significant changes in output emissions from one input factor to chassis dynamometer vehicle tests and, secondly, the difficulty in obtaining

statistical confidence when the tests are conducted with more than one chassis dynamometer test cell and multiple drivers. Controls for the other factors that are known to be important, such as the dynamometer, the electrical system and so on were implemented in this study, however due to the commercial setting where these experiments were carried out many of these controls were achieved via procedural actions and no data was recorded to verify that the factors were in control.

Further examination of Table 7-1 shows that whilst there is very little change in the mean CO_2 emissions there is a large reduction in the spread of the CO_2 emissions. When the driver's aid tolerances are switched off the standard deviation of total bag CO_2 emissions is reduced from 4.46 g/km to 2.52 g/km which is a 43.5% change in the standard deviation. This 43.5% reduction in standard deviation is a very large reduction, but it is not quite as significant as the percentage change figure might first suggest since it is dominated by the reduction in the number of outlying tests. This is evident from Figure 7-4 where it can be seen that all the outlying tests are with the tolerances switch on. Whilst this is still important, as outlying tests are wasteful in resources, the reduction in extreme outliers does not help improve the precision within the normal operating range. However further examination of the data shows that there has been an improvement within the normal operating range. This is less clear from Figure 7-4 but can be seen by examination of the histogram of CO_2 emissions for the two cases, see Figure 7-5, which shows that when the tolerances are switched off the distribution of CO_2 results is much narrower and has a higher peak frequency. This improvement in normal driver precision can also been seen numerically since the average interquartile range has been reduced by 16%, from 4.08 g/km to 3.43 g/km. Figure 7-6 and Figure 7-7, further highlight these findings showing that when the distribution of CO_2 emissions results from individual drivers are examined there is in most cases a reduction in outliers and a reduction in inter quartile range when the tolerances are not displayed. These findings would suggest that when the tolerances are displayed, drivers are more likely to follow a particular style, such as driving close to a tolerance line. When the tolerances are not displayed the author assumes that drivers are forced to drive as close to the target drive trace as they can, rather than adopting a preferred drive style that uses more of the available legal speed tolerance. The author proposes that a human driver tends to subconsciously alter their acceptance criteria when the tolerances are removed from the driver's aid. In conventional testing, with tolerances displayed, human drivers are likely to think they have achieved perfect driving simply by driving within the tolerance lines, irrespective of how close they are to the target speed trace. Conversely when the tolerances are not displayed, to achieve perfect driving, drivers are more likely to attempt to follow the target trace as closely as possible. This could be because without the tolerances displayed they are unsure if they are within them. Alternatively it could be that without having the tolerances displayed drivers are more

aware that any driving away from the target drive trace is generating an error, errors which would be subconsciously ignored when a driver can see that they are within an acceptable tolerance band.

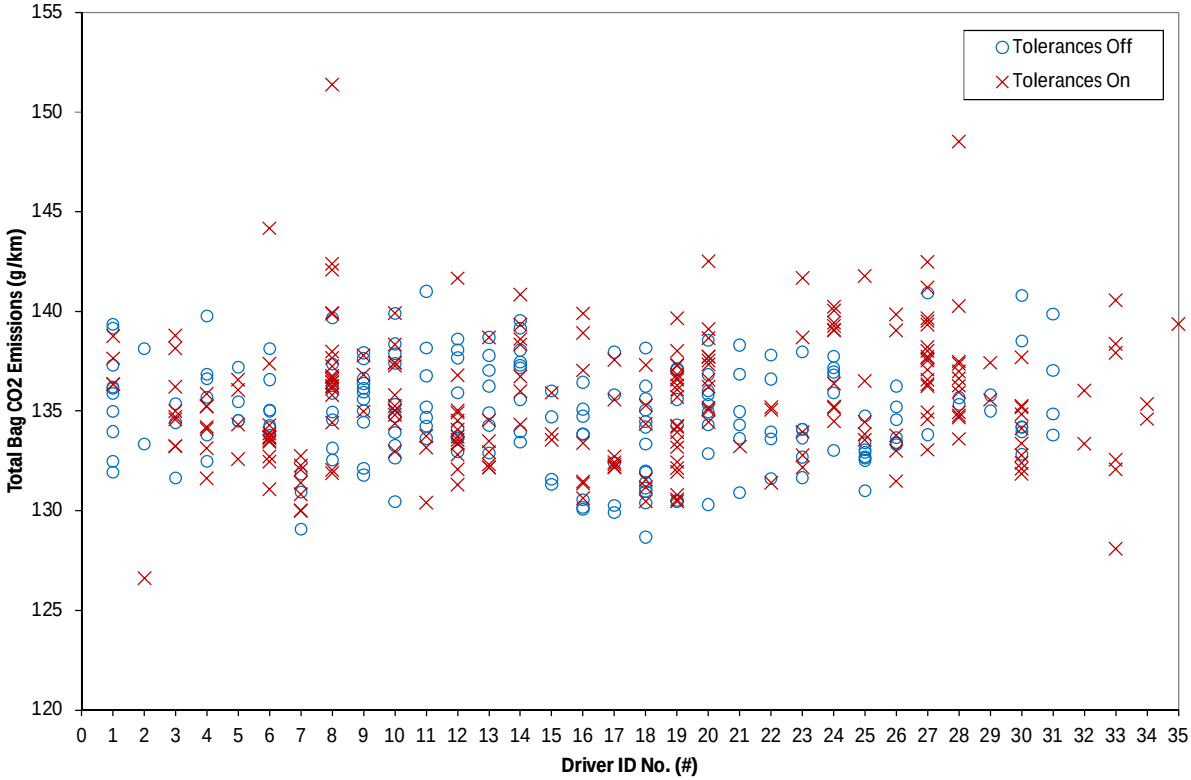

Figure 7-4: Total Bag CO_2 Emissions for all drivers by driver's aid tolerance setting

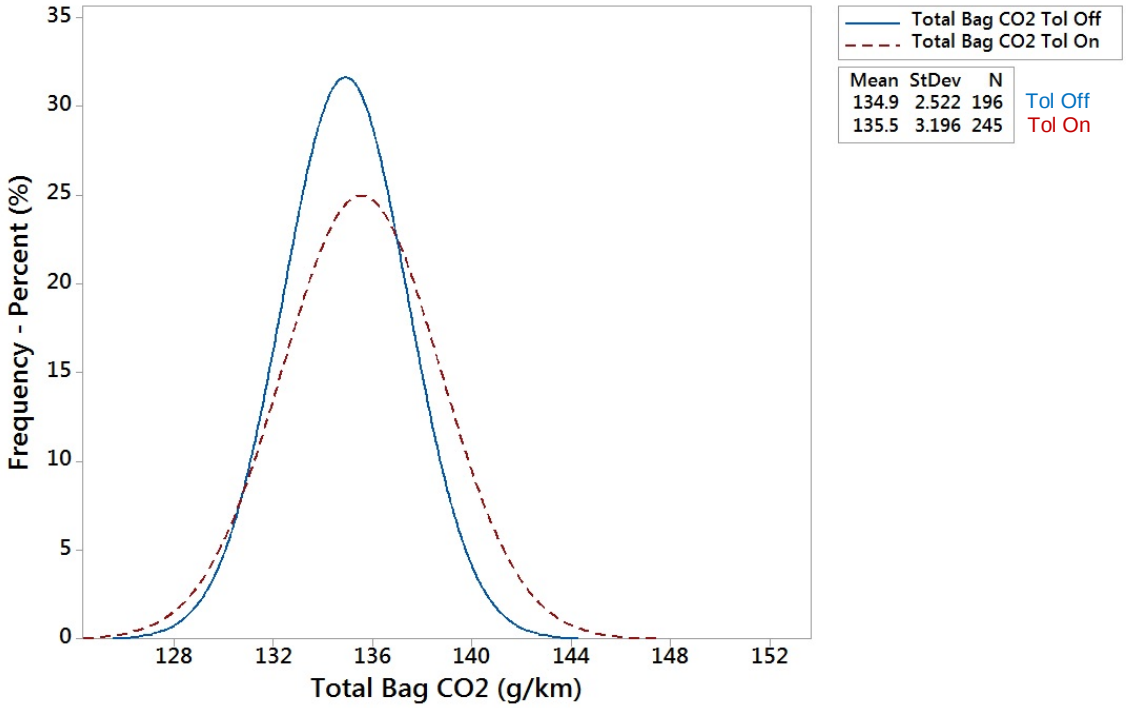

Figure 7-5: Histogram of the total Bag CO_2 Emissions for all drivers grouped by driver's aid tolerance setting. 'Tol Off' stands for driver's aid tolerances switched off and 'Tol On' stands for driver's aid tolerances switched on

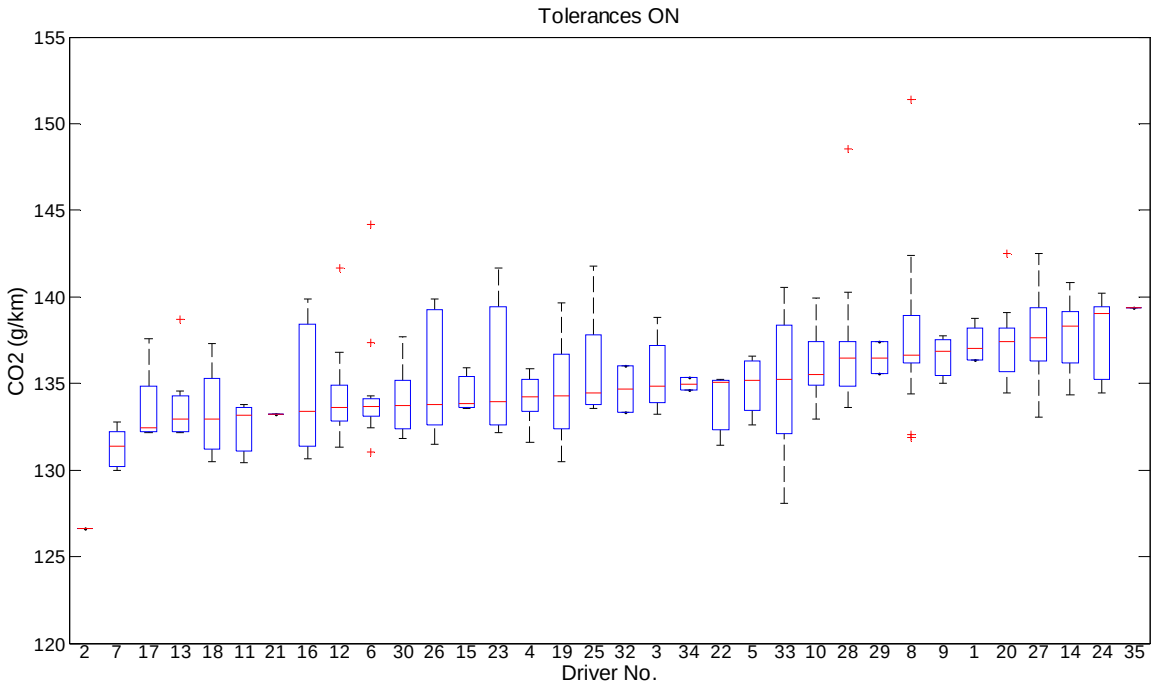

Figure 7-6: Boxplot of total bag CO_2 emissions for all drivers with driver's aid tolerances on

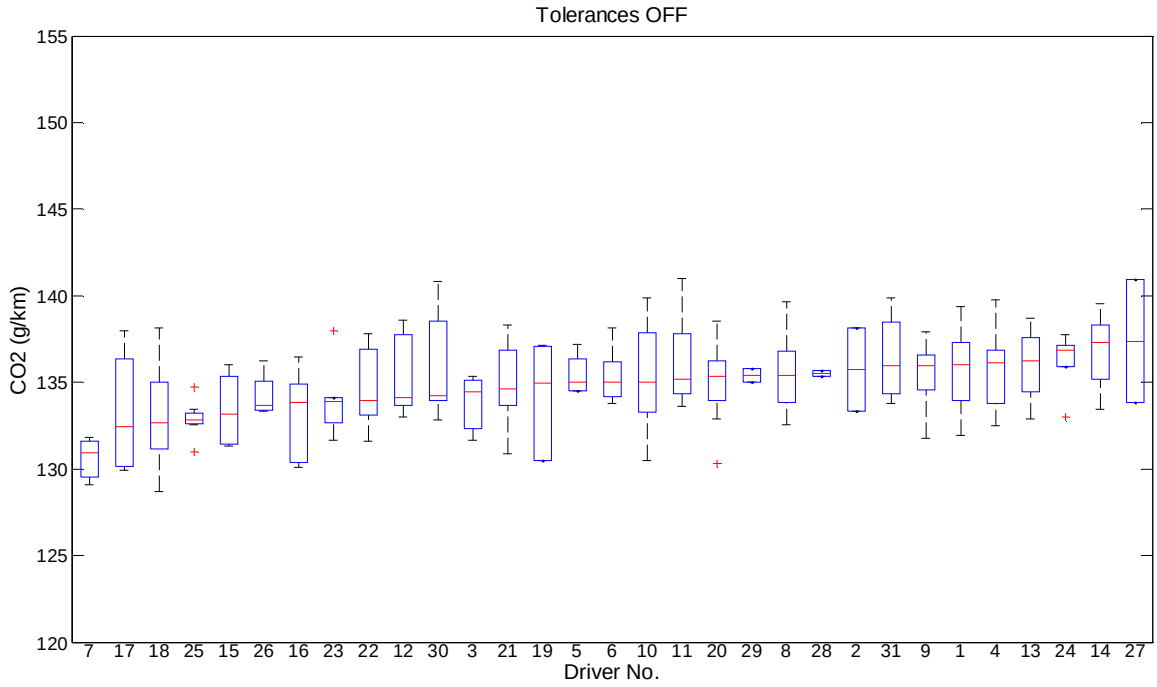

Figure 7-7: Boxplot of total bag CO_2 emissions for all drivers with driver's aid tolerances off

Several metrics were calculated to quantify any changes in the driver input behaviour since these are emissions test input measures and therefore should be less prone, than output emissions results, to give misleading results due to interactions with other variables within an emissions test.

The SAE J2951 drive quality standard defines two groups of metrics; primary and supplementary metrics [33]. The primary metrics are the energy and distance based metrics, ER, DR and EER. The ER and EER are intended to correlate with energy related emissions, namely CO_2 and fuel consumption. The supplementary metrics are intended to quantify other types of driver behaviour that do not necessarily affect the drive energy but can still have effects on the fuel consumption, an example being oscillatory pedal movements [33]. The supplementary metrics are the ASCR and the RMSSE. Another metric which is not part of the SAE J2951 drive quality standard is the CASE metric, which was defined by Chappell et. al. [83].

By examination of Table 7-1 the primary metrics, ER, DR and EER, do not show large differences in the mean results between the two cases, tolerances on and off. The percentage changes are large, in the region of 25-36%, however these results are misleading since the ER, DR and EER metrics are based around zero, so even a small change is proportionally large compared to the absolute value. This is one disadvantage of ER, DR and EER metrics.

The means of the RMSSE and the CASE show clearer differences between the two cases tolerances on and off. When the tolerances are not displayed the mean RMSSE and mean CASE are reduced by 12.8 and 11.1% respectively. Also the spread in RMSSE and CASE are reduced by 35.3% and 25.8% respectively. The changes in mean and spread of CASE are statistically significant at a 95% confidence level. The distribution obtained when the tolerances are off is noticeably narrower and has a higher peak frequency that the distribution obtained from the tolerances on condition, see Figure 7-8. These findings support the theory that when the driver's aid tolerances are turned off, drivers are forced to follow the trace as closely as they can rather than adopting any individual drive style that uses the all the available legal speed tolerance.

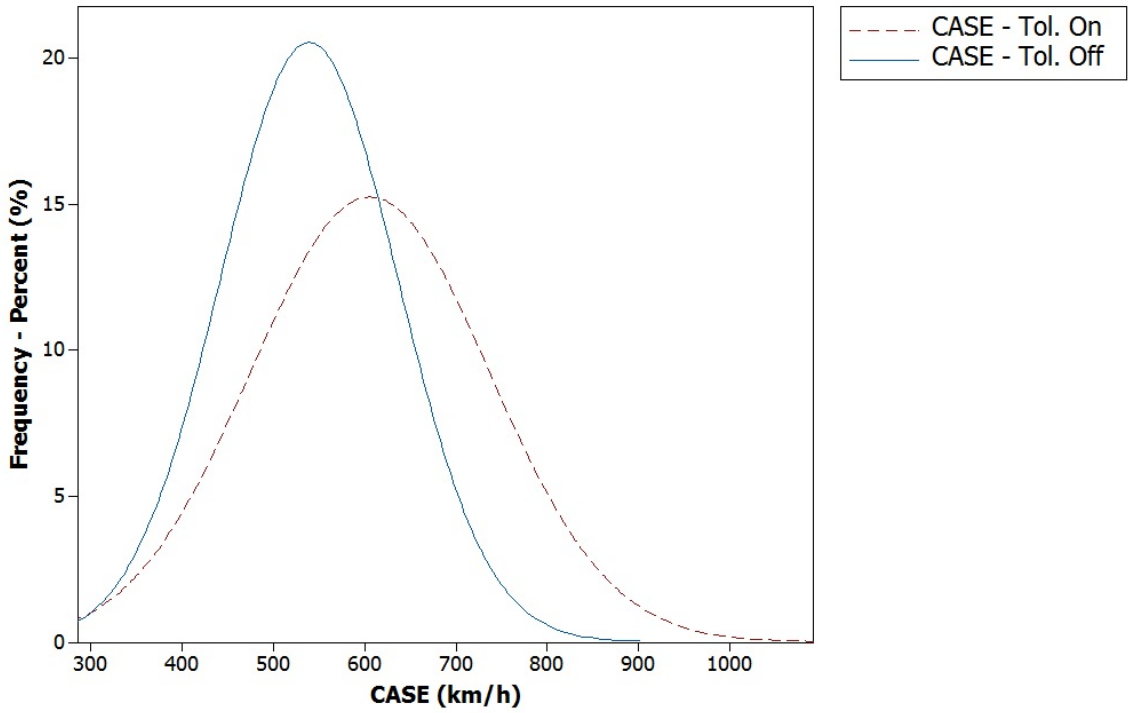

Figure 7-8: Histogram of Cumulative Absolute Speed Error (CASE) for all drivers and the two experimental cases, drivers aid tolerances on and off.

Since the CASE metric is a relatively new metric it is worth validating that it provides a real and robust measure of driver behaviour. Given the difficulties in obtaining confidence in changes in vehicle out emissions, such as CO_2, it is only possible to examine the correlation of the CASE metric against similar standardised metrics; the most similar by calculation is the SAE RMSSE metric, see sections 2.3.5 and 4.2.4 By plotting the end of test RMSSE and CASE metric results from study, the author found an extremely good correlation to a straight line linear fit, with a gradient of 0.001 and a coefficient of determination, or R^2 value, of 0.93. However despite having good correlation with the RMSSE metric, the CASE metric does have useful additional properties that make it potentially more powerful than the RMSSE metric. Discussion of these properties is detailed in later sections of the paper, see sections 7.4 and 7.5.

The change in the ASCR is smaller, being a reduction of only 2.96% when the tolerances are turned off. Since this metric summarises the acceleration error it can be concluded that the speed error differences highlighted by the CASE and RMSSE metrics must have taken the form of longer term speed errors rather than oscillatory or short term aggressive inputs.

7.3.3. *Individual Driver Analysis*

An examination of boxplots of the CASE for each individual driver, see Figure 7-9 and Figure 7-10, again supports the conclusion that individual driver behaviour has been suppressed when the tolerances are not displayed. In Figure 7-9, for the tolerances on,

not only are the the tails of the boxes much longer, there are also many more outlying data points than there are in Figure 7-10, for the tolerances off. Similarly the interquartile ranges are generally smaller in Figure 7-10, indeed on average IQR has been reduced by 30.7% when the driver's aid tolerances are not displayed.

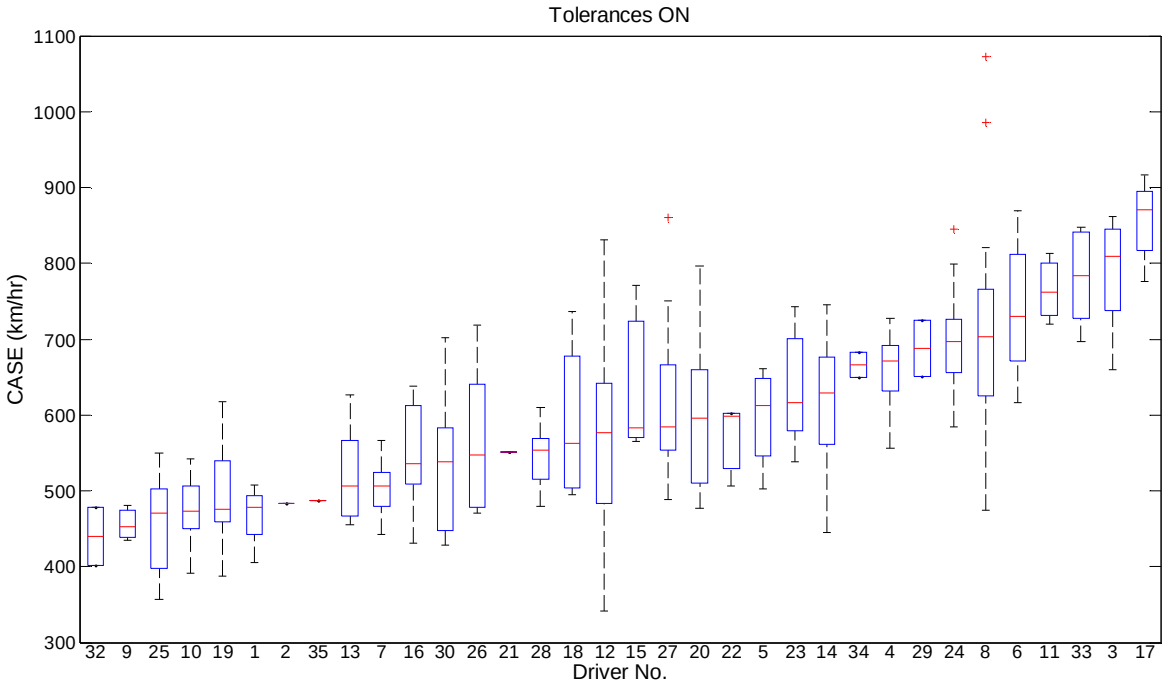

Figure 7-9: Boxplot of CASE for all drivers with driver's aid tolerances on

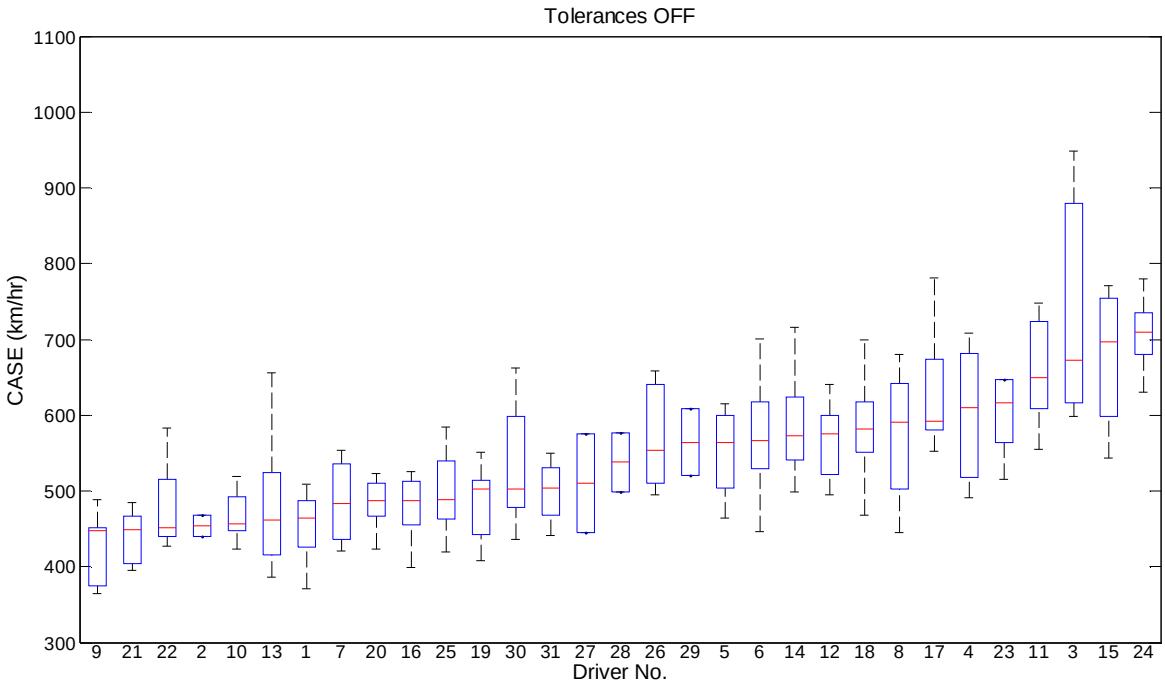

Figure 7-10: Boxplot of CASE for all drivers with driver's aid tolerances off

Figure 7-11 through to Figure 7-18 show how four drivers from the study changed their driver behaviour in different ways when the driver's aid tolerances were turned off. The

figures also provide a comparison of the different driver behaviour metrics for the same data sets.

The first example of a driver behaviour change between the two test cases, tolerances on and off, is driver 17, see Figure 7-11 and Figure 7-12. This is an example of a driver who has reduced their absolute speed error with very little change in precision. Interestingly not all the driver behaviour metrics show a clear distinction between the two experimental cases of driver's aid tolerances on and off. The primary metrics, with the except of the ER metric and to a lesser extent the EER metric, show two distinct groups of results for the two test cases, tolerances on and off. These two groups of results are even more distinctly separated for the supplementary metrics. For example when the tolerances are off the driver has reduced their average end of test CASE from 857 to 631 km/h, a reduction of 26%. Instantaneous divergence of the two groups of results for the tolerances on and off is clearest in the RMSSE, DR and CASE metrics, with the CASE metric showing clear separation earliest in the tests at an elapsed time of approximately 250 seconds, see Figure 7-12. The spread in both the end of test and instantaneous metric results is approximately the same for both tolerances on and off, showing that whilst driver 17 has driven closer to the target speed trace with the tolerances off, they have not improved their precision in their test to test driving behaviour.

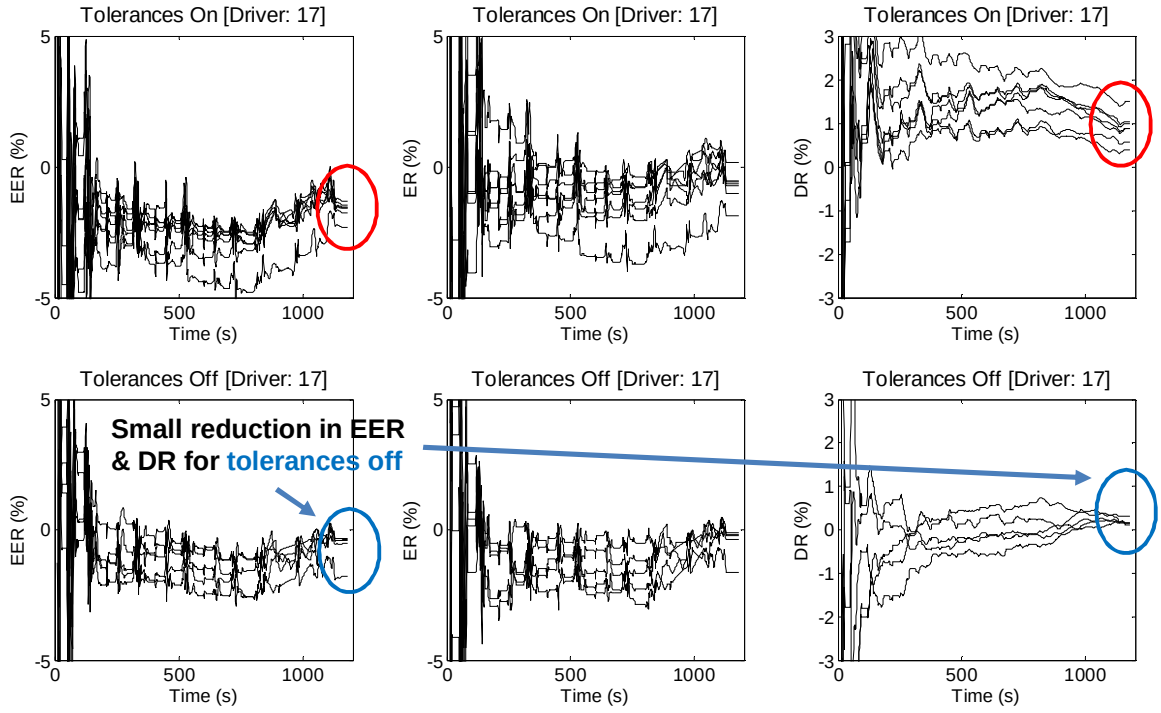

Figure 7-11: Instantaneous SAE primary metrics for driver 17 with driver's aid tolerances on and off

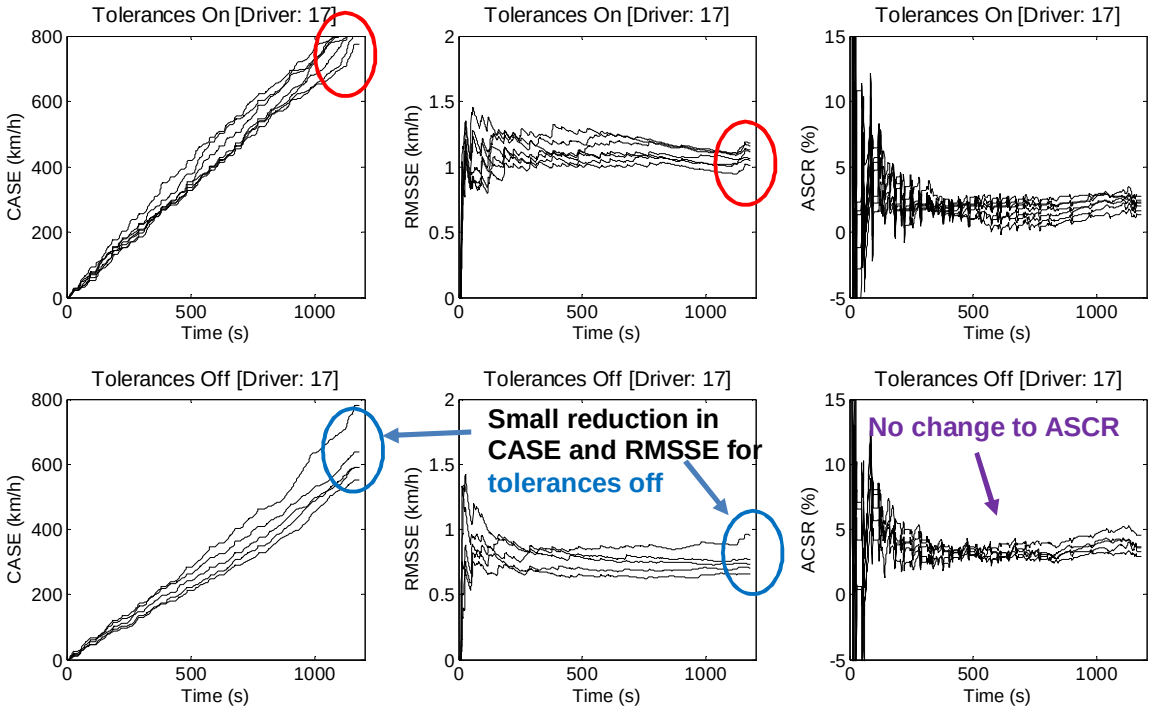

Figure 7-12: Instantaneous CASE and SAE supplementary metrics for driver 17 with driver's aid tolerances on and off

Driver 20, see Figure 7-13 and Figure 7-14, is an example of a driver who has both reduced their speed error and improved their precision when the tolerances are off. As with driver 17, some metrics are almost totally insensitive to the change in driver 20's drive style between the two test cases. Other metrics are more sensitive to changes in either precision, error or both. The EER and ER are the metrics that do not show any notable differences at all between the results for the driver's aid tolerances on and off. The only remaining SAE primary metric, the DR, shows some reduction in the spread for both the instantaneous and end of test results, although the mean seems relatively unchanged. The ASCR shows a similar pattern to the DR metric. For both the ASCR and DR the reduction in the spread of the instantaneous and end of test results is clear, although there appears little difference in the mean. Only the RMSSE and CASE metrics show a clear reduction in both the mean and spread of the results. The reductions are also clear from both the instantaneous and end of test metric results. Driver 20's mean CASE was reduced from 598 to 483 km/h, a reduction of 19% and the standard deviation of CASE was reduced from 98.5 to 33.0 km/h, a reduction of 66.5%.

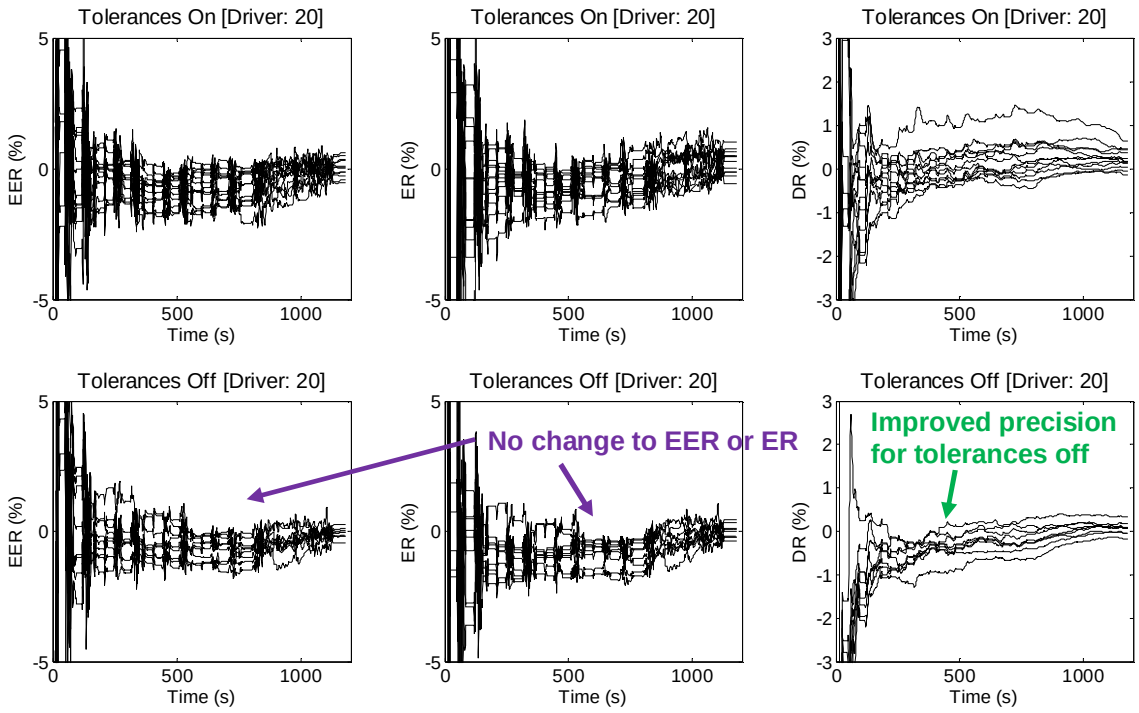

Figure 7-13: Instantaneous SAE primary metrics for driver 20 with driver's aid tolerances on and off

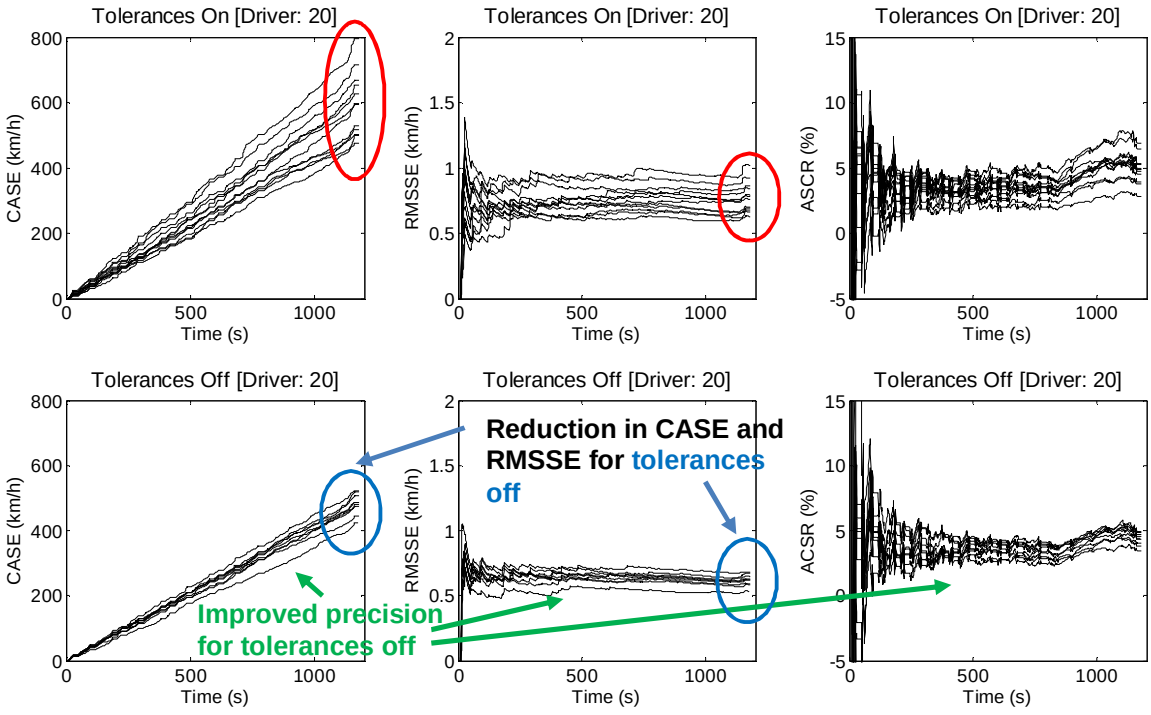

Figure 7-14: Instantaneous CASE and SAE supplementary metrics for driver 20 with driver's aid tolerances on and off

Driver 12, see Figure 7-15 and Figure 7-16, is an example of a driver who has not changed their speed error but has improved their precision when the driver's aid tolerances are off. These changes in driver 12's drive style are not evident from the SAE primary metrics or from the ASCR supplementary metric. The instantaneous and end of

test ER, EER and DR results are much the same for the two cases of driver's aid tolerances on and off. In terms of precision, from the primary metrics, only the DR shows a slight reduction in the spread of the instantaneous and end of test results. Conversely the RMSSE and CASE metrics show a clear distinction between the two cases, tolerances on and off. Both the instantaneous and end of test results show much improved precision when the tolerances are off, with very little change in the mean speed error. The mean CASE result has been relatively unchanged from 571 km/h with the tolerances on to 567 km/h with the tolerances off, a change of only 0.7%. The spread of the end of test CASE results, indicated here by the standard deviation, has been reduced from 131 to 50 km/h, a much larger reduction of 62%.

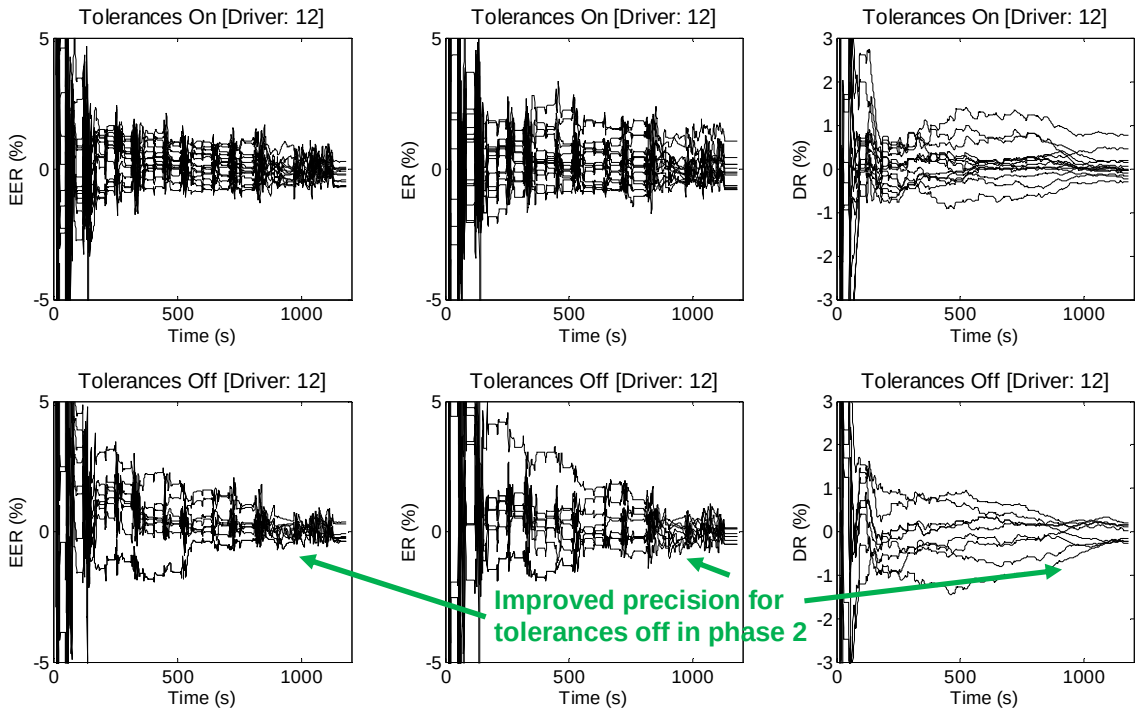

Figure 7-15: Instantaneous SAE primary metrics for driver 12 with driver's aid tolerances on and off

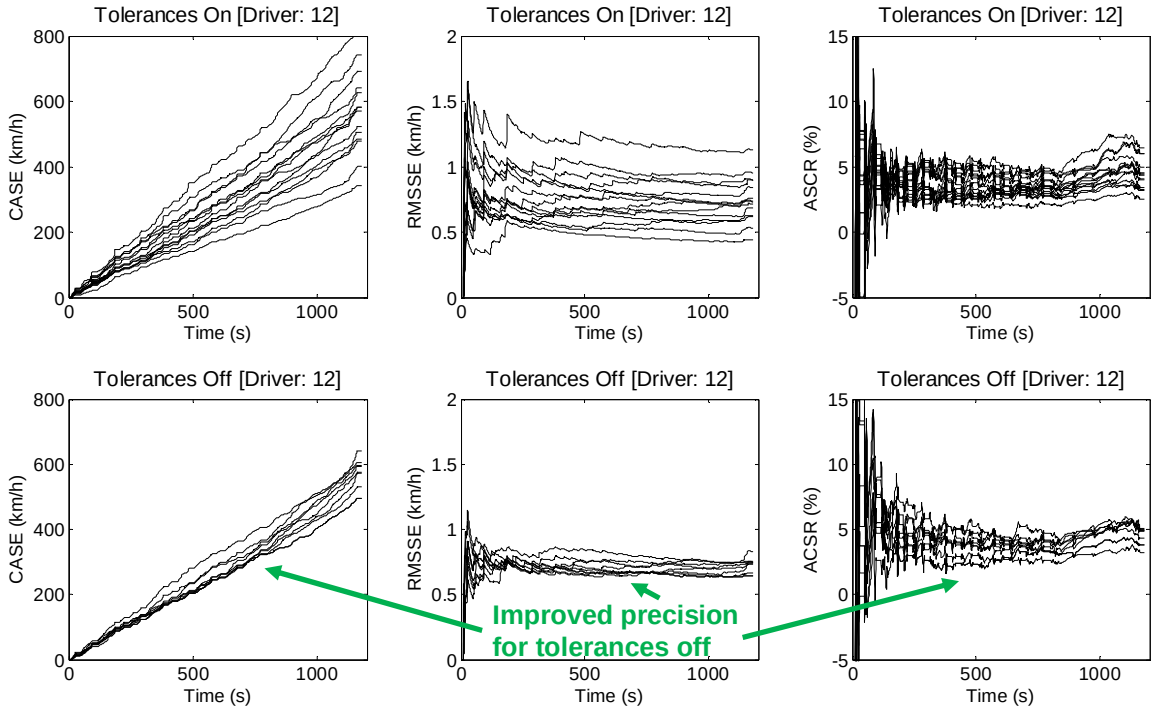

Figure 7-16: Instantaneous CASE and SAE supplementary metrics for driver 12 with driver's aid tolerances on and off

From Figure 7-11 through Figure 7-16 examples have been shown of following driver behaviour changes:

- Reduced speed error with no change in precision (driver 17)
- Reduced speed error with increased precision (driver 20)
- No change in speed error with increased precision (driver 12)

Examining all drivers on an individual basis showed that there are no examples where a driver's average speed error increased with the tolerances off, only examples where it was unchanged or reduced. Similarly for the most part the drivers' precision was either unchanged or improved. However there are three examples, drivers 1, 9 and 11 who had slightly reduced precision when the tolerances were off. It should be noted that all these drivers completed many more tests with the tolerances off than with the tolerances on or vice versa so it is difficult to make a valid comparison between their results for the two test cases. Driver 9 is shown as an example, see Figure 7-17 and Figure 7-18, noting that driver 9 completed only three tests with the tolerances on, but completed 11 tests with the tolerances off. Again, as with the drivers previously examined, the SAE primary metrics and the ASCR show little distinction between the two cases, tolerances on and off. It could be argued that the spread in primary metric results for tolerances on was reduced with an outlier, however given the very small number of tests the author suggests it is more likely

that the full distribution is not fully developed due to the small sample size. Only the RMSSE and CASE metrics show, both instantaneously and via the end of test results, that there is an increased spread in the results when the driver's aid the tolerances off with comparatively little change in the mean speed error. The mean CASE was reduced from 456 to 427 km/h, a change of only 6%. Whereas the spread of the CASE, indicated here by the standard deviation was increased from 23 to 47 km/h, an increase of 51%. As discussed it is difficult to have confidence in the increased spread with the tolerances off given the small number of tests completed in the baseline condition; with tolerances on. However if this reduced precision is a real effect, the author speculates that perhaps these drivers had become so accustomed to driving with the tolerances on that they continued to adopt a unique driving style but without the tolerances to guide them they drove less consistently.

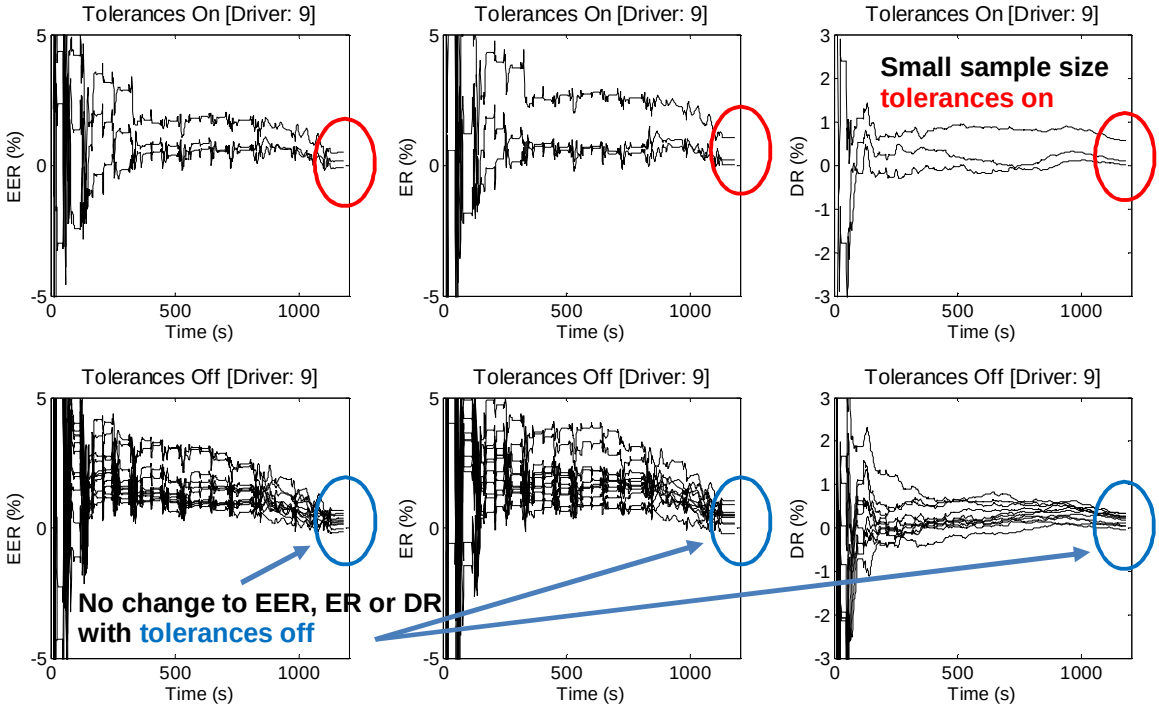

Figure 7-17: Instantaneous SAE primary metrics for driver 9 with driver's aid tolerances on and off

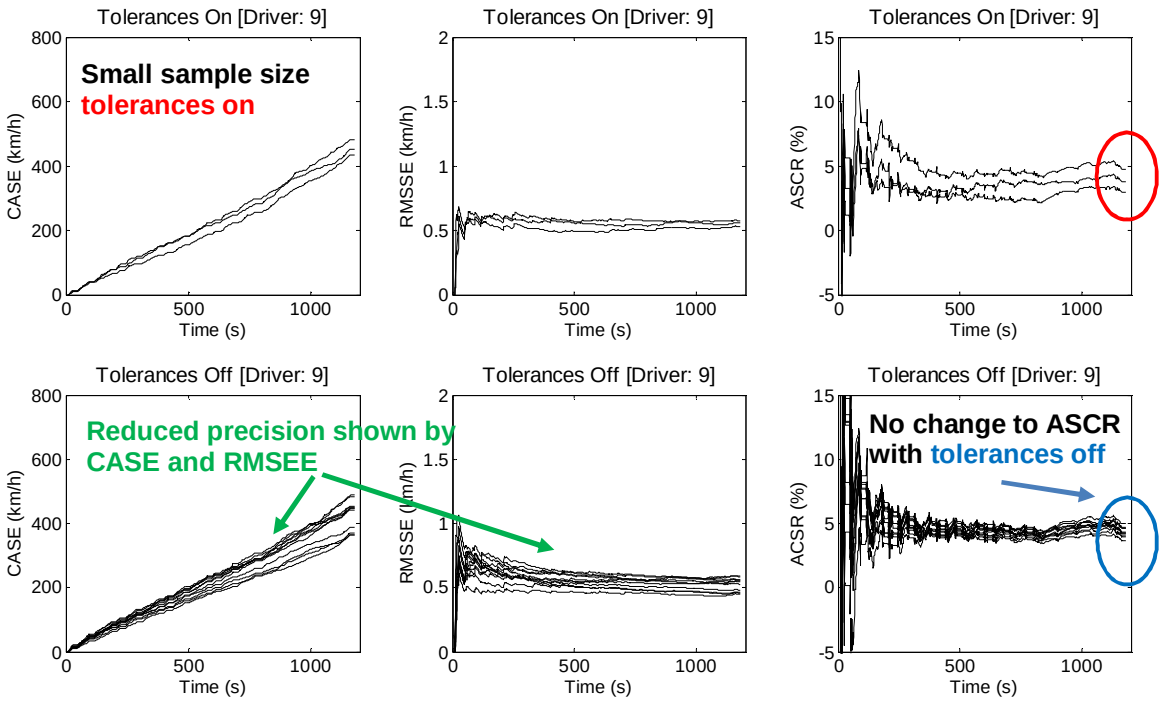

Figure 7-18: Instantaneous CASE and SAE supplementary metrics for driver 9 with driver's aid tolerances on and off

7.4. Comparing Driver Behaviour Metrics

As noted in the previous section, see section 7.3.3, not all of the driver behaviour metrics show that there is a clear distinction in driver behaviour between the two experimental cases of driver's aid tolerances on and off. The SAE primary metrics, ER and EER, along with the supplementary metric the ASCR have been shown to be insensitive to the changes in driver behaviour in this study and the primary DR metric has only been useful in some respects. The RMSSE and CASE metrics have been by far the most powerful and the novel CASE metric particularly so when viewed instantaneously. This clearly demonstrates that not all metrics serve to classify the same types of driver behaviour.

The reasons for this are evident when the calculations, see section 2.3.5, are examined in more detail. The SAE J2951 primary metrics are energy and distance based calculations that function to provide the mean percentage energy or distance error. In the case of the energy based metrics, ER and EER, it is possible to achieve the same end of test result via different paths. For example a driver could drive using less energy than the target speed trace during one portion of a test and then drive using more energy than the target during a later portion of the test. Both these behaviours will generate an instantaneous energy error but since their signs are opposite, assuming their magnitudes are the same, they will cancel each other out and have no effect on the end of test ER or EER result. This characteristic is not exhibited by the DR metric since all distance covered during a

test, including any distance errors, are accumulated and the total distance is always increasing. In this way any error from the target distance, whether positive or negative will always cause a change in the end of test DR metric even though the change may be small.

The RMSSE, ASCR and CASE are all metrics that are based on an absolute error and in this way the problem of errors during the test cancelling each other and not being detected are avoided. However the ASCR is an acceleration error metric and it is therefore possible to have a large speed error that does not generate a large ASCR value simply because the rate of change of speed during the time period that the error took place was small. The RMSSE is a speed error based metric that avoids the problems suffered by the energy metrics since it is based only on the magnitude of the instantaneous speed errors. However since the mean error is used for the end of test metric any speed errors must either be of a large magnitude or endure for a large proportion of the test to have a significant effect on the end of test mean. The CASE metric, much like the DR metric, is robust to these issues. Since the metric is speed based, uses the absolute value and takes a cumulative sum, any errors even if only small are included and are less likely to be ‘averaged out’ or smoothed by the remainder of test. Table 7-2 summarises these differences between the metrics.

Table 7-2: Driver Behaviour Metric Classifications

Driver Behaviour Metric	Energy based metric	Speed based metric	Accelerati-on based metric	Average (Mean) error metric	Cumulative error metric
SAE Energy Rating	✓			✓	
SAE Distance Rating		✓			✓
SAE Energy Economy Rating	✓			✓	
SAE Absolute Speed Change Rating			✓		✓
SAE Root Mean Squared Speed Error		✓		✓	
Cumulative Absolute Speed Error		✓			✓

Despite the SAE J2951 standard recommending the metrics to be used for one number end of test results [33], it is actually useful to examine the SAE metric and other metric results as traces of results calculated instantaneously throughout the test. This enables the identification of differences in behaviour during the tests that are not highlighted from the end of test results.

Studies by Brace et. al. [8] and Chappell et. al. [83] have included throttle pedal position data. These data were not available for the experimental data presented in Figure 7-4 through Figure 7-18. However throttle position data has been proven to correlate with emissions results in the study by Brace et. al. [8], who used throttle position to calculate their pedal busyness metric. This metric was defined as the cumulative sum of the absolute rate of change of pedal position. In addition to the study by Brace et. al. [8] the metric has also shown its usefulness in the work presented in Chapter 4 which was published by Chappell et. al. [83]. However these studies have not proven that the pedal busyness metric is more sensitive as a driver input characterisation tool than speed or acceleration based metrics. To this end, raw data was taken from the DoE study run on the University of Bath chassis dynamometer which resulted in Brace et. al.'s publication. In their experiment eleven noise factors were varied simultaneously via a DoE approach and a response model was built to isolate the fuel consumption effect of individual factors. To achieve a perturbation in pedal busyness Brace et. al. adjusted the robot driver PID control terms to achieve a more oscillatory pedal characteristic resulting in normal and aggressive test conditions. To look at the effect of this two tests were selected from the DoE matrix were the aggressive and normal robot characteristics were in use. The other

noise factors which were simultaneously varied are summarised in Table 7-3 factors that were unchanged are not listed. The resulting driver behaviour metrics, as calculated by Brace et. al. are also given.

Table 7-3: DoE test conditions and corresponding end of test driver metric results

	Test A	**Test B**	**Percentage change (%)**
DoE test condition variables			
Robot driver pedal busyness setting	Aggressive	Normal	
Headwind fan demand (%)	100	60	
Tyre type	Production	Sport	
Vehicle alignment to chassis dynamometer	Normal	Misaligned	
Vehicle restraints	Angled to floor	Horizontal	
Inertia simulation setting (kg)	1470	1617	
Driver metric results			
Pedal busyness (%)	4571	2113	**+116**
Cumulative speed error (Km/h)	363	537	**-32.4**

The results shown in Table 7-3 show that the use of the two robot driver settings has had an effect on both the pedal busyness and speed error metrics, although the effect on the pedal busyness is over three times the relative magnitude if the percentage differences are examined. This suggests that the two metrics are measuring different perturbations. To investigate this the instantaneous traces were plotted in Figure 7-19.

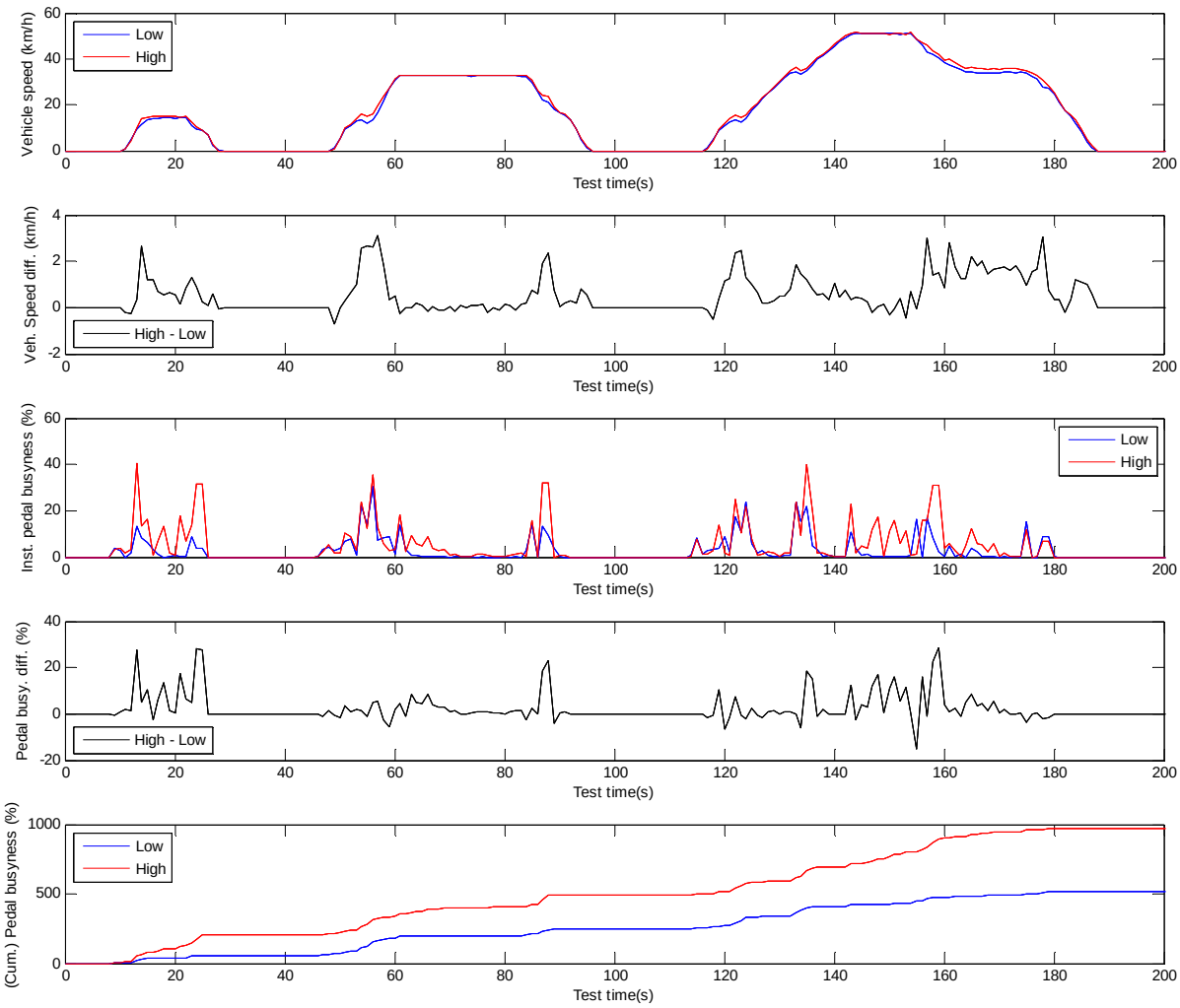

Figure 7-19: Comparison of vehicle speed error and pedal busyness as driver metrics for the first 200 seconds of a NEDC emissions test for high and low robot driver pedal oscillations. Plots show vehicle speed, the difference between high and low vehicle speed, the instantaneous pedal busyness, the difference between instantaneous high and low pedal busyness and the pedal busyness as developed over the test.

Comparison of the individual plots within Figure 7-19 shows that there are some differences in the vehicle speed profile for the two test cases; high and low aggresivity. Indeed the profile of the trace of the second and fourth plots from the top of the figure are very different. During the cruise periods there is very little difference in the speed error for the two test cases, however there are marked changes in the pedal busyness difference as summarised by the first plot down particularly for the first and third vehicle excursions. These plots demonstrate that the pedal busyness metric is giving useful additional insight to driver inputs. This can be explained because the pedal busyness is measuring the root driver input and vehicle speed is some way down the integral chain from the driver pedal input. To provide further verification of this the difference in the pedal busyness was plotted against the difference in the vehicle speed error, as shown in Figure 7-20.

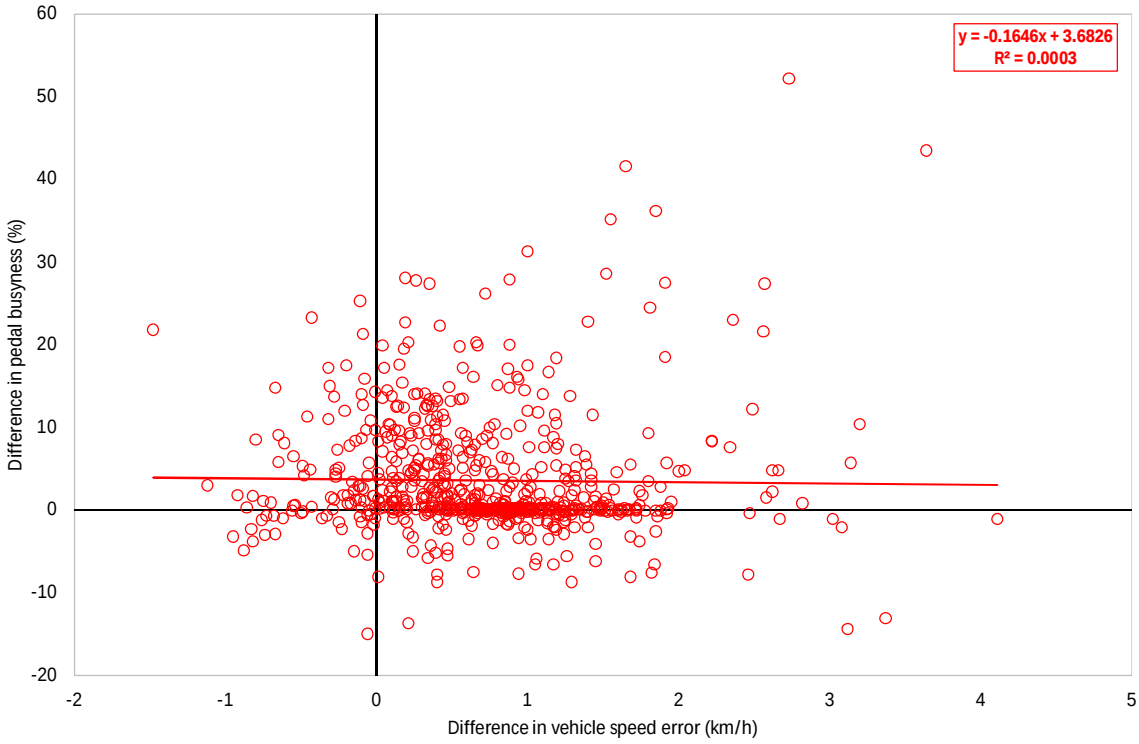

Figure 7-20: Relationship between difference in vehicle speed error and the difference in pedal busyness for high and low aggresivity drives over an NEDC recorded at 1Hz. Idle periods have been excluded.

Examination of Figure 7-20 shows that there is absolutely no correlation between the vehicle speed error and the pedal busyness the coefficient of determination being 0.0003. Clearly the pedal busyness is giving useful additional insight into the driver inputs and therefore ECU logging to record driver pedal inputs is important if not essential to fully classify driver behaviour.

7.5. Real-time Driver Feedback

All the work presented so far has been focused on post-test analysis of driver behaviour. However this approach only allows for retrospective training and the possibility of correcting existing results. Perhaps a better approach that could reduce the number of wasted and invalid tests would be to use the metrics discussed in this chapter to provide instantaneous feedback to the driver. For a metric to be useful in this purpose it must be stable and maintain sensitivity throughout the duration of the test. By examination of Figure 7-11 through Figure 7-18 it can be seen that the primary SAE metrics, EER, ER and DR are not likely to be well suited to this application since they are extremely oscillatory, particularly in the first 300s of the test. A similar problem is prevalent with the SAE supplementary metrics, namely the ASCR and RMSSE. They are initially oscillatory and towards the end of the test they become less sensitive and tend to a straight line constant value. The metrics which exhibit instability in the first portion of the test are those

that calculate an average error, see Table 7-2 and this instability is caused by the fact that at the start of the test a fixed instantaneous error is a much larger percentage of the total energy or error over the length of the test already passed. The only metric that is non oscillatory and is stable throughout the test is the CASE and therefore this metric could form the useful basis of an instantaneous driver feedback system. Further experimental validation work would be required to demonstrate this fully. However the use of ECU pedal data to calculate pedal busyness, the new CASE metric and the use of metrics to calculate instantaneous values during the test are being proposed to the working group as an extension to the SAE J2951 standard. This work is underway and it is planned that a future version of the standard will incorporate some or all of these techniques.

7.6. CO_2 correction and tolerances for Drive Metrics

An idea that is gaining significant traction from legislators, particularly within the forthcoming WLTP, is the idea of correcting CO_2 emissions from TA tests on the basis of drive metric results or to limit the CO_2 influence of driver behaviour by imposing a legal tolerance on the EER result for a test. This idea is relatively speaking in its infancy and there is substantial further work required before it could be implemented. The work of this chapter has shown that reviewing a simple one-number-per-test result for EER is not sufficient to classify the behaviour as there are multiple routes through a test that end with the same EER result. In addition there is limited data to suggest that the correlation between drive metrics and emissions results is suitably stable to enable the implementation of universal correction factors. The author suggests that further validation work is required in this area to develop a robust relationship between drive metrics and emissions results before legislators should consider implementing such controls.

7.7. Chapter Summary and Conclusions

The aim of the experimental data discussed in this chapter was to determine if the precision in driver behaviour could be improved by removing the speed tolerance traces from the driver's aid display during a chassis dynamometer emissions test. A total of approximately 450 tests were completed, 250 with the tolerances on and displayed on the drivers aid, followed by approximately 200 with them not displayed. Tests were completed by 35 human drivers using the same test vehicle across 6 separate chassis dynamometer test cells. From the analysis of the results from these tests the following conclusions are drawn:

- It was found that there was very little change in the mean CO_2 emissions between the two driver's aid configurations, although the scatter was markedly reduced; the standard deviation being reduced by 43.5%.

- An analysis of driver behaviour metrics showed that the SAE J2951 primary metrics, EER, ER along with the supplementary metric, the ASCR, were insensitive to changes in driver behaviour in this study. The results from these metrics showing little change between the two test cases; tolerances on and off. This highlighted that it is not sufficient to simply rely on the SAE J2951 primary energy metrics to classify and understand differences in driver behaviours between tests.

- The SAE J2951 supplementary metric, the RMSSE, along with the newly defined CASE metric and the SAE primary DR metric did prove to be effective tools to understand the driver style differences. The RMSSE and CASE metrics were on average reduced when the tolerances were off by 12.8 and 11.1% respectively. These changes were significant when tested at a 95% confidence level. The spread in these metrics was reduced even more dramatically by 35.3 and 25.8% respectively.

- An analysis of individual driver behaviour showed that most drivers either improved their precision or reduced their speed error from the target or achieved improvements in both precision and error.

- Although the SAE J2951 standard recommends its metrics only as one number end of test or phase results, it provides useful additional insight to examine traces of any of the driver metrics calculated instantaneously throughout any given test. This helps to identify between test or driver patterns, is useful for driver feedback and is the only robust method to identify the common issue of different drive styles during a test which result in the same end of test result via the SAE J2951 metrics.

- Of the two metrics found to be most sensitive to the changes in drive style in this study, the RMSSE and CASE, the CASE metric showed more promise for use in an instantaneous driver feedback tool. This is because it is not unstable at the beginning of the test and is not damped at the end of the test thereby showing more uniform sensitivity with time.

- The use of ECU pedal data to calculate pedal busyness, the new CASE metric and the use of metrics to calculate instantaneous values during the test are being proposed as an extension to the SAE J2951 standard.

Chapter 8. Procedural

8.1. Introduction

The review of the literature showed that the largest effects from procedural factors that have been reported were related to the tyre condition, engine oil level and ambient temperature. Whilst useful data exists within the literature to quantify the size of the effect of these factors, in most cases there is not enough information to enable complete control of the factor. For example for the tyre inflation pressure, there is data that quantifies the expected change in FC for a change in pressure, but not any data that shows the expected variability in tyre pressure in a commercial laboratory testing environment, nor a suggestion of how it might be controlled using typically available resources.

This chapter will investigate the most significant procedural factors to quantify the normal level of variability and to suggest methods to control these factors.

8.2. Tyre inflation pressure

The review of the literature showed the importance of the tyre inflation pressure on the vehicle rolling resistance and hence CO_2 emissions with effects reported in the region of 0.3 – 2.6% change in FC. However no authors in the literature have attempted to quantify the normal variability in tyre inflation pressure. For a commercial laboratory, such as the one studied in this research, it is common for a test vehicle will remain in a temperature controlled environment for the duration of its testing and between test soak periods. The author therefore proposes that the tyre pressure is unlikely to change for the duration of the testing. This would only hold true if the tyre pressure is set correctly when the vehicle enters the lab and if there were no leaks in the wheel/tyre assembly. To investigate this theory a series of relatively random measurements were taken from the quality check vehicles in the commercial laboratory over a period of approximately 150 days. The results are presented in Figure 8-1.

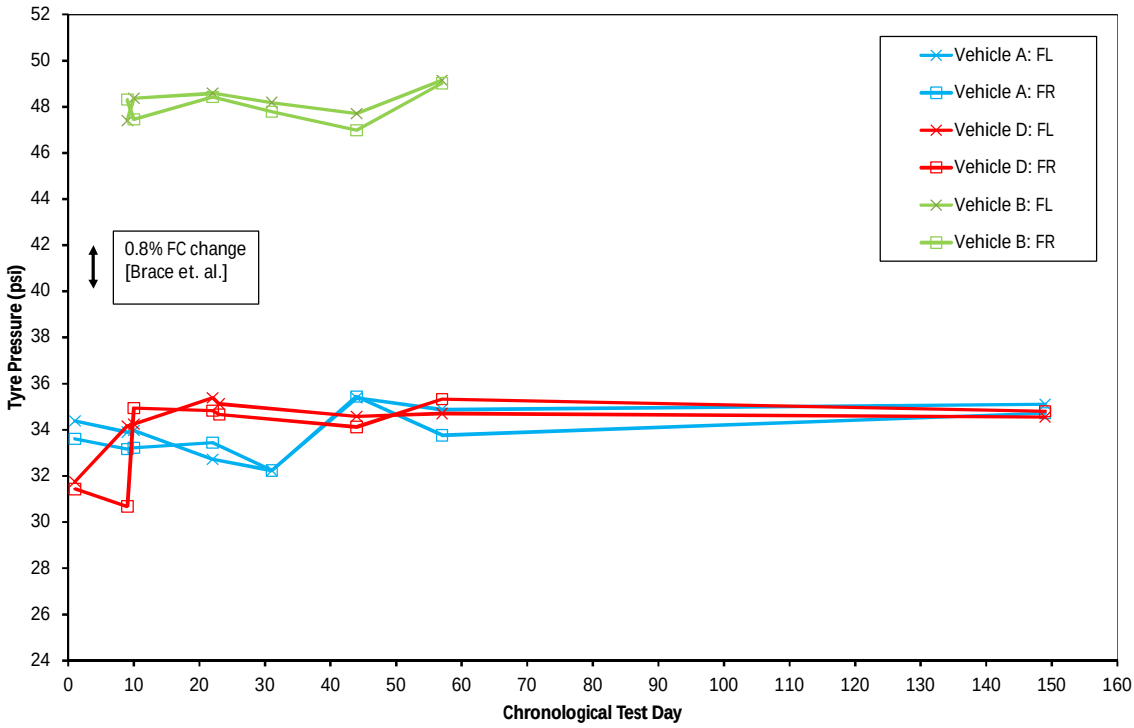

Figure 8-1: Tyre inflation pressure measured from three quality check vehicles during soak conditions within the commercial laboratory. Vehicle A is a gasoline B-car, vehicle D is a C-car and vehicle B is a light commercial. FR is the front right tyre and FL is the front left tyre. All vehicles are front wheel drive. Representative FC sensitivity is shown using data from Brace et. al. [8].

The results presented in Figure 8-1 were obtained by taking tyre pressure readings from the vehicles during soak periods with various steps taken to ensure repeatability of these measurements. For example the measurements were all taken by the same person, the author, using the same calibrated gauge. In addition the measurements were taken at about the same time of day to ensure that the vehicles had been on soak for a similar amount of time prior to the measurement. Only a limited number of measurements could be taken due to practical constraints. However the data that has been captured shows a few interesting trends. Firstly for vehicle D the tyre pressures of both front wheels were approximately 4psi below the target pressure of 36psi. By reference to the work by Brace et. al. [8], see section 2.5.3, this might be expected to cause a change to the FC of as much as 1.6%. At the next measurement it appears that only one wheel has had its tyre pressure adjusted since the front left pressure has increased whilst the front right has slightly decreased. This shows an example of the magnitude of the error that can occur through variability in the human setting of tyre pressures. After this point the tyre pressures remain very consistent for the duration of the experiment. The tyre pressures for the light commercial vehicle, vehicle B, remain very consistent throughout the experiment varying only within approximately ±1psi. Vehicle A shows the most sustained variability in tyre pressure as the measurements are variable throughout the experiment. It is possible there is a slight leak on this vehicle as the pressure steadily decreases for the

readings taken over the first 30 test days. Given the large time lapse between the second to last and last measurements it's not possible to verify this.

A procedure in operation within the commercial laboratory is to check the vehicle tyre pressures when the vehicle enters the laboratory and then to check again for the first chassis emissions test. Following this, checks are only routinely made every sixth emissions test. The tyre pressures are checked in the test cell, after the vehicle has been moved from the soak area and installed onto a dynamometer. The checks are made with devices which are regularly calibrated back to a traceable standard. From the data gathered for Figure 8-1 an example of the regular pressure checks can be identified from the data for vehicle D as occurring between the first and second measurements. However there are not enough measurements or enough data to identify any further checks with any certainty. The success of a tyre pressure check is predominately governed by human error in either seating the fitting onto the tyre valve causing air to be lost during the reading, or in mis-reading the gauge. The second of these error states was reported verbally due to some devices having difficult to read scales. To this end some commercial laboratories have installed automatic tyre pressure checking devices or direct tyre pressure monitoring for a limited number of vehicles. The automatic device takes a user inputted set point and then automatically adjusts the pressure when the fitting is offered up to the tyre valve. Such devices are likely to be good at minimising human error but are costly to install and are not usually easily mobile.

To date only a limited amount of work has been conducted in the area of tyre pressure monitoring and there is much additional work that could be undertaken in the future. With a greater number of measurements of in-field variability of tyre pressures it would be possible to verify the author's assertion that tyre pressures do not change significantly with time when being tested in temperature controlled conditions. If this was proved to be correct procedures for checking tyre pressures regularly within commercial laboratories could be relaxed to avoid the likely scenario that by asking multiple operators to check the tyre pressures one is introducing more sources of uncertainty and increasing the variability. In the absence of this information the author suggests that for a low throughput environment, tyre pressures should be checked prior to every test using a consistent method; the same gauge and the same operator for instance. If a higher throughput is required it may be beneficial to install tyre pressure sensors. These devices can be installed inside the tyre void, typically attached to the rear of the tyre valve and transmit pressure data wirelessly. If this is not feasible then a process where tyre pressures are checked 'every so often' is not very precise but probably is the best that can be achieved in such circumstances.

8.3. Engine oil level

The work of Brace et. al. [8] from the literature showed that the engine oil level can have a significant effect on the vehicle FC over a TA style emissions test. Brace et. al. reported a large change in FC; 2.9% which was statistically significant at 99% confidence. However the change in engine oil level that was tested was very large; in a modern passenger vehicle a change in oil level of 2.5 litres would likely be reducing the volume by over 50%. For example the full fill on a common passenger B-car, such as vehicle A is approximately 4.5 litres. The author of this thesis would argue that in a commercial laboratory environment this factor would be unlikely to be prevalent, since most client vehicles are not tested for a long enough duration for oil consumption to be an issue. For the quality check vehicle scenario it is perhaps prudent to implement checks for the engine oil level, but again, given the relatively low rate at which engine oil consumed the factor is unlikely to be anywhere near the statistically significant level when comparing tests from week to week.

8.4. Ambient Temperature

In the literature there was some discrepancy between the magnitude of the effect of ambient temperature on the vehicle FC and CO_2 emissions. Brace et. al. investigated only a very small temperature change of 3°C and reported a very small effect, 0.2% FC, which was not statistically significant [8]. Whereas Jourmard et.al. [31], Kadijk et. al. [14] and Schmidt [20] all investigated much larger temperature changes, most within the 10°C region and perhaps unsurprisingly reported larger effects of between 2 and 4% change in CO_2 emissions. The results published by Schmidt [20] suggested some vehicles were much more temperature dependant than others as vastly different results were obtained from different vehicles but not enough additional information was given to verify and have confidence in this.

Given that a legal TA emissions test can only occur between 20 and 30°C [9] there is limited scope for temperature to become a factor. However the literature has shown that on some vehicles a change within a 10°C region is enough to cause a change to the CO_2 emissions of at least 2%. To give an indication of the potential scope for this to be become a significant factor, the pre-test start temperature was plotted for a number of tests of quality check vehicles from the commercial laboratory results. These results are shown in Figure 8-2.

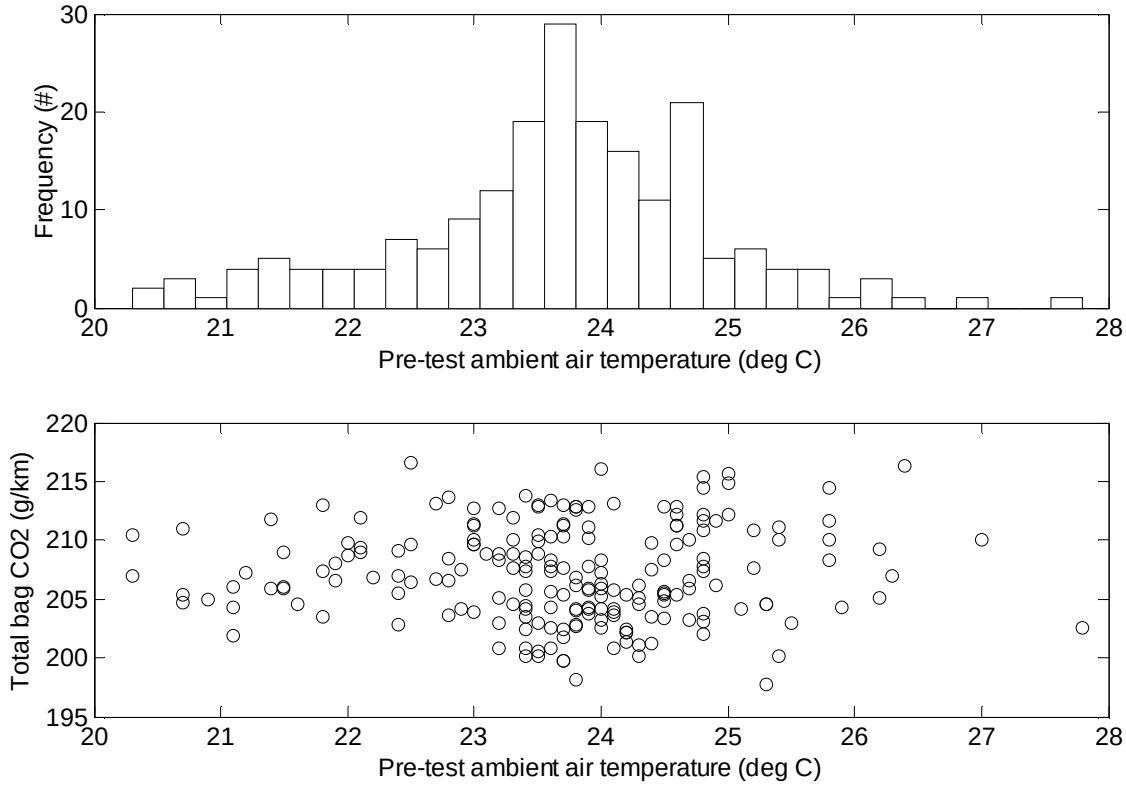

Figure 8-2: Histogram of pre-test ambient air temperature for a number of tests in a commercial laboratory and relationship between pre-test air temperature and total CO_2 emissions for the same tests.

Figure 8-2 shows that there is approximately a range of 8°C in the test start temperature which would suggest a change in CO_2 emissions of just under 2% using data from the literature. However if the data is plotted against the total bag CO_2 emissions there is no correlation between ambient temperature and CO_2 emissions, see Figure 8-2. This could likely be because other significant noise factors are varying at the same time that mask any relationship between ambient temperature and CO_2 emissions given that Figure 8-2 shows a range of 20 g/km, approximately 10%, in CO_2 emissions and the literature suggests the effect of temperature alone is less than 2%. Control of the temperature should be relatively straight forward as it is directly controlled by the installed air conditioning systems. However the data from Figure 8-2 suggests the temperature is not very well controlled in the commercial laboratory. The author speculates that this is because the laboratory extends over a very large area with limited subdivision of areas to control the temperature when external doors are opened. However further measurements of temperature distribution throughout the laboratory would be required to validate this.

8.5. Chapter Summary and Conclusions

In this chapter the likely effects of the three most significant procedural factors identified in the literature were analysed and discussed. Measurements of tyre pressure from quality check vehicles were analysed to understand typical variability in tyre pressure. The likely

prevalence of the variations in engine oil level and ambient temperature were also discussed. From this work the following conclusions can be drawn:

- Tyre pressures on modern vehicles in a temperature controlled environment are unlikely to change significantly on their own unless there is a mechanical failure or leak. Asking multiple operators with multiple different gauges to check and adjust the pressures is believed to introduce more variability than simply not adjusting the pressures at all, although further work is required to prove this definitively.

- The effect of changes in engine oil level are unlikely to be significant in a modern commercial test environment unless there is a mechanical failure on the vehicle.

- Ambient temperature does vary within a commercial laboratory test environment despite the use of temperature control plant which is required to meet the tolerance imposed by the TA authority. Data from the commercial laboratory showed that temperature varied within a range of 8°C, however there was no correlation between ambient temperature and CO_2 emissions when examining a scatter plot these variables. However using data from the literature the estimated effect of an 8°C variation in temperature on CO_2 emissions is just under 2%. It is suggested that ambient temperature might be better controlled with sufficient installed air conditioning plant and good segregation of areas to prevent temperature fluctuations when external doors are opened.

Chapter 9. The Chassis Dynamometer

9.1. Introduction

The importance of the correlation between dynamometer road load and vehicle CO_2 emissions is well founded within the TA testing industry and is discussed by several authors in the literature. Authors have reported sensitivities in the region of 0.6% CO_2 per 1% change in road load force [10] over a TA test and 0.16% change in FC per 1% change in simulated inertia [8].

The aim of this chapter is to answer the question posed by the review of the literature; *is the modern chassis dynamometer capable of providing the required precision and accuracy for modern high precision testing?* In the process of answering this question the fundamental operating systems of the dynamometer shall be examined to understand the sources of uncertainty and how they might be minimised.

9.2. Dynamometer Load cell calibration

Load cells for modern chassis dynamometers are normally strain gauge types mounted between the motor body and the dynamometer frame. The load cells must be accurately calibrated and capable of giving repeatable readings, otherwise none of the other calibration routines will give satisfactory results. As was covered in the literature review, see section 2.4, the DPEQAP defines an acceptance criteria for a load cell calibration of ±0.1% for accuracy, ±0.1% for linearity, ±0.1% for hysteresis and ±0.05% for repeatability [49]. This is much tighter than the tolerance defined in the TA regulations which states that: “the accuracy of matching dynamometer load to road load shall be ±5% at 120, 100, 80, 60 and 40 km/h and ±10% at 20km/h.” [9].

The load cell is normally calibrated by the deadweight calibration method whereby weights are hung from a load arm attached to the dynamometer motor body. The length of the arms is accurately measured during manufacture and inputted into the controller along with accurate measurements of the applied weights. A series of weights are applied to exercise the load cell from its zero position to full scale, normally in both the positive and negative direction, known as a two sided calibration. Although older dynamometers only calibrate in one direction, a one sided calibration, for which the zero point is not included. Since dynamometer motors and load cells are normally located beneath the floor of a test cell it is normal to apply these weights via a swing arm that is connected to the motor load arm via a threaded bar or similar. The connections must be made using knife edges to ensure there is as little friction as possible. Any friction in the connection points will result in less force being applied to the load cell than is applied by the operator at the test cell

floor. To achieve a repeatable load cell reading during the calibration it is essential to minimise any disturbance, movement or vibration in the swing arm since this will cause oscillation in the load cell value and an unrepeatable calibration result. This necessitates the careful loading of the dead weights onto the arm and ensuring that adequate stabilisation time is allowed before load cell readings are taken. For this reason and also for convenience, some dynamometer manufacturers offer an automated calibration, where the weights are applied by actuators minimising any disturbances and meaning the weights can be applied directly to the load cell arm without the need for additional knife edge joints. However such systems are relatively uncommon due to the additional expense of installing them in the first place.

The author's experience of witnessing load cell calibrations being performed in a commercial testing environment showed that if the calibration was performed carefully with due diligence to the concerns discussed, such as stabilisation of the weights prior to taking readings, it was certainly possible to achieve calibrations that were well within the TA legal tolerance. However for achieving the highest precision possible from vehicle testing the TA tolerance is unlikely to be sufficient and as a minimum the user must aim for achieving the much tighter acceptance criteria laid out in the DPEQAP. Data provided by the major dynamometer manufacturer Horiba suggests that it is possible to exceed the DPEQAP criteria by some margin on the latest generation of dynamometers. With a two sided calibration the manufacturer claims to be able to achieve a limit five times smaller than the criteria defined in the DPEQAP for linearity and hysteresis; stating a tolerance of ±0.02%, see Figure 9-1 [35].

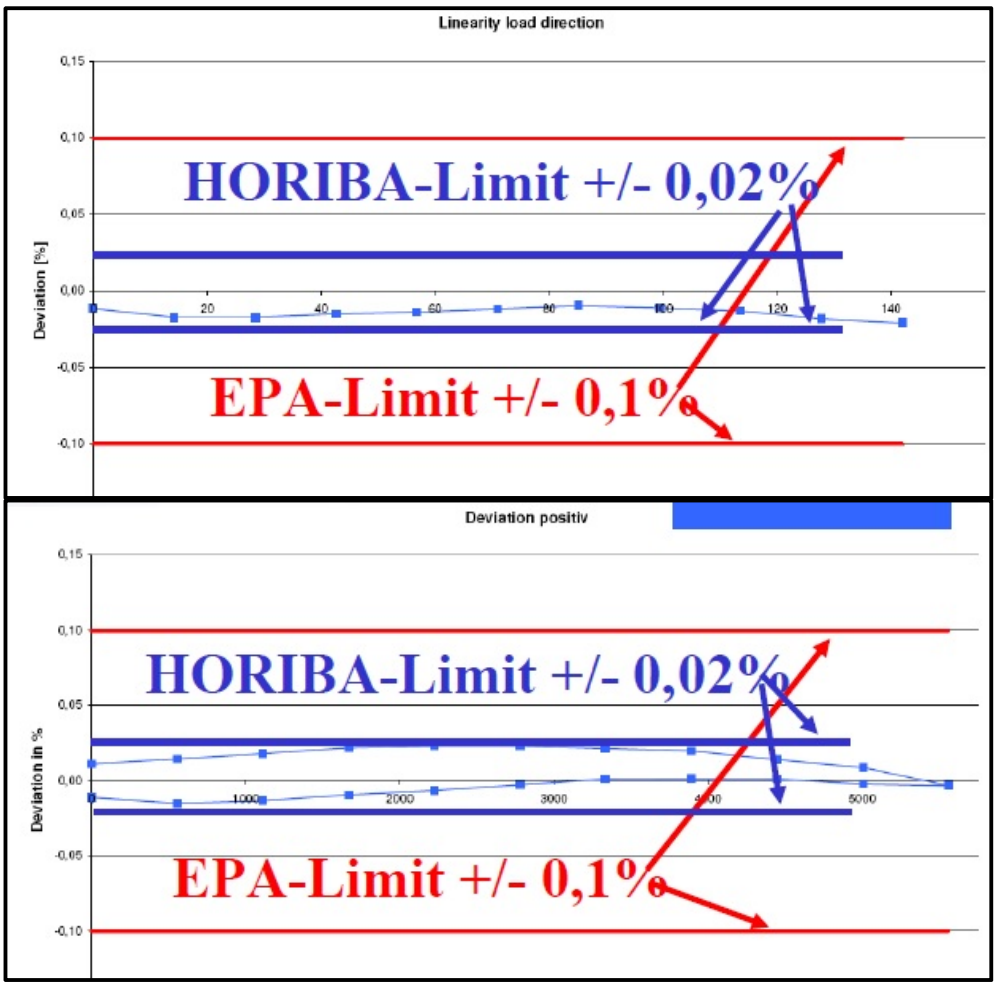

Figure 9-1: Horiba results showing the achievable linearity (top plot) and the hysteresis (lower plot) for a VULCAN chassis dynamometer two sided load cell calibration [35]

The same manufacturer also states a tolerance of ±0.005% for accuracy, which is ten times smaller than the DPEQAP criteria [35]. In both cases data is provided to verify these claims. The manufacturer goes on to explain the disadvantages of a one sided calibration; namely that only one quadrant of operation is calibrated and that deformation of the load arm can be an issue, although the author of this thesis notes that this is the case for either type of calibration. Horiba state that their one sided calibration does not give a linearity or hysteresis that meets the DPEQAP criteria [35]. If the sensitivity reported in the literature by Kadijk et. al. [10] is to be believed the improvement in accuracy provided by the Horiba system would mean errors in CO_2 emissions would be controlled to within ±0.013%. A tolerance that should enable the arbitration of even the smallest changes to modern vehicle technology.

In summary modern dynamometer equipment is more than capable of giving the required accuracy and precision from load cell calibrations. In the absence of any field data to prove otherwise the author concludes that, provided the necessary care is taken during the routine, including ensuring that a two sided calibration is undertaken, the calibration of

load cell is not a significant issue for the accuracy and precision of a modern chassis dynamometer.

9.3. Dynamometer Base Inertia Calibration

For accurate operation, a dynamometer must have an accurate determination of the base inertia of the rotating components coupled between the motor/s and the vehicle wheels. As was discussed in the literature review, see section 2.4, in the case of most modern dynamometers with electrical inertia simulation the base inertia is required to determine the amount of up or down simulation that the electric motor/s must provide during a transient driving manoeuvre. When a dynamometer is brand new the manufacturer could determine the base inertia of the machine by weighing the roller set, using CAD models and by taking product data from the motor manufacturers. However there is a concern that this measure could be inaccurate during the dynamometer lifespan as there will be wear of the rollers, motors and deposits on the roller surface from vehicle tyres. It is therefore commonplace to regularly run a calibration procedure for the base inertia. This procedure is essentially the same as that defined in the DPEQAP where by the dynamometer is accelerated and decelerated, without a vehicle and by applying a fixed force from the motor/s. The time taken to change from the initial speed to the maximum and then back to the initial speed is used to determine the acceleration, from which the mass or inertia can be determined via Newton's second law [49].

In commercial test environments it is common for an inertia calibration to be performed at the start of each shift following a circa 20 minute dynamometer warm up, saving the results and taking them forwards for any testing in that shift. At the University of Bath the inertia calibration is not performed very often at all, normally only if there is a reason to suspect that the base inertia has changed (for example noticeable increase tyre deposits on the rollers). As a useful diagnostic check the base inertia calibration routine is sometimes run without saving and updating the results for subsequent testing.

To obtain an accurate result from the inertia calibration routine, there must be accurate and precise signals from the load cells and the speed encoders. The load cells are required to ensure that the correct force is applied by the motors during the acceleration and deceleration events. This fact is borne out in the DPEQAP roadmap, see Figure 2-15, which shows that if the inertia check is not passed, the corrective measure is to 'perform a torque cell calibration' [49]. The encoder signals are required to ensure that the control system has an accurate measure of the roller speed and so can accurately determine the acceleration between the set speeds. Of course both of these are also required for the other dynamic calibration procedure; the losses calibration which is discussed in the following section.

9.4. Dynamometer Losses Calibration

As discussed in the literature review, see section 2.4, the dynamometer controller must have an accurate model of the losses between the inertia simulation source, typically an AC motor, and the rollers to enable the accurate arbitration of motor torque and therefore load on the vehicle wheels. However the losses can only be calibrated when a vehicle is not in contact with the dynamometer rollers and by running a standalone routine whereby the dynamometer is accelerated at a constant rate and the error in the recorded force is monitored. The study of the literature found that some key components of the losses are the bearing friction, windage on the rollers and motor coast torque losses. The bearing friction is said to be approximately linear with speed and dependant on thermal state due to the fundamental relationship between temperature and viscosity of the lubricating medium [42]. The windage losses are caused by aerodynamic skin friction drag on the surface of the rotating components, which is given in Equation 9-1.

$$F_D = C_D \frac{\rho V^2}{2} A_C$$

Equation 9-1 [91] [92]

Where F_D is the aerodynamic skin friction drag force, ρ is the density of air, V is the velocity, C_D is the skin friction drag coefficient and A_C is the moving surface area in contact with the air. The skin friction drag coefficient is dependent on the Reynolds number of the fluid or air and hence is highly dependent on whether the flow is laminar or turbulent. The drag force is therefore also dependant on the temperature, since changes in the ambient temperature will cause changes in the density of the air. When the temperature is increased the density of the air will also be increased meaning higher windage forces.

The theory therefore shows that for total accuracy the dynamometer's model of the losses must be obtained and be representative of the thermal state during the whole duration of a specific test. If the test to determine the magnitude of the dynamometer losses, typically called a loss calibration, is performed when the dynamometer is very hot and the emissions test using this loss estimation is performed after an overnight soak of the dynamometer there could be a substantial error in the load applied to the vehicle and this may cause a change in the vehicle CO_2 and diesel NO_x emissions. Since both are highly correlated to vehicle load.

However no published studies exist in the literature that quantify the possible magnitude of the effect of losses compensation errors and the importance of the thermal state of the dynamometer. To determine the possible upper and lower bound of the error in the

applied load due to incorrect loss compensation a series of tests were performed in two test rooms at the commercial laboratory studied in this thesis; cell 14 and cell 4. In both cases the loss calibration was performed, firstly, following a long period of soak at the prevailing laboratory ambient temperature of approximately 24°C and secondly following the laboratory standard dynamometer warming procedure, which is to operate the dynamometer at 80kph for 20 minutes. Additionally in cell 4 a repeated warm loss calibration was carried out. The cell 4 test cell is an upgraded twin roller with part mechanical and part electrical inertia simulation, whilst the cell 14 test cell is an old twin roller with majority mechanical inertia simulation and only a small capacity electrical inertia trim capability. When the tests were performed cell 14 had not been operated in several weeks and the cell 4 had not been operated for 3891 minutes, which is over 5 days. These conditions were chosen to provide the absolute worst case 'cold' dynamometer states. A further difference between the two test cells is that cell 4 has bearing heaters that are always on and control the bearings to a set point temperature defined by the manufacturer. Figure 9-2 shows the results from these test cells.

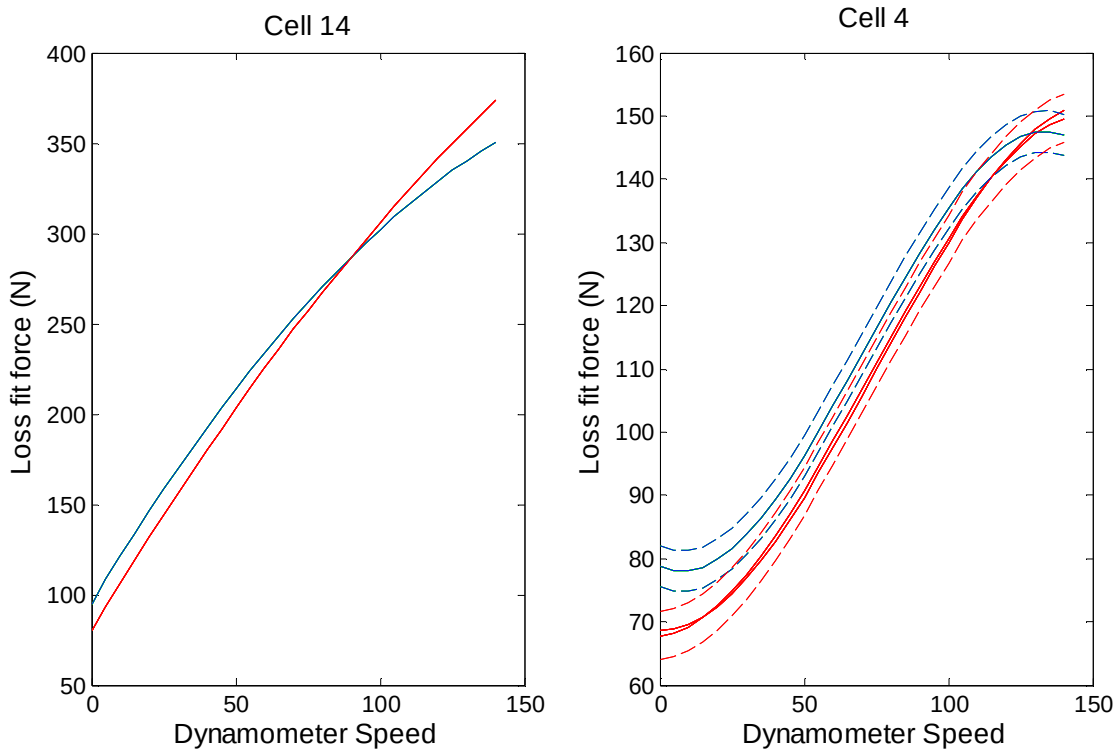

Figure 9-2: Cell 14 and cell 4 loss calibration results for cold and warm states. Blue lines are for the cold dynamometer and red lines are for the warm dynamometer. In cell 4 two calibrations were run with the dynamometer in a warm state. Dashed lines show RMS fit error

The results from cell 4 in Figure 9-2 show that generally when the dynamometer is cold the losses are higher than when the dynamometer is warm. At lower speeds the difference is approximately 10-15% and the difference decreases as the speed increases until approximately 130kph where the lines intersect and the pattern reverses. This result

at high speeds is unexpected, given that the theory states that the losses should be less on a hotter dynamometer and that the literature states that the bearing losses are approximately linear with temperature [42]. The results from cell 14 show much the same pattern, at low speeds the cold dynamometer losses are higher than the hot dynamometer and at higher speeds the pattern is reversed. Interestingly the cross over speed is much lower in the case of cell 14, being approximately 90kph compared with 130kph. The percentage difference between the hot and cold dynamometer losses are about the same for cell 14 as they are for cell 4 being in the region of 15% at their largest. To give an indication of the likely effect on CO_2 emissions the additional uncompensated losses force from using a cold dynamometer with losses calibrated under hot conditions was modelled in a powertrain simulation tool created by the author. This tool is a relatively simple spreadsheet based model which assumes perfect driving, following the NEDC speed profile exactly and uses this speed profile to calculate the tractive force at each 10Hz timestamp. With a calculated tractive force and using gear ratio data for the target vehicle the engine torque is calculated. To give a measure of the CO_2 emissions, an AVL ADVISOR map is used as a lookup table for each timestamp and the results are summed over the drive cycle. The ADVISOR maps are an open source set of data giving instantaneous fuel usage in g/s for the engine speed and torque operating range [93]. For this simulation vehicle data was used from vehicle B and an ADVISOR map from a Mercedes 2.2litre diesel engine was used. The results from this simulation showed that due to the additional force from an uncompensated cold dynamometer the expected change in FC and hence CO_2 emissions over the NEDC was 0.68%. It is only possible to have limited confidence in this result given the limitations of the simplistic spreadsheet model. These include the prefect driver, instantaneous gear changes, no warm up, engine fuel map data starts at 1250rpm, no clutch slip and no driveline efficiency included. However the indications are that dynamometer loss errors from incorrect thermal state could be in the region of 0.7%.

Given the choice, an engineer seeking a high precision result would always choose the more modern dynamometer with lower overall losses since the overall force error in the loss estimation is likely to be much lower. Figure 9-2 also shows a tolerance on each calibration result in the form of the RMS fit error. The error bands are overlapping for a large proportion of the speed range and this suggests that it is difficult to have confidence in the observed difference between the results except at the very low speeds. However the repeated warm loss calibration result from cell 4 is a very close match to the other warm calibration result and so this restores some confidence in the difference between the cold and warm cases. To have any statistical confidence it would be necessary to perform repeated cold and warm measurements in exact replicate conditions and include measurements from other test cells, however this data is not available.

The inclusion of the tolerance lines in Figure 9-2 highlights a potential source of error in the loss calibration procedure. For that particular test cell, cell 4, the tolerance lines are from the RMS fit error between the measured data and the resulting curve fit. The accuracy of resulting loss compensation is therefore a function, not only of the measured force during the test but also of the accuracy of the curve fitting algorithm. As the study of the literature showed the bearing friction is expected to be linear and the windage a squared function. It is therefore unsurprising that most dynamometer manufacturers use a second order fit and very surprising that some use a third order fitting algorithm for the losses force. The fit is unconstrained with no initial conditions to give sensible constraints on the locations of the minima. From examination of Equation 9-1 it is expected that the loss force minima would occur at zero speed and the resulting profile would be a quadratic showing increasing loss force with rotational speed. The bearing friction should theoretically provide a linear offset from zero. It can therefore be concluded that the loss fit profiles produced by dynamometers are inaccurate since they do not follow this trend and instead show points of inflexion part way through the speed range of the machine. In an attempt to examine if this variability in the fitting algorithm could be affecting the results further experimentation was conducted in cell 4 where a series of losses calibration routines were run in quick succession. Initially the losses from the cold dynamometer, following an overnight soak were obtained. The dynamometer was then run through a standard 20 minute warm up and the losses re-evaluated. In an attempt to capture the effect of the cool down of the dynamometer on the losses calibration, the losses calibration routine was then re-run a following four times allowing gaps between each calibration where the dynamometer was left idle. The results are shown in Figure 9-3.

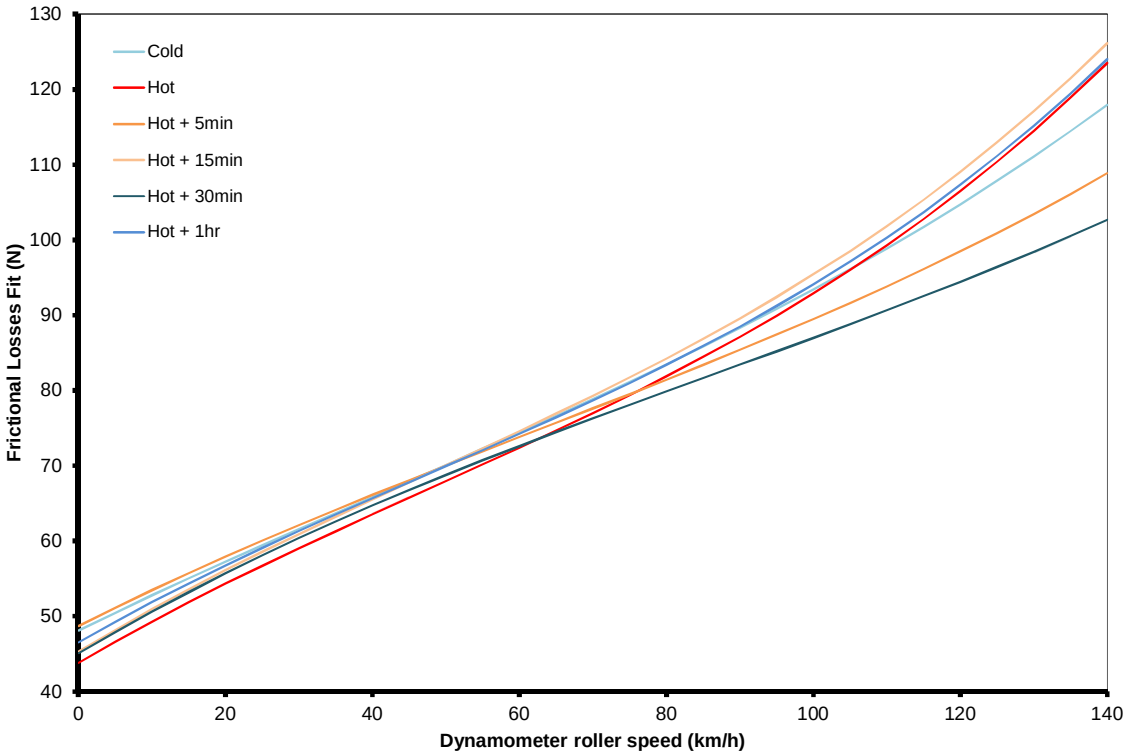

Figure 9-3: Cell 4 loss calibration results for a cold, warm and cooling down dynamometer

Interestingly the loss curves resulting from the experiment in cell 4 do not follow in the order that might be expected; the losses from the cold dynamometer are actually near to the mean loss force from all conditions throughout the speed range. The losses fit from the hot dynamometer are the lowest as is expected but only below approximately 70 km/h. For the intermediate conditions, the loss force appears to be fairly randomly ordered, showing absolutely no correlation between apparent thermal state and the loss force. If the RMS fit errors are included it is not possible to have any confidence in the apparent differences between the conditions at speeds below approximately 100 km/h.

To investigate the cause of the seemingly random variability seen in Figure 9-3 and to determine if that is a result of poor curve fitting or noise in the fundamental signals, such as speed and force, data from two sources were examined. Firstly the chassis dynamometer at the University of Bath which uses the same basic principle for the test, with parameters that are user configurable for the fixed deceleration rate. In this case during commissioning of the dynamometer a deceleration time of 400 seconds was chosen with a start and end speed of 120 and 20 km/h respectively. By simple calculation, via application of the suvat equations, this yields an acceleration of -0.25 km/h/s.

Figure 9-4 shows a typical losses calibration result that has been obtained on the University of Bath's chassis dynamometer. The control system GUI shows both the previous, in other words applied, and the new losses calibration fit results within a plot of

the friction loss force with respect to roller speed. In addition and unlike many other systems, the measured force is also shown.

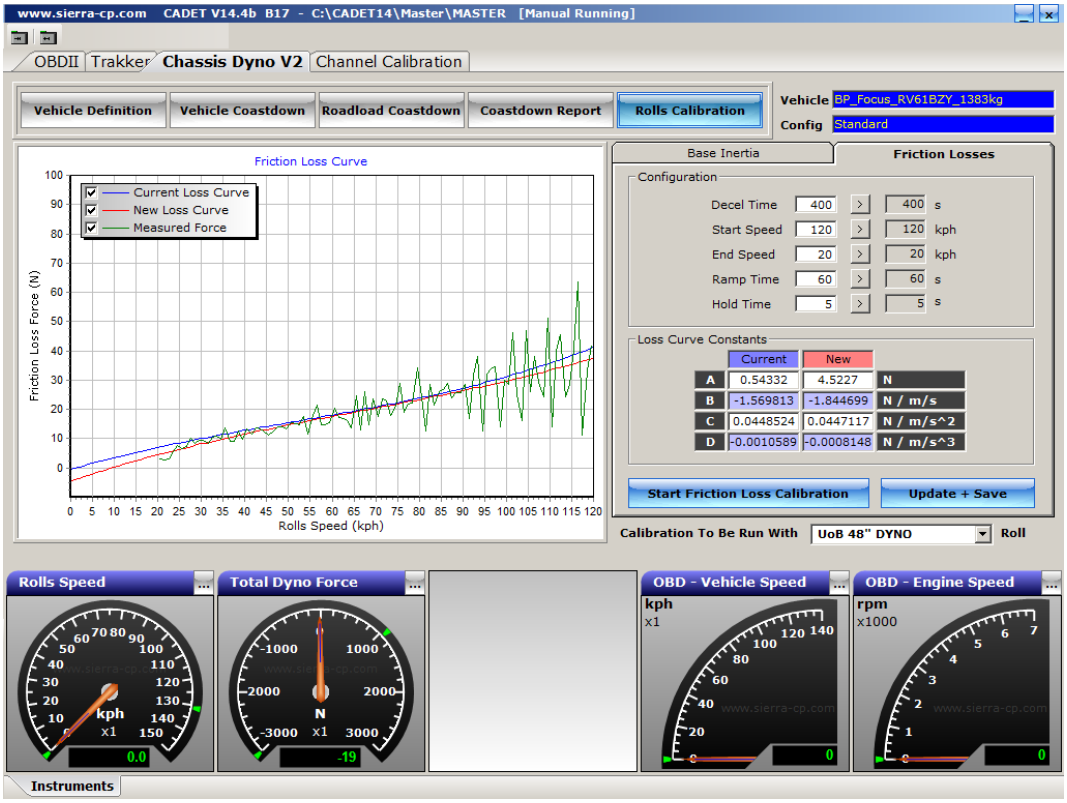

Figure 9-4: Typical friction calibration results display on the University of Bath chassis dynamometer via the Sierra CP Engineering CADET host system

It is immediately clear from Figure 9-4 that the University of Bath chassis dynamometer can suffer the same issues with respect to over fitting of the friction force curve since the resulting profiles for the two tests are not repeatable nor do they follow the expected pattern described earlier. What is particularly striking is the large amount of noise in the measured force signal. The noise increases with speed and for the higher speeds extends as far as ±100% of the fitted loss force. Conversations with the manufacturers to try and understand their calibration routines and examine the sources of errors are difficult because of course manufacturers are naturally cautious to divulge information about how their system works if it highlights any significant limitations or reveals a ‘trade secret’ that gives the company a competitive edge over its rivals. However it is clear from Figure 9-4 that the noise on the force signal is an issue for the accurate determination of loss force. By examining the raw data from both the University of Bath chassis dynamometer and chassis dynamometers within the commercial laboratory where the speed, acceleration and force are logged during loss calibrations it was found that the root cause of the noise on the force signal is a result of noise on the acceleration signal. The reason for this is that the acceleration or deceleration rate during calibrations is relatively low and hence if data is recorded at high frequency the change in speed between each timestamp is very small. It is therefore of utmost importance that the encoder signal has very high resolution.

This is why most dynamometer manufacturers choose encoders with at least 10,000 lines per revolution, giving a resolution of 0.036° or approximately 0.38mm linear distance at the roller surface. The University of Bath chassis dynamometer uses encoders with only 2,000 lines per revolution which in the author's opinion goes some way to explain the high noise in the signal, given that the resolution in linear distance is quite large at 1.92mm compared with 0.38mm for the 10,000 line encoders.

Of the three dynamometers examined in this section of the thesis, the total calibrated losses are by far the lowest for the Bath University chassis dynamometer whilst the losses from the cell 14 dynamometer are by far the largest, being nearly ten times larger, regardless of thermal state. This highlights an important point; given the fundamental limitations of the losses calibration routine, in terms of noise sensitivity and also curve fitting accuracy the smaller the magnitude of the losses the less likely these errors are to have a significant effect on the total load applied to the vehicle and hence the CO_2 emissions. To this end manufacturers have made several strides to reducing the magnitude of the parasitic losses in chassis dynamometers, by removing devices such as drive belts, flywheels and bearings along with introducing bearing heaters.

One improvement which has been implemented in the commercial laboratory is a tractive force monitor. The idea behind this is covered within the DPEQAP [49] which is to monitor the dynamometer motor force during constant speed operation of the dynamometer when there is no vehicle in contact with the rollers. In this condition, if the losses and base inertia are accurately calibrated for, from Newton's second law the motor force required to maintain a constant speed should be zero. The tractive force monitor, therefore keeps a check on the motor force and highlights an error if the force goes outside of tolerance. Typically this tolerance was set in the region of ±5 to ±10N depending on the capability of the dynamometer. When an error was flagged a coloured status light would turn red on the dynamometer control PC screen. This is an effective tool however the only issue is that an operator can ignore the controller's request for re-calibration and proceed to use the dynamometer anyway. These actions can be logged by the controller but there is not necessarily easy visibility of them within a standard test cell environment. A method to address this will be discussed in section 9.8 of this chapter.

In conclusion the losses calibration procedure used throughout the chassis dynamometer industry relies upon firstly accurate and noise free signals; namely speed and force, secondly accurate calibration of the base machine inertia and thirdly stable and reproducible loss curve fitting algorithms. These remain challenging but are not impossible to achieve. The best that can be hoped for is to minimise the magnitude of the losses through considered design of the dynamometer system. Although in some respects a

smaller loss force presents a greater challenge to measure, the corresponding opportunity for large force errors is minimised and therefore the overall effect on the vehicle emissions should be reduced.

9.5. Interaction of Calibrations

Typically the inertia calibration is performed before the losses calibration, however the losses must be accurately calibrated to ensure that the control system has an accurate model of the conversion from motor input current to force at the roller surface. Equally the base inertia must be accurately calibrated in order for the losses force to be accurately calculated. It is therefore necessary to iterate these processes and this is typically achieved, with a new dynamometer by starting with the manufacturer supplied data from CAD models and manufacturer data for the base inertia. This is then used to calibrate the losses and then the process can be iterated until consistent results are achieved. One difficulty with this is that any noise in the signals makes it very difficult to know if a stable solution has been achieved. This is a fundamental issue with the machine and further highlights the critical importance of an accurate load cell calibration combined with minimising any noise on the load cell and roller/motor encoder signals.

9.6. Coastdown Testing for Road Load Setting and Verification

The traditional method for setting and validating the load applied by the dynamometer to the vehicle is the coastdown test which is defined within the SAE standards J2264 [46] and J1263 [44]. The coastdown test is normally completed after first running a preconditioning cycle, often a NEDC, to ensure that the vehicle is thermally stable. These principles were introduced in section 2.4. During a coastdown test the dynamometer and vehicle are accelerated up to a pre-defined stabilisation speed, normally around 135kph. Then the vehicle transmission is put into neutral and the dynamometer is allowed to coastdown to zero whilst the dynamometer simulates and applies the road load to the vehicle. The time taken to coast is recorded and compared to track recorded times or to times from previous dynamometer based results. A coastdown test normally consists of more than one repeat run; the normal practice within commercial laboratories is three to five runs for each coastdown test, whilst the University of Bath have historically used three repeat runs for coastdown tests.

During a test sequence for a vehicle in the commercial laboratory studied in this thesis it is not normal practice to perform a coastdown test after every emissions test, instead the frequency is typically more like once every six tests. In fact there is a process that prevents a test requestor from asking for more coastdown tests than this because the coastdown tests are so time consuming. The only exception to this is for quality check

vehicles where a coastdown test is always performed. The impact of this policy is that coastdown results from client vehicles are relatively sparse and when they are performed it is not uncommon for the dynamometer road load to be iterated because the coastdown results appear to have drifted. The main reason the load is iterated is because there is a need to keep the dynamometer road load close to the track road load so that the vehicle loading remains equivalent to that which the vehicle would experience in the end goal of TA. If the coastdown results from client vehicles are at all suspect it can present a real challenge and difficult judgement calls frequently have to be made regarding whether or not to iterate the dynamometer vehicle load when there is no real confidence in the coastdown results. In the author's opinion, an iteration of the road load in these circumstances is risky since it will chase the special cause variability and is therefore highly unlikely to result in an improvement in the accuracy or precision of CO_2 emissions from the vehicle.

Common practice at the University of Bath is slightly different. Here a coastdown test is performed after every single emissions test. However, crucially, this is done purely for verification and the results are never used to iterate the dynamometer road load once a test sequence has been started, this process was chosen historically to minimise sources of imprecision and because accuracy is normally much less important than precision for testing in an academic context.

The sources of inaccuracy and imprecision for a coastdown test are numerous and many were introduced in the literature review, see section 2.4 and the earlier sections of this chapter. In addition the author has extended the list of factors through discussions with experienced commercial laboratory staff, dynamometer manufacturers and though an examination of the systems. These factors are summarised in three categories; procedural, dynamometer and vehicle which are shown on the fishbone diagram in Figure 9-5.

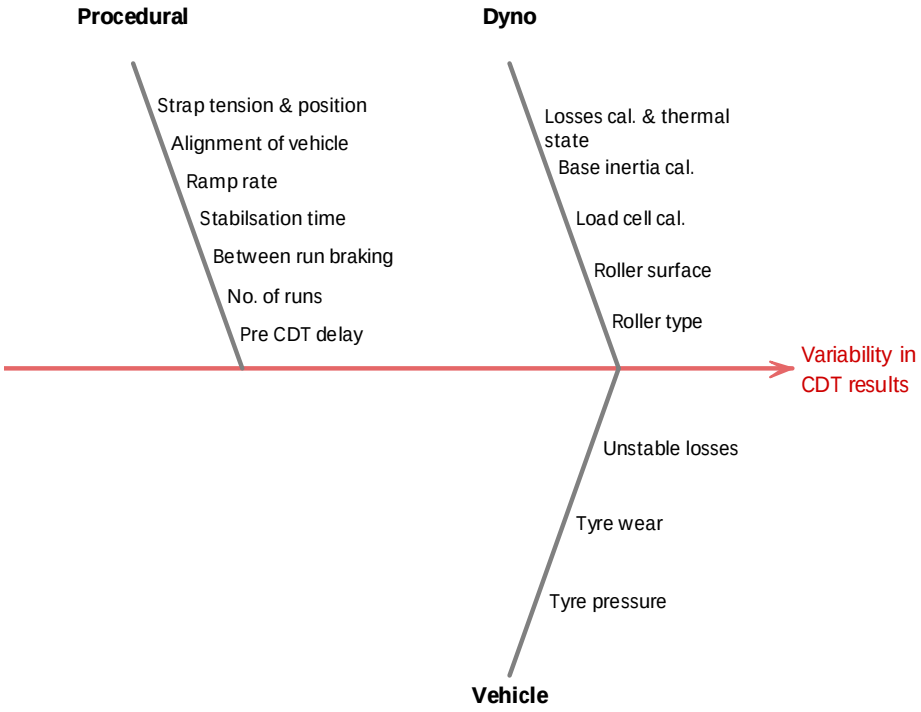

Figure 9-5: Coastdown test fishbone diagram

By examination of Figure 9-5, the factors that are caused by the dynamometer are all covered within the DPEQAP, which was introduced in the literature review. The DPEQAP gives procedures for validating that the dynamometer is within acceptable tolerances for each of these sources of error, whether these standards are sufficient to achieve the required precision is questionable. However it has at least been shown earlier in the chapter that in most cases the acceptance criteria can be met or exceeded for these calibration standards by a considerable margin. However keeping check of these factors is no small task and methods for dealing with this will be covered later in this chapter.

For many years the coastdown process consisted of accelerating the vehicle up to speed by driving it and accelerating through the gears. However this process has the potential to introduce significant variability, since there are likely to be changes in the procedure used between different operators and drivers. For example, if a driver accelerated aggressively during this period the tyres would be hotter going into the coastdown and the rolling resistance would be affected. As discussed in the literature review, see section 2.5.3, Genta [55] has shown that a hotter tyre carcass results in reduced rolling resistance which would be expected to increase coastdown times.

With the introduction of increased electrical inertia simulation within chassis dynamometers it has become possible to use the dynamometer electrical machine/s to accelerate the vehicle prior to the coastdown tests. This upgrade has the significant advantage that the acceleration rate can be pre-set and accurately controlled by the dynamometer so that it is the same for every test run. The University of Bath has been

using this procedure for many years and, although no data exists to prove the fact, it has been reported verbally that it was beneficial in removing the driving variability for the pre coastdown acceleration. But this fact is verified by the move of the SAE who updated their SAE J2264 standard to recommend that dynamometer driven coastdowns are used [46]. The commercial laboratory studied in this thesis installed this upgrade to some of its test cells during the course of the project by enabling a small change to the control system. Data was collected from two vehicles on one of these dynamometers; cell 12, to establish the effect of the change in coastdown process. The results are shown in Figure 9-6.

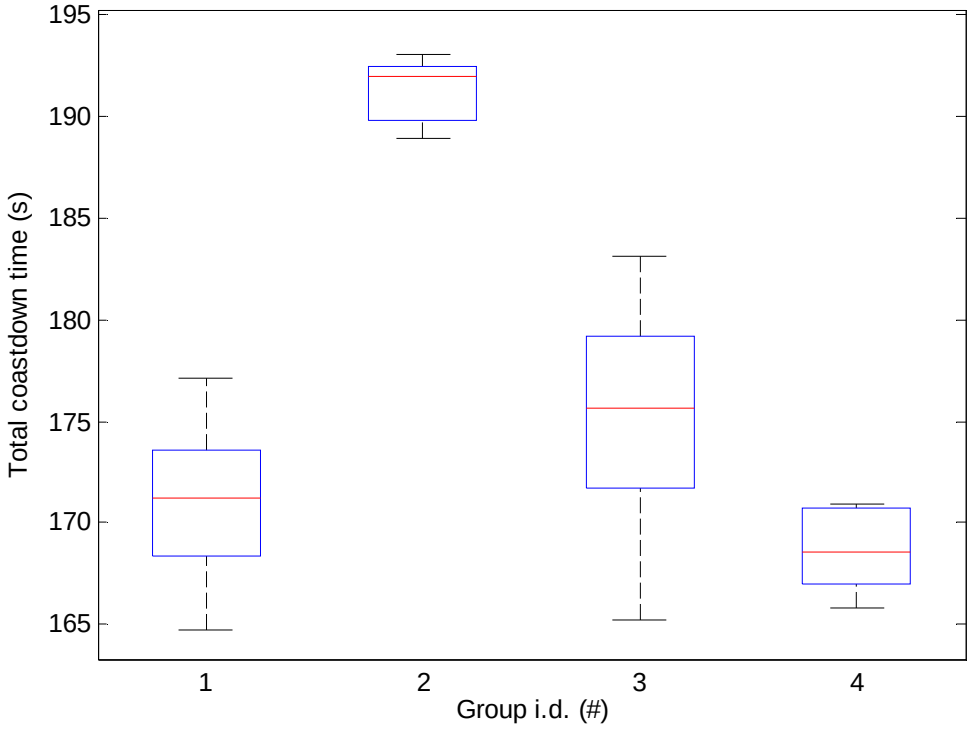

Figure 9-6: Comparison of coastdown time variability prior and post auto coastdown upgrade on the cell 12 dynamometer. Groups 1 - 4 are in order; vehicle A pre upgrade, vehicle A post upgrade, vehicle B pre upgrade and vehicle B post upgrade, respectively.

By examination of Figure 9-6 it can be seen that the precision of the coastdown results has been substantially improved for both vehicles, the IQR has been halved in both cases and the length of the boxplot tails reduced such that they fit within the pre-upgrade IQR for each vehicle. Interestingly the mean has also been substantially changed for each vehicle. Vehicle A has seen an increase in mean total coastdown time of approximately 20 seconds and the vehicle B has seen a reduction in the mean total coastdown time of approximately 10 seconds. The data shown in Figure 9-6 covers only four tests before and after the upgrade for each vehicle, however only a maximum of ten tests could be included at the time of the analysis as no more had been completed on each vehicle post upgrade. The results for ten tests are not substantially different and still show a mean shift

for both vehicles, although the mean shift for vehicle B is reduced slightly. These mean shifts do bring the results into question slightly, particularly for vehicle A were the shift was approximately 12%. The mean shift for vehicle B was only approximately 4%, which is much smaller but still significant to the coastdown time. Whether these changes are significant in CO_2 emissions it is hard to say. With the limited number of channels that are logged in a standard vehicle tests from which these are taken it is impossible to ascertain if another noise factor is contributing to the mean shift. The mean shift for vehicle A was

When completing a coastdown test it is normal to carry out a number of runs and take the average data forward for verification or iteration of the dynamometer road load. Typically in both commercial and academic settings anywhere between three and five runs are completed. Within a commercial setting this is not ideal because of the time taken to complete the runs and hence there is a desire to keep the number of runs to a minimum. Ideally vehicles would be stable across the three runs since the coastdown tests are always performed post-test so the vehicle should be relatively thermally stable. However experience shows that this is often not the case. To quantify this a large number of coastdown test results were collated from vehicles tested within the commercial laboratory. In total data from 1376 coastdown tests were used, 1170 were a vehicle with manual transmission was tested and 179 where a vehicle with automatic transmission was tested. These data sets included all types of vehicle from B through to C car to light commercials, therefore the absolute total coastdown times are very different within this data set. To enable the results to be compared on a like for like basis it was assumed that the average result for the first three runs was the correct result and the error to this value was calculated for each of the runs. The results are shown in Figure 9-7.

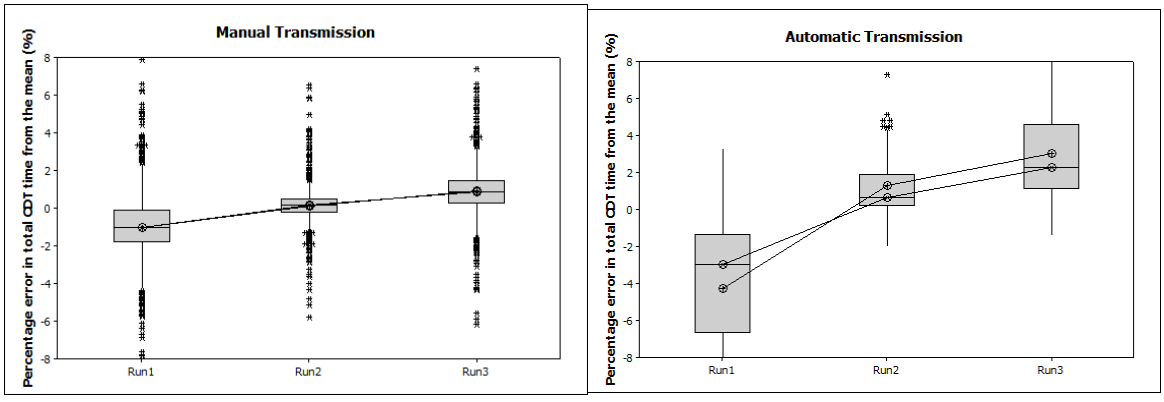

Figure 9-7: Boxplots of the error for each coastdown test run compared to the average result for a large number of manual and automatic transmission vehicles tested in the commercial laboratory.

By examination of Figure 9-7, there is a surprising difference between the total time results for the three runs. On average there is a clear trend that the total coastdown time increases with run number for a coastdown test. This suggests that the vehicle and or also

the dynamometer are not stable during a typical coastdown test. For vehicles with a manual transmission the error for each of the runs one, two and three to the mean is -1.04, 0.13 and 0.91% respectively. For the vehicle with an automatic transmission, these figures are much larger; -4.30, 1.29 and 3.00% respectively. An ANOVA analysis shows that these differences are statistically significant at 95% confidence. This suggests that automatic vehicles are much less stable than manual vehicles. The vehicles for which the data was collected include both production specification and prototype vehicles. There is a commonly held belief that the vehicle losses within a prototype vehicle are much less stable than production vehicles. Data from one of the production quality check vehicles would seem to support this. The results from this vehicle show that there is no statistically significant difference between runs 1, 2 and 3 for a pool of 64 tests.

As was mentioned in the previous section the coastdown test is the current industry standard benchmark for validating dynamometer road loads. However there are many factors that can affect the coastdown results and it is clear that there are sources of inaccuracy and imprecision that do affect the coastdown result but do not directly affect the CO_2 emissions from a corresponding emissions test. This causes difficulties when using coastdown results for test validation since it is entirely conceivable that an outlying coastdown result from a vehicle might have absolutely no correlation with what happened during the preceding emissions test. For example the coastdown stabilisation time is likely to affect the time recorded from the subsequent coastdown test. A long stabilisation time is likely to put more heat into the vehicle tyres, unless they are in thermal equilibrium with the surroundings and cause a change in rolling resistance. This will affect the recorded time but will have no impact of the CO_2 emissions recorded from a TA test unless the road load is iterated off the coastdown results.

An important question is how suitable is the coastdown test at determining if the forces applied during a test are accurate. In other words is the coastdown condition actually equivalent to any operating points during an emissions test. To answer this question it is first necessary to understand any differences between the operation of the dynamometer during a coastdown event and during a drive cycle.

During a drive cycle, when the vehicle is at rest there is theoretically only the F0 component of the dynamometer road load force acting on the dynamometer rollers, since all other terms in the road load equation are speed dependant, see Equation 2-11. In reality the dynamometer is often not able to apply this force statically without there being a resulting motion of the vehicle wheels, as such some dynamometer controllers apply a holding torque around zero speed. The details of this are unpublished since they are the intellectual property of each dynamometer manufacturer. As the vehicle starts to move the

inertia force starts to play a part. The base inertia of the dynamometer will always be present and unless acted upon by an external force will maintain the speed of the vehicle assuming its mass is exactly equal to that of the rollers. In reality this is unlikely and instead the dynamometer motor/s must apply a force to account for the difference between the base machine inertia and the test vehicle inertia. The direction and magnitude of this force will depend on whether the test vehicle has an inertia that is greater or smaller than the dynamometer, whether the dynamometer is accelerating or decelerating and therefore also on the balance of these. For example if the inertia of the test vehicle is only slightly larger than the base inertia and the dynamometer acceleration is high, the overall resistive force applied by the motor/s will be increased. In addition to the inertia, the dynamometer must also simulate the dyno road load forces such as the aerodynamic drag and tyre losses which are governed by Equation 2-11. If the vehicle is in contact with the rollers but not driving the road load forces are likely to be dominant since these are the only external forces on the vehicle acting to change the speed of the vehicle driven wheels. This is the mode of operation of the chassis dynamometer and vehicle during a coastdown test. However during a drive cycle when the vehicle is in gear and the powertrain is applying force to the rollers this is the dominating force in determining the speed of the rollers. To investigate this phenomenon data was taken from a variety of sources including the University of Bath chassis dynamometer and the dynamometers within the commercial laboratory. The data was used to calculate, knowing the base inertia of the dynamometers, the inertia and road load components of motor force that are applied to a vehicle during drive cycle and coastdown tests.

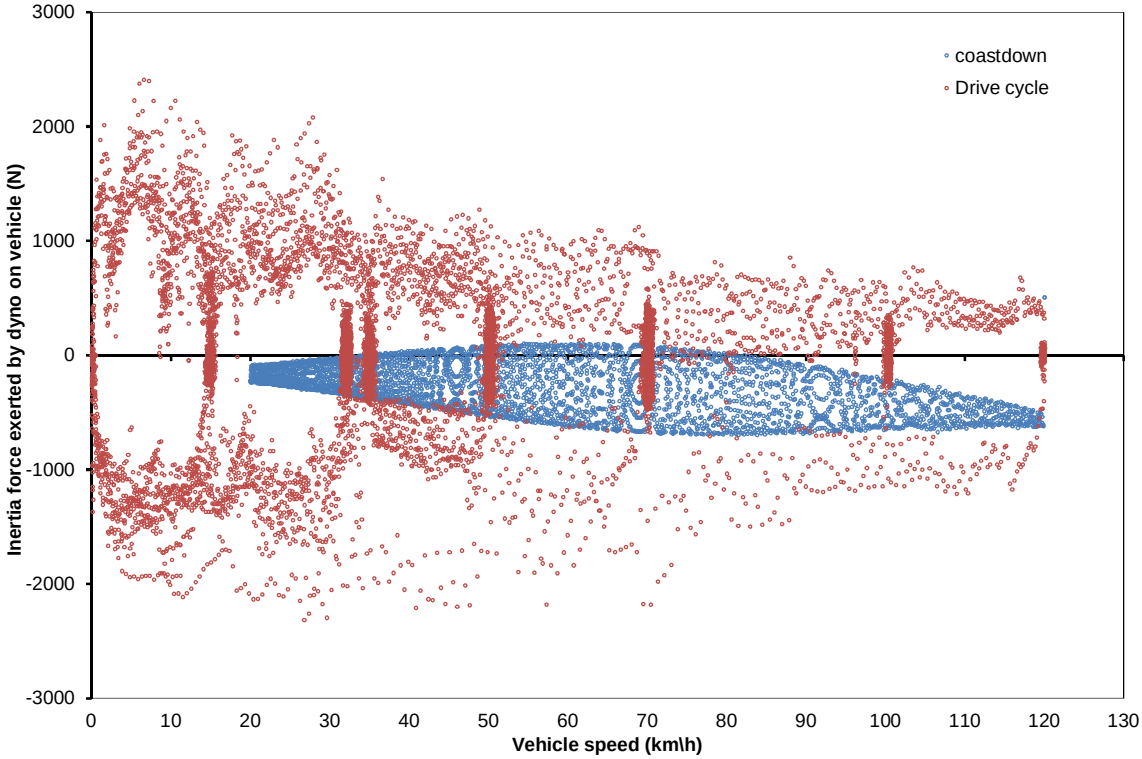

Figure 9-8: Calculated inertia component of force applied by the dynamometer motor to the vehicle during a NEDC test and a coastdown test for a C-car tested on the University of Bath chassis dynamometer. Data collected at 10Hz.

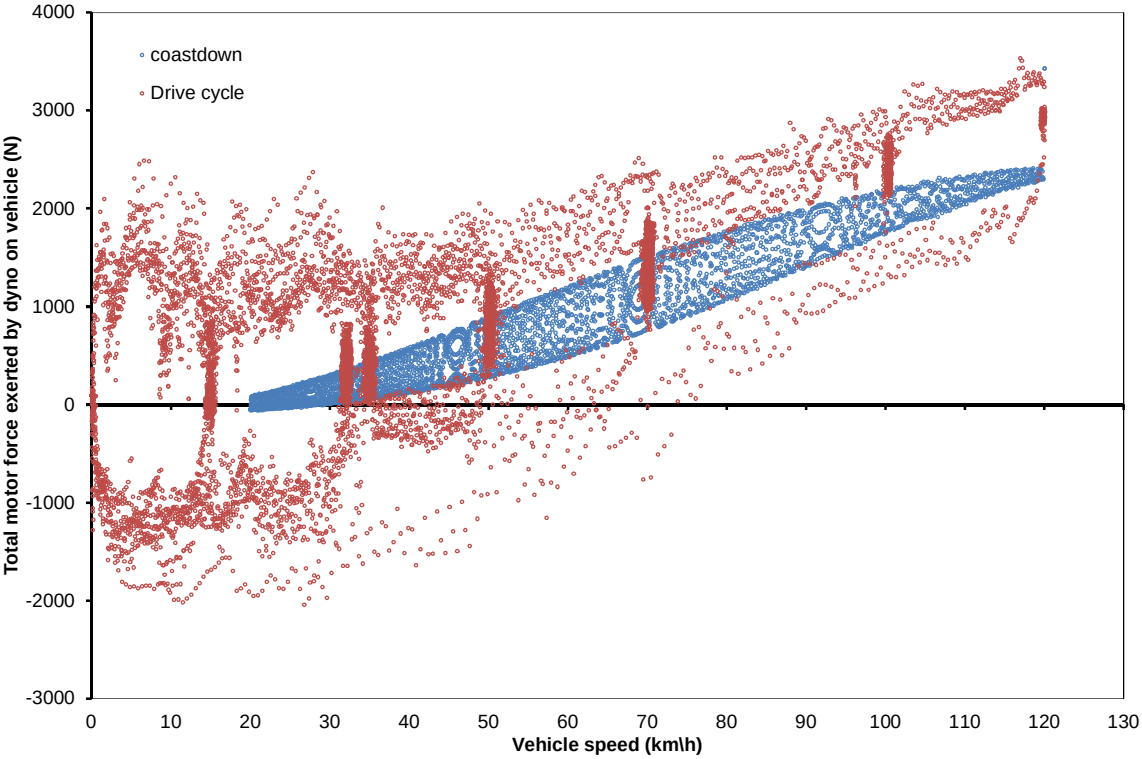

Figure 9-9: Calculated total motor force, including inertia and dynamometer road load components, applied by the dynamometer motor to the vehicle during a NEDC test and a coastdown test for a C-car tested on the University of Bath chassis dynamometer. Data collected at 10Hz.

Figure 9-8 and Figure 9-9 show the results calculated for a C-car that was tested on the University of Bath chassis dynamometer. The pattern of repeated vertical blocks in the drive cycle data is from the cruise conditions in the NEDC. During cruise conditions the acceleration is zero and hence the calculated force clusters around the cruise speeds. The regions with high noise between the cruise points represent the parts of the cycle where the vehicle is being driven and is accelerating or decelerating. If the vehicle is not start stop equipped the CO_2 emissions are generated in all portions of the cycle, with the only exception being the deceleration events in the bottom half of the plot due to deceleration fuel shut off. Figure 9-8 shows that, in agreement with theory, the inertia forces during a coastdown are much lower than they are during the drive cycle. For this vehicle the test mass was very close to the base inertia of the dynamometer and therefore the total inertia simulation force was centred approximately around zero. Figure 9-9 shows that when the dynamometer road load forces are added in the total applied force by the motor is still less than it is during the driving portions of the test. Generally speaking the data in both plots is quite noisy, this is due to noise on the speed and acceleration signals which is an issue particular to that dynamometer at the time of the experiments and should not distract from any conclusions drawn from the other patterns in the data. In summary both Figure 9-8 and Figure 9-9 highlight that the coastdown test is really verifying a condition of operation which is not repeated during the emissions test. However given that the applied motor force is dependent on the difference between the base and vehicle inertias an alternative, lighter vehicle was also analysed. The results are shown in Figure 9-10 and Figure 9-11.

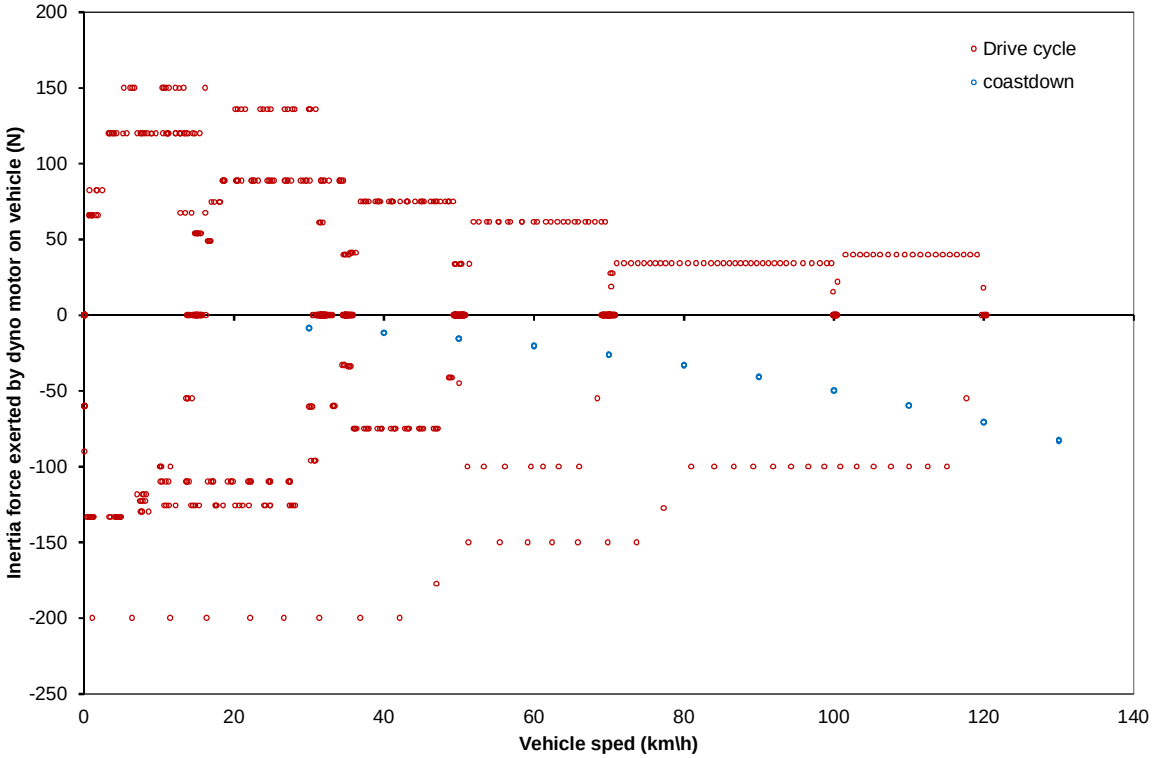

Figure 9-10: Calculated inertia component of force applied by the dynamometer motor to the vehicle during a NEDC test and a coastdown test for vehicle A tested on the cell 12 chassis dynamometer. Data collected at 1Hz.

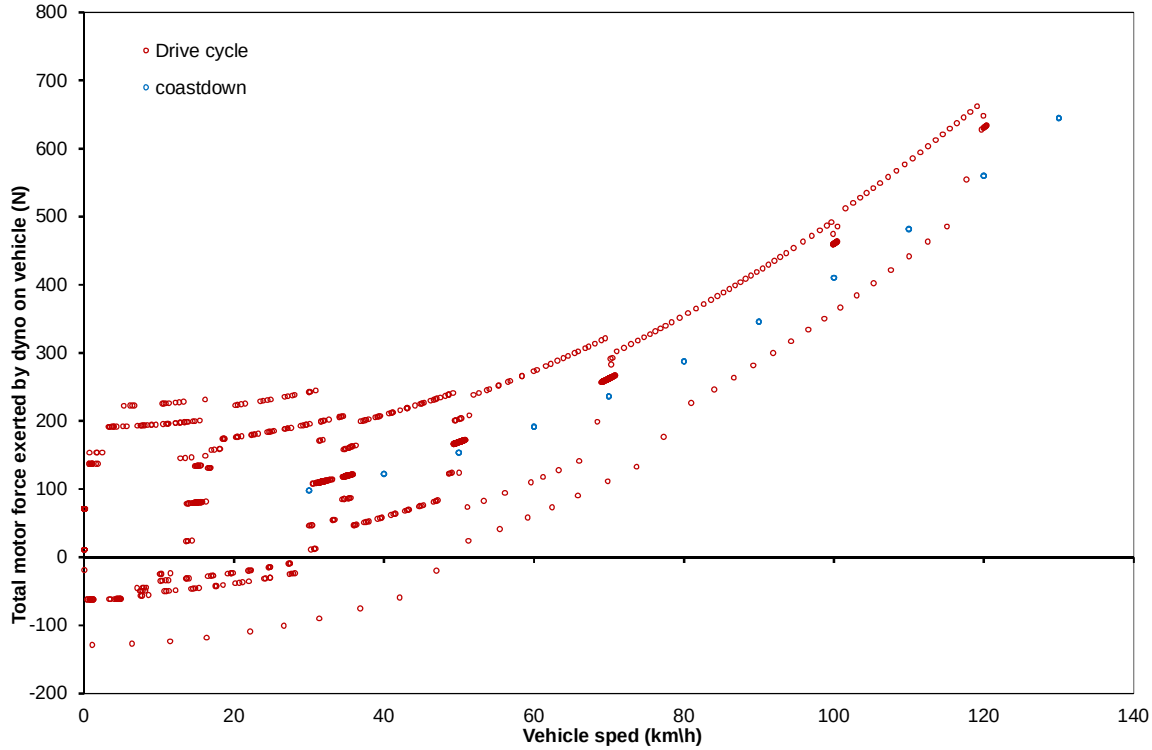

Figure 9-11: Calculated total motor force, including inertia and dynamometer road load components, applied by the dynamometer motor to the vehicle during a NEDC test and a coastdown test for a vehicle A tested on the cell 12 chassis dynamometer. Data collected at 1Hz.

Figure 9-10 and Figure 9-11 show the same patterns observed in Figure 9-8 and Figure 9-9 although there is a lot less noise evident in the data. The reduced noise is partially

due to a reduction in logging frequency from 10Hz to 1Hz and partially due to there not being an issue with the raw speed signal for Figure 9-10 and Figure 9-11. In Figure 9-10 the coastdown forces are not coincident with either the cruise or driving forces seen during the NEDC test. When the dynamometer road load force is included, as shown in Figure 9-11 this holds true for higher speeds but at lower speeds the applied force during the coastdown is nearly coincident to what appears to be a cruise force during the drive cycle.

In summary the coastdown test is a useful tool for diagnosing dynamometer loading faults but it cannot be the only tool used to check loading on a vehicle during a drive cycle since the magnitude of applied force is vastly different during driving conditions and coastdown conditions. The reason for this discrepancy is that there is no external driving force applied to the dynamometer during a coastdown and hence coastdown tests are dominated by the dynamometer road load force only whereas drive cycle tests are dominated by the inertia force.

9.7. The importance of dynamometer road load on CO_2 emissions

So far in this chapter it has been shown that coastdown tests are dominated by dynamometer road load forces whilst drive cycle tests require accurate generation of both dynamometer road load and inertia forces, particularly if the cycle is highly transient. The split of inertia and dynamometer road load forces between drive cycles and coastdown tests have been discussed but in this section of the chapter the link between these forces and the CO_2 emissions will be investigated. The end goal of a TA style emissions test is to ensure that the CO_2 emissions are accurate to the driving conditions during the test, however in an effort to achieve this one question posed is: *what forces are most dominant during an NEDC and are there certain parts of the cycle which are more important in terms of* CO_2 *emissions? Given the increased variability in the coastdown test process as the speed decreases can the final speed gates be discounted if only a very small proportion of the* CO_2 *emissions are produced at these speeds?* These questions will be answered in this section.

By examination of Figure 1-1 it is evident that the NEDC is composed of a mixture of acceleration, cruise, deceleration and idle events. In order to quantify the relative split of these for a cross section of modern vehicles the cycle was split into its modes and the proportion of the total cycle power was calculated for four vehicles tested within the commercial laboratory. The results are shown in Figure 9-12.

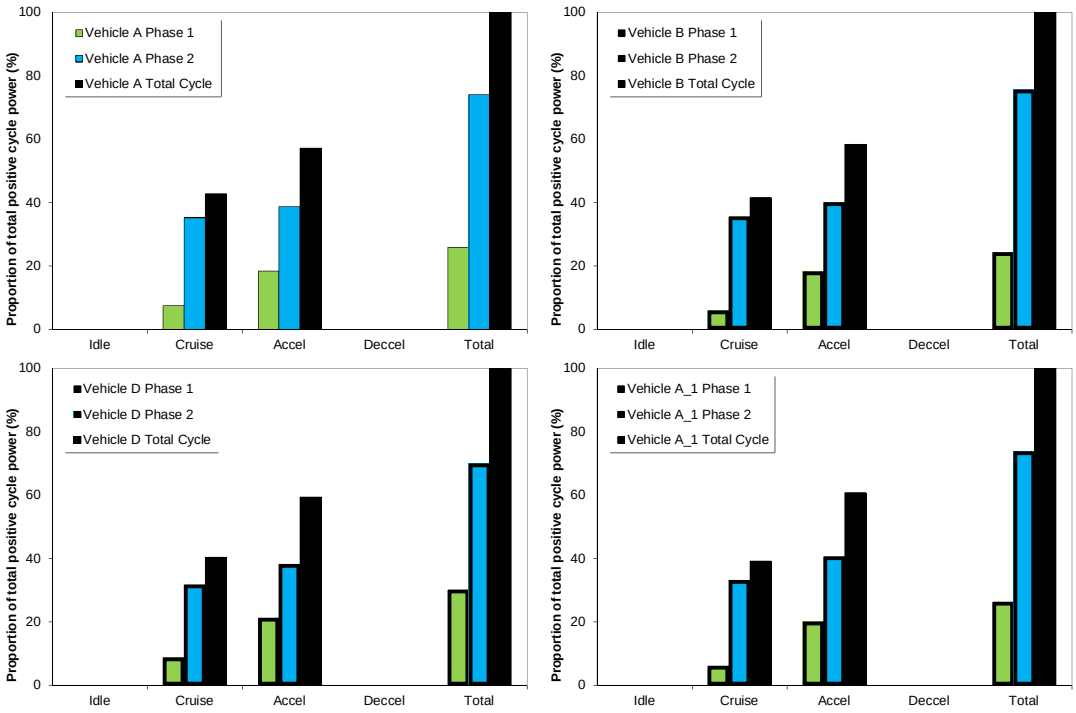

Figure 9-12: Proportion of total positive cycle power by driving mode and cycle phase for four vehicles tested over the NEDC. Vehicle A_1 is a high fuel economy version of vehicle A.

Figure 9-12 shows that the highest proportion of positive cycle power can be attributed to acceleration events, for both phases of the cycle and for the cycle as a whole. The highest proportion of cycle power during these acceleration events occurs in phase 2 of the test, where nearly double the percentage of cycle power occurs compared to phase 1. Of the cruise events, again phase 2 has the highest proportion of the cycle power, interestingly the proportion of total cycle cruise power occurring in phase 2 is approximately four times the percentage that which occurs in phase 1. Overall phase 2 contains over double the percentage of total cycle power that phase 1 does, so in terms of cycle power, phase 2 is much more important than phase 1. Interestingly there is no difference in these trends across the four vehicles, despite these vehicles having very different dynamometer road loads and inertias.

Given the relative differences in the inertia and dynamometer road load forces observed between the coastdown test and the NEDC drive cycle, the split of these force components was plotted for the NEDC for the same four test vehicles as was shown in Figure 9-12, the results are shown in Figure 9-13.

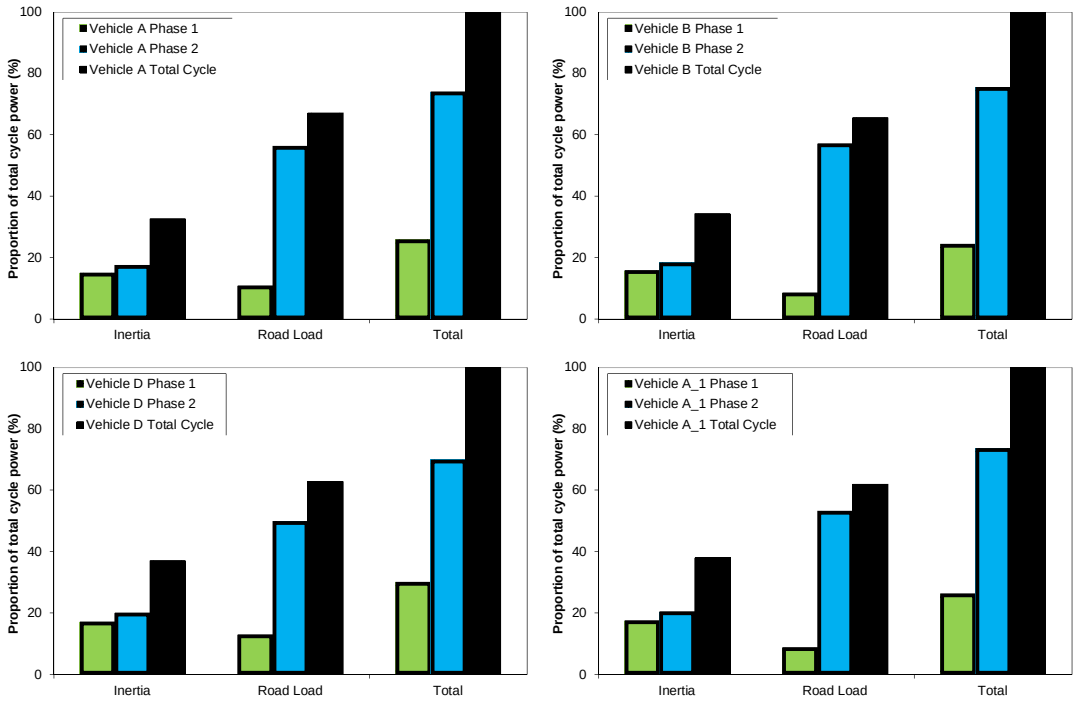

Figure 9-13: Proportion of the total cycle power by inertia and dynamometer road load force component and cycle phase for the four vehicles tested over the NEDC. Vehicle A_1 is a high fuel economy version of vehicle A.

Figure 9-13 shows that during the NEDC the dynamometer road load forces contribute to a higher proportion of the total cycle power than the inertia forces. For all vehicles the proportion of total cycle power attributed to the dynamometer road load component is approximately double that which is attributed to the inertia component. Again there is little difference between the four test vehicles, despite their large difference in inertia and dynamometer road load forces.

The analyses of cycle power are useful because vehicle out CO_2 emissions are produced whenever the engine is running and are produced in proportion to the applied load on the engine. This is clearly demonstrated if the instantaneous fuel power, which is equivalent to the CO_2 emissions, is plotted against the instantaneous cycle power as is shown in Figure 9-14 for vehicle A tested in the commercial laboratory investigated in this research.

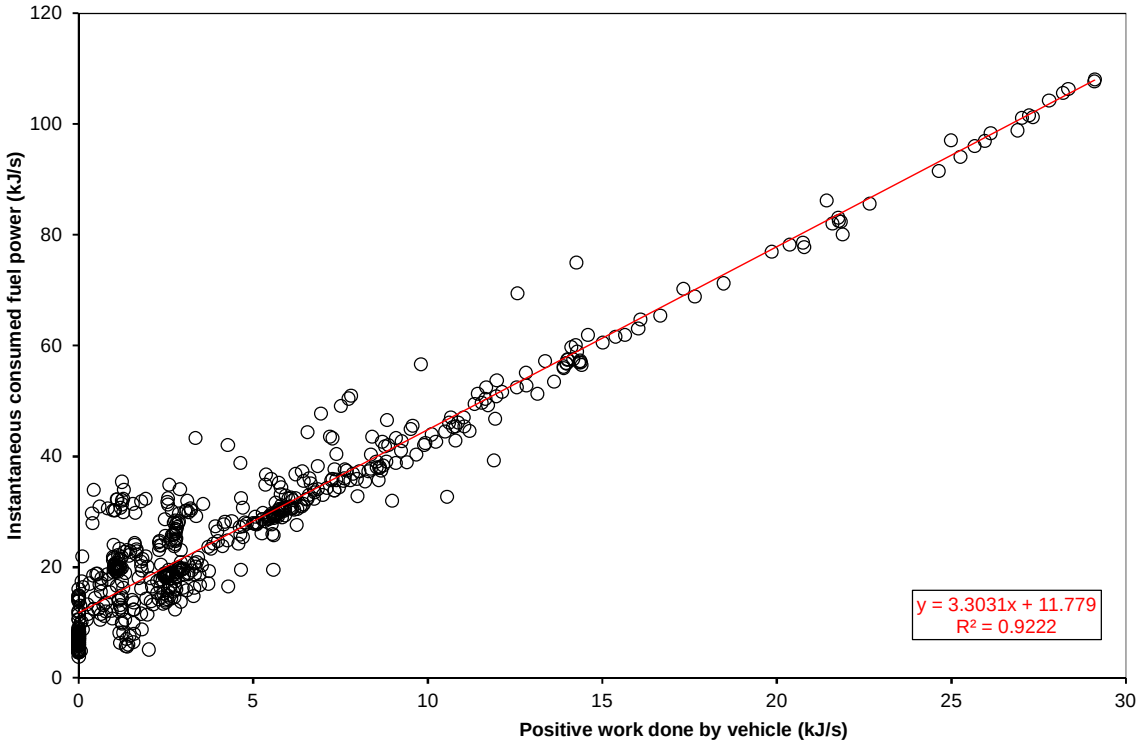

Figure 9-14: Relationship between the positive work done by vehicle A against the dynamometer load and the instantaneous consumed fuel power for the same vehicle tested at in the commercial laboratory.

Figure 9-14 shows that there is an extremely strong correlation, the coefficient of determination being 0.92, between the positive dynamometer road load work done and the instantaneous consumed fuel power; hence CO_2 emissions. However the gradient of the relationship must be vehicle dependant because of the inherent efficiency differences between vehicles. In an effort to quantify the relative importance of the forces applied to a vehicle during a TA style test it is therefore necessary to normalise the CO_2 emissions for a given vehicle. This normalisation was carried out for batch of tests carried out on vehicle A when tested at the commercial laboratory. A batch of tests was used to even out any variability in the measurement of the CO_2 emissions by the CVS system and analysers. The results of this analysis are shown in Figure 9-15.

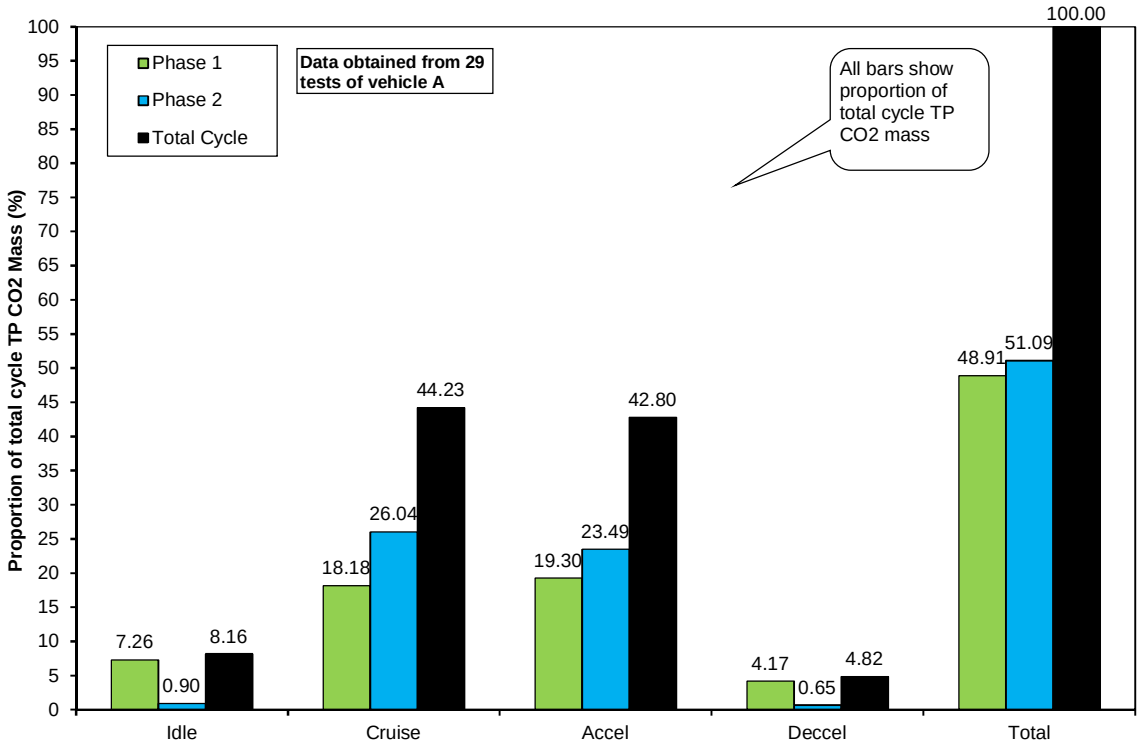

Figure 9-15: Proportion of the total CO_2 mass emissions by mode and phase for 29 tests on vehicle A at the commercial laboratory.

Figure 9-15 shows that in terms of CO_2 emissions there is very little difference between the cruise and acceleration sections of the NEDC with 44 and 43% of the CO_2 mass emissions respectively occurring in each. By phase there is also very little difference, with 49 and 51% of the CO_2 mass emitted during phase 1 and phase 2 respectively. According to the results of Figure 9-12 and Figure 9-13 the acceleration events and phase 2 should have resulted in a much greater proportion of CO_2 emissions when compared with cruise events and phase 1 respectively. However this is not reflected in the CO_2 mass emission results. The reason for this difference by phase is due to the long periods of idling and deceleration that occur in phase 1. During these periods there is no positive cycle power, however CO_2 emissions are still generated (unless the vehicle is stop start equipped). If the CO_2 emissions from the idle and deceleration events are subtracted from their corresponding phase totals, the resulting values become 37.5 and 49.5% for phase 1 and 2 respectively. This is closer to the results obtained in Figure 9-12 and Figure 9-13 but still not an exact match. The reasons for this are unclear from this analysis. Therefore in an effort to understand these phenomena the CO_2 mass emissions were summed for each mode of the NEDC and are present for the same 29 tests of vehicle A in Figure 9-16.

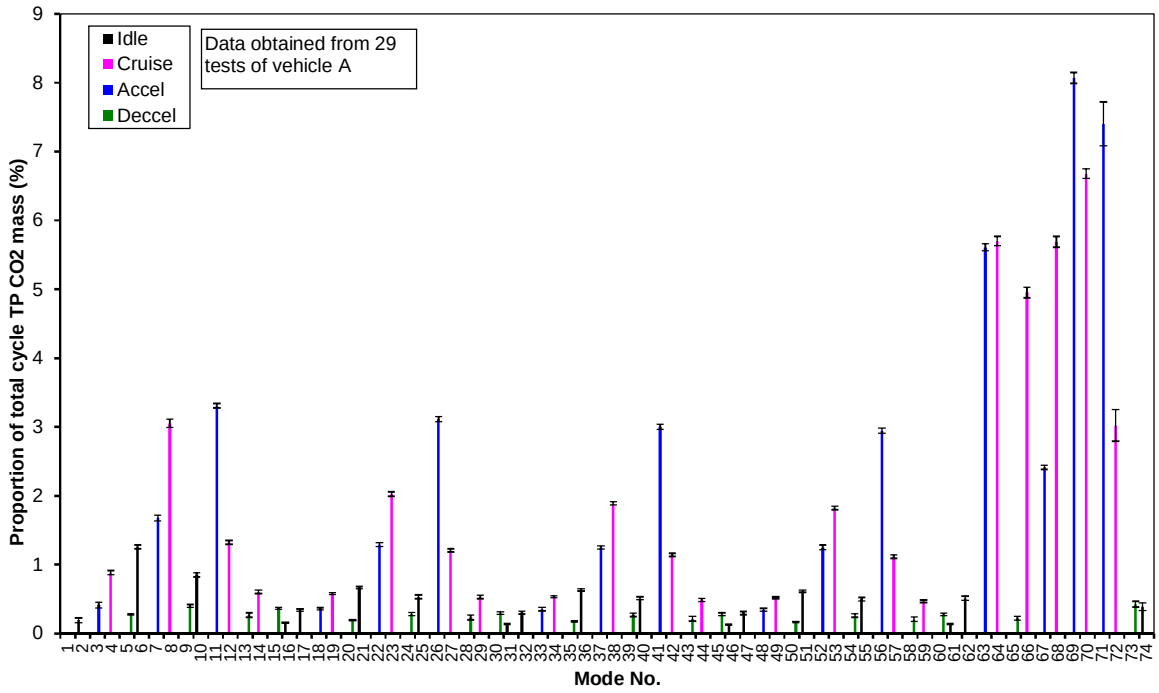

Figure 9-16: Proportion of total cycle CO_2 mass emissions for each mode of the NEDC averaged over 29 tests of vehicle A tested at the commercial laboratory. The error bars show the 95% confidence intervals based on the standard error of the mean.

Figure 9-16 shows that there are several key driving modes in phase 1 which appear to be contributing to the fact that the total phase 1 CO_2 emissions are higher than expected. These are the acceleration modes, 11, 26, 41 and 56. This must be because on average this vehicle was driven more aggressively during these phase 1 acceleration events than it was during the phase 2 acceleration events. With a further round of experimentation and data analysis for a different vehicle it could not be determined if this pattern was vehicle specific or more generic but it seems likely to be a case of special cause variability effecting either this vehicle or this batch of 29 tests.

In summary to the questions posed at the start of thesis section; the dominant forces during a NEDC test are the acceleration modes and phase 2 of the cycle. However, despite the excellent correlation between CO_2 emissions and road load force during driving events, when the NEDC is analysed on a CO_2 basis it appears that phase 1 and 2 are of almost equal importance due to the idling modes during phase 1. Similarly the split between cruise and acceleration events is much less clear.

9.8. Six-Sigma Process Control and the Dynamometer Dashboard

The DPEQAP, which was introduced in the literature review, see section 2.4, has defined several procedures and a roadmap see Figure 2-15, for ensuring that a chassis dynamometer is fit to test. As has been shown in this chapter, these acceptance criteria serve as a useful minimum standard that must be achieved for any emissions chassis dynamometer. In many cases these standards can be exceeded by modern chassis dynamometers. For the losses and inertia calibrations, the results themselves in isolation are fairly meaningless; an operator is unlikely to know if the resulting coefficients from a loss force calibration are correct or an outlier without a history of results to refer to, even then the coefficients alone could be hard to interpret. This is one way in which SPC techniques are useful to record and present a history of results, highlighting when a result is unusual, i.e. special cause. Using these ideas the author of this thesis developed and pioneered the 'Dynamometer Dashboard' within the commercial laboratory studied in this research. This is a tool based in the Microsoft Excel programme and automatically reads data from the laboratory's chassis dynamometers, processes this data and displays the results in an SPC based format. The initial idea for the Dynamometer Dashboard was to create a one page screen where a traffic light system could be used to show the live status, in terms of quality, of each dynamometer within the laboratory. This idea was based on screens that are typically found within manufacturing plants or vehicle assembly lines, where the status of the entire line can be easily seen by all staff within the facility.

The first step in the design of the Dynamometer Dashboard was to create a front screen format and decide on what status indicators would be used for the front screen. A simple format was decided upon, where by the dynamometer or test cell would be listed on the left and various status indicators displayed within each row to the right. The choice of the categories for the status indicators was based upon the procedures that are identified within the DPEQAP and upon what raw data was available to use from the laboratory dynamometers. Additional categories that were desirable but for which no data existed yet were added to allow for future expansion, but were initially greyed out. The categories that were decided upon were Servicing, Fault log, Load cell calibration, Inertia calibration, Losses calibration, Unloaded coastdown and the Tractive force monitor. Not all the dynamometers within the laboratory save their results to the dynamometer control PC hard drive, allowing for polling from the network and copying to the Dynamometer Dashboard. Those dynamometers not yet equipped with this functionality were also greyed out. Of the dynamometers which do save results, these are typically saved into a .csv format file. In addition on the specific dynamometers in this laboratory all command and fault messages between the control PC and real time controller were saved to a Microsoft Access database file at regular intervals. The same Access database also

contained the load cell calibrations. If the tractive force monitor flagged an issue, this would also be saved to the Access database file. The paper records of the servicing and load cell calibrations for the dynamometers were, under an existing process, manually transcribed to excel files which were saved onto a shared server drive. Some work was required to configure the regular copying of these data files from the dynamometer control PC's to the server, thereby allowing the Dynamometer Dashboard to access the data. The server was configured to check for any new data on the test cell control PC's every 15 minutes and copy the relevant files across.

The result of selecting these criteria for the service indicators was a 16 by 7 matrix representing all the criteria and all the dynamometers or test cells within the laboratory, see Figure 9-17. Initially this was configured so that if the results within the category were within specification, the matrix cell would be shaded green and if there was a problem it would be shaded red. In the end this design was not well received because although defects should signify that corrective action is taken it might not be necessary to stop the test cell and therefore suffer the financial penalty of a completely non-functional test cell. Following several phases of iteration a final format was agreed. This format was to display a green cell with the text 'OK' if the checks within that category were satisfactory and then to display a yellow cell with the text 'Warnings' if there were issues with the results from that check on that given dynamometer. If there was a sufficiently large error in the results, according to the SPC criteria, then a red cell with the text 'Defect' would be displayed. In certain test cells it was not possible to copy the necessary raw data across from the dynamometer control PC's to the server because the raw data was not being saved by the control PC. This was the case in the older test cells; cell 9 and cell 14, hence for these test cells the entire row is blacked out on the Dynamometer Dashboard. Other test cells were undergoing upgrades during the creation of the Dynamometer Dashboard and hence the raw data was only available for some of the checks, namely the Servicing and Load cell calibration. These cells for the Inertia calibration, Losses calibration and Unloaded coastdown were therefore greyed out. For all test cells the Fault log and Tractive Force monitor checks were not implemented before the conclusion of this research. In the case of the Fault log this was because of a technical issue in copying the Access database file onto the server and in the case of the Tractive Force monitor was because the results from this were not being saved on any of the dynamometers within the laboratory.

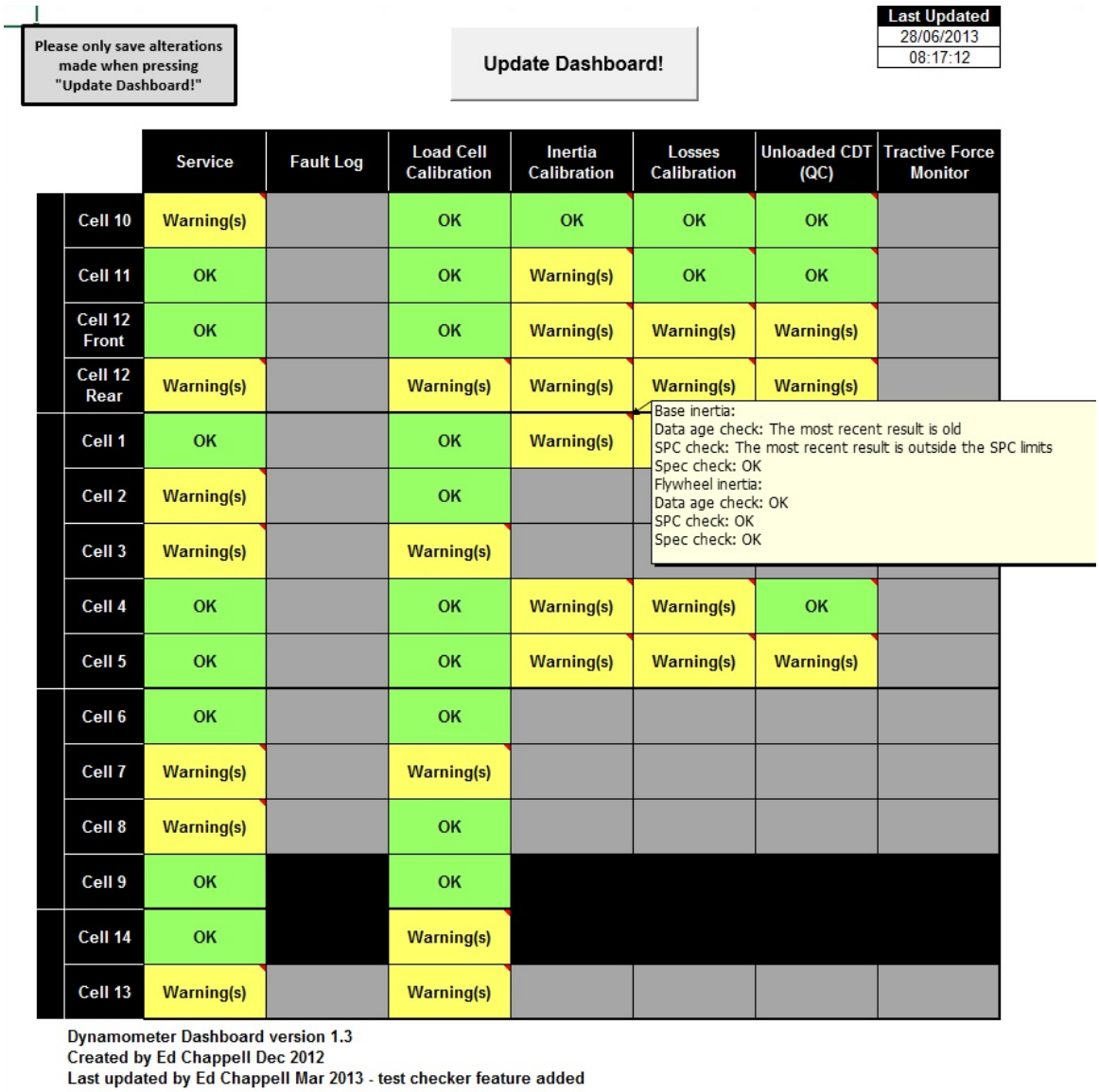

Figure 9-17: Snapshot of the Dynamometer Dashboard front screen, with the cursor hovering over the inertia calibration result for cell 1, showing an example of the warning messages displayed to the user.

At the design phase it was hoped that the Dynamometer Dashboard would be displayed on a monitor within the laboratory so that it could be viewed by all staff, however difficulties were encountered in trying to achieve this, both technically and politically. Instead a local version of the Excel file was saved onto a secure Microsoft SharePoint site and could then be viewed and or downloaded by users at their convenience. The file would require updating so that it displayed the latest status. Therefore a button was added at the top of the screen to '*Update Dashboard*!'. With an updated Dynamometer Dashboard the user could then easily tell if the dynamometer was ready to test by checking if all the criteria had been met and the status indicators were green for all checks on that dynamometer. If there were any warnings or defects the user could hover over the cell with their cursor and a text box would appear with a message about the issue. To determine which colour to highlight the cells within the Dynamometer Dashboard and also

what message should be displayed within the text boxes it had to be decided what checks were required for each criteria.

For some this was simple, in the case of the servicing, the Dynamometer Dashboard was coded simply to check if the last service had been performed within 90 days of the current date. If the service was overdue the cell highlight is changed from green to yellow and the text box message updated to say that the service is overdue. Additionally where the next service had been scheduled a further check was performed to see if the scheduled service was overdue. If so, again the cell colour would be changed to yellow and the text box message updated. Essentially the same set of checks was performed for the load cell calibration criteria with the same resulting colour status and text box messages. A feature was added were the user could click on the title cell for each column of checks and this would open a worksheet tab containing the raw data that was used for the analysis. The page includes both a copy of the manual log for servicing and calibration, along with links to the calibration result files that are saved on the laboratory computer server. In addition, a permanently visible page was added to the Dynamometer Dashboard that showed the service and calibration timelines for each dynamometer within two Excel plots. The page was created so that the timelines for each dynamometer could be easily visualised. More vivid colours were chosen for the calibration timeline as this was perceived to be more critical to achieving high quality results than a slightly late service. The page is shown in Figure 9-18.

Figure 9-18: Dynamometer Dashboard load cell and calibration timeline plots.

For the inertia calibration, Losses calibration and Unloaded coastdown test the checks required to determine the status to be displayed were significantly more complicated.

Firstly a large amount of code was required to automate the functions of the Dynamometer Dashboard when the ‘update’ button was pressed by the user. Firstly code was required to identify, list and sort the available results files from the dynamometers; comparing these with the data already loaded into the Dynamometer Dashboard to determine which files were new. To process the data, again a large amount of work and code had to be written by the author to automate the calculation of the SPC limits and plot the necessary control charts. The amount of visual basic code written by the author is too large to include in this thesis or in an appendix as it amounts to over well over 100 pages when formatted. The limits that were calculated were based on both SPC and specification limits. This is because the laboratory has specification limits, normally based from the DPEQAP and there was a desire to see how the dynamometer results compared to both these limits and SPC limits. Also for users not familiar with SPC techniques the specification limits are often perceived to be easier to interpret.

Using the principles obtained from section 3.3, an X-bar and R-chart was used for the results from the unloaded dynamometer only coastdowns. This is because there are three runs within each test, so the results are easily grouped. I and MR charts had to be used for the results from the inertia and losses calibrations, since there is just one result per test. For the losses tests, the loss force at a fixed speed, 80km\h was chosen and calculated. This was done because the result from the test is a set of coefficients which cannot be processed within the SPC framework. Instead of using the entire history of results from each dynamometer to calculate the SPC limits, a moving window of the thirty most recent tests was used. This is because the entire history of results contains many results which are known outliers, for example from dynamometer commissioning and to write a visual basic code to automatically exclude these outliers would be a difficult task, beyond the scope of this thesis. To calculate the SPC limits a standard template was created across several hidden pages of the Dynamometer Dashboard, this was populated via the visual basic code with the thirty most recent results and embedded formulae within the page were used to calculate the SPC limits which were copied across to a data saving page for use later. These working pages were hidden following the completion of the processing. In fact the Dynamometer Dashboard contains a total of 17 pages or tabs as they are often known. Of which 12 are unhidden and re-hidden each time the dashboard is updated and only 5 are permanently visible. To display the results of the SPC processing a permanently visible page was created with the SPC charts displayed. A drop down box was positioned at the top of this page so that the user could select which

dynamometers results to view. This is shown in detail in Figure 9-19 and Figure 9-20 for the test cell 1.

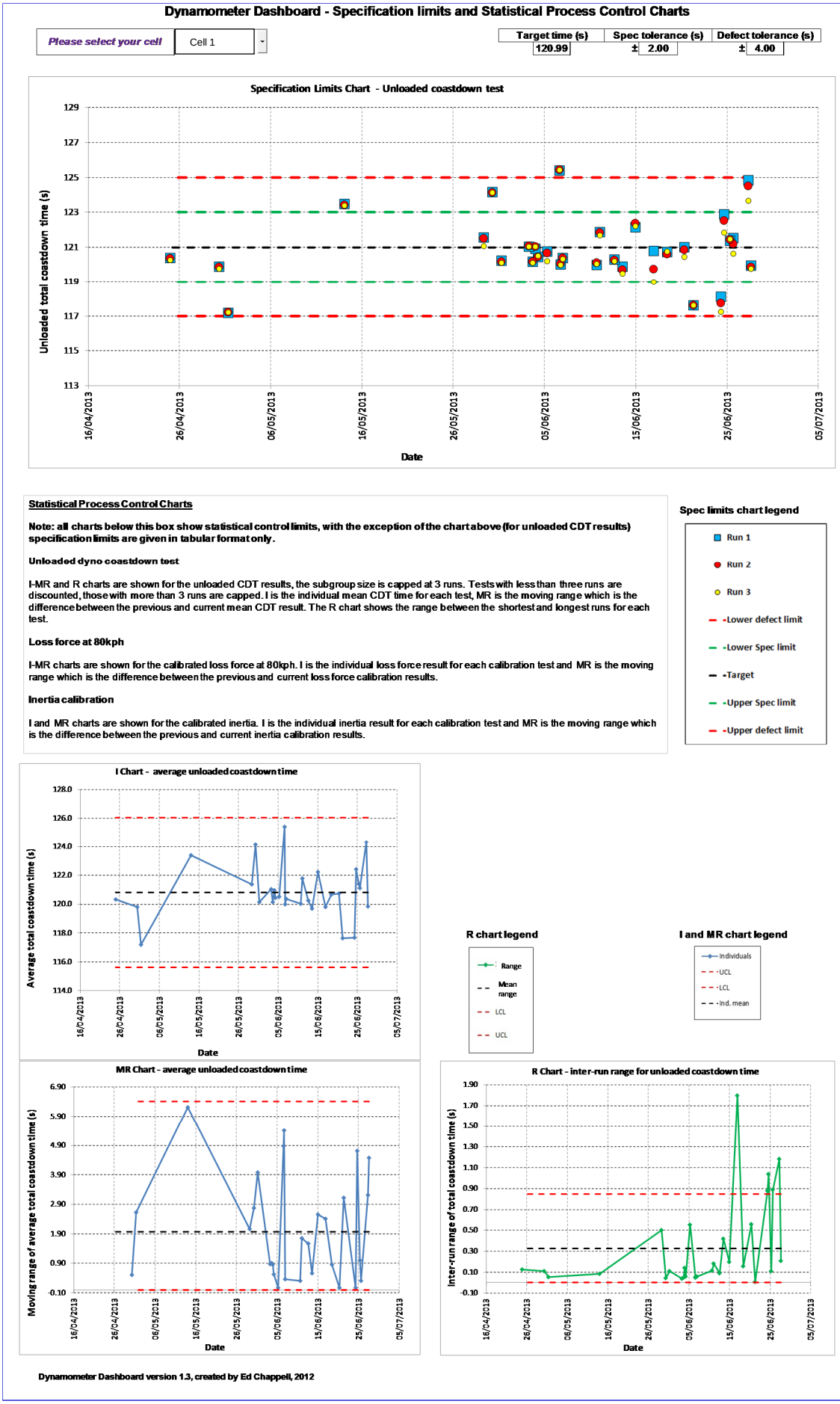

Figure 9-19: Close up print preview style view of the SPC page 1 from the Dynamometer Dashboard.

Figure 9-20: Close up print preview style view of the SPC page 2 from the Dynamometer Dashboard.

The principle behind the design of the SPC plot pages shown in Figure 9-19 and Figure 9-20 was to show the unloaded coastdown and calibration results. The unloaded coastdown results are intended to be an overall dynamometer system check, shown at the top of the page with the largest and most visually striking plot. This plot is a specification limit plot which shows the results of the dynamometer only coastdown check against the specification limits in green and the defect limits in red. Both of these being fixed specification limits based off user experience of the staff within the commercial laboratory and also on desired targets. Since there are three runs for each dynamometer coastdown test, the three runs are plotted using cursors that create a bull's-eye pattern when they align and there is no variability between the runs. A visual check of the plot to see if there is variability between the runs is helpful, since a common and easily identifiable error state occurs if the dynamometer is too cold, whereby the runs get longer as the test progresses. In addition to the specification chart there are also SPC charts for the dynamometer coastdowns in the form of I-MR charts which are also shown on page 1 of the SPC plots, see Figure 9-19, which use the average total coastdown time from the three runs. These serve mainly to assist the visualisation of the data but also allow the user to check the results against the SPC criteria highlighted in Table 3-1 as these checks are automated and hidden within the visual basic code. On page 2 of the SPC plots, see Figure 9-20 there are several I-MR charts which show the individual calibration results for the inertia and losses calibrations. There are two sets of plots because the older dynamometers have two base inertias due to the presence of a clutch controlled flywheel.

To serve as additional clarification for inexperienced users, a page was added to the Dynamometer Dashboard which explains the roadmap to achieving high quality results from chassis dynamometers. This roadmap was based on the information and procedures shown in the DPEQAP [40] and was tailored to the data available to the Dynamometer Dashboard. The roadmap page is shown in Figure 9-21. The roadmap shows how the Dynamometer Dashboard can be used to check each stage within the map with respect to the validation criteria. If all stages are passed then the dynamometer is regarded as ready to test and able to produce high precision and high accuracy results.

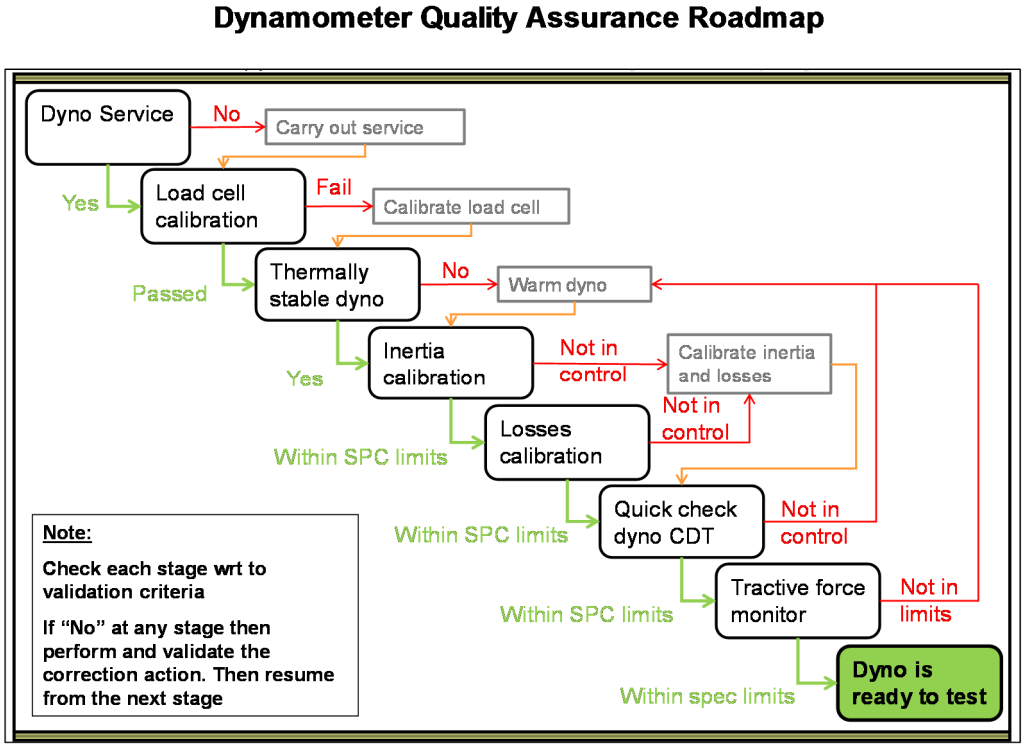

Figure 9-21: Snapshot of the Dynamometer Dashboard quality assurance roadmap page.

A further feature that was included in the second major release of the Dynamometer Dashboard is the test checker which is shown in Figure 9-22. This one page tool allows a user to enter a test number and load data from the dynamometers that shows the history and status of the dynamometer leading up to and immediately prior to that emissions test. This feature was created as experienced users often found themselves having to manually navigate the history of results to understand the variability and status of the dynamometer for a given test where there might have been a suspected dynamometer fault. The same colour highlighting system was used for the dynamometer inertia and loss calibration status messages. In addition the elapsed time between the start of the emissions test and the last dynamometer calibration, for inertia and losses, is calculated by the test checker. If this time falls within the length of a typical shift then the cell is highlighted green, if not a yellow highlight is used with corresponding messages in each case. A shortened version of the Xbar-R chart from the SPC page was also included, although in this case only showing the most recent unloaded coastdown results. Using the loss force fit coefficients from the 20 most recent dynamometer calibrations, a new plot was included at the bottom of the test checker page. This shows the curve for the most recent loss calibration in purple and the previous 20 calibrations in grey. This plot, whilst not conforming to traditional SPC formats, was found to be useful to visualise where a loss calibration might have gone wrong. The theory being that if the purple line, for the most recent calibration, was significantly different in profile or had a substantially different y-axis intercept there was likely to be something wrong with that calibration.

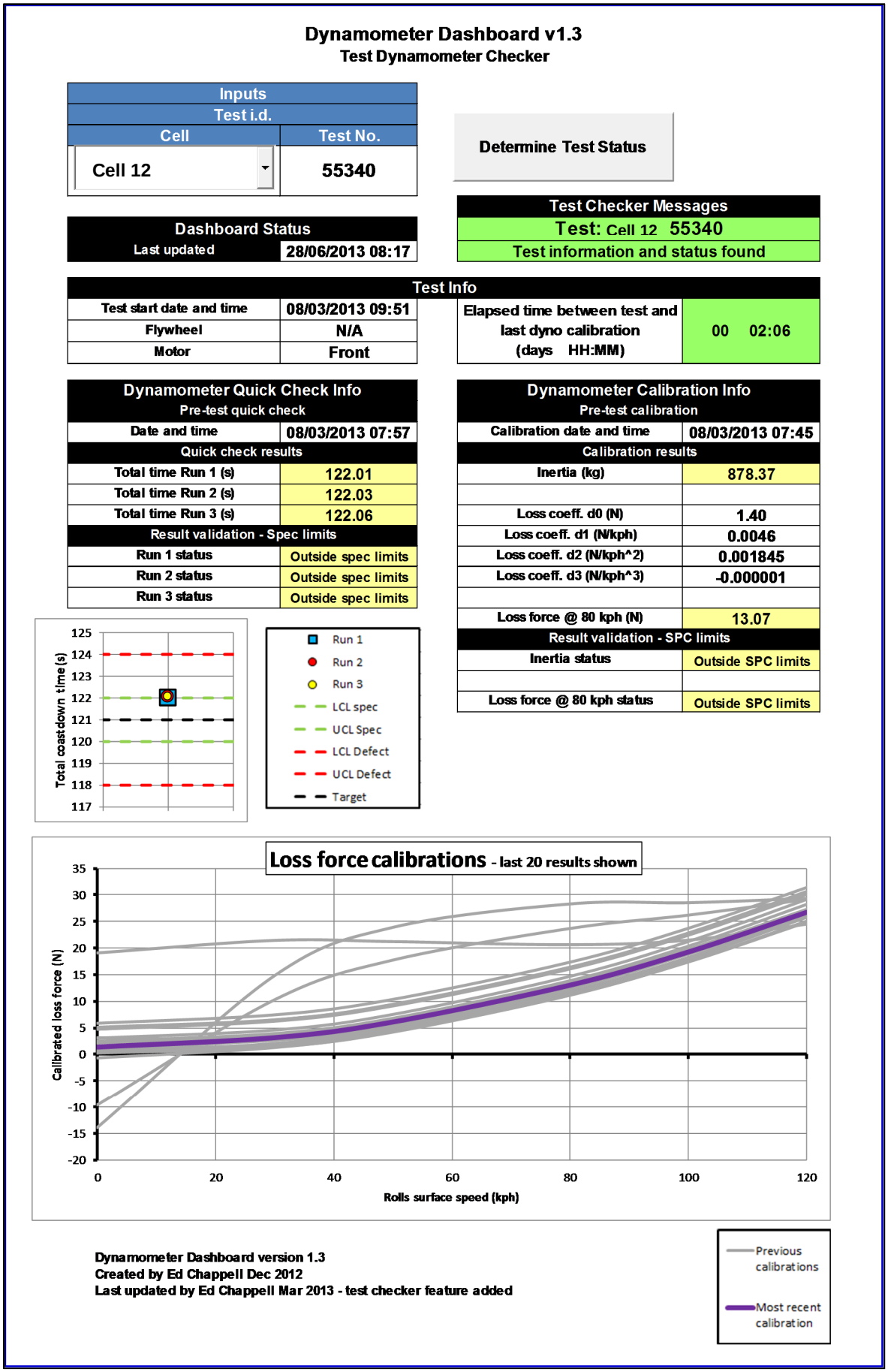

Figure 9-22: Snapshot of the Dynamometer Dashboard test checker page with an example test from Cell 12 loaded to show the typical results that are displayed.

Once the author had got the Dynamometer Dashboard fully written, de-bugged and running within the commercial laboratory it proved a very useful tool for dynamometer quality control which is still in active use. Usage of the Dynamometer Dashboard generally fell into two modes, prevention and post test analysis.

Once the Dynamometer Dashboard was up and running it proved very useful and the following are some examples of typical usage cases where the dynamometer dashboard enabled improved precision within the commercial laboratory. The Dynamometer Dashboard was kept frequently updated and often checked at the start of each shift so that any warnings or defects were investigated before testing started. This is probably the most common usage case. Warnings in these circumstances were typically a result of the operator forgetting to warm and calibrate the dynamometer prior to use. This would result in a warning that the most recent calibration on that dynamometer was out of date and was easily rectified with a gentle reminder to the operator in that test cell. Unsurprisingly instances of these reduced as operators became more aware that they were easily highlighted within the Dynamometer Dashboard. This improved precision by making the dynamometer state more consistent each shift, given that other noise factors were still varying it was not possible to see this within the CO_2 emissions results, however the author reasons that the consistent usage will result in higher precision from the dynamometer at least.

Mechanical issues with the dynamometers were also easily highlighted by the Dynamometer Dashboard, for example a negative result for the loss force fit on cell 11 was seen via the Dynamometer Dashboard and when investigated it was found that there was insufficient hydrostatic lift on the dynamometer bearings causing an offset to the load cell reading. Testing was therefore stopped and the fault rectified. When repaired the precision of the calibration results from cell 11 was noticeably improved. Again the impact of this was not seen in CO_2 emissions, but clearly the improved calibration precision will result in higher precision of the vehicle loading. Although an example was not witnessed by the author, it would also be possible to identify failing bearings via the increase in loss force. Aside from mechanical failures, sometimes operators would run an unloaded coastdown at the start of a shift but not warm and calibrate the dynamometer. This would be obvious if the dynamometer had been idle during the preceding night shift, because the coastdown results would be much shorter than the target time and the three runs would be converging in time towards the target as the dynamometer warmed.

For post-test analysis the test checker tool was most useful. Several examples were seen by the author where a laboratory client had achieved an unusual emissions result from a particular test and had contacted the quality team for an answer. A common

misconception is that these issues were caused by the dynamometer and often, having run the test checker tools, it was clear that the dynamometer was in a good state for the shift where the emissions test was completed. Often in these cases, when other analysis tools were used to investigate the historical coastdown results from that vehicle it was found that the vehicle was not behaving consistently due to a mechanical issue or as was often the case because experimenters were changing calibration variables too frequently on the vehicle without validating baseline conditions. Other times, although less frequently, it was obvious from the test checker that the dynamometer was not in a proper state when the client's test was completed and therefore the loading on the vehicle was not as desired. In this case corrective actions could be taken, if they had not already been prompted by complementary warnings on the dynamometer Dashboard front screen so that when the test was repeated the dynamometer status was within the specification and SPC limits.

However by far the most striking impact of the Dynamometer Dashboard was only apparent when the history of dynamometer unloaded coastdown results were studied. By examining a window of unloaded coastdown test results from all dynamometers for 3 months after the implementation of the Dynamometer Dashboard and for a 3 month window prior to its implementation it was found that the precision of unloaded coastdown results was nearly halved; the coefficient of variation in total coastdown time dropping from 6.64 to 3.97%. The resulting distribution of coastdown times, as shown in Figure 9-23 is narrower and has a higher peak value of frequency.

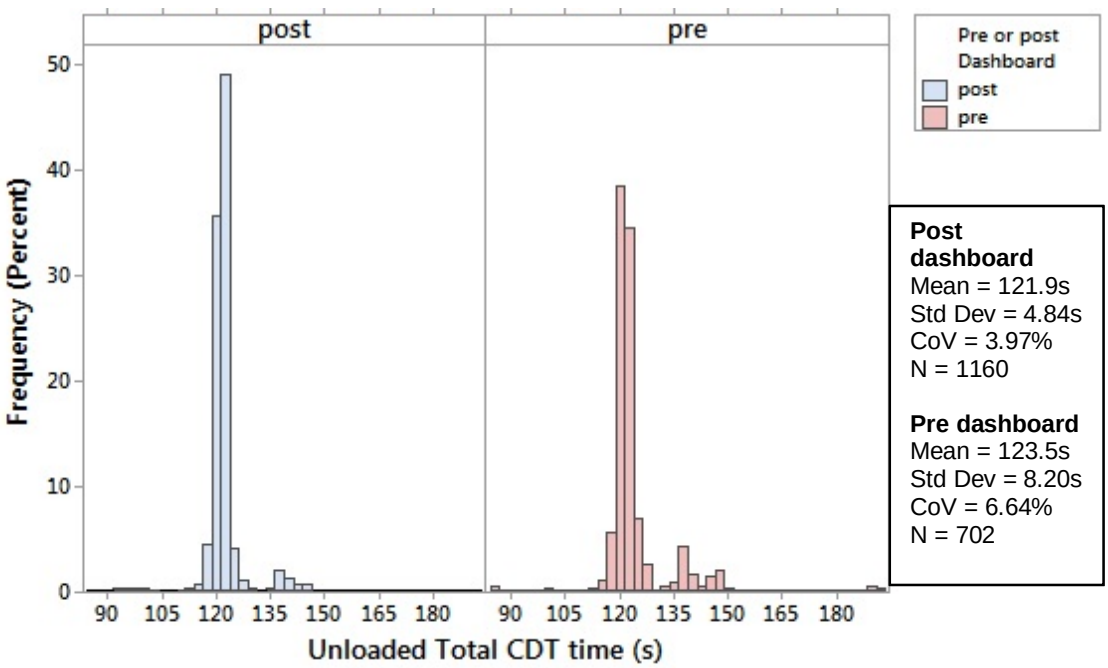

Figure 9-23: Distribution of unloaded (dynamometer only) coastdown times before and after the implementation of the Dynamometer Dashboard within the commercial laboratory.

The significant improvement in precision of unloaded coastdown times really demonstrates the impact of the Dynamometer Dashboard. Since these coastdowns are performed without a vehicle and serve only to validate the status of the dynamometer it was not possible to relate these results back to an improvement in the precision of CO_2 emissions. However the DPEQAP roadmap shows that unloaded coastdown time is a useful metric for determining the quality of the dynamometer and it stands to reason that an improvement in CO_2 emissions would follow if all other factors were controlled at the same time.

9.9. Chapter Summary and Conclusions

In this chapter the primary sources of imprecision from the chassis dynamometers were examined. An automated statistical process control tool was developed for ensuring that the DPEQAP procedures are controlling the dynamometer precision. From this work the following conclusions are drawn:

- The DPEQAP and EPA quality procedures defined a useful benchmark standard for verifying the chassis dynamometer. However to achieve the highest precision it is necessary to go beyond these standards and many manufacturers are now able to offer dynamometers that are capable of achieving such high levels of precision and accuracy. For example a load cell calibration may now only be contributing to a CO_2 error in the region of ±0.0126%.

- Errors from loss calibrations can be minimised by advancements in chassis dynamometer design that reduce the absolute magnitude of the losses. Care is still needed to ensure that the curve fitting algorithm has produced sensible results which can be checked through SPC validation techniques.

- A great deal of attention is required to monitor the procedural usage of the dynamometer to ensure that dynamometers with high frictional losses are adequately warmed prior to operation.

- SPC tools are most useful in the application of monitoring the health and status of dynamometers and it is recommended that these techniques are implemented in any chassis dynamometer laboratory. These tools reduce the number of defective tests thereby improving precision and making financial savings for a commercial laboratory.

- Coastdown testing to validate the load applied by the dynamometer is the industry standard procedure for validating dynamometer load and is useful in this respect, however it must be considered that it does not fully represent the driving modes

during a NEDC test and perhaps even less so for the future WLTP cycle. The coastdown method therefore, effectively only evaluates the dynamometer road load portion of the applied load and does not fully validate the inertia simulation portion of the applied force. This shows that it is important to validate the response time of the chassis dynamometer control system and the results of base inertia calibration via the use of SPC techniques.

- The modern chassis dynamometer is capable of achieving the required precision and accuracy for modern high precision testing. However this can only be achieved when the necessary attention is paid to the procedural usage of the dynamometer and to the calibration of the dynamometer systems.

Chapter 10. Conclusions

10.1. Summary

The research in this thesis has looked at the key sources of noise for imprecision in CO_2 emissions from chassis dynamometer tests, including methods to improve and control these factors culminating in demonstrations of improvements. Chapter 1 has introduced the subject area and outlined the aims and objectives of the work. Chapter 2 reviews the literature in this field and identifies the key sources of imprecision from chassis dynamometer tests. Chapter 3 reviews statistical methods for improving and validating test precision. Chapter 4 looks at the best that can be achieved in current practice and poses a universal methodology for the use of response modelling for post-test verification of noise factor control along with the correction of CO_2 emissions results. Chapter 5 looks at the standard of precision that is typically achieved in a commercial setting, including a data mining study. Chapter 6 begins four chapters that study the most significant noise factors in detail by looking at the vehicle electrical system. Chapter 7 considers driver behaviour, Chapter 8 procedural factors and Chapter 9 the chassis dynamometer. Finally Chapter 10 summarises and draws conclusions from the research.

10.2. Conclusions

The conclusions from the work presented in this thesis are presented against the objectives that were laid out in Chapter 1. The main outcomes are presented in line with the overall aim of the thesis.

1. *"Review the literature relating to sources of imprecision and inaccuracy for chassis dynamometer based vehicle tests. Use existing data to attempt to rank the sources and establish the factors that have the largest impact on variability of* CO_2 *emissions."*

   The primary sources of imprecision in CO_2 emissions that are covered in the literature have been reviewed in five main areas; the vehicle electrical system, driver behaviour, the chassis dynamometer, procedural factors and the emissions measurement system. The key noise factors in the electrical system are the auxiliary loads and battery charging with effects to the CO_2 emissions covering a large possible range from 1 to 50%. The key noise factors for driver behaviour are speed error and gear changing with CO_2 effects of up to 5.5 and 4.5% respectively. There is much scope for further work to classify driver behaviour and to analyse the usefulness of the newly published SAE J2951 drive quality

standard. The noise factors from the chassis dynamometer are comparatively well understood in the literature with sensitivities in the region of 0.65% CO_2 per 1% change in road load. Procedural factors are numerous but are generally recorded to have small individual effects in the region of a few percent. The emissions measurement system is an important area but is not within the scope of this thesis.

2. *"Examine statistical methods for determining confidence in small differences between results and explore the application of regression modelling to chassis dynamometer testing"*

   High statistical confidence in experimental results is best achieved by improving the precision of the measurements which is the key motivator for the research presented in this thesis. Six sigma and process control techniques have shown that for complex multiple input single output systems, such as chassis dynamometer FC tests, precision of the output measurement can only be improved by controlling all the important input factors. An improvement in just one factor is unlikely to show a significant improvement in the output result. It has been demonstrated that statistical process control tools are useful to identify if these key input factors are under control once improvements are implemented.

3. *"Understand the current best practice for high precision chassis dynamometer testing by analysing data recorded from a series of chassis dynamometer emissions tests were the knowledge and recommended tolerances gained from the literature are implemented."*

   The suggested tolerances and controls from the literature and from the study published by Brace et. al. [8] were successfully implemented during a chassis dynamometer based FC trial, achieving the target 0.5% CoV for the FC results and in some cases bettering this to 0.2%. From the use of regression response modelling it was shown that no recorded noise factors varied in such a way that effected the FC results. It was shown that regression response modelling can be universally applied to chassis dynamometer test plans to determine if known factors are adequately controlled. In addition if a known factor does cause a significant effect on fuel consumption this method can be used to correct for the effect of noise factors providing a good fit can be obtained for the response model.

4. *"Understand the standard practice in industry by gathering historical data from a commercial laboratory. Perform a data mining exercise to identify any sources of imprecision that are exposed by this data."*

Historic data from a commercial laboratory was analysed and it was found that the basic level of variability was relatively high, the CoV of total bag CO_2 emissions being approximately 2.5%, some five times higher than was achieved in the high precision study. Very few of the known important noise factors which had a significant effect on the CO_2 emissions were recorded as part of the standard suite of vehicle and emissions logging equipment. Response models were constructed using the available data and although these had a relatively poor level of fit, the coefficient of determination being between 0.432 and 0.802, these did indicate that coastdown time, dynamometer run time status, air humidity and soak time were of some importance. Despite the introduction of additional logging, in the form of ECU DAQ, to achieve the response model with a coefficient of determination of 0,802, there is still approximately 20% of the variability in the CO_2 emissions that remains unexplained and uncontrolled.

5. *"Guided by the findings from the literature perform detailed studies into the most significant sources of imprecision, identifying the root causes of their effects, proposing methods to improve the precision and if possible demonstrating these methods by controlling the factors."*

   From the literature, the most important noise factors were classified as being part of four main groups; the vehicle electrical system, driver behaviour, procedural factors and the chassis dynamometer machine. Studies were therefore conducted in each of these areas and the following conclusions are drawn from each area.

   Vehicle electrical system

   Sources of imprecision from the vehicle electrical system fall into two areas, auxiliary loads and SLI battery charging. An experimental study of auxiliary loads on a relatively simple vehicle found that the largest are from the air conditioning system, HVAC blower, headlamps and heated rear window. By measuring the steady state CO_2 emissions, a linear fit with a gradient of 2.3 kJ/s fuel energy per kJ/s electrical energy was determined between the average change in electrical power from auxiliary loads and the change average modal consumed fuel power. For the test vehicle in question, with no loads switched on, the engine was consuming 120kJ/s fuel energy and with the highest electrical load switched on this was increased to around 700kJ/s. If all electrical auxiliary loads are switched on simultaneously the change in CO_2 emissions is vast. Testing showed a change in the hot test CO_2 emissions of 43% for the test vehicle in question. On a separate test vehicle the effect of charging the SLI battery pre-test on CO_2 emissions was found to be 2.2% at 95% confidence. Charging the battery is also beneficial in

improving the precision of the alternator load during subsequent emissions tests, although this did not translate to the bag CO_2 emissions. A linear fit of the data with a gradient of 3.1 kJ/test fuel energy per kJ/test alternator energy was developed between the change in alternator energy during the test and the change in consumed fuel energy. The difference between the two gradients, which were 2.3 and 3.1 respectively, was due to vehicle technology differences. Battery charging was found to improve the precision and also simultaneously reduce the mean CO_2 emissions, meaning there was little effect on the CoV. All these findings showed that recording the alternator and battery current is essential and that ensuring minimal pre-test vehicle disturbances are important if the SLI battery is not being charged.

Driver behaviour

A study of a relatively simple change to the driver's aid, where by the legal speed tolerances are not displayed reduced the standard deviation of CO_2 emissions by 43.5%. An analysis of driver behaviour metrics showed that SAE J2951 primary metrics, EER, ER along with the supplementary metric, the ASCR, can be insensitive to certain changes in driver behaviour. Instead the SAE 2951 supplementary metric, the RMSSE, along with the newly defined CASE metric and the SAE primary DR metric proved to be more effective tools to understand the driver style differences in the experiment conducted on the driver aid change. The RMSSE and CASE metrics were on average reduced, when the tolerances were not displayed, by 12.8 and 11.1% respectively. These changes were significant when tested at a 95% confidence level. Despite the SAE J2951 standard recommending their metrics as one-number end of test metrics, it was found that useful additional insight can be gleamed from using the metrics as instantaneous tools. Of the two metrics found to be most sensitive to the changes in drive style in this study, which were the RMSSE and CASE; the CASE metric is more indicative as an instantaneous driver feedback tool. This is because the CASE is not unstable at the beginning of the test and is not damped at the end of the test thereby showing more uniform sensitivity with time.

Procedural

Studies of the most significant procedural factors showed that tyre pressures can be relatively easily controlled provided the tyre pressures are correctly set prior to the start of any test sequence. In a commercial environment frequent checking of tyre pressures by multiple operators with multiple gauges is likely to introduce more variability than not checking at all, for a relatively short duration test

sequence. Ambient conditions, such as temperature can be relatively easily controlled providing suitable plant is installed with sufficient power capacity to achieve a temperature tolerance range of 2.5°C which according to the literature would cause a change in CO_2 emissions of less than 0.5%.

Chassis dynamometer

The causes of imprecision from the chassis dynamometer are well understood and documented within the EPA attachment A and DPEQAP procedures. An automated SPC dashboard tool was therefore developed to ensure the important factors are controlled. This was demonstrated to be highly beneficial in a commercial testing lab, resulting in an improvement in the unloaded coastdown precision from 6.64 to 3.97% CoV. The traditional method for validating the road load applied to a vehicle is the coastdown test, however it was shown that this test does not fully represent the driving modes of an NEDC test. The coastdown method effectively only evaluates the dynamometer road load portion of the applied load and does not fully validate the inertia simulation portion of the applied force. This shows that it is important to validate the response time of the chassis dynamometer control system and the results of base inertia calibration via the use of SPC techniques described. By implementing automated coastdown testing the precision of coastdown times was improved by a factor of approximately two.

The aim of this thesis was to identify the sources of imprecision affecting vehicle fuel consumption measurements from chassis dynamometer tests, to understand the fundamental physical mechanisms that cause these factors to be important, to propose and finally if possible demonstrate methods for controlling these sources. The following points summarise the main sources of imprecision and the control methods proposed through this research.

- **Vehicle electrical system,** which can be controlled by:
    - Charging the SLI battery between tests for research work
    - Not using auxiliary devices
    - Installing current measurement devices on the vehicle
- **Driver behaviour,** which can be controlled by:
    - Removing the tolerances from the driver's aid
    - Recording accelerator pedal data
    - Calculating metrics that allow for classification of driver behaviour

- **Procedural,** which can be controlled by:
    - Tyre pressures can be controlled by limiting the number of checks and installing measurement devices
    - Installing plant to control ambient conditions, temperature and pressure, to a high precision
- **Chassis dynamometer,** which can be controlled by:
    - Using modern dynamometers with low parasitic losses
    - Following the DPEQAP procedures
    - Implementing SPC tools to validate dynamometer quality status
    - Critically evaluating the response time of the dynamometer

The impact of the research presented in this thesis is summarised in Figure 10-1 which shows that the precision in the output, namely the CO_2 emissions, has been improved from 2.6 to 0.4% as measured by the coefficient of variation. This is shown in the red and green bars of Figure 10-1. A chassis dynamometer emissions test is a complex system with multiple input factors varying simultaneously. As such individual input factors cannot always be directly correlated to output CO_2 emissions. Figure 10-1 therefore also shows the baseline level of precision in the important noise factors, expressed by the coefficient of variation for a suitable input factor metric, and then the improved precision that has been achieved through the demonstration of the control methods discussed in this thesis. These are shown in the dark and light blue bars on Figure 10-1. These dark and light blue bars shows that substantial improvements in precision have been demonstrated in the fields of driver behaviour and the chassis dynamometer. There is clearly large variability in the vehicle electrical system from the battery charging and auxiliary loads, however only a very small improvement in precision was seen from the battery charging because although the standard deviation of alternator energy was reduced the mean was also reduced at the same time. Further work is needed to measure the improved precision from the implementation of the recommendations from this research regarding electrical auxiliaries and tyre inflation pressure. In addition Figure 10-1 shows via the grey bars, those noise factors that can have a significant effect on the result of individual emissions tests by quantifying the predicted percentage change in CO_2 emissions from maximum perturbation of each factor. Of these factors the numerous ancillary electrical loads have by far the largest potential impact on CO_2 emissions, followed by ambient conditions, pedal busyness, battery charging and dynamometer losses calibrations. With further experiments it would be possible to measure the distribution of these noise factors shown

by the grey bars of Figure 10-1 and therefore replot them as light and dark blue bars with data for the precision of the relevant input metrics, but these data were not available.

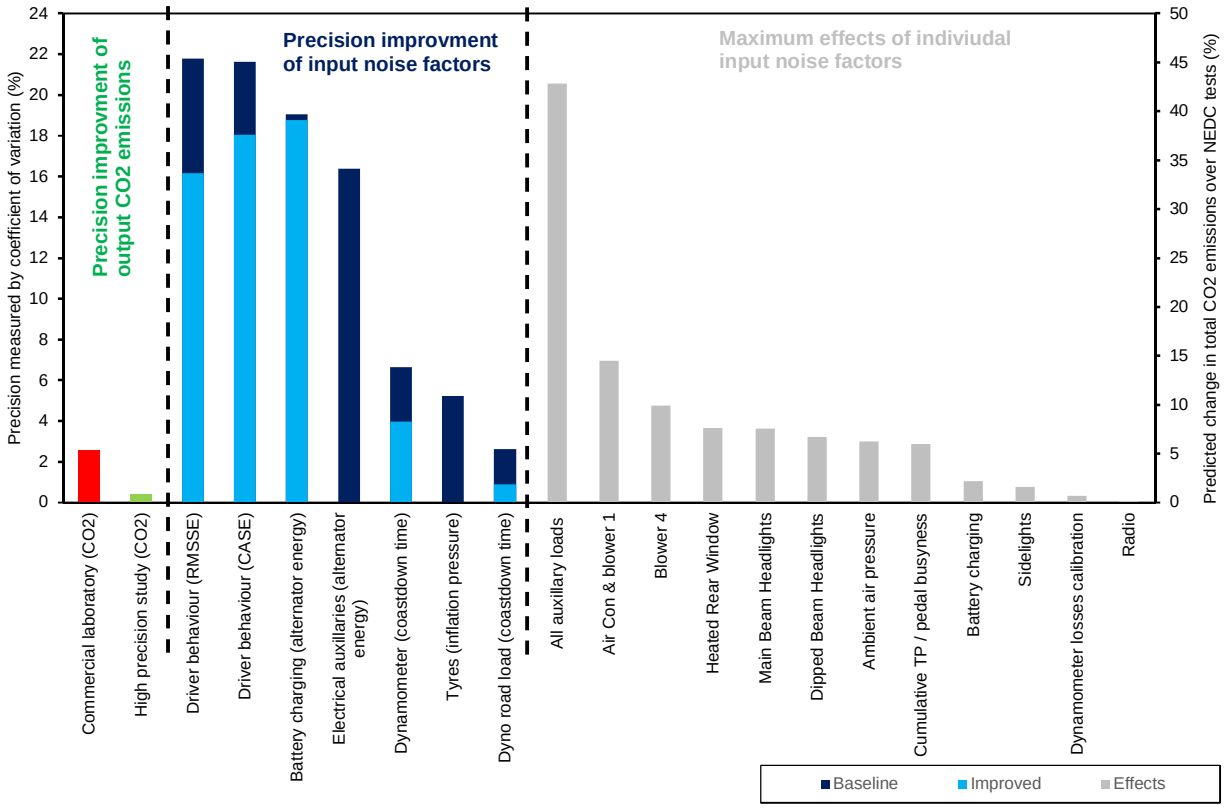

Figure 10-1: Summary of the measured improvements made to the precision and the measured maximum effect of key noise factors made by the author in this thesis. The red bar shows the level of precision of CO2 emissions before the work started and the green bar shows the level of precision of CO2 emissions achieved through this work, both on the primary y-axis. The blue bars show the precision of input factors measured through metrics with the baseline shown in dark blue and the improvement in light blue, both on the primary y-axis. The grey bars show on the secondary y-axis the maximum effect of individual noise factors possible during one emissions test.

Through this research three major contributions have been made to the state of the art. Firstly, from the work on driver behaviour an extension is proposed to the Society of Automotive Engineers J2951 drive quality metric standard to include the a newly developed Cumulative Absolute Speed Error metric and to suggest that metrics are reviewed across the duration of a test to identify differences in driving behaviours during a test that do not cause a change to the end of test result. Secondly, the need to instrument the vehicle and test cell to record variability in the key noise factors has been demonstrated. Thirdly, a universal method has been developed and published from this research, to use response modelling techniques for the validation of test repeatability and the correction of CO_2 emissions.

10.3. Outlook and further work

The research from this thesis has prompted the start of a number of further research programmes and significant research equipment funding for the PVRC at the University of Bath.

Specifically the research from this thesis helped underpin the submission and argue the case for a successful £2 million ESPRC equipment grant, number EP/K040391/1, to upgrade the chassis dynamometer test facility at the University of Bath.

Following the conclusions from this thesis, further research work that could be undertaken is suggested below:

- The noise factors for which a sample of normal variability was not taken in this research could be revisited to enable the full verification of the improvement made in precision through this research.

- The installation of wheel torque transducers on a vehicle would enable the loading on the vehicle to be measured both accurately and instantaneously during an emissions test. The measured torque could be fed into the chassis dynamometer controller and used to adjust the dynamometer speed to achieve the exact theoretically required load at the vehicle wheels. If successful this would alleviate the issue of the coastdown test not being fully representative of the NEDC driving modes and would negate the need to control the tyre condition. This proposal was included the EPSRC equipment grant, number EP/K040391/1, and will be carried out during late 2015.

- A real time driver feedback display could be prototyped using the SAE and CASE metrics. If successful this would enable a driver to control to both vehicle speed and also their energy use during an emissions test.

- Given the increased penetration of current measurement devices on production vehicles, the feasibility of interrogating these should be examined. If successful this would enable to control of electrical variability without the need to additional costly instrumentation to be installed or vehicles to be modified substantially.

References

1. Gense, N.L.J., Jackson, N. and Samaras, Z., ***Euro 5 technologies and costs for Light-Duty vehicles. The expert panels summary of stakeholders responses***. 2005, TNO Science and Industry: Delft, Netherlands.
2. European-Commission, ***Commission Staff Working Document. Accompanying document to the Proposal from the Commission to the European Parliament and Ccouncil for a regulation to reduce CO2 emissions from passenger cars. Impact Assessement.*** 2007.
3. Fontaras, G. and Samaras, Z., ***On the way to 130g/km CO2—Estimating the future characteristics of the average European passenger car.*** Energy Policy, 2010. 38 (4): p. 1826-1833.
4. European Commission. ***Reducing CO2 emissions from passenger cars***. 2010 [cited 16th August 2011]; Available from: http://ec.europa.eu/clima/policies/transport/vehicles/cars_en.htm.
5. Bartz, W. J., ***Gear oil influences on efficiency of gear and fuel economy of cars.*** Proceedings of the Institution of Mechanical Engineers, Part D: Journal of Automobile Engineering, 2000. 214 (2): p. 189-196.
6. Bannister, C. D., Hawley, J. G., Ali, H. M., Chuck, C. J., Price, P., Chrysafi, S. S., Brown, A. and Pickford, W., ***The impact of biodiesel blend ratio on vehicle performance and emissions.*** Proceedings of the Institution of Mechanical Engineers, Part D: Journal of Automobile Engineering, 2010. 224 (3): p. 405-421.
7. Akehurst, S., Hawley, J. G., Pegg, I. and Piddock, M. ***Front End Auxiliary Drive (FEAD) Configurations Focusing on CO2 Benefits***. in *SAE 2004 Wold Congress & Exhibition*. 2004: SAE International. SAE Technical Paper No. 2004-01-0596.
8. Brace, C. J., Burke, R. and Moffa, J., ***Increasing accuracy and repeatability of fuel consumption measurement in chassis dynamometer testing.*** Proceedings of the Institution of Mechanical Engineers, Part D: Journal of Automobile Engineering, 2009. 223 (Compendex): p. 1163-1177.
9. United Nations, ***ECE 83-06. Uniform Provisions Concerning the Approval of: Vehicles with Regard to the Emission of Pollutants according to Engine Fuel Requirments***. 2013: InterRegs Ltd.
10. Kadijk, G. and Ligterink, N., ***TNO 2012 R10237: Road load determination of passenger cars***. 2012, TNO.
11. Stone, R., ***Introduction to Internal Combustion Engines***. Third Edition ed. 1999: Palgrave.
12. Schafer, F. and van Basshuysen, R., ***Reduced Emissions and Fuel Consumption in Automobile Engines***. 1995: Springer-Verlag / SAE International.
13. European Commission, ***Regulation (EC) No 715/2007 of the European Parliament and of the Council on type approval of motor vehicles with respect to emissions from light passenger and commercial vehicles (Euro 5 and Euro 6) and on access to vehicle repair and maintenance information***. 2007: European Commission.
14. Kadijk, G., Verbeek, M., Smokers, R., Spreen, J, Patuleia, A., Van-Ras, M., Norris, J., Johnson, A., O'Brien, S., Wrigley, S., Pagnac, J., Seban, M. and Buttigieg, D., ***Supporting Analysis regarding Test Procedure***

Flexibilities and Technology Deployment for Review of the Light Duty Vehicle CO2 Regulations 2012, TNO.
15. Mock, P., German, J., Bandivadekar, A., I., Riemersma., Ligterink, N. and Lambrecht, U., ***From laboratory to road: A comparison of official and 'real world' fuel consumption and CO2 values for cars in Europe and the United States***. 2013, ICCT.
16. Mock, P., Kühlwein, J., Tietge, U., Franco, V., Bandivadekar, A. and German, J., ***The WLTP: How a new test procedure for cars will affect fuel consumption values in the EU***. 2014, ICCT.
17. Hawley, J. G., Bannister, C. D., Brace, C. J., Akehurst, S., Pegg, I. and Avery, M. R., ***The effect of engine and transmission oil viscometrics on vehicle fuel consumption****.* Proceedings of the Institution of Mechanical Engineers, Part D: Journal of Automobile Engineering, 2010. 224 (Compendex): p. 1213-1228.
18. Reasbeck P., Smith J.G., ***Batteries for Automotive Use***. 1997, Taunton: Research Studies Press Ltd.
19. Alder, Ulrich, ***Automotive Electric/Electronic Systems***. 2nd Edition ed. 1995, Stuttgart: Robert Bosch GmbH.
20. Schmidt, Helge, ***Factors influencing NEDC CO2 emissions during type approval of passenger cars***. 2010, TuV Nord.
21. Jurgen, Ronald K., ***Automotive Electronics Handbook***. Second Edition ed. 1999: McGraw Hill Inc.
22. Venkkateshraj, A.V.K., Vijayakumar, B., Narayanan, V. and Anandakumaran, N.K.R. ***High Power and High Efficiency Alternators for Passenger Cars***. in *SIAT 2007*. 2007: The Automotive Research Association of India. SAE Technical Paper No. 2007-26-058.
23. Bischof, H., Gröter, H. P. and Schenk, R. ***High Output Alternator Concepts***. in *International Congress & Exposition*. 1999: SAE International. SAE Technical Paper No. 1999-01-1092.
24. d'Ambrosio, C., Genovese, M., Ferre, A., Simonsson, J., Berger, H., Midi, M., Abele, M. and Schmieder, G., ***Energy Efficient Vehicles for Road Transport - EE VERT; Deliverable D1.2.1.*** 2009.
25. Montalto, I., Tavella, D., Casavola, A. and De Cristofaro, F., ***Intelligent Alternator Employment To Reduce Co2 Emission and to Improve Engine Performance****.* SAE Int. J. Alt. Power., 2012. 1 (1): p. 1-11. SAE Technical Paper No. 2011-01-2444.
26. Plint, M. A. and Martyr, A. J., ***Engine Testing Theory and practice***. Second Edition ed. 2002: Butterworth-Heinemann.
27. Bielaczyc, P. and Szczotka, A. ***Analysis of Uncertainty of the Emission Measurement of Gaseous Pollutants on Chassis Dynamometer***. in *SAE Wold Congress & Exhibition*. 2007: SAE International. SAE Technical Paper No. 2007-01-1324.
28. Society of Automotive Engineers, ***J2951: Drive Quality Evaluation for Chassis Dynamometer Testing***. Surface Vehicle Recommended Practice. 2011, Warrendale, PA: SAE International.
29. Gonder, J., Earleywine, M. and Sparks, W., ***Analyzing Vehicle Fuel Saving Opportunities through Intelligent Driver Feedback****.* SAE Int. J. Passeng. Cars - Electron. Electr. Syst., 2012. 5 (2): p. 450-461. SAE Technical Paper No. 2012-01-0494.
30. Vagg, C., Brace, C. J., Wijetunge, R., Akehurst, S. and Ash, L., ***Development of a new method to assess fuel saving using gear shift***

indicators. Proceedings of the Institution of Mechanical Engineers, Part D: Journal of Automobile Engineering, 2012. 226 (12): p. 1630-1639.
31. Joumard, R., Laurikko, J., Han, T.L., Geivanidis, S., Samaras, Z., Meretei, T., Devaux, P., Andre, J., Cornelis, E., Lacour, S., Prati, M.V., Vermeulen, R. and Zallinger, M., ***Accuracy of exhaust emission factor measurements on chassis dynamometer***. Journal of the Air and Waste Management Association, 2009. 59 (Compendex): p. 695-703.
32. Joumard, R., Andre, M., Laurikko, J., LeAnh, T., Geivanidis, S., Olah, Z., Devaux, P., Andre, J.M., Cornelis, E., Rouveirolles, P., Lacour, S., Prati, M.V., Vermeulen, R. and Zallinger, M., ***Accuracy of exhaust emissions measurments on vehicle bench (Report LTE 0522)***. 2006: France.
33. Moore, W., Sutton, M. and Donnelly, K. ***Development of Long Haul Heavy Duty Vehicle Real World Fuel Economy Measurement Technique***. in *SAE 2013 World Congress & Exhibition*. 2013: SAE International. SAE Technical Paper No. 2013-01-0330.
34. D'Angelo, S., Brownell, C., Brownell, C. and Mears, W.G. ***Evaluating the Performance of Chassis Dynamometers with Electric Inertia Simulation***. in *International Congress & Exposition*. 1996: SAE International. SAE Technical Paper No. 960716.
35. Bender, S., ***Chassis Dynamometer VULCAN - Technical Presentation***. 2012.
36. Plint, M. A. and Martyr, A. J., ***Some limitations of the chassis dynamometer in vehicle simulation***. Proceedings of the Institution of Mechanical Engineers, Part D: Journal of Automobile Engineering, 2001. 215 (Compendex): p. 431-437.
37. Chapin, C. E. ***Road Load Measurement and Dynamometer Simulation Using Coastdown Techniques***. in *Passenger Car Meeting & Exposition*. 1981: SAE International. SAE Technical Paper No. 810828.
38. Schürmann, D., Krause, N. and Kinne, D. ***The Influence of Testing Parameters on Exhaust Gas Emissions***. in *Passenger Car Meeting & Exposition*. 1978: SAE International. SAE Technical Paper No. 780649.
39. Yasin, T.P. ***The Analytical Basis of Automobile Coastdown Testing***. in *Automotive Engineering Congress & Exposition*. 1978: SAE International. SAE Technical Paper No. 780334.
40. Carlson, R.B., Lohse-Busch, H., Diez, J. and Gibbs, J., ***The Measured Impact of Vehicle Mass on Road Load Forces and Energy Consumption for a BEV, HEV, and ICE Vehicle***. SAE Int. J. Alt. Power., 2013. 2 (1): p. 105-114. SAE Technical Paper No. 2013-01-1457.
41. El-Sharkawy, A.E. ***Reliability Analysis of Dynamometer Loading Parameters during Vehicle Cell Testing***. in *SAE Wold Congress & Exhibition*. 2007: SAE International. SAE Technical Paper No. 2007-01-0600.
42. Thompson, J.K., Marks, A. and Rhode, D. ***Inertia Simulation in Brake Dynamometer Testing***. in *20th Annual Brake Colloquium and Exhibition*. 2002: SAE International. SAE Technical Paper No. 2002-01-2601.
43. Horiba Ltd. ***VULCAN EMSCD48***. 2013 [cited 26/11/2013 2013]; Available from: http://www.horiba.com/automotive-test-systems/products/mechatronic-systems/vehicle-test-systems/details/vulcan-emscd48-626/.
44. Society of Automotive Engineers, ***J1263 Road Load Measurment and dynamometer Simulation Using Coastdown Techniques***. 2010: SAE International.

45. Society of Automotive Engineers, ***J2263 Road Load Measurement Using Onboard Anemometry and Coastdown Techniques***. 2008: SAE International.
46. Society of Automotive Engineers, ***J2264 Chassis Dynamometer Simulation of Road Load Using Coastdown Techniques***. 2014: SAE International.
47. Mears, W.G., D'Angelo, S. and Paulsell, C.D. ***Performance Tests of a Large-Roll Chassis Dynamometer with AC Flux-Vector PEU and Friction-Compensated Bearings***. in *International Congress & Exhibition*. 1993: SAE International. SAE Technical Paper No. 930392.
48. Enviromental Protection Agency, ***Attachment A RFP C100081T1 Specifications of Electric Chassis Dynamometers***. 1991: US EPA.
49. Aguirre, C.J., Brezenski, M., Cetnar, C., Chang, T., Detloff, B., Hopson, S., Fagerman, T., Johnson, S., Karim, J., Owens, F., Paulina, C., Pearl, R. and VanAcker, C., ***Dyanmometer Performance Evaluation and Quality Assurance Procedures***. 2000.
50. Zhu, W., Wang, D., Qi, F. and Yang, D. ***Measurement and analysis to DIW of chassis dynamometers for automobile emissions testing***. in *4th International Seminar on Modern Cutting and Measurement Engineering, December 10, 2010 - December 12, 2010*. 2011. Beijing, China: SPIE.
51. Sato, Y., Kusakabe, T., Satonaka, T., Nakamura, S., Ogawa, Y. and Noguchi, S. ***An Analysis of Behavior for 4WD Vehicle on 4WD-chassis Dynamometer***. in *SAE 2010 World Congress & Exhibition*. 2010: SAE International. SAE Technical Paper No. 2001-01-0926.
52. Mogi, E., Notomi, S., Mizone, T., Yamazaki, S. and Hosoi, K. ***Study on Contribution of Tire Driving Stiffness to Vehicle Fuel Economy***. in *SAE Wold Congress & Exhibition*. 2012: SAE International. SAE Technical Paper No. 2012-01-0794.
53. Clark, S.K., ***Mechanics of Pneumatic Tyres***. 1971, Washington DC: U.S. Department of Commerce.
54. Gerresheim, M. ***Dependance of vehicle fuel consumption on the tyre-wheel assembly***. in *Automobile Wheels and Tyres*. 1983. Sutton Coldfield, UK: IMechE.
55. Genta, G., ***Motor Vehicle Dynamics, Modelling and Simulation***. 2006, London: World Scientific.
56. Wong, J.Y., ***Theory of Ground Vehicles***. Fourth Edition ed. 2008: John Wiley & Sons, Inc.
57. Transportation Research Board, ***Tires and Passenger Vehicle Fuel Economy, Informing Consumers, Improving Performance***. 2006, National Research Council.
58. Pacejka, H. B., ***Tire and Vehicle Dynamics***. 2012: Elsevier.
59. Taghavifar, H. and Mardani, A., ***Investigating the effect of velocity, inflation pressure, and vertical load on rolling resistance of a radial ply tire***. Journal of Terramechanics, 2013. 50 (2): p. 99-106.
60. Lindemuth, B.E., Gent, A.N., McDonel, E.T., Assaad, M.C., Ebbott, T.G., Padula, S.M., Trinko, M.J., Pottinger, M.G., Marshall, K.D., Turner, D.M., Grosch, K.A., LaClair, T.J., Walter, J.D., Gardner, J.D., Queiser, B.J., Popio, J.A., Dodson, T.M., Isayev, A.I. and Oh, J.S., ***The Pneumatic Tire***. 2006, National Highway Traffic Safety Administration: USA.
61. Peralta, M., Paulina, C., Duoba, M., Amann, G. and Bohn, T. ***Evaluating the Effects of Restraint Systems on Four Wheel Drive Testing Methodologies: A Collaborative Effort between NVFEL and ANL***. in

SAE World Congress & Exhibition. 2009: SAE International. SAE Technical Paper No. 2009-01-1522.
62. Silvis, W.M., Harvey, R.N. and Dageforde, A.F. ***A CFV type mini-dilution sampling system for vehicle exhaust emissions measurement***. in *International Congress & Exposition*. 1999. SAE Technical Paper No. 1999-01-0151.
63. Sherman, M.T., Lennon, K. and Chase, R.E. ***Error Analysis of Various Sampling Systems*** in *SAE 2001 World Congress*. 2001. SAE Technical Paper No. 2001-01-0209.
64. Bannister, C.D., ***Vehicle Emissions Measurement***, in *Mechanical Engineering*. 2007, University of Bath: Bath.
65. Box, G.E.P., Hunter, J.S., Hunter, W.G., ***Statistics for experimenters. Design, innovation and discovery.*** Second ed. 2005, New Jersey: John Wiley.
66. Armitage, P., ***Statistical Methods in Medical Research***. 1971, Blackwell Scientific Publications.
67. Mathworks. ***Making Quality Measurements***. 2011 [cited 8th November 2011]; Available from: http://www.mathworks.co.uk/help/toolbox/daq/f5-30343.html.
68. Ropke, K., Nessler, A., Haukap, C., Baumann, W., Kohler, B.U. and Schaum, S. ***Model Based Methods for Engine Calibration - Quo Vadis***. in *presented at the 3. Internationales Symposium fur Entwicklungsmethodik*. 2009. Herausforderungen im Spannungsfeld neuer Antriebskonzepte, Kurhaus Wisebaden, Germany,.
69. Burke, R., ***Investigation into the Interactions between Thermal Management, Lubrication and Control Systems of an Engine***, in *Mechanical Engineering*. 2011, University of Bath.
70. Atkinson, A.C. and Donev, A.N., ***Optimum Experiemental Designs***. 1992, Oxford: Clarendon Press.
71. Draper, N.R. and Smith, H. , ***Applied Regression Analysis***. Third ed. 1998: John Wiley & Sons.
72. Eriksson, L., Johansson, E., Kettaneh-Wold, N., Wilkström, C. and Wold, S., ***Design of Experiments: Principles and Applications***. 2000: Umetrics Academy.
73. DeVor, R.E., Chang, T. and Sutherland, J.W., ***Statistical Quality Design and Control - Contemporary Concepts and Methods***. 1992, New York: Macmillian.
74. Oakland, J.S., ***Statistical process control***. 2008, Butterworth-Heinemann
75. Dvorak, T., Malone, L. and Hoekstra, R. ***Statistical Process Control and Design of Experiment Process Improvement Methods for the Powertrain Laboratory***. in *SAE Poertrain & Fluid Systems Conference & Exhibition*. 2003: SAE International. SAE Technical Paper No. 2003-01-3208.
76. Taghizadegan, S., ***Essentials of lean six sigma***. 2006, Elsevier.
77. Wheeler, D. and Chambers, D., ***Understanding Statistical Process Control***. 1990, North Ammerica: Addison-Wesley Publishing
78. Minitab Inc. ***Minitab 17 Online Help Resource: Understanding Variables control charts in Minitab***. 2014 [cited Feb 2015; Available from: http://support.minitab.com/en-us/minitab/17/topic-library/quality-tools/control-charts/understanding-variables-control-charts/variables-control-charts-in-minitab/.

79. Stapenhurst, T., ***Mastering Statistical Process Control a handbook for performance improvement using cases***. 2005, Oxford; Boston: Elsevier/Butterworth-Heinemann.
80. Minitab Inc. ***Minitab 17 Online Help Resource: Using tests for special causes in control charts***. 2014 [cited Feb 2015; Available from: http://support.minitab.com/en-us/minitab/17/topic-library/quality-tools/control-charts/basics/using-tests-for-special-causes/.
81. Truscott, W.G., ***Six sigma continual improvement for business : a practical guide***. 2003, Butterworth-Heinemann.
82. Cross, J., ***Complex Process***. 2015. Personal E-mail, Sent to: C. Brace and E. Chappell.
83. Chappell, E., Brace, C. and Ritchie, C., ***The control of chassis dynamometer fuel consumption testing noise factors and the use of response modelling for validation of test repeatability***. Proceedings of the Institution of Mechanical Engineers, Part D: Journal of Automobile Engineering, 2013. 227 (6): p. 853-865.
84. Vehicle Certification Authority. ***Car Fuel Data***. 2009 [cited 20th October 2009]; Available from: www.vcacarfueldata.org.uk/search/vehicleDetails.asp?id=15171.
85. British Standards Institution, ***BSI ISO 10521-2:2006 Road Vehicles. Road load. Part 2: reproduction on chassis dynamometer***. 2006: BSI.
86. Cochran, William G. and Cox, Gertrude M., ***Experimental Designs***. Second ed. 1968, New York: John Wiley & Sons Inc.
87. Met Office, ***Extremes - National Meteorological Library and Archive. Fact sheet 9 — Weather extremes (Version 01)***. 2011, Met Office.
88. Ghazikhani, M., Ebrahim Feyz, M., Mahian, O. and Sabazadeh, A., ***Effects of altitude on the soot emission and fuel consumption of a light-duty diesel engine***. Transport, 2013. 28 (2): p. 130-139.
89. United Nations, ***ECE R101: Uniform Provisions Concerning the Approval of Passenger Cars Powered by An Internal Combustion Engine Only or Powered by a Hybrid Electric Powertrain with regard to the Measurment of the Emission of Carbon Dioxide and Fuel Consumption and Electric Range and of Categories M1 and N1 Vehicle Powrred by an Electric Powertrain Only with Regards to the Measurment of Electric Energy Consumption and Electric Range***.
90. Heywood, J.B., ***Internal Combustion Engine Fundementals***. International ed. 1988: McGraw-Hill.
91. Shevell, Richard S., ***Fundamentals of Flight***. Second ed. 1989, New Jersey: Prentice Hall.
92. Matthews, Clifford, ***Engineers' Data Book***. Third ed. 2010: Wiley.
93. AVL, ***ADVISOR 2003***. 2003, AVL List GmbH.